ENVIRONMENTAL CHANGE AND EROSION, POUNAWEA WETLAND, OTAGO, NEW ZEALAND

Finn Gadsby

A thesis submitted in partial fulfilment of the degree of

Master of Science

At the University of Otago, Dunedin, New Zealand

December 2022

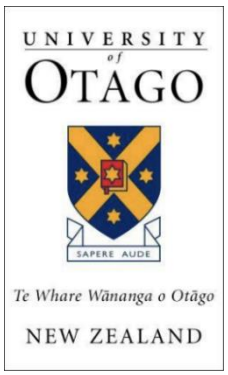

Oblique aerial image of Pounawea Wetland looking east during a UAV drone survey, June 17th 2022

Abstract

Coastal wetlands are dynamic environments that provide a range of high value ecosystem services. Salt meadow wetlands are rare and not well studied in southern New Zealand. Pounawea Wetland (also referred to as the 'Hungerford Point Saltmarsh') provides a unique opportunity to examine how environmental change has contributed to lateral erosion of the wetland edge; and the potential for erosion mitigation strategies. This research aims to (1) document environmental change and the morphodynamics of Pounawea wetland over the last century; (2) examine this change in relation to changing boundary conditions; (3a) determine the spatial patterns and rates of sediment deposition during inundation events; and (3b) examine how sea-level rise will affect future wetland evolution.

Aerial photographs, satellite imagery, and UAV (drone) imagery, from 1948–2022, is used to examine estuary and catchment morphodynamics, shoreline erosion, and vegetation zonation. Shoreline erosion rates were calculated using the Digital Shoreline Analysis System (DSAS). The more exposed margins of the wetland (eastern and western margins) have eroded 60–93 m since 1948; while the more sheltered areas have eroded between 3–30 m over the same period. The average yearly shoreline retreat is -0.67 ± 0.05 m/yr. The rate of erosion increased from 1948–1985, following the erosion of Cabbage Point, a vegetated sand spit. The erosion of this spit likely increased ocean wave propagation into the estuary during periods of north-easterly winds and easterly swells. Wetland species migration from lower to upper marsh was identified through historic aerial images. The podocarp forest receded by 10–50 m between 1967 and 1985.

The severity and frequency of weather events did not increase in the period 1972–2022. Wind and pressure data from Nugget Point climate station, 10 km north-east of Pounawea did not illustrate an increase in potential erosion events (defined with respect to wind speeds > 7 m/s; wind direction 180°-270°; and pressure < 990 hPa).

Deforestation upwind of Pounawea wetland has resulted in an increase in wind speed across the estuary during southerly to south-westerly wind events and consequent increase in significant wave heights along the wetland margins, resulting in an increase in the rates of lateral erosion of the wetland edge. Computational fluid dynamics (CFD)

modelling was used to demonstrate the reduction in wind speed across the estuary in the lee of an upwind forest. Scenarios using different porosities (Cd = 0.005, 0.05 and 0.15) were modelled and all results demonstrated that a forest upwind of the wetland (on the Hinahina side of the estuary) would reduce wind speed across Catlins Estuary by 50–80%.

Sediment, comprised of mineral sand and rock fragments, is accumulating on the surface of the wetland, however, the wetland is eroding faster than the rate of vertical accretion. Sediment accumulation was measured using artificial grass mats during six inundation events that encompassed both high and low energy wave environments. The spatial distribution of sediment deposited on the wetland during inundation events is not evenly distributed. Over 60% of the sediment that accumulated on the eight artificial mats was deposited within 2 m of the wetland edge. Consequently, the margins of the wetland have a higher elevation than the wetland core. Sediment accumulation increases with an increase in wind speed and significant wave height; The wetland edge is accreting faster than SLR, however, this area is periodically eroding at a rate of -0.67 ± 0.05 m/yr and sediment deposited at the edge is eroded.

CFD modelling was also used to examine the effects of rising water-levels on the wall shear stress experienced at the wetland edge. Seven water levels were modelled (0.2-1.4 m, at 0.2m increments) to illustrate different tidal stages and future sea-levels. Results illustrated an increase in the amount of shear stress on the wetland edge up to the level of wetland inundation (0.8 m), beyond this point, wall shear stress decreased. The modelled decrease in wall shear represents waves breaking across the surface of the wetland rather than against the wetland edge. Pressure is exerted on the wetland edge as water level rises, resulting in turbulence and erosion; upon inundation, wall shear stress decreases and the potential for sediment accumulation on the wetland increases.

Pounawea Wetland is a vulnerable, low-lying, and eroding salt meadow. Processes of accretion have been identified, however, the wetland is eroding faster than it is accreting. Two key environmental drivers of wetland change are identified; land use change and sea-level rise. Short, medium and long-term mitigations strategies are proposed to reduce wetland edge erosion and increase ecosystem services. Nature-based solutions such as oyster reefs can attenuate waves to mitigate shoreline erosion, stabilise sediment, improve water quality and provide habitat for fisheries. The combination of oyster reefs, sand renourishment of Cabbage Point and an upwind shelterbelt would

reduce wind speed and wave height across the estuary thereby reducing the potential for lateral erosion. The simultaneous use of multiple strategies has the potential to provide the most effective strategy for erosion mitigation. However, sea-level rise will continue to accelerate, and inundation of the wetland will become more frequent by 2100 and by 2150 the wetland will be inundated every day. Sediment accumulation may increase during this period, but lower marsh species are not suited to spend extended periods of time inundated. Pounawea wetland is eroding faster than it is accreting and if this trend continues (it may slow or accelerate) then the wetland will cease to exist by 2150, and possibly much earlier.

Acknowledgements

To my supervisor Associate Professor Mike Hilton, your knowledge, quick wit and humour have made the last two years enjoyable and a constant learning experience. Thank you for the help planning and executing fieldwork, the encouragement to get into the field when conditions were less than ideal. Thank you for the honest comments related to my writing. I hope and feel as though it has improved over the last two years. It has been an interesting two years with a significant setback half way through but your reassurance that it would be alright and that this thesis was a learning experience helped me to the end.

To Dr Duc Nguyen, thank you for teaching me the basics of CFD and help in the field, your enthusiasm and encouragement was well received.

To Dr Douglas Fraser, thank you for your help all things MATLAB related, your time and energy trying to relay information and processes was invaluable.

To Dr Sophie Horton, thank you for all your help and guidance on processing the RBR data through Ruskin and MatLab, and for always taking the time to answer my constant questions.

To Chris Garden, your GIS wizardry is unmatched, thank you for always taking the time to answer my questions even if they were highly repetitive.

To Dr Teresa Konlechner, your knowledge on vegetation and nature-based solutions was instrumental for this thesis.

To Dr Sarah Mager, thank you for fielding my questions about sedimentation and calculations related to sediment depth.

Campbell, thank you for last two and bit years, it's been quite the journey filled with plenty setbacks and moments of triumph. Your help on field trips, GIS and so many other aspects of this thesis has proved immeasurable.

Maddie, thanks for your help on fieldwork, formatting and the positive reinforcement to finish the thesis, it really helped. Also, the weekly formula one chats were a much-needed distraction.

To Callum, thanks for your help on fieldwork.

To Mike McPhee at the Owaka Museum, thank you for the historical images and information related to Pounawea Wetland and the Catlins Estuary.

To my friends, thanks for the support and always asking how long I had left, this gave me the motivation to get it done.

To my family, thanks for the support, motivation and belief. Thank you also for helping me proof read.

Thank you, Dad, for your unwavering support to pursue further education. You have always supported me in everything I do and it means a lot. Your help proofreading towards the end was invaluable. The words of encouragement in these final months and reminding me to reflect on everything I have achieved rather than all the work still to go was exactly what I needed to hear.

Finally, this thesis is dedicated to my mum. I know she would be proud of where I am today and the way in which I have overcome the challenges of this thesis.

Table of Contents

List of Figures

Chapter 1

Chapter 2

Chapter 3

Chapter 4

Chapter 5

Chapter 6

List of Tables

List of Abbreviations

CBA	Cost-benefit Analysis
Cd	Drag coefficient
CFD	Computational Fluid dynamics
DEM	Digital Elevation Model
DoC	Department of Conservation
DSM	Digital Surface Model
DSAS	Digital Shoreline Analysis System
ENSO	El Nino Southern Oscillation
GCPs	Ground Control Points
GHG	Greenhouse gas
GIA	Global Isostatic Adjustment
Hs	Significant Wave Height
hPa	Hectopascal
IPCC	Intergovernmental Panel for Climate Change
IPO	Inter-Decadal Pacific Oscillation
IUCN	International Union for Conservation of Nature
LiDAR	Light Detection and Ranging
LINZ	Land Information New Zealand
LRR	Linear Regression Rate
MHW	Mean High Water
MHWN	Mean High Water Neap
MHWS	Mean High Water Spring
MLLW	Mean Lower Low Water
MSL	Mean Sea Level
MWAC	Modified Wilson and Cook

NEE	Non-Erosion Event
NIWA	National Institute for Water and Atmospheric Research
NSM	Net Shoreline Movement
NZCPS	New Zealand Coastal Policy Statement
ORC	Otago Regional Council
PEE	Potential Erosion Event
RMSE	Root Mean Square Error
RTK-GPS	Real Time Kinematic-Global Positioning Service
SAM	Southern Annular Mode
SLR	Sea-level Rise
SSI	Storm Surge Intensity
UAV	Unmanned Aerial Vehicle
VLM	Vertical Land Movement
VP	Velocity Profile

1. Introduction

The coast is a dynamic environment, evolving and adapting to changing environmental conditions. The world is facing a climate emergency from exponential greenhouse gas (GHG) emissions entering and warming the atmosphere leading to sea-level rise. Coastal habitats act as a barrier between human infrastructure and the natural world. The deterioration of this barrier has the potential to accelerate coastal erosion, increase storm surge, degrade habitats and negatively affect ecosystem services (Arkema *et al.*, 2015; Costanza *et al.*, 2007; Kittinger and Ayers, 2010). This chapter will introduce the study site, outline the research aims, justify the study and outline the thesis structure.

1.1. COASTAL WETLANDS

Coastal wetlands are located in areas of land - sea interaction through marine tidal cycles. They act as a natural buffer for wave attenuation and provide habitat for wetland species (Chagué-Goff and Goff, 2003; Möller *et al.*, 2014). Salt meadow wetlands are formed in sheltered environments, typically on intertidal sand flats where silt and sediment can accumulate (Thannheiser and Holland, 1994). Salt meadow vegetation is low-lying (<3 cm tall) and forms interwoven communities of plants (Johnson and Gerbeaux, 2004). This low vegetation is not effective for wave attenuation but can trap sediment deposited onto the wetland which helps the wetland vertically accrete (Partridge and Wilson, 1988; Thannheiser and Holland, 1994). Known internationally as 'herbfields' these wetlands have different vegetation zones dependent on the wetland elevation - increases in elevation are associated with an increase in species richness (Moeslund *et al.*, 2011). Each zone is usually defined by species tolerance to salt water intrusion. Salt meadow wetlands are occasionally inundated during storms or spring high tides (Thannheiser and Holland, 1994), however, extended exposure to saline water can lead to decay (Partridge and Wilson, 1989).

Wetlands have biophysical, ecological, social and cultural values that may be threatened by erosion and eustatic sea-level rise. These values can be summarised through ecosystem services (Arkema *et al.*, 2015; Spalding *et al.*, 2014). Ecosystem services are the conditions and processes of ecosystems that generate or help to generate benefits for people (Guerry *et al.*, 2015). Costanza *et al.* (1998) estimated the value of global ecosystem services to be US $33 trillion per annum (Costanza *et al.*, 1998). The way in which ecosystem services are valued has developed alongside the growing body of literature that recognises their importance for coastal protection; ecological biodiversity; economic stability and societal development (Feagin *et al.*, 2010; Arkema *et al.*, 2015; Himes-Cornell *et al.*, 2018; Nelson *et al.*, 2013).

Erosion of wetland environments has not been widely researched in New Zealand, especially salt meadow wetlands. Robertson *et al.* (2018) discussed Southland wetland loss since the 1990s but attributed the loss of wetlands to drainage and land-use change for agricultural intensification. The Pounawea Wetland (Hungerford Saltmarsh) has not been drained or altered yet it is eroding at the margins. Understanding why the wetland is eroding is necessary because salt meadow wetlands are rare and should be effectively managed. The biodiversity value of coastal wetlands as a habitat for flora and fauna is critical. Pounawea Wetland has been identified as a regionally significant wetland, therefore, understanding why it is eroding is important to ensure this regionally significant wetland can be a functioning habitat for species.

1.2. COASTAL HAZARD MANAGEMENT

Coastal hazards such as erosion and inundation are increasing because of eustatic sea level rise (Zhang *et al.*, 2004). As populations increase, cities and communities expand into areas that are suboptimal for development, many of these areas are near the coast (Gracia *et al.*, 2018). Growth at the coast increases pressure on coastal infrastructure and protection mechanisms. Over 85% of New Zealanders live within 5 km of the coast (Lawrence *et al.*, 2018) and New Zealand's infrastructure has lagged behind its growth for several decades (Simonson and Hall, 2019). The need for resilience and adaptable environmental solutions to coastal hazard management is increasing.

Coastal environments are dynamic, and erosion and accretion drive coastal morphodynamics. For decades, coastal erosion has been addressed in a reactionary manner (Zhang *et al.*, 2004), meaning that after an erosion event (storm surge) strategies are implemented to address the issues where infrastructure failed. The response is usually to build larger and stronger hard infrastructure (Gracia *et al.*, 2018). Hard infrastructure such as seawalls, breakwaters and groynes modify the hydrodynamic and sedimentary regimes by attenuating wave energy (Firth *et al.*, 2014; Morris *et al.*, 2018; van Rijn, 2011). Advances in the understanding of the drivers of erosion such as sediment imbalance, and storm surge provide an opportunity for a proactive approach to coastal erosion. Computer modelling allows for detailed assessment of at-risk areas based on environmental indicators. The use of modelling to simulate erosion events and the reaction of different implementation strategies has increased (Brown *et al.*, 2006; Cowell *et al.*, 1992; Ramakrishnan *et al.*, 2018).

Hard infrastructure is increasingly viewed as economically and ecologically unsustainable (Morris *et al.*, 2018). The restoration and creation of natural habitats for coastal hazard management, specifically, shoreline erosion and wave attenuation has increased over the last two decades (Arkema *et al.*, 2013; Morris *et al.*, 2018; Narayan *et al.*, 2016; Seddon *et al.*, 2020; Sutton-Grier *et al.*, 2015; Temmerman *et al.*, 2013).

Nature-based solutions (NBS) protect the coastline and increase ecosystem services by decreasing turbidity, stabilising sediment and provide habitat/nursey environment for fisheries (Himes-Cornell *et al.*, 2018). NBS are also cost effective and adaptable to changing environmental conditions (Narayan *et al.*, 2016; Reguero *et al.*, 2018). Implementation of NBS within New Zealand is limited, however, case studies from overseas illustrate the potential for NBS to be utilised as an alternative method for coastal hazard management (Duarte *et al.*, 2013; Möller *et al.*, 2014; Morris *et al.*, 2019; Scyphers *et al.*, 2011; Sutton-Grier *et al.*, 2015).

1.3. SEA-LEVEL RISE

Global mean sea level rise (GMSLR) is accelerating due to ocean thermal expansion, mass lost from glaciers and polar ice sheet melt (Alley *et al.*, 2005). The effects of GMSLR on low-lying coastal nations and communities are likely to be costly financially, ecologically and socially. Sea-level rise (SLR) has been accelerating since the industrialisation of the world in the 1800s and has increased significantly in the twentieth century (Fox-Kemper *et al.*, 2021). The rate of SLR is not consistent around the world. In New Zealand, Hannah (2004) calculated the mean rate of SLR to be 2.1 mm yr^{-1} (Hannah, 2004); Gehrels *et al.* (2008) calculated a rate of 2.8 ±0.5 mm yr^{-1} from the start of the twentieth century (Gehrels *et al.*, 2008). The Intergovernmental Panel on Climate Change (*IPCC*) projects ~0.6–1 m of SLR by 2100 depending on global commitments to reduce greenhouse gas emission (IPCC, 2021a).

As sea-level rises, low-lying coastal environments such as wetlands are going to be inundated more frequently and storm surge will reach further inland. Increases in storm surge will likely accelerate erosion of all coastal margins. Salt meadow environments will be particularly vulnerable because the herbaceous vegetation is not suited to thrive in high energy environments (Thannheiser and Holland, 1994). The effects of SLR are not likely to be reversed in the next 50 years, therefore, understanding how environments are going to be impacted is critical for implementing mitigation strategies. SLR is going to affect Pounawea Wetland, so providing a comprehensive analysis of morphodynamics, land use change and external pressures on the wetland is required to accurately assess the wetlands future.

1.4. STUDY SITE: POUNAWEA WETLAND, OTAGO

Pounawea Wetland is located on the southeast coast of Otago, New Zealand (Lat. S46°, 28', Long. E169°,41', Figure 1.1). The wetland is classified as a salt meadow wetland, with a lower, middle and upper marsh (Partridge and Wilson, 1988). The lower marsh is made up of low-lying herbaceous species that form a 'carpet' or 'turf' like area, depicted in Figure 1.2 as brown vegetation however this is just winter die-off. The

middle marsh is comprised of shrubs and the upper vegetation zone is a native podocarp forest (Figure 1.2). The current study has focused on the wetland edge and lower marsh zone processes, however, historical aerial imagery provided insights to how vegetation boundaries have shifted over time (chapter 3).

Figure 1.1: Location of NIWA climate station at Nugget Point (yellow star); Pounawea Wetland (red star); and Hinahina (orange star).

Pounawea Wetland (currently 6 ha) is steadily decreasing in size. The accommodation space of the wetland is confined by the podocarp forest and high terrain to the north and the Catlins Estuary to the south. Pounawea Wetland is classed as 'Schedule 9 Regionally Significant Wetland' and is deemed to have a high diversity of wetland habitat types. The Otago Regional Council (ORC) acknowledge the scarcity of this type of coastal wetland and its proximity to a mature coastal forest (ORC, 2020a). Pounawea Wetland is located adjacent to the Catlins Estuary. The Catlins Estuary is a mesotidal estuary with a spring tide range of 1.76 m. Catchment characteristics and land use change will be discussed in sections 3.6 and 3.7.1.

Figure 1.2: Oblique image of Pounawea Wetland, orientated north-east. Three vegetation zones have been outlined; lower marsh (brown vegetation); middle marsh (grey/green shrubs) dominates north of the creek but areas of higher elevation in the lower marsh region are occupied by shrub vegetation; podocarp forest. Image taken on June 17th 2022 during a UAV survey of the wetland.

The predominant wind directions at Nugget Point are north-east and south-west (Figure 1.3). Stronger winds (>9 m/s) are mostly from the south-west. Pounawea Wetland is somewhat sheltered from north-east winds by the podocarp forest and terrain, whereas, south-west winds flow from the surrounding hills across the estuary undisturbed for 3 km. The processes related to wind flow, speed and direction, are discussed in chapters 4, 5 and 6.

Pounawea Wetland provides a unique opportunity to investigate changes in morphodynamics of the estuary system, processes of lateral wetland edge erosion and the potential impact of sea-level rise. This salt meadow wetland is low-lying, vulnerable and rare. Understanding the processes causing erosion should help to develop a strategy to protect this and other low-lying wetlands.

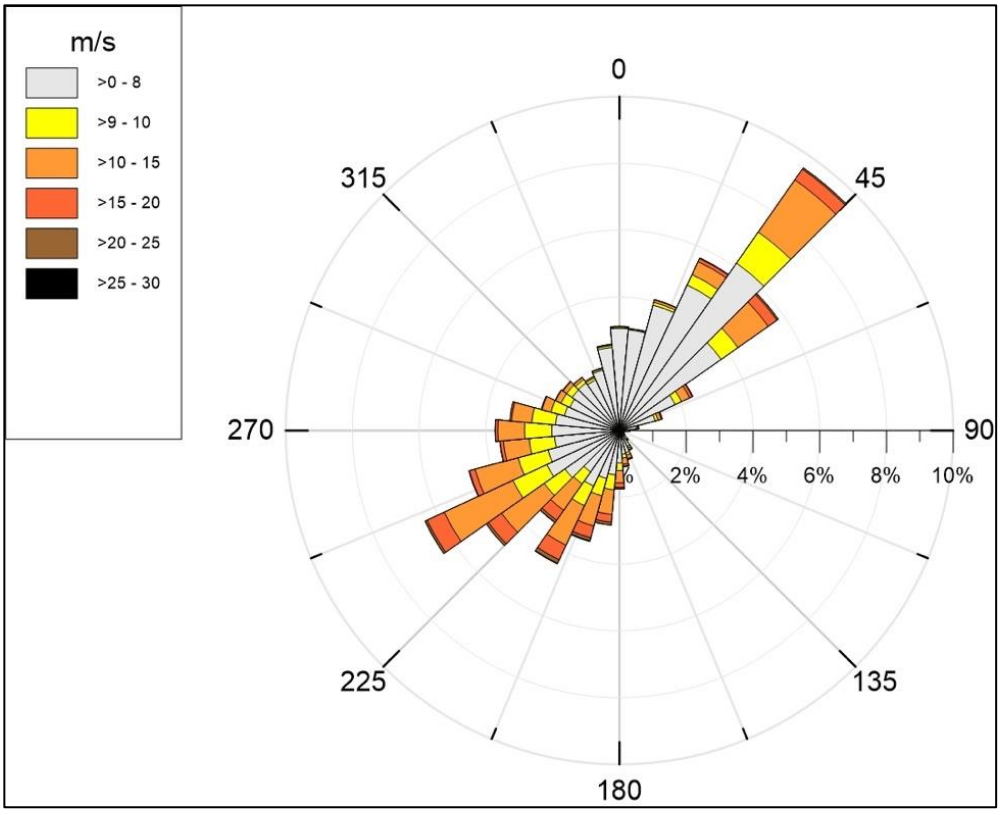

Figure 1.3: Wind rose from Nugget Point climate station data (1972-2022). The dominant wind is from the north-east and south-west, stronger gusts from the south-west.

1.5. RESEARCH AIMS

Wetlands are dynamic environments that are known to adapt to environmental change (Cahoon *et al.*, 2006; Spencer *et al.*, 2016b). Understanding what is driving environmental change is important if mitigation solutions are to be effective. This research aims to investigate the environmental drivers of wetland change at Pounawea Wetland. Research on New Zealand coastal wetlands is limited; therefore, this provides an opportunity to investigate an eroding salt meadow wetland, the result of which could improve management strategies to protect these environments from coastal erosion and sea-level rise.

It is important to understand the processes of sedimentation and spatial distribution of sediment across Pounawea Wetland. Wetland accretion is recognised as a mechanism that might allow wetlands to keep pace with sea-level rise (Kirwan *et al.*, 2016; Morris *et al.*, 2016; Nolte *et al.*, 2013), however, rates of sediment accretion are variable (Phillips, 2018; Schuerch *et al.*, 2018). Understanding the rate of sediment accretion at Pounawea Wetland enables more informed decisions to be made relating to the drivers of environmental change and the implementation of mitigation strategies.

There is a significant lack of New Zealand research on nature-based solutions involving wetlands. Studies overseas have illustrated wave attenuation and ecosystem services benefits of wetland and oyster reef environments (Arkema *et al.*, 2015; Himes-Cornell *et al.*, 2018; Morris *et al.*, 2018; Narayan *et al.*, 2016; Temmerman *et al.*, 2013). The application of such methods in a New Zealand context has scarcely been considered, but, there is clearly a potential for greater use of nature-based systems in vulnerable coastal areas. The application of mitigation strategies that protect and enhance the environments is a significant opportunity to improve coastal resilience, this research will aid in that understanding and its application to low-lying salt meadow wetlands.

The Pounawea Wetland has experienced significant morphological change since 1948 (the date of the first aerial photograph). Historical information and observations related to the wetland are sparse. Pounawea Wetland has featured as a study site for several studies in varying disciplines; notably a stratigraphic investigation (Gehrels *et al.*, 2008); archaeology (Garland and Wadsworth, 2019; Hamel, 1977; Hamel, 1978; Lockerbie, 1959); and studies of wetland flora (Partridge, 1984; Partridge and Wilson,

1988; Partridge and Wilson, 1989). Historical accounts detail the Catlins River/Estuary system with respect to the dense vegetated landscape that covered the surrounding areas (Thomson, 1889; Tyrrell, 2006; Wilson, 1993). The erosion or accretion of the Pounawea Wetland has not been well documented or discussed in the literature and this is to be the first detailed account of the historical erosion and accretion that has taken place. Stevens and Rogers (2017) did acknowledge the loss of salt marsh ecosystems within the Catlins Estuary, estimating over 300 hectares has been lost because of wetland drainage and land use conversion to grass pastures for agriculture, however, the Pounawea Wetland was not specifically discussed (Stevens and Robertson 2017).

The aim of this research is to identify the drivers of marginal wetland erosion at an eroding salt meadow wetland in South Otago, New Zealand. This research uses analysis of historical aerial imagery, climate data, field observations and computational fluid dynamic modelling to address the following research aims and determine:

1. Environmental change and morphodynamics of the Pounawea Wetland.
2. The frequency and severity of changing boundary conditions.
3. The spatial patterns and rates of sediment deposition during inundation events and how sea-level rise will affect processes of erosion at the wetland edge.

1.6. THESIS STRUCTURE

A brief overview of the background to the study has been presented in chapter 1. The aims and justification of the thesis have been outlined and the study site was introduced. Rising sea-levels have increased pressure on low-lying coastal communities and environments. Salt meadow wetlands are unique and therefore are not well studied globally or in New Zealand. Pounawea Wetland provides an excellent opportunity to study an eroding wetland to identify the causes of erosion and discuss how mitigation strategies could be implemented to decrease lateral erosion.

Chapter 2 details the relevant literature on coastal wetland environments, sea-level rise, hydrodynamic processes, and coastal hazard management practices including nature-based solutions. The review outlines current knowledge and identifies gaps in the literature to justify the aims of the thesis.

Chapter 3 examines environmental change and morphodynamics of the Pounawea Wetland. Aerial and satellite imagery and UAV surveys are used to document wetland vegetation and landform changes within the Catlins Estuary. This chapter details wetland elevation, species zonation, wetland edge erosion and calculates rates of lateral erosion.

Chapter 4 investigates the changing boundary conditions and their effect on Pounawea Wetland. Long term wind and pressure data from Nugget Point climate station is used to examine changes in the frequency of potential erosion events (PEE). Computational fluid dynamics (CFD) is used to model the effects of deforestation on wind speed and wave formation across the estuary.

Chapter 5 explores the processes of wetland inundation, erosion and sedimentation. Empirical research and CFD modelling are used to describe and explain the processes of sediment accumulation onto the wetland during inundation events and how SLR will affect wetland edge erosion.

Chapter 6 discusses the key findings of the thesis in relation to the two key drivers of environmental change. Short, medium and long-term mitigation strategies are proposed and discussed. The chapter concludes by discussing the global approach to coastal wetland management.

Chapter 7 summarises the key findings of this thesis in relation to the research questions. The chapter concludes with the limitations of the study and future research opportunities.

2. Literature Review

2.1. INTRODUCTION

Coastal wetlands protect the coast while providing habitat for obligate flora and fauna. However, coastal wetlands are under increasing pressure due to land use changes and the acceleration of sea-level rise (SLR) and erosional processes. Wetlands act as a buffer, reducing wave attenuation through vegetation density and the width of the wetland (Cahoon *et al.*, 2006; Chagué-Goff and Goff, 2003; Gedan *et al.*, 2010; Leonardi *et al.*, 2018; Möller *et al.*, 2014; Shepard *et al.*, 2011). The loss of these environments either naturally or through human intervention is a concern for coastal communities and ecosystems alike.

This literature review will focus on New Zealand coastal wetlands, specifically, wetland formation, species zonation and processes contributing to wetland erosion. This thesis includes consideration of future management options, specifically, nature-based solutions. Nature-based solutions (NBS) have gained traction in recent years as there is an awareness to move away from hard infrastructure (sea walls, breakwaters) due to their expensive upkeep and negative environmental impact on the coastal ecosystem. The precise definition of NBS is still up for debate by scholars but the International Union for Conservation of Nature (IUCN) define NBS as:

"actions to protect, sustainably manage, and restore natural or modified ecosystems, that address societal challenges effectively and adaptively, simultaneously providing human well-being and biodiversity benefits" (Cohen-Shacham et al., 2016, p. xii).

Coastal wetlands are underrepresented within the scientific literature in New Zealand. New Zealand literature is skewed towards dunes and beach zone processes. For this reason, the bulk of literature on wetland erosion is sourced from outside of New

Zealand, mainly from Europe or the Gulf of Mexico region. However, the bulk of this literature is focused on grass wetlands (Temmerman *et al.*, 2012; Phillips, 2018; Möller *et al.*, 2014; Leonardi *et al.*, 2018; Cahoon *et al.*, 2018).

The focus of this review is to explain the environmental conditions of wetland formation and species zonation and how external forces are driving environmental change within wetland environments. This review seeks to understand the current literature and identify gaps within the literature to help form research objectives. The review begins with the description of wetlands and coastal wetland geomorphology and salt marsh vegetation zonation. Following this, New Zealand wetlands are classified and Otago coastal wetlands are discussed. Section 2.3 examines the external influences on wetland environments. This section reviews tides; wind and waves; storm surge; wave attenuation and ecosystem energy absorption; coastal eutrophication; sea-level rise; vertical land movement; and atmospheric pressure. Section 2.4 reviews environmental management practicalities such as; coastal resilience; nature-based solutions; hybrid infrastructure; and ecosystem services. To conclude, a summary of findings related to the relevant literature is discussed.

2.2. WETLANDS

Wetlands are diverse and interconnected with the surrounding ecosystem. Wetlands are exposed to climatic, hydrological, bio-geomorphic and development stresses that affect each wetland differently (Enwright *et al.*, 2016; Leonardi *et al.*, 2018; Möller *et al.*, 2014; Scott *et al.*, 2014a; Zhu *et al.*, 2022). The term ‘wetland’ is broad by nature:

*“**Wetlands** is collective term for permanently or temporarily wet areas, shallow water and land-water margins. Wetlands may be fresh, brackish or saline, and are characterised in their natural state by plants and animals that are adapted to living in wet conditions (Environment Council, 1983).”* (Chagué-Goff and Goff, 2003, p. 3).

A wetland is not just a habitat for aquatic and land-based species, they are an essential part of the earth's ecosystem. Wetlands have been referred to as 'nature's supermarket' and the 'kidneys of the landscape' (Mitsch and Gosselink, 2015). The expansive food-chain and rich biodiversity flourishing within the wetland are second to none. Wetlands are similar to kidneys, they filter natural and human waste, stabilize and cleanse the water supply and protect the shoreline.

Wetlands are dynamic over both short and long timescales. Wetlands have the ability to preserve environmental change, such as those resulting from sea level change, cyclones, tsunamis, storm-surges, earthquakes, floods and human activity (Chagué-Goff and Goff, 2003). Studying preservation of climatological events is important for understanding historical climate conditions and how wetland morphology and catchment characteristics have developed through time.

2.2.1. Coastal wetlands

Coastal wetlands are described by way of the interplay of the land, sea, and a period of inundation taking place at the coastline (Scott *et al.*, 2014b). Coastal wetlands, also known as salt marsh, are an intertidal area that is driven in large part by marine tidal cycles. The vertical range of a salt marsh is ruled by way of the tides, which determine the exposure time for marsh vegetation taking place within distinct elevation ranges between mean sea level and the highest tides (Figure 2.1). The tidal range is an important control on salt marshes – tides bring nutrients for estuarine and nearshore species and oxygen for aquatic plant groups and invertebrates (Phillips, 2018). The salt marsh environment is inclusive of intertidal (mudflats), subtidal and supratidal (wet coastal platforms). The hydrological processes of salt marshes are driven by adjacent saline and brackish estuary water as well as the ground water table. Above and below ground exchanges of water are occurring continuously at salt marshes, that is why salt-marshes can be known as a throughflow wetland (Goff *et al.*, 2003). The salinity of a salt marsh is between 5-35%.

Salt marshes are formed in sheltered coastal environments, namely estuaries, coastal lagoons and embayments. The majority of salt marshes were formed in the last 5,000 years, once sea level was relatively stable after periods of tectonic uplift and post-glacial ice sheet loading (Scott *et al.*, 2014b). Salt marshes often occur in areas of low

topography. These are the same areas that humans have colonised and the corresponding degradation of salt marshes through land reclamation for development or agricultural purposes has significantly reduced the area of coastal wetlands globally (Scott *et al.*, 2014b). Salt marshes provide a number of ecosystem services. Firstly, they act as a buffer to wave action and storm surge and provide shoreline stabilisation and erosion control. Secondly, they filter sediments and nutrients from coastal water. Thirdly, they provide a breeding ground for fish, birds and vertebrates. Finally, salt marshes have recreational, cultural and aesthetic value (Goff *et al.*, 2003).

2.2.2. **Coastal wetland geomorphology**

Coastal wetlands are formed at the intersection of the sea and land where low gradient tidal flats have formed due to the decrease in discharge and the ability for sediment to settle.

The interaction between the tidal prism and basin geometry is the first process that initiates wetland development. Limited tidal prisms will give rise to smaller inlet/marsh systems with shallow channels and larger systems developing in relict morphology will tend to have deeper channels (Fagherazzi and Furbish, 2001).

The combination of estuarine morphology and sediment deposition are responsible for tidal flats. However, both processes are defined by the accommodation space of the estuary. Accommodation space is the volume between the estuary bed and the level of high water (Balson, 2000). Changes in sea-level, estuary morphology and sedimentation rates can all impact the accommodation space of an estuary (Muto and Steel, 1997). Vertical or lateral movement of sediment can increase or decrease accommodation space. Rees *et al.* (2000) has shown erosion events that alter the morphology of the estuary system coincide with reduced accommodation space during the Holocene period (Rees *et al.*, 2000). Reduction in the accommodation space means that there is less habitable space for vegetation to establish and therefore saltmarshes cannot form. Madsen *et al.* (2007) illustrated that once accommodation space was available and sedimentation rates were high, morphological change within the estuary environment can occur quickly (Madsen *et al.*, 2007). Furthermore, lateral migration and erosion of the estuary margins will become more common.

The formation of coastal wetlands (salt marsh) is initiated by the accretion of sediment on tidal flats. Sediment is gradually deposited to higher elevations relative to sea level during high tide or flood events. Over time, the rate of inundation decreases which allows for propagules of pioneer species to colonise the exposed sediment. Rates of sediment deposition generally increase as plants colonise the exposed mudflat. Sediment is deposited during inundation events and trapped by plants and their roots systems, effectively building depositional terraces on the tidal mudflat (Johnson and Gerbeaux, 2004; Marani *et al.*, 2011). Sediment trapping and accretion increase the elevation of the marsh which causes there to be a decrease in the depth and duration of inundation. As a result, species that prefer higher elevation and are less salt tolerant inhabit the upper marsh zone and a succession of plant communities develop across the wetland (Cahoon *et al.*, 2018).

Shoreline erosion and sediment transportation and deposition are natural processes. Salt marsh erosion can occur by a number of processes including; wave action which undermine the miniature scarps at the shoreline; foreshore morphology; substrate cohesion; and soil properties and below-ground root biomass (Houttuijn Bloemendaal *et al.*, 2021; Marani *et al.*, 2011; Riddin and Adams, 2021; Wang *et al.*, 2017). Erosion can also be accelerated by crabs (burrowing) and by silt cohesiveness being weakened by the alternation of freshwater and seawater (Johnson and Gerbeaux, 2004). The effect of bioturbation of crabs has been contested. Needham (2011) argues that the interlinking nature of crab hole communities decrease erosion potential (Needham, 2011). Sediment eroded at the shoreline can be uplifted and deposited to areas of higher marsh elevation demonstrating that wetlands are dynamic. The ability to accrete vertically or laterally is fundamental to the survival of wetlands.

2.2.3. Salt marsh vegetation

Salt marsh vegetation develops across three to five marsh zones that are formed along the salt marsh gradient (Bertness and Ewanchuk, 2002; Chirol *et al.*, 2018; Scott *et al.*, 2014b). Using a three-marsh model, the upper marsh makes up roughly 20%, the middle marsh forms the next lowest 20%, and the lower marsh makes up the remaining 60% (Scott *et al.*, 2014b). A conceptual model by Chirol *et al.* (2018) illustrates four marsh zones associated with salt marsh environments and includes the mudflat zone

(Figure 2.1). The boundaries depicted in Figure 2.1 are not representative of marsh structure described by Scott *et al.* (2014). Marsh boundaries are defined by elevation and species occupation, but it is important to remember that these are dynamic environments that experience overlap. The three marsh zones are not strictly defined by the species that inhabit them. Plant tolerance to salinity and water logging are other factors that influence species zonation across marsh zones (Pennings and Callaway, 1992). Species zonation for the lower marsh is dependent on the salinity tolerance of the species, whereas, in the upper marsh, species are excluded by their competitive superiors, meaning the most dominate species thrive (Pennings and Callaway, 1992).

Terrestrial halophytic vegetations begin to colonise between the tidal levels of mean high-water neap (MHWN) and mean high-water spring (MHWS). Species at Pounawea colonise from mean high water (MHW). The limitations of salt marshes can be found where saline influence is so far reduced that halophytes are in the minority (Beeftink, 1977). Marsh elevation is not the only influence in zonation across salt marshes. Pennings *et al.* (2005) discovered a paradigm within regularly flood salt marshes. They discovered that there is an inverse relationship between competitive ability and stress tolerance, meaning that the competitively superior plants occupy the least stressful zones (areas of least inundation), and the competitively inferior plants are displaced to the stressful zones (Pennings *et al.*, 2005). The results of this paradigm were not reflected in salt marshes that were irregularly flooded (Costa *et al.*, 2003).

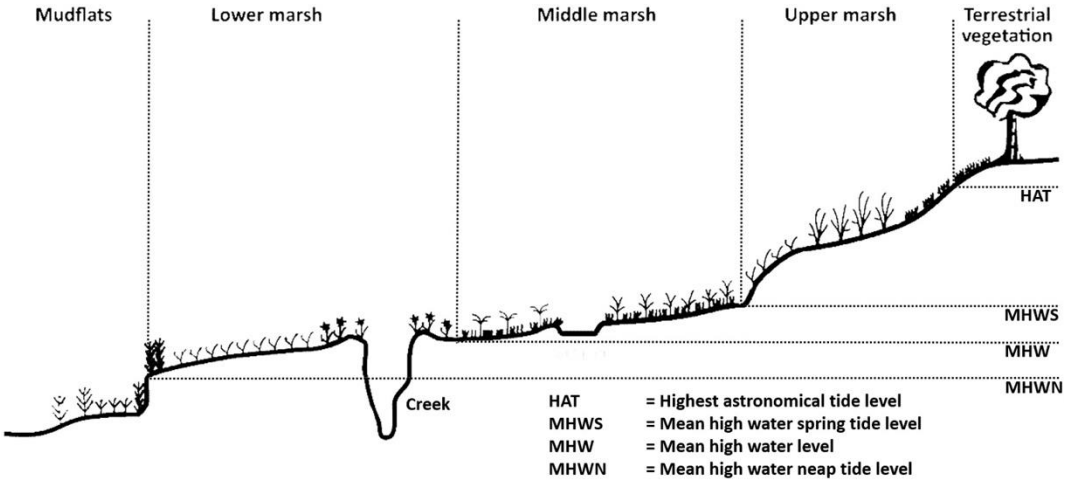

Figure 2.1: Salt marsh vegetation zones and the associated tidal level (Chirol *et al.*, 2018).

Salt marshes typically develop in calm and protected embayments, lagoons and estuaries. These sheltered environments are a defining factor in the establishment of saltmarsh vegetation. For successful seedling establishment there are two requirements. Firstly, there must be a period following inundation where seeds can disperse, strand and anchor. Secondly, there needs to be a period of limited wave exposure, reducing the chances of sediment re-suspension, tidal-flat erosion and seed overtopping (Balke *et al.*, 2015). Tidal-flat elevation, water levels and magnitude of external forces (wave height) are all contributing factors to seedling disturbance and disturbance magnitude (Balke *et al.*, 2014). This concept is called the 'Window of Opportunity'. Spring tides offer more opportunity for seedling dispersal to higher elevations compared to neap tides. Storm surge can provide a disproportionately higher amount of viable seeds but can also be labelled as 'Windows of Risk' as newly established seeds can be eroded at the shoreline margins (Zhu *et al.*, 2022).

2.2.4. New Zealand wetlands

New Zealand's unique climatic and geographical location has enabled a wide range of wetland types to establish and flourish (Figure 2.2, b), however, land reclamation for agriculture has significantly reduced wetland area in New Zealand. Prior to European colonisation, 2,500,000 ha of wetlands existed, roughly 250,000 ha or 10% exist today (Johnson and Gerbeaux, 2004). Draining wetlands for agricultural land reclamation and development are two central causes for the loss of New Zealand wetlands in the last 50 years. The Resource Management Act (1991) acknowledged the importance of these environments and recommended they be protected. Wetland drainage around New Zealand continued following this recommendation. A study by Pompei and Grove (2010) focused on freshwater wetlands in the Canterbury region. This study identified 102 sites that showed substantial (>25%) loss since 1990 (Pompei and Grove, 2010). Loss of wetlands continues today, small wetlands on private land are typically exempt from the rules that protect New Zealand wetlands (Myers *et al.*, 2013). The National Policy Statement for Freshwater Management mandates mapping of small wetlands down to 0.05 ha (Dymond *et al.*, 2021). Mapping wetlands is important to document change, either natural or unnatural.

2.2.5. Wetland classification

The classification of different wetland environments has been a point of argument between ecologists for years. Often described as a halfway world between terrestrial and aquatic environments, wetlands exhibit characteristics of both (Mitsch and Gosselink, 2015). The dynamic nature of wetlands often creates overlap between different wetland types, making it difficult to distinctively classify the wetlands of New Zealand. A wetland classification system created by Johnson & Gerbeaux (2004) details a range of factors that influence wetland morphology and the vegetation around New Zealand (Johnson and Gerbeaux, 2004).

Johnson & Gerbeaux (2004) identify nine environments based on the hydrological and landform setting, salinity and temperature. These nine environments are; marine; estuarine; riverine; lacustrine, palustrine, inland saline, plutonic; geothermal; and nival. The initial classification of these nine environments is not a strictly defined due to the dynamic nature of wetlands (Figure 2.2). The wetland class is made up of nine classes; bog; fen; swamp; marsh; pakihi and gumland; seepage; shallow water; ephemeral wetland; and salt marsh. Once again, these environments have a significant amount of overlap (Figure 2.2). This literature review will focus on the estuarine environment that produces salt marshes.

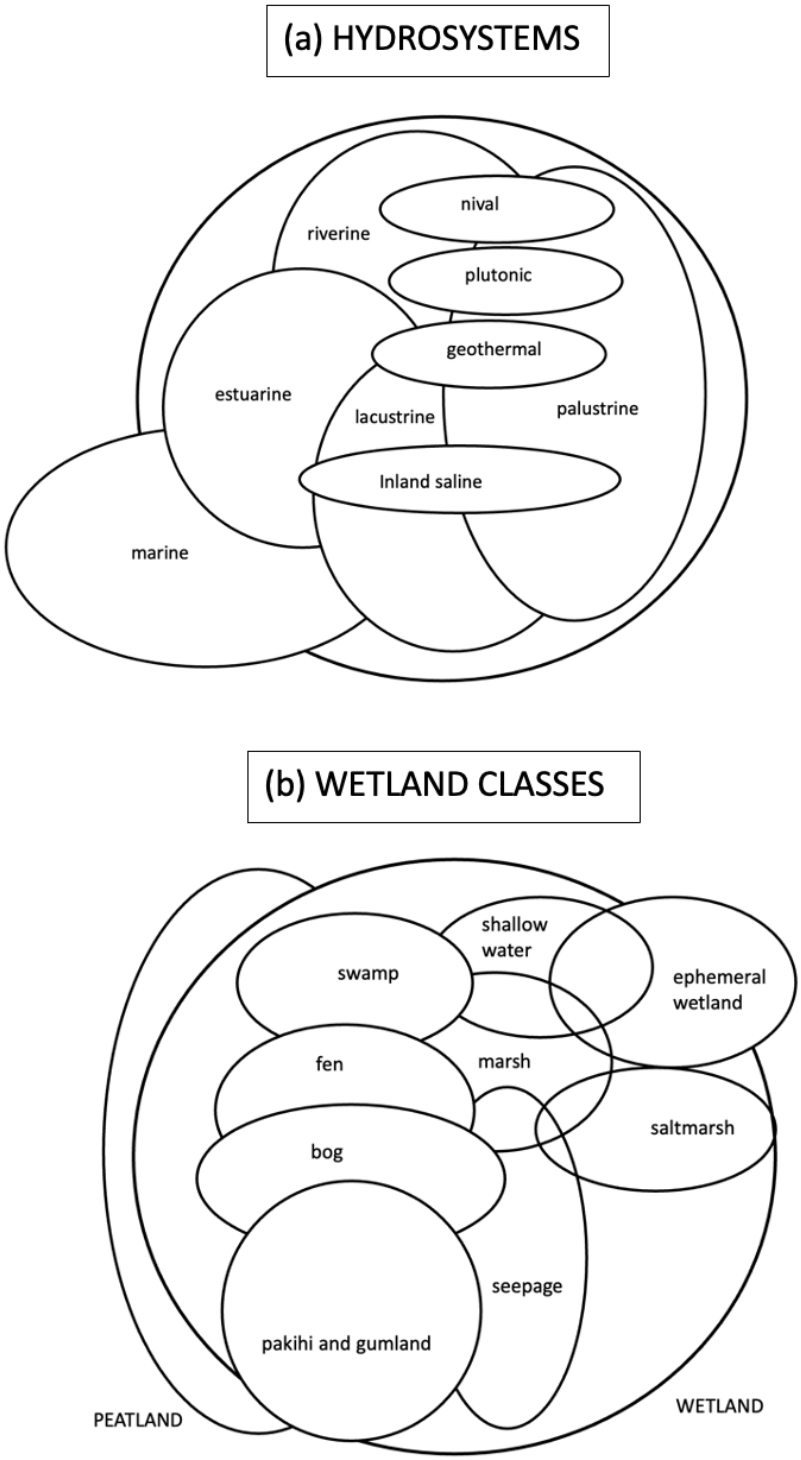

Figure 2.2: (a) Conceptual arrangement of hydrosystems in relation to wetland as represented by the shaded circle; (b) conceptual arrangement of wetland classes, (Johnson & Gerbeaux, 2004).

2.2.6. Otago coastal wetlands

The majority of wetlands in New Zealand were formed after the last glacial period (c. 18,000 years ago) (McGlone, 2009). Coastal wetlands are thought to be younger (5000 years) given their proximity to sediment inputs and erosive processes that both create and destroy wetlands. Otago wetlands are unique due to the absence of two dominant wetland species, *Avicennia marina* subps. *australasica* (mangrove) and *Junus maritimus var. australiensis* (sea rush) (Partridge and Wilson, 1988). The southern boundary of these species can be found north of Otago. The absence of these two species creates a wetland where low-lying herbaceous species dominate the lower and middle marsh areas. Partridge and Wilson (1989) noted that Otago wetland species die back in winter and grow in summer, during the season of highest salinity (Partridge & Wilson, 1989). Pounawea features a salt turf/salt meadow like environment that dominates the lower and middle margins of the wetland.

Salt meadows are formed in the presence of silt and sand flats and are commonly associated with river deltas due to the increase in nutrient enrichment. Salt meadows are found in sheltered environments, the dominant vegetation of salt meadows cannot tolerate high surf surge (Thannheiser and Holland, 1994). Salt meadows are known overseas as 'herbfields' and these environments are generally made up of herbaceous species, low in stature (<5cm tall) and tightly intertwined plant communities (Johnson and Gerbeaux, 2004). Zonation patterns can be found at salt meadows and it is thought that species richness increases as meadow elevation increases (Moeslund *et al.*, 2011). The species zonation pattern at Papatowai (30km south of Pounawea), observed by Thannheiser and Holland (1994) is seen below (Figure 2.3).

The salt meadow found at Pounawea is located adjacent to an estuary where incoming tides and river flows from storms are able to inundate the wetland and the dense carpet of plants is able to stabilize sediment (Thannheiser and Holland, 1994). The Pounawea salt meadow is made up of three dominant halophytic species; *Sarcocornia quinqueflora; Samolus repens var. repens; Selliera radicans* (Figure 2.4). It is these species that form the dense, carpet like marsh that enables silty and sandy sediment to stabilise. The upper marsh is made up of *Apodasmia similis* (jointed wire rush, oioi). Environmental factors such as soil salinity, moisture, nutrient concentrations and inundation frequency can all affect salt meadow species differently even when the elevation range of a salt meadow can be measured in decimetres (Moeslund *et al.*, 2011).

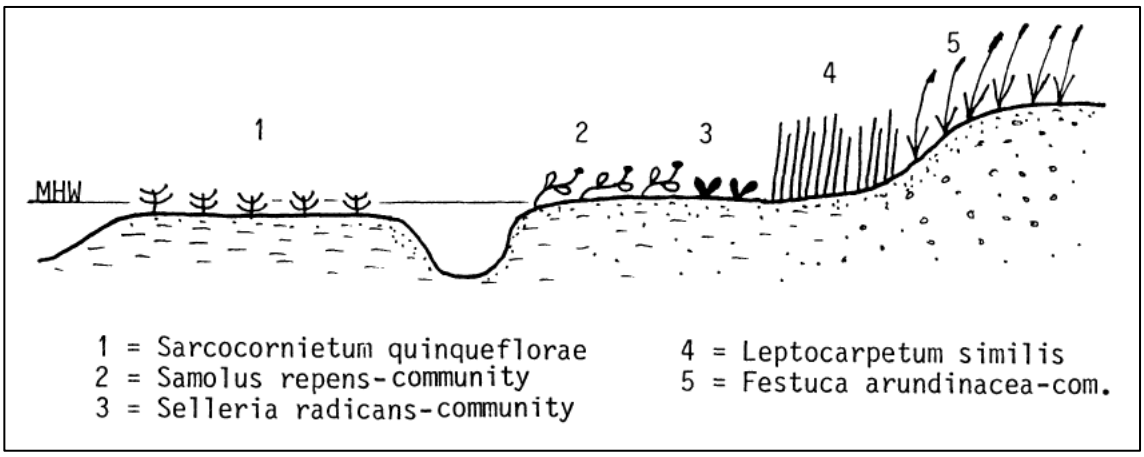

Figure 2.3: Vegetation zonation of the salt meadows near Papatowai (South Island), (Thannheiser and Holland, 1994).

Figure 2.4: Lower and middle marsh vegetation species; *Sarcocornia quinqueflora* (red box)*; Samolus repens var. repens* (blue box)*; Selliera radican*s (yellow box).

One of the issues facing Otago wetlands is the lack of evidence for the on-going rate of habitat loss or rates of erosion in the post-European area (Robertson *et al.*, 2018). The decline of wetlands through Māori and European settlement is well documented and accounts for the vast majority of wetland decline (Robertson, 2016; Ausseil *et al.*, 2011). However, the continual decline of wetlands in some regions is being ignored and reasoning for the decline is not being explored.

2.3. EXTERNAL INFLUENCES ON WETLAND ENVIRONMENTS

2.3.1. Tides

Tides are caused by the gravitational attraction of the solar system bodies (Stephens *et al.*, 2013). The earth's tidal system is influenced by the moon and sun. Tides are semidiurnal and have tidal maximums and minimums that span a 14-day cycle (Pugh and Woodworth, 2014). Tidal maximums occur at spring tide, occurring after new and full moons when the sun and moon are aligned (Figure 2.5). The tidal minimum is neap tides that occur after the first and third quarter of the moon, where the moon and sun are perpendicular to each other (Figure 2.5). Perigean-tides occur once a month when the moon reaches a perigean, its closest approach to earth. The highest perigean-spring tides occur 6-7 months apart, these tides are also known as king-tides and occur when perigean tides align with a full or new moon (NOAA, 2021).

Lunar perigee (super tides, 8.85-year cycle) and regression of the lunar nodes (18.61-year cycle) are both tidal events that increase tidal elevation and inundation (Haigh *et al.*, 2011). The former influences sea level as a quasi-4.4-year cycle (Menéndez and Woodworth, 2010).

Tidal fluctuation in the estuarine hydro system governs the distribution of subtidal, intertidal, and supratidal zones. Tidal reaches of estuaries experience regular alternation of ebb and flood flow, this decreases further upstream (Johnson and Gerbeaux, 2004).

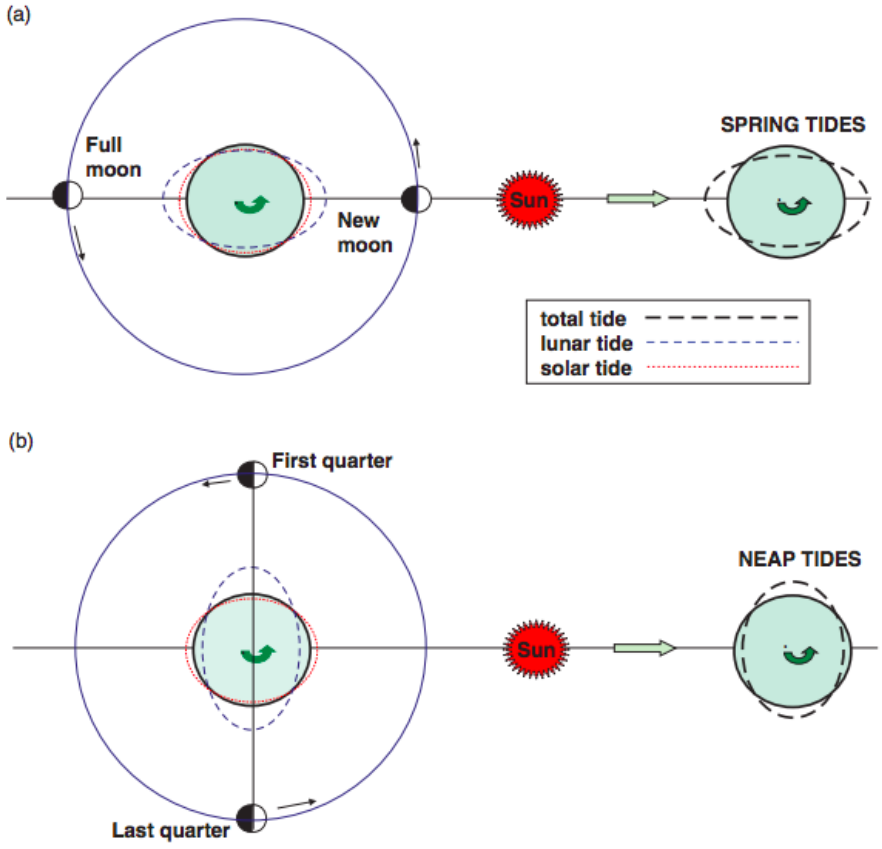

Figure 2.5: Spring-neap tidal cycles are produced by the relative motions of the moon and sun, at 14.8-day intervals. The lunar and solar equilibrium tides combine to produce (a) spring tides and (b) neap tides (Pugh and Woodworth, 2014).

2.3.2. Wind & waves

Salt meadow environments are not usually exposed to the open coast and therefore are not significantly impacted by long-period swell waves. These environments are, however, exposed to local source, fetch limited, wind waves. Karimpour *et al.* (2017) demonstrated that wave growth in shallow estuaries is a function of wind fetch to water depth ratio (Karimpour *et al.*, 2017). Fetch is defined as the unobstructed distance that wind can travel over water in a constant direction (Fagherazzi and Wiberg, 2009). Water depth and the duration of the wind event can impact fetch and wave action. Marani *et al.* (2011) theorised that wind waves and marsh erosion would have a positive linear relationship, Finotello *et al.* (2020) confirmed this theory through observed wave data and historical bathometry change (Finotello *et al.*, 2020). The results stipulated that wind-

induced erosion of the salt marsh margins was reduced when the marsh edge is gently sloping, facing shallow tidal flats and the marsh edge is present in mid-low portions of the upper intertidal zone where halophytes are established (Finotello *et al.*, 2020).

Fetch-limited wind waves of any size can, over long periods of time cause erosion. A study by Leonardi *et al.* (2016) found that the majority of marsh erosion occurred during moderate storms condition with a return period of 2.5 months, violent storms or hurricanes cause <1% of erosion (Leonardi *et al.*, 2016). It is important to note that this study did not focus on salt meadow environments.

Wind waves act in a similar manner to tidal currents, the generated waves exert a bed shear stress which influences the sediment transport regime (Hunt *et al.*, 2015). Sediment can be suspended and uplifted onto the marsh area and settle. At the same time, wind waves can erode the shoreline margins and sediment is transported offshore. Fagherazzi & Wiberg (2009) state that salt marsh platforms located between MSL and MHHW are increasingly affected by fetch, wave height and bottom shear stress, which creates the greatest potential for erosion (Fagherazzi and Wiberg, 2009).

2.3.3. Storm surge

A storm surge is defined as a rise in mean sea level due to the effects of atmospheric pressure, wind and wave set up (Lane *et al.*, 2009; Murty and Flather, 1994). Storm surge can also be influenced by rainfall and the interaction with tidal conditions (Gönnert *et al.*, 2001). The significant hazards associated with storm surges are flooding of low-lying coastal areas and acceleration of shoreline erosion. Nicholls *et al.* (1999) modelled flooding from future storm surges with moderate sea-level rise and coastal population change and predicted that the number of people affected by flooding would increase five-fold by 2080. These predictions assume no change in storm frequency or intensity (Nicholls *et al.*, 1999). Research on how climate change will affect frequency and intensity is not certain. May *et al.* (2013), Walsh *et al.* (2016) and Knutson *et al.* (2010) argue that storm surge frequency will remain constant, whereas, Pye & Blott (2008), Bengtsson *et al.* (2009) and Jiménez *et al.* (2017) believe that frequency of surges will increase due to increasing cyclonic activity, thereby, increasing storm surge incidence and magnitude (Bengtsson *et al.*, 2009; Jiménez *et al.*, 2017; Knutson *et al.*, 2010; May *et al.*, 2013; Oh and Moon, 2012; Pye and Blott, 2008; Walsh *et al.*, 2016).

Bell *et al.* (2000) concluded that return periods for storm surges will increase as a result of SLR as well as estimating the New Zealand wide maximum surge to be one-metre (Bell *et al.*, 2000). The literature is relatively old and this raises some questions about the relatability of the source material. A recent study by Adam *et al*. (2020) illustrated that there was not enough evidence to support a statistically significant increase in the frequency and magnitude of storm surge on the open coast of Southern New Zealand, but, concluded that the one-metre surge maximum proposed by Bell *et al.* (2000) was likely an underestimation (Adam *et al.*, 2020). Significant changes in technology have enabled greater accuracy in predicting storm surge, this would impact the decisions made by governments and communities.

Wetlands are buffers between the land and sea and their effectiveness in wave attenuation is reliant on a number of morphological and vegetation variables. Research by van Loon-Steensma *et al.* (2014) indicated that dense or high vegetation (15-25 cm) is almost as effective as widening the salt marsh by 350 m and plants with low heights (5–15 cm) had no wave dampening effects (van Loon-Steensma *et al.*, 2014). On the contrary, Spencer *et al.* (2016) simulated storm surge conditions in a 310 m long and 5 m wide flume with a 40 m wetland area and tested effectiveness of salt marsh species to attenuate waves. Two of the three species are not common in Otago wetlands but the results highlighted the effectiveness of *Puccinelliua* as a soil stabilizer (Spencer *et al.*, 2016a) and this species is found in South Island wetlands (Thannheiser and Holland, 1994). Rupprecht *et al*. (2017) demonstrated that flexible low-growing plant canopies showed high resilience to storm surge conditions (Rupprecht *et al.*, 2017).

Salt marsh survival is dependent on the rate of shoreline erosion. Leonardi *et al.* (2016) illustrated that the relationship between salt marsh erosion and wave energy remained linear (Leonardi *et al.*, 2016). As wave energy increases the amount of erosion seen at the marsh edge remains linear, there is not a threshold where wave energy can exceed and accelerated marsh erosion occurs. This is contrary to the idea that larger storms are responsible for dramatic increases in coastal erosion. Leonardi *et al.* (2016) explains "*Based on the analysis of two decades of data, we find that violent storms and hurricanes contribute less than 1% to long-term salt marsh erosion rates. In contrast, moderate storms with a return period of 2.5 mo are those causing the most salt marsh deterioration. Therefore salt marshes seem more susceptable to variations in mean wave energy rather than changes in the extremes." (Leonardi et al., 2016, p. 64)*. This concept

is depicted in Figure 2.6 and it can clearly be seen that strong wind events are not the main cause of salt marsh erosion.

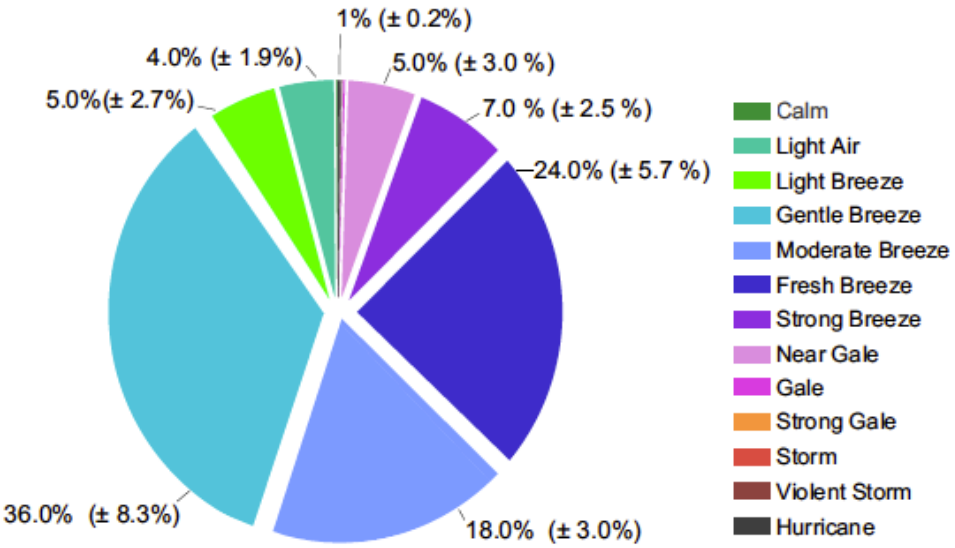

Figure 2.6: Average contribution of different wind categories to salt marsh erosion rates (Leonardi *et al.*, 2016).

2.3.4. Wave attenuation & ecosystem energy absorption

Wave attenuation is the reduction in wave height or energy that occurs as waves pass over coastal habitats (Morris *et al.*, 2018). Wave attenuation at wetlands is achieved through frictional drag introduced by vegetation (Shepard *et al.*, 2011). Coral reefs, mangroves, salt marshes, seagrasses and oyster beds are coastal environments associated with wave attenuation. These provide shoreline and coastal protection from high energy wave events or storm surge. The literature across these coastal environments share the common theme of this review. The ability of the natural coastal environments to protect the coast is widely underdeveloped and underutilised. There has been significant improvement in the last ten years that has illustrated the effect nature-based environments have on wave attenuation at the coast (Arkema *et al.*, 2013; Duarte *et al.*, 2013; Gittman *et al.*, 2017; Himes-Cornell *et al.*, 2018; Möller *et al.*, 2014; Morris *et al.*, 2018; Narayan *et al.*, 2016; Pinsky *et al.*, 2013; Shepard *et al.*, 2011; Slobbe *et al.*, 2012; Sutton-Grier

et al., 2015). The majority of these studies occur in the Gulf of Mexico which is highly prone to hurricanes.

Little work has been done locally in New Zealand on salt marshes even though this environment has been shown to reduce wave attenuation. The protection potential for coastal wetlands was calculated by Manis *et al*. (2015), they showed that wetlands had a 6.9% reduction in wave attenuation initially and 31.4% after one year. Other studies showed 72% reduction in wave height across wetlands (Narayan *et al.*, 2016). Möller *et al.* (2014) conducted a controlled experiment in a 310-metre wave flume tank using a natural section of transplanted salt marsh. The salt marsh was inundated and waves were generated to replicate extreme storm events. The results showed that up to a 60% of observed wave reduction can be attributed to vegetation (Möller *et al.*, 2014). Moreover, the marsh substrate remained stable to surface erosion even when vegetation was eroded or stems broken.

The studies mentioned above were conducted overseas in tussock dominated wetlands. Pounawea Wetland is a salt meadow or herbfield with low vegetation profiles thereby limiting the ability to attenuate waves. A study by Mury *et al.* (2020) used multispectral drone imagery to model the wave attenuation potential of salt meadow communities in France. Observed wave height measured using pressure sensors highlighted two areas where wave attenuation was heightened. These areas being: (1) the marsh edge, the marsh scarp would create a topographical slope change and wave over wash was induced and (2) the upper marsh, where vegetation density and height was at its highest (Mury *et al.*, 2020). The gap in literature related to salt meadow wave attenuation in New Zealand is an area that should be explored in greater depth.

2.3.5. Coastal eutrophication

Eutrophication is defined by Nixon (1995) as ‘an increase in the rate of supply of organic matter to an ecosystem’ (Nixon, 1995). The intensive use of agricultural fertilizers (nitrogen and phosphorus based fertilizers) and nitrate leeching from livestock has seen the rates of coastal eutrophication significantly increase worldwide (Castro and Freitas, 2011). Wetlands have an inherent ability to filter nutrients but increasing eutrophication is compromising this ability, moreover, it is causing salt marsh loss. Results from Deegan *et al.* (2012) showed an increase in the above-ground leaf biomass,

an increased microbial decomposition of organic material, and coastal eutrophication caused the dense, below-ground biomass of bank-stabilizing roots to decrease (Deegan *et al.*, 2012). This compromised the geomorphic stability of the marsh, creek bank erosion occurred and marsh loss ensued. The potential loss of salt marsh area due to increasing coastal eutrophication, driven by increased nutrient loading will impact the ecological function and ecosystem services of the salt marsh environments.

2.3.6. Sea-level rise

Global mean sea-level rise (GMSLR) has increased significantly since the industrialization of the world in the 1800s. The 20th century saw the greatest rise in GMSL in 3000 years (Fox-Kemper *et al.*, 2021). The fastest rise was seen in the Western Pacific from 1993-2018. The main drivers of GMSL rise are ocean thermal expansion and mass lost from glaciers (Alley *et al.*, 2005). These two processes contributed to 38% and 41% of the total change from 1901 to 2018 (Fox-Kemper *et al.*, 2021). The GMSLR for the pre-satellite period (1901-1990) was calculated to be 1.38 mm yr^{-1}, (0.81 to 1.95 mm yr^{-1} highly likely), this increased to 3.25 mm yr^{-1} from 1993-2018 (Nerem *et al.*, 2018).

The use of precision satellite altimeter data has increased the accuracy of the SLR acceleration measurement. Over the last 25 years (1993-2018) the rate of acceleration was estimated to be 0.084 ± 0.025 mm/y^2 (Nerem *et al.*, 2018). This acceleration of SLR aligns with predictions made by the Intergovernmental Panel on Climate Change (IPCC) report (Fox-Kemper *et al.*, 2021). The significance of the acceleration can be summed up by stating that the projected rise of 650 mm by 2100 is double what would be observed if SLR was at a constant rate of 3 mm/yr (Nerem *et al.*, 2018).

The *IPCC* report concluded that GMSL will continue to rise until at least 2100 because the processes driving GMSL are not likely to slow down quick enough to avoid the rise in sea-level that is predicted. A range of shared socioeconomic pathways (SSP) have been used to predict the rate of SLR, currently the world is on track to use SSP2-4.5 (Figure 2.7). The pathways shown in Figure 2.7 are made with medium confidence (66% probability of occurrence), therefore, the confidence bands should be considered when assessing SLR projects (Fox-Kemper *et al.*, 2021).

Sea-level rise around New Zealand was estimated by Hannah (2004) to be 2.1 mm yr^{-1}, the original data estimated an increase of 1.61±0.24 mm yr^{-1} but had not accounted for present-day isostatics-glacial effects (Hannah, 2004). Sea-level rise at Pounawea was reconstructed using foraminiferal analyses and the results showed a considerable increase in the rate of sea-level rise during the 20th century. A slow but steady rise of 0.3±0.3 mm yr^{-1} from AD 1500 to AD 1900, this increased significantly to 2.8±0.5 mm yr^{-1} at the start of the 20th century (Gehrels *et al.*, 2008).

Projecting future sea level is challenging, due to the complexity of many aspects of the climate system. As climate research into past and present sea levels leads to improved computer models, projections have consistently increased. Kulp and Strauss (2019) projected that in low emission scenario, sea level will rise 300 mm by 2050 and 690 mm by 2100, relative to the level in 2000. In a high emission scenario, it will be 340 mm by 2050 and 1110 mm by 2100 (Kulp and Strauss, 2019). The figure below is from the IPPC 2021 Sixth Assessment Report and it illustrates a the predicted global mean sea-level (GMSL) that could occur under a range of emission scenarios (IPCC, 2021a).

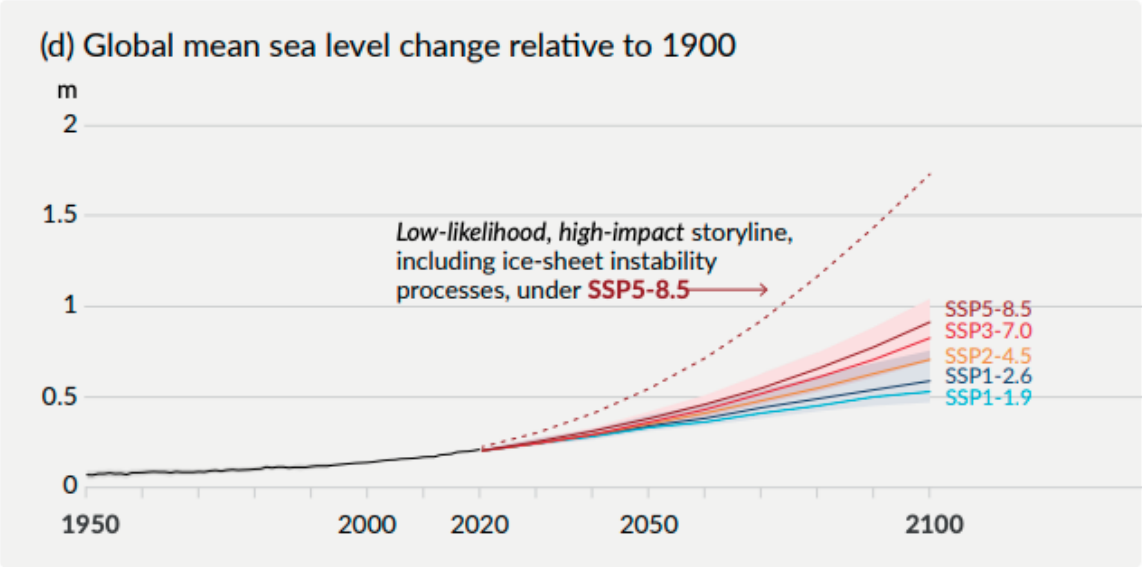

Figure 2.7: IPCC Share Socioeconomic Pathways (SSPs) and their forecasted effect on global sea-level relative to 1900. Figure from the IPCC Summary Report for Policy Makers 2021 (IPCC, 2021b).

Since 1900 there has been a recorded mean sea level (MSL) rise of ~2 mm/yr causing coastal areas to experience storm inundation more frequently (Stephens *et al.*, 2017). In New Zealand, $22 billion worth of coastal infrastructure and 133,265 people live within a 1.5 m elevation of MHWS (Mean Height Water Springs) (MfE, 2017). This highlights the significant risk and potential cost that many New Zealander's and the government will face in the future.

2.3.7. Vertical land movement

Vertical land movement (VLM) influences local sea level. As discussed in section 2.3.6, sea-level around the globe is not consistent and variations in sea-level exist regionally. Movement of the land through tectonic uplift and subsidence, and ice sheet melting causing global isostatic adjustment (GIA) are causes of VLM (Hendtlass *et al.*, 2020). Vertical uplift caused by earthquakes will result in a net decrease in sea-level and subsidence will result in a net increase in sea-level (King *et al.*, 2020). Subsidence is most prominent in low lying areas or deep-seated sedimentary basins or deltas (Hendtlass *et al.*, 2020). Over time sediment compacts causing the land to sink. Subsidence can be exacerbated when water is pumped out of basins for farming, land-use development or agriculture (Hendtlass *et al.*, 2020).

The New Zealand coastline has been mapped for VLM by the *NZ SeaRise: Te Tai Pari O Aotearoa programme*. This programme has calculated vertical land movement for every 2 km of coastline (Figure 2.8). VLM is calculated using global positioning satellite technology and synthetic aperture radar systems mounted on satellites (Envisat and Sentinel) orbiting Earth. Results from VLM calculations have been applied to SLR projections to accurately predict future local sea-level around New Zealand (Denys *et al.*, 2020).

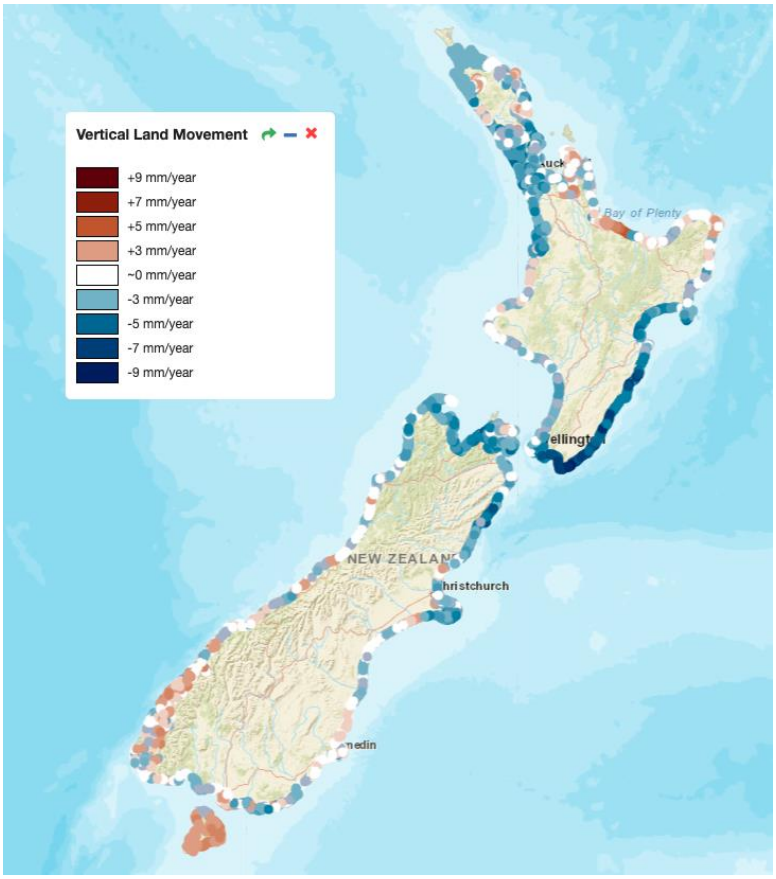

Figure 2.8: Vertical Land Movement (VLM) of New Zealand, calculated by the *NZ SeaRise: Te Tai Pari O Aotearoa programme*. Subsidence represented by the blue areas and uplift by the brown areas (https://searise.takiwa.co/map/6233f47872b8190018373db9/embed).

2.3.8. Atmospheric pressure

The "inverted Barometer effect" relates open coast sea level and surface air pressure (Pugh, 2004). A change in surface air pressure over the ocean results in a change in the sea surface in the amount of 1cm/mbar. If surface air pressure decreases then sea-level increases and vice versa. The nature of this relationship does not alter global sea level averages because water is almost incompressible but it does create opportunities for observed local sea level trends to be influenced by long-term patterns of surface air pressure changes (Church and White, 2006). It is crucial to understand and account for the impact that atmospheric pressure can have on sea-level, especially, when analysing the frequency and magnitude of inundation events on wetland land environments.

2.4. ENVIRONMENTAL MANAGEMENT

2.4.1. Coastal resilience

Resilience can be summed up by Holling (1973) as a "measure of persistence of systems and of their ability to absorb change and disturbance and still maintain the same relationship between population or state variables" (Holling, 1973, p. 2). Coastal resilience encompasses this definition, whether it is sub-tidal, inter-tidal ecosystems or human development that is trying to adapt to changing environments, the goal is the same, to survive and thrive.

Coastal resilience requires an interconnected approach with the natural ecosystem. This is a consistent message throughout the literature, an integrated approach with nature builds community resilience, which can add value to ecosystem services (Arkema et al., 2013; Arkema et al., 2015; Miller et al., 2010; Narayan et al., 2016; Saleh and Weinstein, 2016; Slobbe et al., 2012; Zuniga-Teran et al., 2020). Resilience is constantly developing and setbacks will occur but communities and governments must learn and adapt accordingly.

Wetlands are a naturally resilient environment that have adapted to changes in environmental conditions continuously. Wetlands are resilient in two ways; firstly, wetlands can accrete vertically. This is achieved when plants trap sediment and the elevation of the wetland increases (Traill et al., 2011). Moreover, the stability of the wetlands is reliant on both indirect and direct biotic processes. Indirect biotic process includes, plants trapping sediment through their roots or plant litter trapping sediment on the surface. Direct biotic processes include; surface and subsurface processes. Surface process include the build-up up of decaying organic matter or the formation of living benthic mats (algal, roots), these surface processes can be layered and create vertical accretion whilst also impacting the compaction and erosion potential of the wetland (Cahoon et al., 2006). Subsurface process including root production and decomposition of organic material impact soil volume which influences expansion or subsidence of the subsurface wetland area (Cahoon et al., 2006).

Secondly, wetlands can migrate landwards if they are not able to vertically accrete faster than the rising sea level. Landward migration is becoming more common, however, human encroachment on the coastal environment has limited the ability for wetlands to migrate, this phenomenon is called 'coastal squeeze' (Silva et al., 2020). The resilience of wetlands is further enhanced by the biologically diverse ecosystems that make up wetland environments.

2.4.2. Nature-based solutions

Nature-based solutions (NBS) have the potential to protect coastal wetlands from SLR and storm surge; and simultaneously provide ecosystem services. Reefs (coral & oyster); salt marshes; seagrasses; mangroves; and dunes are a few of the nature-based environments that could be reintroduced to help mitigate SLR and climate change induced coastal hazards. These ecosystems act as a natural barrier (buffer) and dissipate waves to reduce the wave energy that reaches the coastline (Arkema *et al.*, 2013; Seddon *et al.*, 2020). The effectiveness of these environments to dissipate wave energy is dependent on location; the ratio of wave height to water depth; habitat width; vegetation type; age; height; and density (Narayan *et al.*, 2016; Shepard *et al.*, 2011). The ecosystem services provided by these environments include; coastal protection; erosion control; act as natural water filters by removing nutrients from sediment; reducing turbidity; increasing water quality; habitat/nursery environments for fisheries; and support tourism and recreation (Himes-Cornell *et al.*, 2018).

NBS not only increases wave attenuation and coastal protection but these natural ecosystems can act as 'carbon sinks' through carbon capture and sequestration from the atmosphere (Duarte *et al.*, 2013; Himes-Cornell *et al.*, 2018; Vuik *et al.*, 2019). Blue ecosystems such as; seagrasses; salt marshes; mangroves & macroalgae make up 0.2% of the ocean floor but contribute 50% of carbon burial in marine sediments (Duarte *et al.*, 2013), they are hugely important in the wider picture of carbon sequestration. These ecosystems are undervalued for their capacity to work as carbon sinks and offer protection against erosion and SLR. The loss of vegetated coastal habitat is alarming, 25-50% are gone, consequently, the loss of carbon sinks equates to 12-20% of anthropogenic GHG emissions (Duarte *et al.*, 2013).

Nature-based solutions provide the greatest cost/benefit return of any coastal protection strategies, but, long-term studies are required to realise the potential (Duarte *et al.*, 2013; Narayan *et al.*, 2016; Reguero *et al.*, 2018; Temmerman *et al.*, 2013; Turner *et al.*, 2007; Vuik *et al.*, 2019). On average, coastal habitats reduce wave heights between 35% and 71%. Coral reefs reduce wave heights by 70%, salt-marshes by 72%, mangroves by 31% and seagrass/kelp beds by 36% (Narayan *et al.*, 2016). Salt marshes were the most effective at reducing wave height but occur in sheltered environments. Narayan *et al.* (2016) synthesised 52 restoration projects from four coastal habitats and provided a cost-benefit analysis (Table 2.1). The results showed that mangroves and salt marshes were extremely cost-effective, however, they did observe significant differences in the cost of implementation around the world, especially, between Europe and Asia. A cost-benefit analysis (CBA) for the Humber estuary, UK, revealed that after 25 years of tidal marsh restoration on reclaimed land, it is economically more beneficial than maintaining dykes (Turner *et al.*, 2007), similar conclusions were found by Temmerman *et al.* (2013). The CBA (Figure 2.9) highlights the significant benefit of natural infrastructure with respect to the potential for averting costs associated with damages (Reguero *et al.*, 2018).

Dune restoration is a mitigation strategy to protect beaches and development in the dynamic zone. Dune restoration can occur by the removal of invasive species and the planting of native species that will return the dune morphology to a natural state (Hesp and Hilton, 2013). Dune restoration is an ongoing process that sometimes requires continuous replanting of species to maintain the natural morphology of the foredune (Bergin *et al.*, 2007).

Sand spits are a natural protective barrier that can attenuate wave energy and be an effective habitat for birds (Hanley *et al.*, 2014). Sand spits are dynamic and subject to erosion, accretion and movement (Osswald *et al.*, 2019; Robin *et al.*, 2020; Bateman *et al.*, 2020). Sandspit erosion is not uncommon as discussed by Robin *et al.* (2020) and Bateman *et al.* (2020), sand is either transferred offshore, onshore or redistributed within the estuary system.

Costanza *et al.* (1998) estimated the economic value of coastal wetlands in the United States for coastal protection and concluded that coastal wetlands currently provide 23.2 billion dollars per year in storm protection services (Costanza *et al.*, 1998). This value was obtained in the 1990s and it is sure to have increased considerably as research on climate change and SLR has increased. Furthermore, over half of United States salt

marshes (and their associated ecosystem services) have been lost due to direct and indirect human impacts. Human modifications to the coastal zone have resulted in decreased sediment supply to marshes, altered hydrological functioning, and increased subsidence, all of which contribute to marsh loss and decrease coastal protection services (Shepard *et al.*, 2011).

Table 2.1: Cost of coastal protection methods using nature-based solutions (Narayan et al. 2016).

Habitat	Reported Restoration Project Costs^ as US $ Per m^2: Median (Range)	Estimated Replacement Cost Ratios*: Average (*95% CI*)	% of Projects implemented for coastal protection	% of Projects in High Exposure Regions #	% of Projects reporting coastal protection benefits♆
Coral Reefs (*n = 19*)	115.62 (2–7490)	NA	5	80	ER– 5; FL– 5
Oyster Reefs (*n = 4*)	135.63 (107–316)	NA	75	50	NA
Salt-Marshes (*n = 17*)	1.11 (0.01–33)	2 (0.95–3.01)	69	77	ER– 6; FL– 41; ST– 18; BC– 6
Mangroves (*n = 12*)	0.1 (0.05–6.43)	5 (3.1–6.9)	76	35	FL– 50; ST– 34; BC– 41

n = total no. of projects for each habitat type. CI = confidence interval.
^: Project costs not scaled; areas for which costs are reported vary across studies (see S3 Table).
*: Replacement cost ratio = submerged breakwater cost / nature-based defence cost (see Methods).
#: High exposure regions defined as regions with > 10 J/m^2 average annual wave energy based on global deep-water wave climate dataset in [44].
♆: Coastal protection benefit types = ER–savings in erosion damage costs; FL–savings in damages costs from storms; ST–savings in costs of adjacent coastal structures; BC–project benefit / cost ratio > 1.
Note: some projects report multiple benefits (see S3 Table).

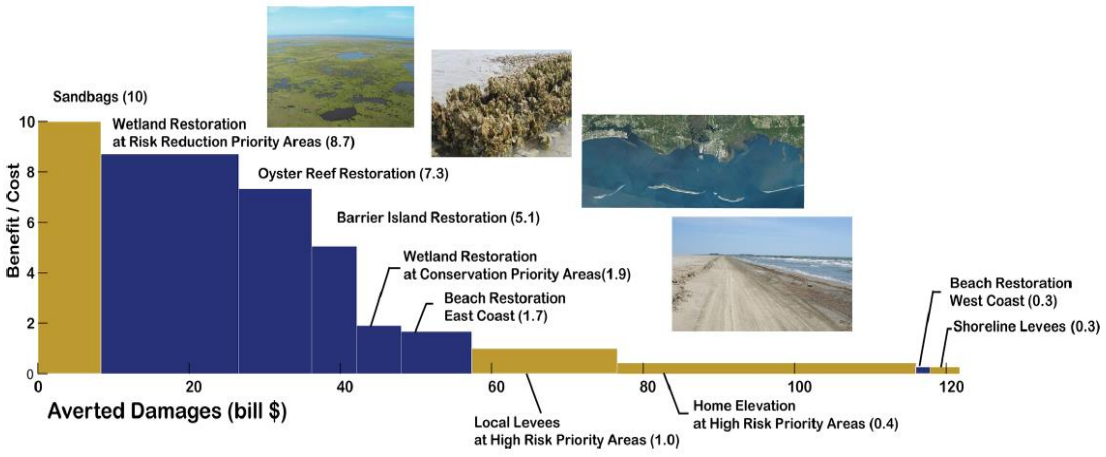

Figure 2.9: Cost-benefit analysis of coastal defence measures. Benefit to cost ratios are represented in the vertical axis and the horizontal axis expresses the aggregated benefit (averted damages), the width of the bars represents the individual benefit from each measure (Reguero et al., 2017).

2.4.3. Hybrid infrastructure

Hybrid infrastructure is a combination of hard and soft engineering, maximising the strengths and minimising the weaknesses of each approach (Sutton-Grier *et al.*, 2015). Nature-based restoration is not suited to all environments, in high energy zones storms can uplift new seedlings, undoing months of planning and planting. Therefore, it can be beneficial to use temporary seawalls to help dissipate wave energy and provide a stable environment for seedlings to lay down roots and build resilience (Figure 2.10). Furthermore, there is also the option for nature-based infrastructure to protect built infrastructure.

Oyster reefs can be artificially constructed and then placed in front of seawalls or dikes to dissipate wave energy, reduce storm surge and enhance ecosystem services (Morris *et al.*, 2018). This could be a practical solution for densely populated urban areas that do not have the space for a full-size nature-based coastal defence. Hybrid infrastructures enable a multi-objective outcome that benefits a range of ecosystem services, whilst not encroaching on urban lifestyle and development (Firth *et al.*, 2016; Miller *et al.*, 2010). The work completed by Firth *et al.* (2016) and Miller *et al.* (2010) suggests a solutions-based approach that understands the urban environment and challenges these areas face. Hybrid infrastructure allows for innovation and adaptation to changing environments without an overhaul of the lifestyle to which humans have become so attached.

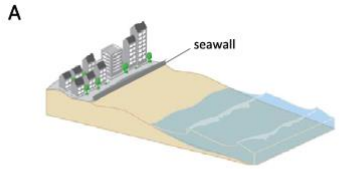

Built defences

strengths

- Ready to withstand storm events as soon as constructed
- Significant expertise, experience, and good state of knowledge on their implementation and functioning

weaknesses

- Does not adapt with changing conditions (e.g. sea level)
- Possible coastal habitat losses
- False sense of security, possibly causing increased damages during storms
- Only provides storm protection benefits, no co-benefits

Natural defences

strengths

- Provides many-co-benefits
- Potential to self-recover after storms
- Can be cheaper
- Potential to adapt changing conditions, and grow stronger in time

weaknesses

- Can take long time before ecosystem is established and ready to provide adequate defence
- Likely require large space
- Growing but still limited expertise in their implementation
- Variable levels of coastal protection depending of the ecosystem, and external forcing, which is possibly difficult to quantify/

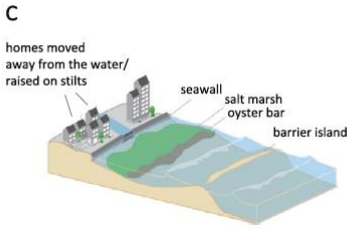

Hybrid defences

strengths

- Provides some co-benefits
- Can provide greater level confidence than natural solutions alone
- Can be used in areas with smaller space than the required for natural solutions alone
- Capitalize best characteristics of built and natural infrastructures

weaknesses

- **Growing but still limited expertise in their implementation**
- Does not provide same benefits than natural systems alone
- Can still have some negative impact on the ecosystem

Figure 2.10: Coastal defence classes, built, natural and hybrid. Strengths and weaknesses are outlined (Sutton-Grier *et al.* 2015).

2.4.4. Coastal armouring - hard infrastructure

Coastal armouring has been the primary method prioritised for coastal protection within New Zealand and around the world. Coastal armouring otherwise known as 'hard' or 'grey' infrastructure has been the method of coastal protection for several decades based on the recommendations from; the Shoreline Protection Manual (CERC, 1984); Coastal Engineering Manual (USACE, 2002); Overtopping Manual (Pullen *et al.*, 2007); and the International Levee Handbook (CIRIA, 2013). Coastal armouring is the physical protection of the coast using built infrastructure such as; seawalls; breakwaters; dikes; and groynes. Armouring is popular in highly urbanised areas, 50% of Sydney harbour is armoured by seawalls and 60% of the Ventura coastline in California has some form of armouring (Firth *et al.*, 2013). The purpose of coastal armouring is to modify hydrodynamic and sedimentary regimes to slow coastal erosion and protect vulnerable areas or to improve recreational conditions (Firth *et al.*, 2013; Schoonees *et al.*, 2019).

Coastal armouring can be dated back to the 13th century but its usage in the 21st century is being called into question (Charlier *et al.*, 2005). Hard infrastructure achieves its functional objective of coastal protection, however, as these structures begin to age and deteriorate, the costs begin to outweigh the benefits. The potential implications of

hard infrastructure include; loss or damage of natural landforms; irreversible coastline modification; aggravation of erosion processes downdrift; and negative visual impact. The financial and ecological impacts of these structures have been scrutinised by academics and the findings illustrate that there needs to be a movement away from hard infrastructure towards a more ecologically friendly solution (Firth *et al.*, 2014; Morris *et al.*, 2018; Schoonees *et al.*, 2019; Slobbe *et al.*, 2012; Stancheva *et al.*, 2011; Temmerman *et al.*, 2013).

2.4.5. Stakeholder involvement and public participation

Stakeholder involvement and public participation are crucial societal elements to the success of nature-based solutions. The key to successful policy implementation is for communities to feel involved, either, in the deliberation process, through contributing ideas, criticism or feedback (Allen *et al.*, 2018; Evans *et al.*, 2017; Gillgren *et al.*, 2018; Jurjonas and Seekamp, 2018; Lawrence *et al.*, 2018). The 21st century has seen vast improvements in technology and globalisation, creating a more integrated world, where values and knowledge can be shared more easily and freely. In the past, stakeholder involvement and public participation were seen as ad-hoc or a public relations necessity, rather than constructive and meaningful engagement with concerned or interested parties (Gillgren *et al.*, 2018). Robust community engagement at both local and national levels is desperately needed for there to be effective management of CC, SLR strategies and coastal protection. Stakeholder engagement builds trust and provides a sense of investment in the future. Without engagement governments and local councils may implement policy without considering the wider community impacts or how the community feels about the policy. This was evident in Franz Joseph after floods blew out embankment ponds and threatened wastewater ponds. Westland District Council quickly approved a solution without proper consultation, businesses and community groups were shocked by the lack of communication and discussion for alternatives (Strong, 2017).

Education and open dialogue between experts, elected officials, planners and the public are what academics believe can drive support for nature-based solutions and sustainable development. Local councils and governments must realise they will need the support of communities if they wish to implement coastal protection strategies. These changes may drastically change the nature of coastal communities both visually and

economically. The processes at the coast are integrated both on land and in the water. This needs to be reflected in the policy creation, implementation, public participation and stakeholder engagement (Arkema *et al.*, 2015; Gillgren *et al.*, 2018; Guerry *et al.*, 2015; Lawrence *et al.*, 2018; Vuik *et al.*, 2019). Stakeholder engagement and public participation are relevant to the wider theme of utilizing nature-based processes to mitigate and protect vulnerable coastal areas from SLR and climate change impacts. The integrated nature of the environment and ecosystem services means that stakeholder engagement and public participation are more valuable than ever before.

2.5. SUMMARY

Wetlands are a critically important part of the natural environment that are under increasing pressure to survive. Increases in sea-level will continue to erode coastal wetlands. These environments are dynamic and highly adaptative, however, coastal development has limited landward transgression of many wetland environments. The need to protect and restore these environments is of critical importance. Research on salt meadow environments in Otago, New Zealand is limited, greater understanding of how low-lying coastal wetlands will adapt to SLR is needed.

Globally, there is a growing recognition for the importance of the natural environment for coastal defense. The expense of hard infrastructure and the negative environmental effects are more frequently being acknowledged and alternative solutions are increasingly sought out. Nature-based solutions provide coastal protection, ecosystem benefits and are cheaper to implement and maintain. Measures to understand wetland erosion and the provide solutions for erosion mitigation are central themes through this review. Pounawea Wetland is a low-lying salt meadow environment that is laterally eroding. Understanding why and how this erosion is occurring and the potential mitigation solutions is the purpose of this thesis.

3. Environmental Change and Morphodynamics of the Pounawea Wetland

3.1. INTRODUCTION

Coastal wetlands are low-lying environments vulnerable to small changes in environmental conditions (Chagué-Goff and Goff, 2003; Spencer *et al.*, 2016b). This chapter aims to document the environmental change and morphodynamics of the Pounawea Wetland. Historic aerial imagery and UAV imagery flown for this study is used to calculate the rate of shoreline erosion from xx to xx. Understanding the spatial and temporal patterns of historic erosion will help predict future shoreline erosion by identifying vulnerable areas susceptible to accelerated erosion and assessing the processes that have resulted in accelerated erosion. This is achieved by using past erosion as an indicator for future erosion, however, future environmental conditions will not be the same. Sea-level is rising and this is going to alter the environmental conditions and morphodynamics of the wetland. Sea-level rise (SLR) will be discussed in chapter 4 & 5. This chapter will focus on past rates of wetland edge erosion, Catlins Estuary morphodynamics and wetland vegetation change.

The Catlins Estuary system has undergone significant land-use change since being colonised by European settlers in the 1860s. The wetland has been eroding since the first aerial image was made available in 1948. If erosion was to continue at its current rate, the lower and middle saltmarsh zones will be eroded by 2150. This chapter will begin with the description of the methods used for this chapter, followed by the results, discussion and conclusion. The methods section below details how erosion was analysed and calculated. The results section provides an over-arching view of environmental change and morphodynamics of the Catlins Estuary. Additionally, the results section discusses historic and current vegetation zonation. The discussion will examine and discuss the findings presented in the results section and identify what is causing the wetland to erode. Finally, a summary of key findings is provided.

3.2. METHODS

3.2.1. Shoreline erosion

Shoreline erosion was analysed using 75 years of aerial imagery. The data was geo-referenced using common landmarks (houses, road intersections) and analysed through Arc GIS™. The aerial imagery was not evenly distributed across the 75-year period, five images span the period 1948–1985 (Table 3.1). Polygon shapefiles of the wetland edge were created for each aerial image. One limitation of this approach was that the time and subsequent tidal cycle was not clear from the images. The effect of shadowing in the upper marsh boundary caused by the podocarp forest was dealt with by attributing the shadowed areas to the forest. Whilst not entirely accurate this method was transferrable to images with poor resolution. Shadows present on the middle and lower marsh were attributed to shrubs and classified in that manner.

Table 3.1: Summary of data sources and date of capture.

Data Type	**Year**
Aerial Photograph	1948
Aerial Photograph	1967
Aerial Photograph	1975
Aerial Photograph	1982
Aerial Photograph	1985
Aerial Photograph	1997
Satellite Imagery	2006
Satellite Imagery	2015
Satellite Imagery	2019
UAV	Nov-21
UAV	Mar-22
UAV	Jun-22

Rates of shoreline erosion were calculated in two ways. The first method involved subtracting the total marsh area (square metres) from the sum of the marsh area of the next aerial photograph and dividing by the number of years between images (Flester and Blum, 2020). This method was applied to Manuka and Cabbage Point and the Pounawea Wetland. The same process was used to calculate vegetation area change. The second method used Digital Shoreline Analysis System (DSAS) version 5.1 to calculate rates of shoreline change (Nagdee *et al.*, 2019). DSAS is an extension tool used through Arc GIS. A baseline was established and polyline shapefiles of each shoreline image were created and used as inputs for the DSAS model. DSAS creates transects perpendicular to the baseline, intersecting each historical shoreline, transects were spaced 5 m apart (Himmelstoss *et al.*, 2018). Statistical outputs were calculated using a 95% confidence interval. Linear Regression Rate (LRR) was chosen as the primary output parameter. LRR uses all data points, irrespective of changes in accuracy or trend, the method is purely computational and easy to deploy (Himmelstoss *et al.*, 2018). DSAS is susceptable to outlier effects but historical shorelines at Pounawea are uniform meaning that shoreline erosion has occurred periodically. Net Shoreline Movement (NSM) was also computed by calculating the distance between the oldest and youngest shoreline profiles (Himmelstoss *et al.*, 2018).

Beta Shoreline Forecasting uses historical shoreline position data and the Kalman filter (Kalman, 1960) to forecast shoreline position. The use of model-derived position and shoreline historical positions was developed by (Long and Plant, 2012). DSAS was created for shoreline beach environments and incorporates two assumptions; (1) the beach is a littoral cell; and (2) processes responsible for change are linear and have be relatively constant through time (Fenster *et al.*, 1993; Nagdee *et al.*, 2019). DSAS has been successfully used to map wetland erosion (Baral *et al.*, 2018; Kuleli *et al.*, 2011; Yan *et al.*, 2021), however, unlike overseas literature the Pounawea Wetland is not parallel to the coast. There are a number of spatial, hydrodynamic and environmental processes that underpin wetland morphodynamics that may not be included in the DSAS tool. DSAS outputs should be treated carefully and used as a tool to infer conclusions rather than a definitive proof of erosion.

Internal erosion was not included in the calculations of total eroded area (Table 3.4). Poor image resolution meant it was difficult to accurately represent these features. Elsewhere, it is acknowledged that internal erosion would impact the morphology of the wetland (Ganju *et al.*, 2015).

3.2.2. Surveying

Surveying was largely completed using a ground controlled Unmanned Aerial Vehicle (UAV) and specific shoreline profiles that were deemed to be strategic. The UAV allowed for aerial observations and imagery to be captured during desirable conditions. Shoreline profiles and wetland morphological features were recorded using highly accurate instrumentation explained below.

Real-Time Kinematic Global Positioning Systems

Real-time kinematic global positioning systems (RTK-GPS) are widely used in coastal surveying and topographical mapping. RTK-GPS are highly precise and relatively inexpensive compared to LiDAR surveys, allowing for land-based surveys to be repeated and completed without significant preparation or cost (Lee *et al.*, 2013). RTK-GPS comprises of a base station (stationary) and rover (portable GPS). The rover relays the surveyed coordinates via a signal relative to the base station. The base station is set up over a known vertical datum (Figure 3.1, b) that was installed and surveyed in 2020 relative to an established vertical datum set up by Land Information New Zealand (LINZ). The RTK-GPS has a vertical accuracy of 2 mm and a horizontal accuracy of 4–9 cm (Lee *et al.*, 2013). This level of accuracy was used to measure the ground control points (GCPs), transect profiles and areas of interest.

Ground Control Points

GCPs are used in conjunction with the UAV to accurately measure the topography of the survey area. Each GCP represents a known location and elevation measured using the RTK-GPS to a vertical accuracy of 2 mm. GCPs are used because the internal GPS of the UAV is not accurate enough to map the small changes in surface elevation. The RTK-GPS measures the x, y, z co-ordinates of each GCP and this information is later

inputted in Pix4D to form the digital elevation model (DEM) and orthomosiac images. Black and white tiles were used as GCPs, these were spread out across the wetland in a grid like pattern ~ 20 m apart (Figure 3.1, a). GCPs were placed outside of the desired survey area to ensure accuracy, the podocarp forest restricted the ability to widen the survey margins. GCPs were placed in areas of varying height (-0.5–0.95 m) to ensure greater vertical accuracy (Martínez-Carricondo *et al.*, 2018).

Unmanned Aerial Vehicle

A DJI Phantom-4 Pro V2 UAV was used to capture overlapping vertical images and orthophotographs. The overlapping images (75% overlap) were inputted into Pix4D and digital elevation models were created. DEMs are used to display the morphology of a landscape, the temporal change over time and to extract profiles. A digital surface model (DSM) is created by using the elevation of the surface, including vegetation (Hugenholtz et al., 2013; Jaud et al., 2016). A DEM refers to a grid-based representation of topography built by the interpolation of topographic points on a regular grid (Jaud et al., 2016). The survey points (GCPs) and their x,y,z co-ordinates are imported into ArcGIS and then converted to a DEM (Moloney et al., 2018). The survey area took 20 minutes to fly at 55 m and 35 m elevation and each survey produced ~450 images. Technical issues with the UAV meant the November 2021 flight did not go ahead as planned. Flights in March and June were successful and the outputs are used in this chapter.

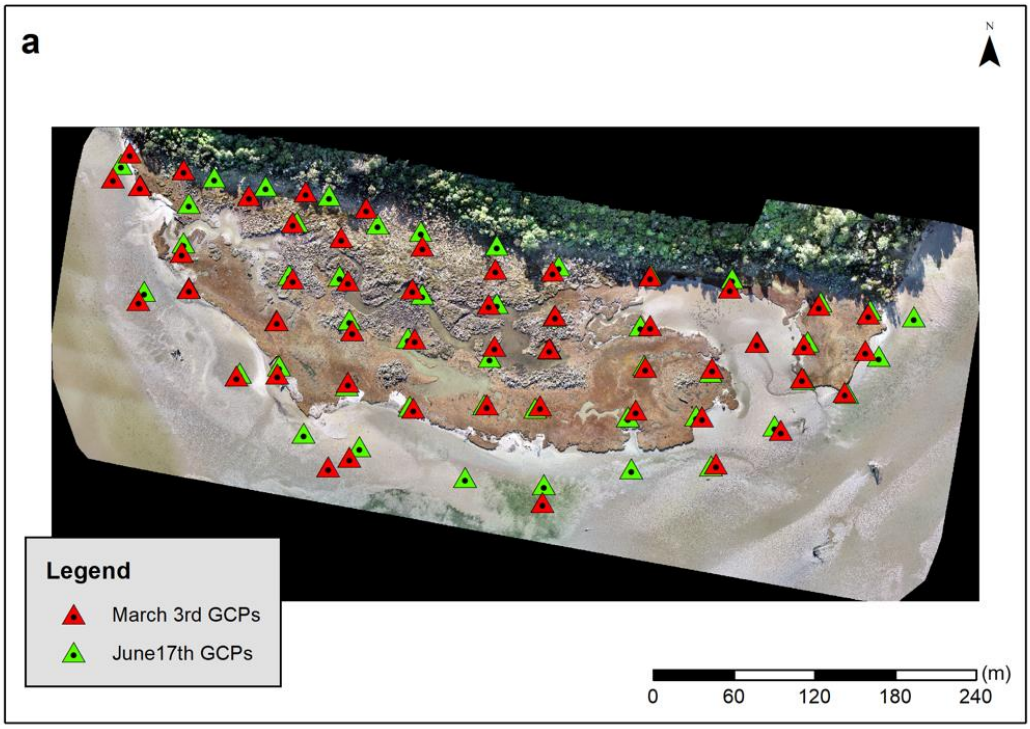

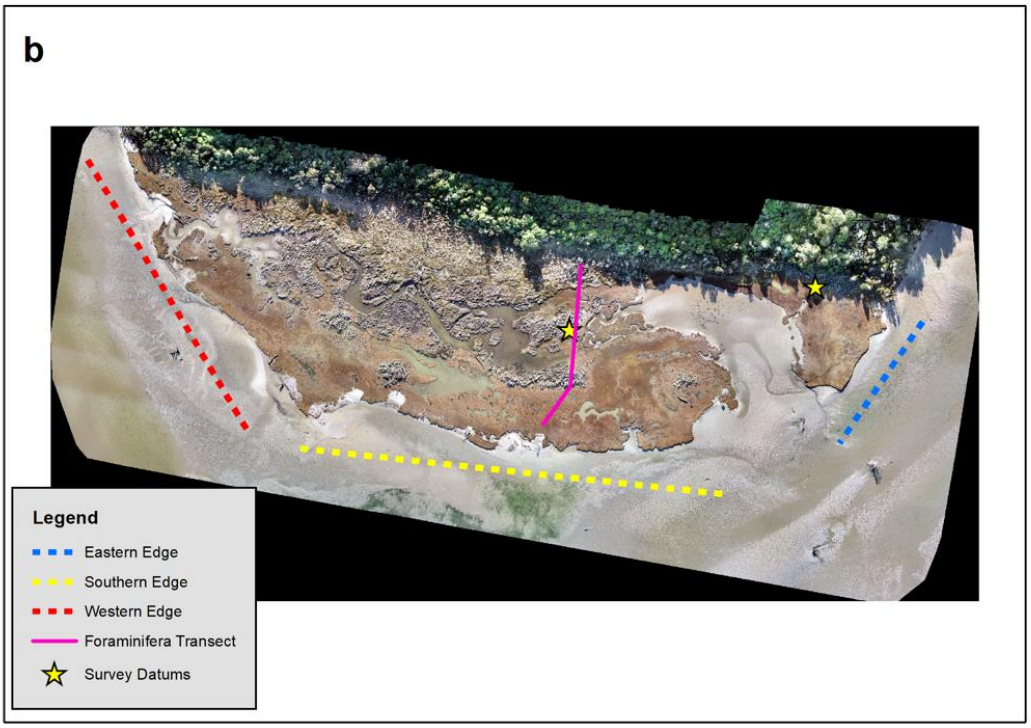

Figure 3.1: (a) GCP layout for March 3rd and June 17th UAV flights; (b) Survey datums used for all RTK base station locations and the survey transect (pink) used by Southall *et al*. (2006). Dashed lines represent the sections of the wetland shoreline that will be discussed throughout this thesis; blue - eastern edge; yellow - southern edge; red - western edge.

3.3. WETLAND ELEVATION AND TOPGRAPHY

Pounawea Wetland is a low-lying and gently sloping wetland with three distinct vegetation zones. The wetland is gently sloping, increasing by ~0.1 m across the wetland. This elevation change is not inclusive of the transition from intertidal sand flat to the wetland. The elevation of the shoreline edge varies around the wetland therefore the elevation change from the intertidal sandflats to marsh edge can be between 0.3–0.7 m (Figure 3.4, Figure 3.5, Figure 3.6).

The topography of the wetland is mostly flat with areas of undulation, depressions and raised mounds (Figure 3.3). Another prominent feature are the internal erosion pools that are spread across the wetland reaching depths of 0.1–0.4 m. These pools are illustrated using the orange arrows (Figure 3.4, Figure 3.5 and Figure 3.6). The potential cause of these pools will be discussed in section 3.8.2. These three elevation profiles illustrate the significant rise in elevation from the intertidal sandflats to the wetland. Transect sites were chosen because they extend across different morphologies. The location of each profile (Figure 3.4, Figure 3.5, Figure 3.6) on the wetland is depicted in Figure 3.2.

Figure 3.2: Location of profile transects at Pounawea Wetland, transect 1 left, transect 2 centre, transect 3 right. Image captured on 3rd March 2022 by the UAV.

The DEM (Figure 3.3) highlights the morphology of the wetland, depicting a flat surface south of the creek, there is ~0.2 m of elevation variability south of the creek. North of the creek, taller vegetation is present, the DEM clearly identifies this area (white area, transect 1 & 2), it is worth noting that the DEM is recording the top of the vegetation rather than the ground surface. The shoreline edge of the wetland is slightly raised in the DEM and this is confirmed in the transect profiles.

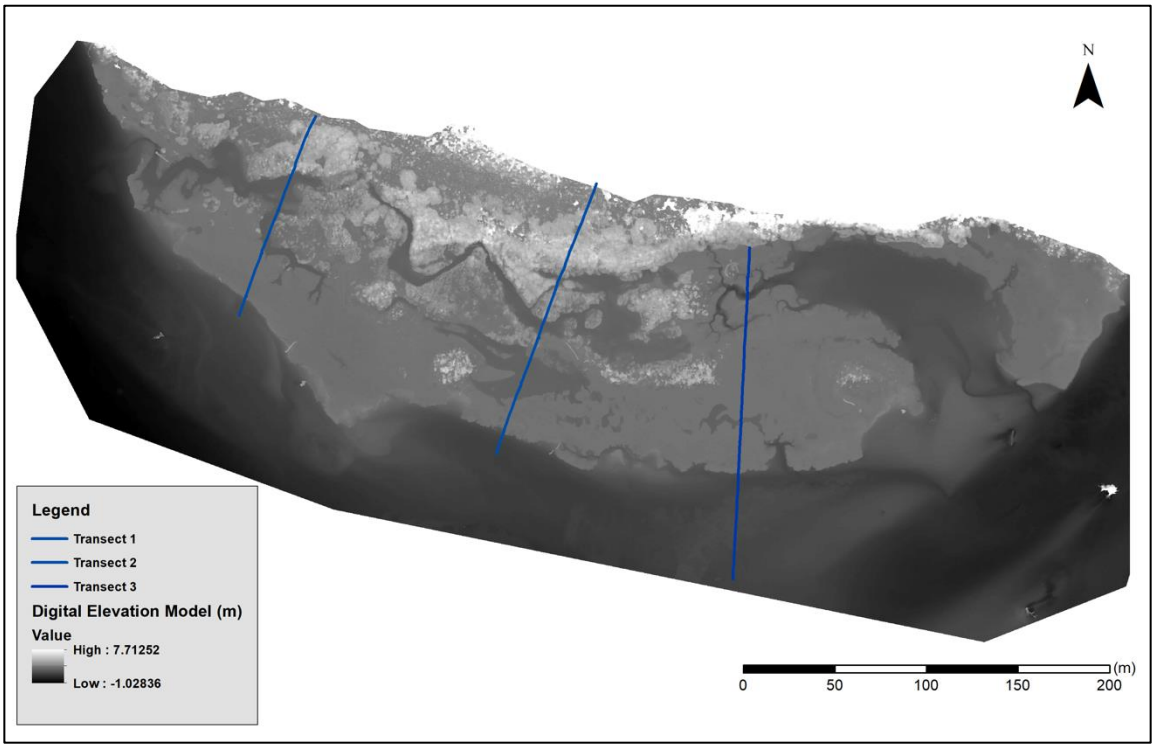

Figure 3.3: DEM of Pounawea Wetland, transects 1, 2 & 3 are included. The DEM has been clipped in Arc GIS to remove the podocarp forest to reduce the vertical height scale.

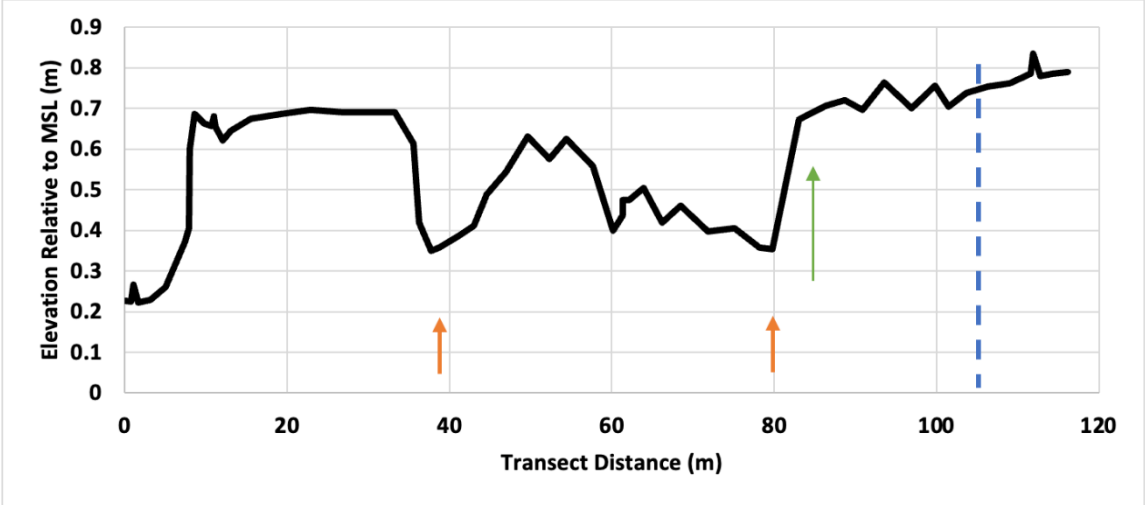

Figure 3.4: Profile of transect 1, moving from seaward edge to the podocarp forest. Orange arrows: depressions; green arrow: zone 2 & 3 boundary; blue dashed line: 1948 podocarp forest boundary

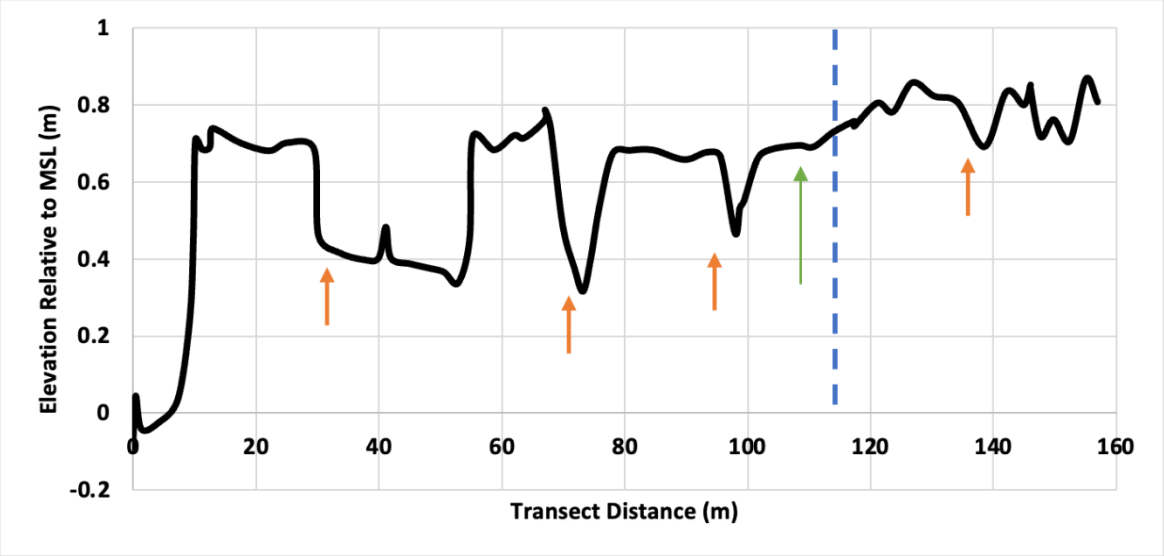

Figure 3.5: Profile of transect 2, moving from seaward edge to the podocarp forest. Orange arrows: depressions; green arrow: zone 2 & 3 boundary; blue dashed line: 1948 podocarp forest boundary

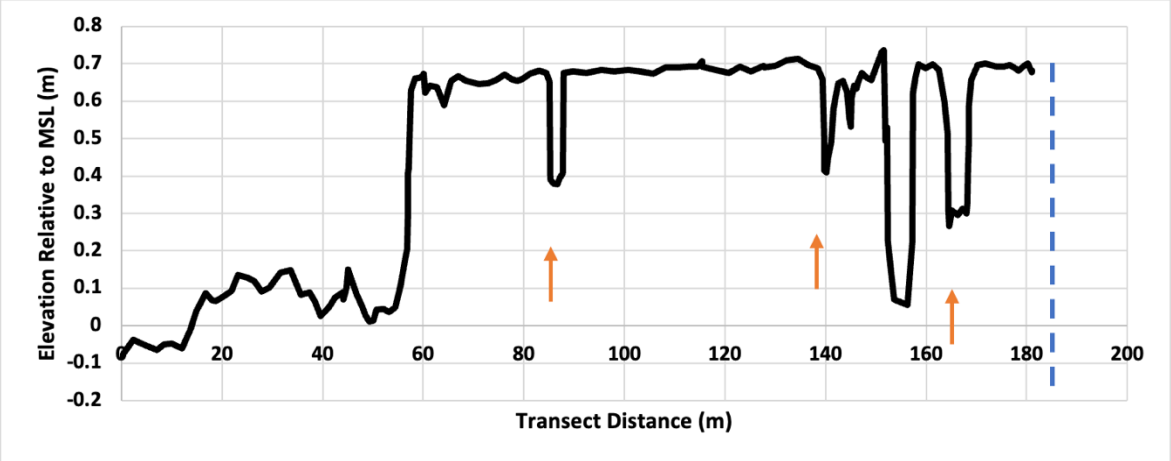

Figure 3.6: Profile of transect 3, seaward edge to the start of zone 2 at the back of the salt marsh. Orange arrows: depressions; blue dashed line: 1948 podocarp forest boundary

3.4. WETLAND STRATIGRAPHY

The wetland is at least late Holocene in age and the tectonic stability of the region is of interest because it indicates whether the wetland has been uplifted faster or slower than SLR. The subduction of the Australian Plate underneath the Pacific Plate has caused vertical land movement (VLM) and subsidence across New Zealand (King *et al.*, 2020). The stratigraphy described by Hayward *et al.* (2007) does not suggest VLM in the last one thousand years (Hayward *et al.*, 2007). Several studies undertaken at or including Pounawea discuss the historical sea-level. These studies focused on the use of live and dead foraminifera to reconstruct late Holocene sea-level (Gehrels *et al.*, 2008; Hayward *et al.*, 2007; Southall *et al.*, 2006). However, recent work by King *et al.* (2021) proposes that the acceleration of sea-level rise from 0.3 ± 0.3 mm/yr (AD 1500–1900) to 2.8 ± 0.5 mm/yr (1900-present) may have been influenced by VLM that was not picked up by Gehrels *et al.* (2008) or Southall *et al.* (2006). The influence of VLM will be discussed in the next chapter.

The stratigraphy of the Pounawea Wetland was analysed by Gehrels *et al.* (2008) from a single transect through the wetland (Figure 3.1, b). The results indicate 300 mm of silty peat underlaid by 100 mm of organic silt. Below these layers are sands that contain foraminifera; *Ammonia* spp.; *Elphidium* spp.; *Trochammina inflata* and *Cibicides marlboroughensis* (Figure 3.7) (Hayward *et al.*, 2007). These species can be associated with a high-intertidal sandflat environment. Further analysis of the sediment cores dated a *Paphies australis* shell and an *Anstrovenus stutchburyi* shell to an age of 1665 ± 48 ^{14}C yr BP and 3756 ± 36 ^{14}C yr BP respectively. Both shells were found in the sand environment, leading Gehrels *et al.* (2008) to conclude that the Late Holocene sea level in this area was -0.2 ± 0.2 m (Gehrels *et al.*, 2008). Furthermore, three ^{14}C dates acquired from a detrital plant fragment found at 0.39 m depth provided an average age of the wetland of 413 ± 23 ^{14}C yr BP (Gehrels *et al.*, 2008). The age of the wetland is not something that is easily defined but through the work of Gehrels *et al.* (2008) it is likely that the wetland is at least 400 years old.

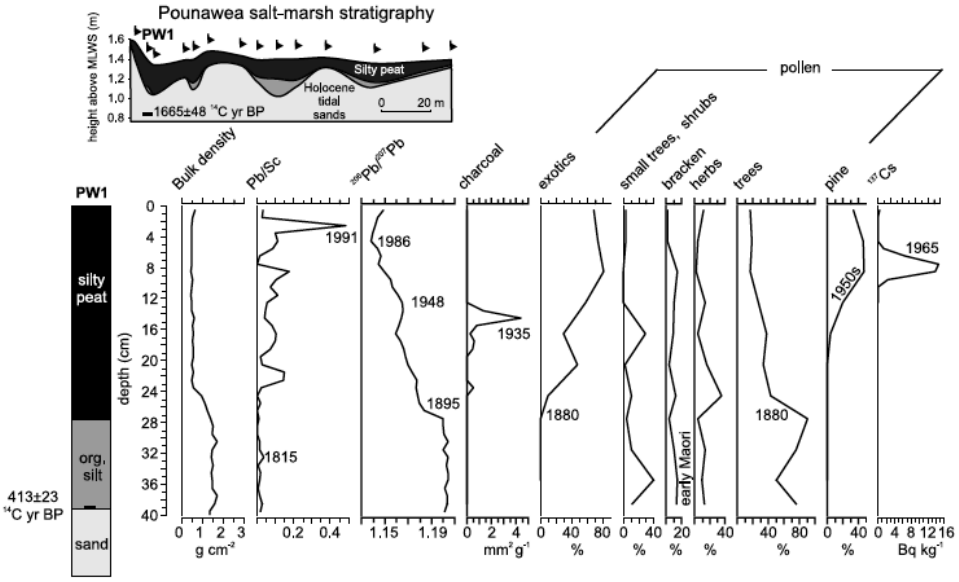

Figure 3.7: Litho-and chronostratigraphy of Pounawea salt marsh (Gehrels *et al.*, 2008).

3.5. VEGETATION AND SPECIES ZONATION

Otago salt meadow/marsh communities have been studied and classified by other academics (Partridge and Wilson, 1988; Southall *et al.*, 2006; Thannheiser and Holland, 1994). This section uses a modified version of these classifications. Three classification zones have been used for this section instead of the four used by Southall *et al.* (2006).

The native podocarp-Broadleaf forest consisting of matai (*Prumnopitys taxifolia*), miro (*Prumnopits ferruginea*), totara (*Podocarpis totara*), kahikatea (*Dacrycarpus dacrdioides*) and rimu (*Dacrydium cupressinum*) (Stevens and Robertson 2017) mark the upper boundary of the Pounawea Wetland and is labelled 'podocarp forest or zone 1. This forest is a remanent of what was once a common sight before the logging industry was established in the Catlins (Wilson, 1993). The second classification zone labelled 'shrubs or zone 2' is comprised of *Coprosma propinqua, Plagianthus divaricatus* (ribbonwood), *Leptocarpus similis* (jointed wire rush/oioi), *Phormium tenax* (flax), *Leptospermum scoparium* (mānuka) and *Agrostis stolonifera*. This zone consists of all species that are not featured in the podocarp forest or are herbaceous species. The third zone labelled 'salt meadow/marsh or zone 3' comprises of all small herbaceous vegetation, primarily, *Selliera radicans, Samolus repens* (sea primrose), *Sarcocornia quinqueflora* (beaded glasswort).

These three vegetation zones occupy the Pounawea Wetland. The spatial boundaries of the zones have changed since the first aerial photograph in 1948. Species migration and erosion of the shoreline margin have all contributed to the evolving wetland environment that is present today.

Wetland elevation and gradient change is a determinant in species zonation (Moeslund *et al.*, 2011; Partridge and Wilson, 1988; Thannheiser and Holland, 1994). Transect 1 & 2 extend across all three vegetation zones whereas transect 3 ends before the podocarp forest. An increase in the slope of the wetland, signalling the transition from the salt meadow zone to the shrub zone, indicated by the green arrows in Figure 3.4 & Figure 3.5. This slope increase is not seen in Figure 3.6 because the transect ends at zone 2, instead, it very gradually rises from 0.629 m to 0.681 m, an increase of 0.052 m across 180 m (the slope increase excludes the significant increase seen at the scarp edge). The overall slope increases for Figure 3.4 is 0.19 m over a 116 m transect. The slope increases of Figure 3.5 is 0.098 m across a 157 m transect.

The rollback of the podocarp forest likely enabled lower and middle marsh transgression. The movement of the podocarp forest boundary since 1948 is shown below (Figure 3.8). Since the boundary change of the podocarp forest, species from zone two have colonised this new habitat. On the northern side of the creek *Leptocarpus similis* and *Phormium tenax* are found. This area can be seen in Figure 3.2 as the dark brown/charcoal area that expands east and west parallel to the creek, alternatively, the 1948 podocarp forest boundary runs right through this area of flax and oioi (Figure 3.8). The podocarp boundary receded a maximum of 56 m at the south face of the wetland and only 17 m at the east and 10 m at the west edges (Figure 3.8). Interestingly, the western and eastern sides receded further than the south facing edge between 1985–2022. During the same period the south podocarp boundary receded ~0–2 m. The initial recession at the southern margin from 1948–1985 changed rapidly, between 30–56 m. Initially, the western and eastern edges did not recede at the same rate, but are now aligned with the southern margin.

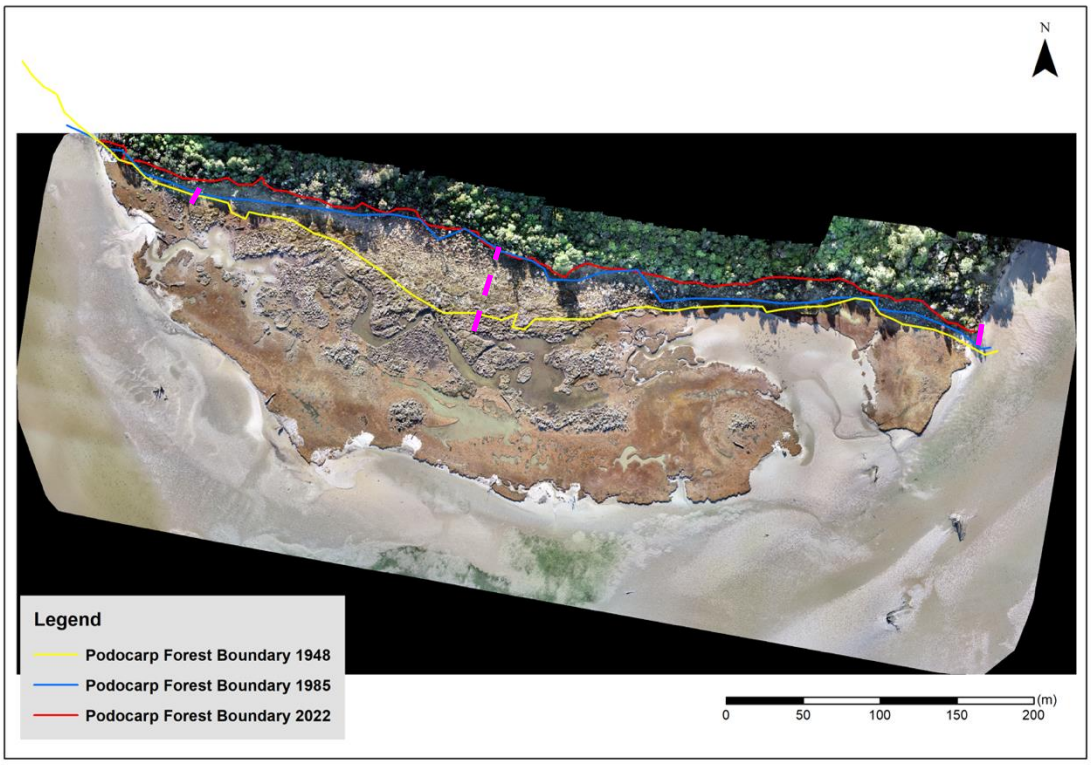

Figure 3.8: Historical podocarp forest boundary, 1948–2022, purple lines illustrate where distance measurements were taken.

The lower marsh zone has been subject to erosion and boundary changes. The migration, erosion and development of zone 2 is illustrated in Figure 3.9. In 1948, shrubs dominated the southern marsh edge, spanning a length of 260 m and a width of 50 m at its widest (Appendix A, Figure A1). This zone may have included *Spartina anglica* before its removal. A contributing factor to the shoreline erosion could have been the spray program undertaken by the Department of Conservation to eradicate *Spartina anglica* from the wetland. An area of shrubs found at the eastern edge side of the wetland (before the inlet arm) has been documented to have increased in size between 1948–1985 then decreased between 1985–2022. The last seven years (2015–2022) the area has reduced significantly, vegetation has retreated towards the centre of the established community. Four areas have remained relatively stable over the 75 years of aerial imagery (Figure 3.10). Three of these areas display an increase in vegetation cover between 1945–1985, the areas then decrease and are now smaller than in 1945, except one. The vegetation appears to have receded inwards and towards the centre of the 1945 vegetation outlines. The plant community furthest right in Figure 3.10 has become sparse.

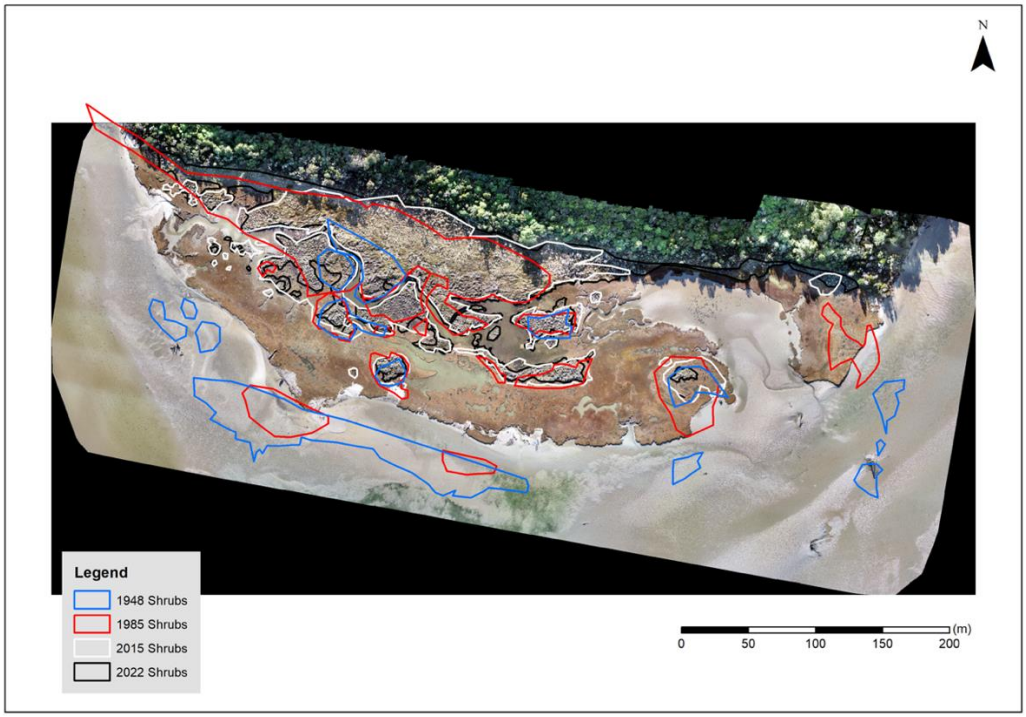

Figure 3.9: Shrub zone plant communities. Plant communities were outlined using historical imagery and Arc GIS, 1948 & 1985 boundaries are not perfect representations of the boundary of shrub zonation, poor image resolution made it difficult to precisely define the margins.

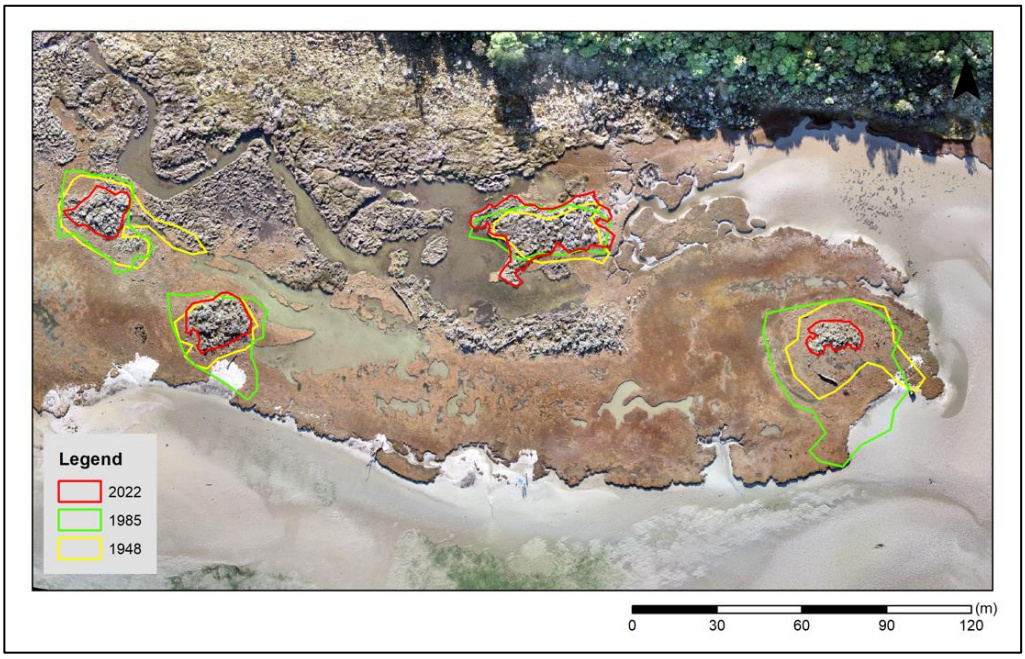

Figure 3.10: Close up of shrub vegetation movement from 1948–2022.

Salt marsh vegetation has not been mapped in any of the figures displayed. This is because all areas that are not zone 1 or zone 2 are considered salt marsh. Area's not outlined in Figure 3.8 and Figure 3.9 are considered to be zone 3 - salt marsh (land-locked erosion, creek and inlet entrance are excluded). The three dominant species are *Selliera radicans, Samolus repens* (sea primrose), *Sarcocornia quinqueflora* (beaded glasswort). *Puccinellia stricta* and *Suaeda novae-zelandiae* and other herbaceous species are found in the lower marsh but are less prominent. Southall *et al.* (2006) observed the lowest elevations of the salt marsh were inhabited by *S. repens & S. quinqueflora* and *S. radicans and S. repens* occupied the intermediate elevations (Southall *et al.*, 2006). Field work confirmed the zonation of Southall *et al.* (2006) to be accurate. *S. radicans* was not found at the marsh edge or at any depressions or the margins of eroded areas. *S. radicans* can be seen in Figure 3.2 as the bright green surface of the salt marsh. At the marsh edge there is a light brown tinge to the UAV orthomosaics, this is an entanglement of *S. repens and S. quinqueflora*. These two species can be found in wetland depression or the shoreline edge. An area dominated by *S. radicans* and at least 20 metres away from the marsh edge *S. repens* and *S.quinqueflora* are observed (Figure 3.11). It is difficult to see from the image but this area is a depression. It is unclear when or how the depression was formed but these are common across the wetland. Partridge & Wilson (1988) noted that in areas of *Sacocornia quinqueflora*, surface firmness is lacking (Partridge and Wilson, 1988). Through ground observations it was noted that *S. quinqueflora* felt spongey comparative to the firm carpet feel of *S. radicans*. There are dozens of depressional areas and parts of the wetland that are starting to erode from within (Figure 3.11). These areas will continue to erode and the damage to the wetland may become significant.

Species zonation is constantly adapting, the threats of shoreline erosion and inundation will significantly impact salt marsh vegetation. Shrub vegetation appears to be resilient, the landward boundary change has reduced the risk of inundation and mortality. Similarly, salt marsh vegetation has taken this opportunity to establish in areas formerly occupied by shrub vegetation. Shoreline erosion and inundation are the most prominent risks to all vegetation species of the wetland. The frequency and subsequent consequences of wetland inundation will be outlined and discussed in chapter 5. Shoreline and land-locked erosion will eventually collide and the loss of salt marsh vegetation could be extensive.

Figure 3.11: *S. repens* and *S. quinqueflora* inhabiting a depressional zone surrounded by *S. radicans*. Photo is looking south and was taken on the 18th March 2022.

3.6. CATLINS ESTUARY CATCHMENT CHARACTERISTICS

The Catlins Estuary is a large (830 ha), mesotidal (1.76 m spring tidal range), shallow (mean depth ~1–2 m at high tide), tidal lagoon type estuary (Stevens and Robertson 2017). The estuary is fed by two freshwater rivers, the Catlins and Owaka Rivers. The estuary is a single tidal entrance channel featuring a bar at high tide that can be difficult to navigate and has been the sight of several strandings and sinkings, most notably '*The Surat'* in 1874 (Tyrrell, 2006). The Catlins River mean flow is ~3.7$m^3.s^{-1}$, whilst the Owaka River mean flow is ~3.1$m^3.s^{-1}$ (Stevens and Robertson 2017, p. 1). The flow rate upstream of the Catlins Lake (March-August 2022) is shown below (Figure 3.12). Flow rate is important because high flow means high levels of suspended sediment and possible wetland accretion. Three large peaks are clearly identifiable, located around May 21–23 reaching ~39$m^3.s^{-1}$ and July 13–16, peaking at ~58$m^3.s^{-1}$ and July 25–28, peaking at 43$m^3.s^{-1}$ (Figure 3.12). The flow rates are monitored by the Otago Regional Council (ORC) and the recording site is upstream near Houipapa (Figure 3.13).

A DEM of the Catlins Estuary indicates the low gradient environment of the Pounawea Wetland. The wetland has formed a terrace above the intertidal sandflats (Figure 3.3) There is a gentle increase in slope from south to north, increasing at the podocarp forest boundary (Figure 3.4, Figure 3.5 and Figure 3.6).

Sedimentation rates have increased in the Catlin's Estuary since European colonisation due to land use change and wetland drainage. Rather than being dominated by sandy sediments and infilling slowly with mud and clay, New Zealand estuaries have seen dramatic increases in sedimentation rates, roughly ten times higher than pre-human periods (Gibb and Cox, 2009; Swales and Hume, 1995). Deforestation has contributed to the upper basin (Catlins Lake) to rapidly infill with fine silts (Robertson *et al.*, 2017). Increased rates of erosion and run-off have seen increases in soft mud in Otago coastal estuaries. Soft mud cover percentage of the Catlins River is estimated at 29%, the highest percentage of the seven rivers studied as part of the 'Otago Estuaries, State of the Environment Report 2010' (Otago Regional Council, 2010). The same report investigated species richness via coring in the predominantly sandy intertidal region and the downstream area of the Catlins River experienced the greatest level of species richness (10.3) (Otago Regional Council, 2010).

Macroalgae was observed during fieldwork which could have two consequences for the wetland; (1) adds mass to the wetland; (2) cloaks the surface and kills or fertilisers vegetation. The presence of macroalgae (*Cladophora, Ulva)* in the lower basin intertidal sandflats and on the wetland (Figure 3.14) could be a result of excessive coastal eutrophication levels in the upper basin (Plew *et al.*, 2020; Teichberg *et al.*, 2010). Specifically, increases in nitrate and phosphorus might contribute to more macroalgae. Larger deposits of macroalgae on the wetland may impact vegetation photosynthesis. The effects of macroalgae are beyond the scope of this thesis but it is important to recognise the potential link between water quality and macroalgae abundance.

Results from fine-scale monitoring of the Catlin's Estuary in 2016 highlighted differences in water quality metrics between the upper and lower basins. This is not uncommon in New Zealand estuaries given the amount of sediment that enters estuaries. Sediment accumulates in the Catlins Lake upper basin where it settles and ultimately affects the water quality through increases in suspended sediment and poor oxygenation. Regular flushing of the lower basin reduces these risks. The upper basin (Catlins Lake) exceeded the eutrophication threshold of $0.4 mgl^{-1}$ of total nitrogen, this limit was not

exceeded by the lower estuary but algae was still present (Robertson *et al.*, 2017). The overall quality of the Catlins Estuary system is deemed to be 'moderate' (Stevens and Robertson 2017). High rainfall events lead to increases in turbidity, nitrate and phosphorus levels. This is to be expected due to farm run-off, debris, sediment and surface water make their way from the surrounding hills and valleys into the estuary system.

The intertidal zone of the Catlin's Estuary (Owaka River included) amounted to 2.3% (14.9ha) and a moderate risk rating was given (Stevens and Robertson 2017). The majority of the mapped eutrophication occurred in the Catlins Lake basin and the riverbanks of the Owaka River. Eutrophication levels differed between the upper and lower basin. Low redox levels in the upper basin reflect the poor oxygenation levels mentioned above. Moreover, these low redox levels mean species would need to be tolerant of low oxygen environments (Robertson *et al.*, 2017). This tolerance is reflected in the reduction of species richness found at the upper basin. The potential for eutrophication in the lower basin was described as low and not likely to be a risk to aquatic life and processes (Robertson *et al.*, 2017). Eutrophication is present in the lower basin and this is demonstrated by the algae deposited on the wetland (Figure 3.14).

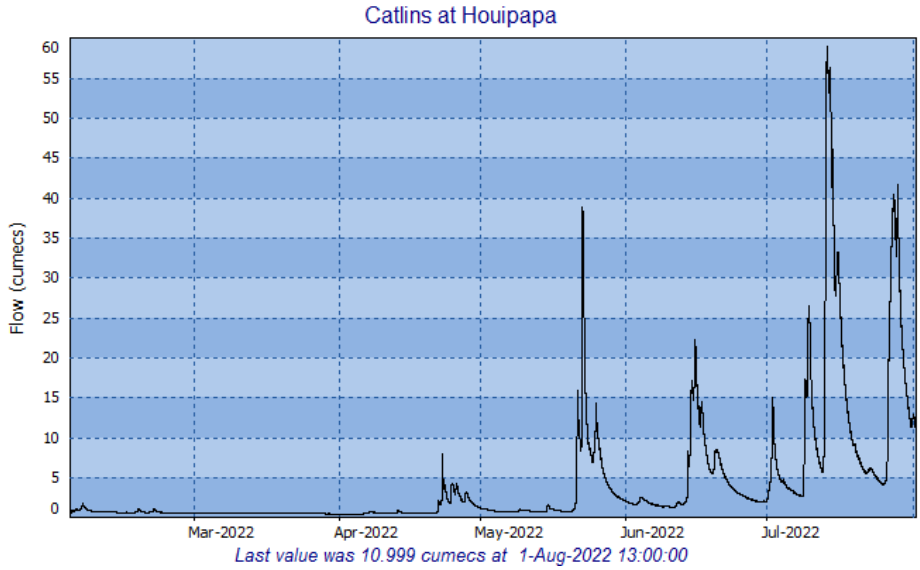

Figure 3.12: Average water flow for the past 180 days measured in cumecs (m^3s). Graph courtesy of the Otago Regional Council.

Figure 3.13: Flow recording station for the Catlins River located at Houipapa (red pin). Image from Google Earth ™.

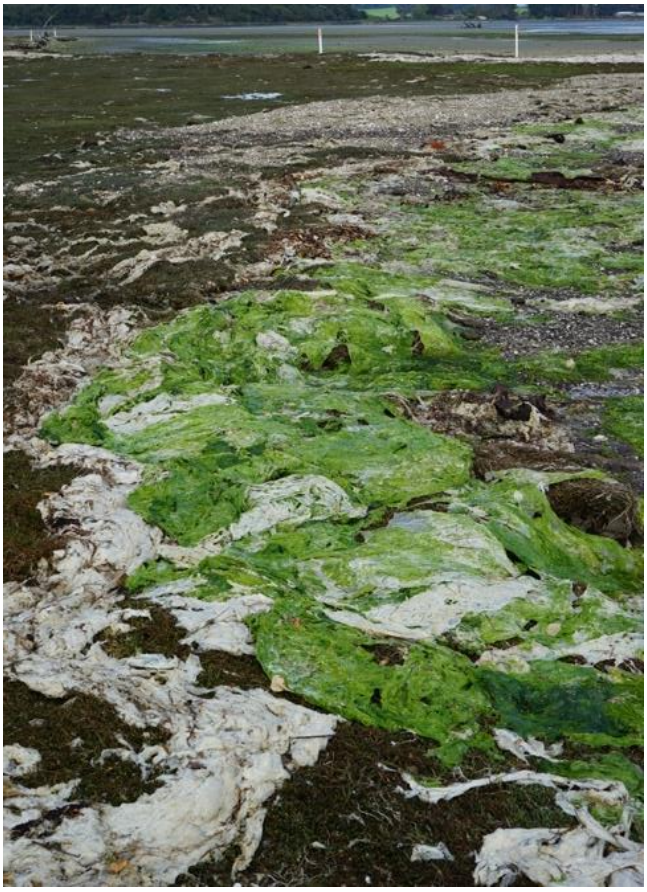

Figure 3.14: Macro algae deposited on the wetland. Photo taken by Mike Hilton on 8th November 2021.

3.7. CHANGES TO VEGETATION AND LAND-USE

3.7.1. Land-use change

Land-use change is an essential driver of environmental change (Luisa Martínez *et al.*, 2014; Scott *et al.*, 2014a). Wetland environments have suffered extensive losses within New Zealand driven by wetland drainage and agriculture expansion (Myers *et al.*, 2013; Robertson *et al.*, 2018). Extensive land-use change has seen the wider Catlins area transformed from dense native forest to pasture. The Catlins was known for its forests of rimu, totara, miro and silver beech (Arthur, 1971). "In pre-history Pounawea was a low lying river flat of swamp, scrub and sandhills, dominated by bush-clad hills, and a prominent bank of sea-shells visible on the spit between Surat Bay and Catlins River." (Arthur, 1971, p. 9). The depiction of Pounawea described by Arthur (1971) is markedly different from the environment found at Pounawea today. Cleared forests and intensive land use change for agriculture is widespread. Behind the upper reaches of the Pounawea salt marsh a section of native podocarp forest remains. Early European settlers observed ever extending evergreen forests and abundance of land and sea birds that littered the coast (Tyrrell, 2006).

Archaeological digs at Pounawea are few, but there has been discoveries of what appears to be summer camps located at Manuka Point (this area has since been eroded but can be seen on the right hand side in Figure 3.15), Hinahina and Jack's Bay between the 14th and 17th century (Hamel, 1977; Tyrrell, 2006). Salt-marsh foraminifera found in the silty sediment overlain the Late Holocene sands sustained levels of *Pteridium* (bracken) spores which may have been deposited after the initial forest clearance of early Polynesian settlers in the 14th century (Gehrels *et al.*, 2008; Newnham *et al.*, 1998).

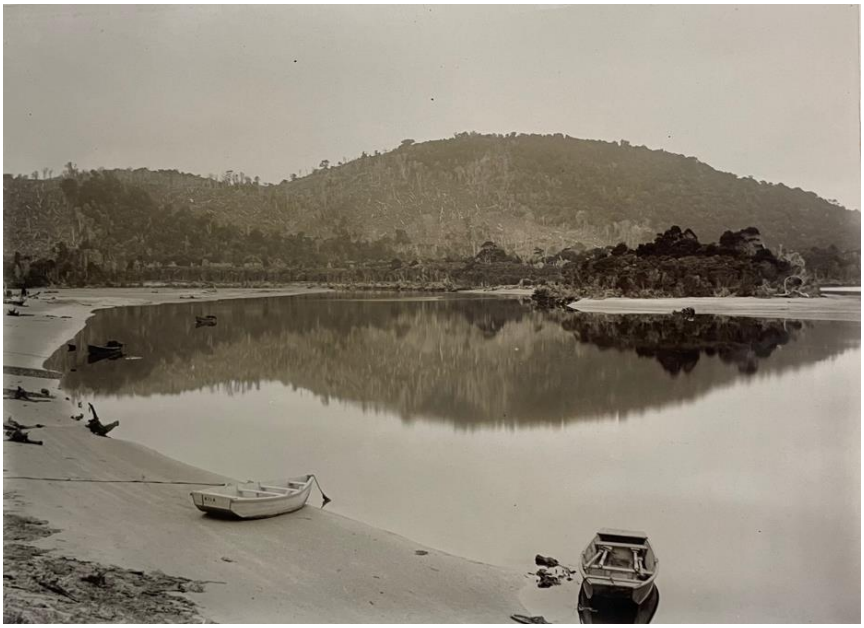

Figure 3.15: Catlins Estuary (1905) looking North, Manuka Point seen on the right has since been eroded. Photo curtesy of the Hocken Library.

Changes to the wetland morphology and morphodynamics of the estuary came in the form of significant forest clearance. Early European settlers purchased large blocks of the Catlins for logging purposes. Saw- milling became a prominent industry for the Otago region. The first saw mills were constructed in 1865, one of these was 'The Big Mill' located at Catlins Lake. Large sections of forests were cleared but native forest still exists at Pounawea (Partridge and Wilson, 1988). An early photograph taken in 1905 shows the Pounawea settlement in the foreground and patches of de-branched trees primed for felling are littered throughout (Figure 3.16). Saw milling had not yet reached its peak (1910-1940) but the surrounding area was already sparse (Wilson, 1993). The podocarp forest extended to the shoreline from both sides of the estuary. The effects on forest removal on wetland shoreline erosion will be discussed in the next chapter.

Figure 3.16: Photograph from 1905 depicting Pounawea township and the surrounding forested landscape. Photo courtesy of the Hocken Library.

The clearance of native forest and development of viable agricultural land took less than 100 years. The removal of forest may have had consequences for wetland evolution. The removal of forest was not always straightforward. The nature of the landscape meant parts of the Catlins were not accessible for several decades due to lack of infrastructure and technology. A lack of government financial support or incentives for forest clearance and high capital costs were the main barriers that only a select few were able to overcome. This changed in 1887 with the establishment of the Government settlement schemes and a worldwide shift and demand for dairy farming (Wilson, 1993). Large areas of forest that lay undisturbed on farm blocks which had previously been too expensive to consider clearing were quickly removed and converted into pasture. A detailed timeline of forest clearance from farmland can be seen in Figure 3.17. From this figure we can see a significant loss of native forest on farmland between 1890–1940 and further support from the government for forest clearance from 1950 through till 1970. Forest clearing, milling and intensive land-use change significantly altered the Catlins Estuary catchment.

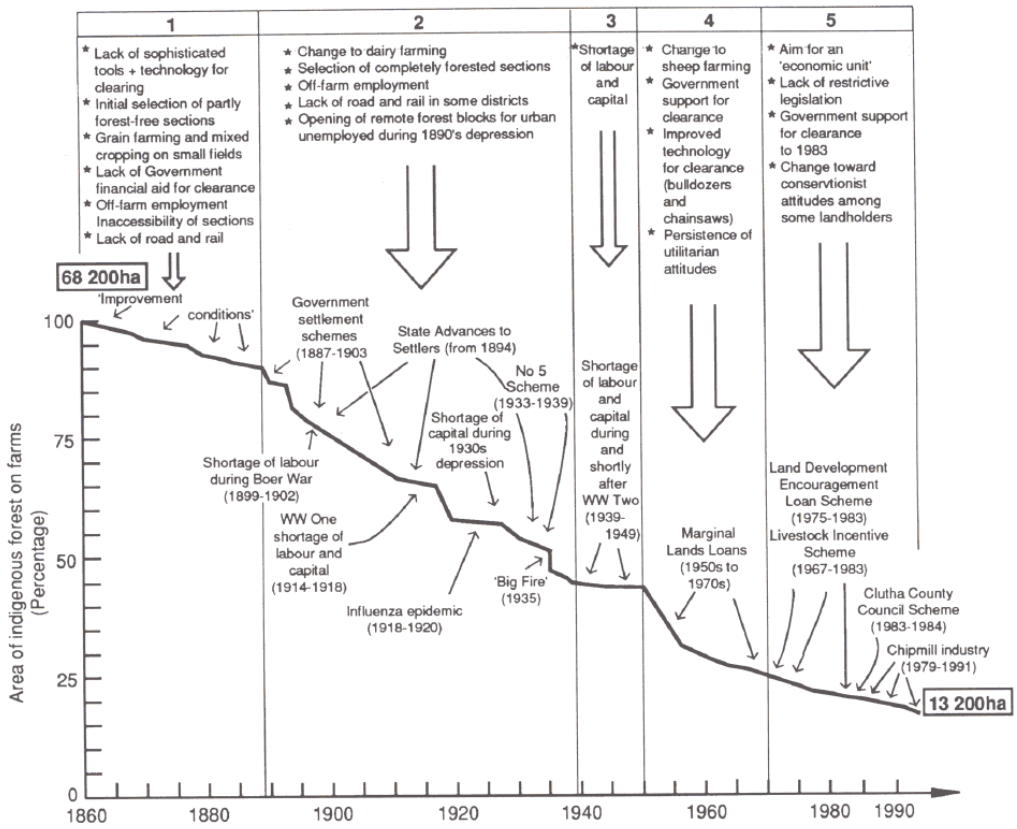

Figure 3.17: The pace of indigenous forest clearance on farms in the Catlins District, 1861–1991 (Wilson, 1993b).

The estuary margins have undergone deforestation over the last 130 years. The podocarp forest extended across the landscape reaching elevations of 200 m and pushed right up to the river banks (elevation ~2 m) has been replaced with roads and pasture land. James W. Thomson, a pioneer of the logging industry and owner of "The Big Mill" wrote about his first experience at the Catlins and Owaka Rivers, he said "On every side except seawards we were surrounded by hills, wooded from their summits to the very water's edge…The over-hanging branches of the trees almost meeting in some places, gave us rather the impression that we were in a kind of immense arcade." (Thomson, 1889, p. 3). Stevens & Robertson (2017) mapped the terrestrial boundary extending 200 m inland of the Catlins and Owaka Rivers (Figure 3.18). Pasture land is the dominant landscape class, extending right up to the estuary edge.

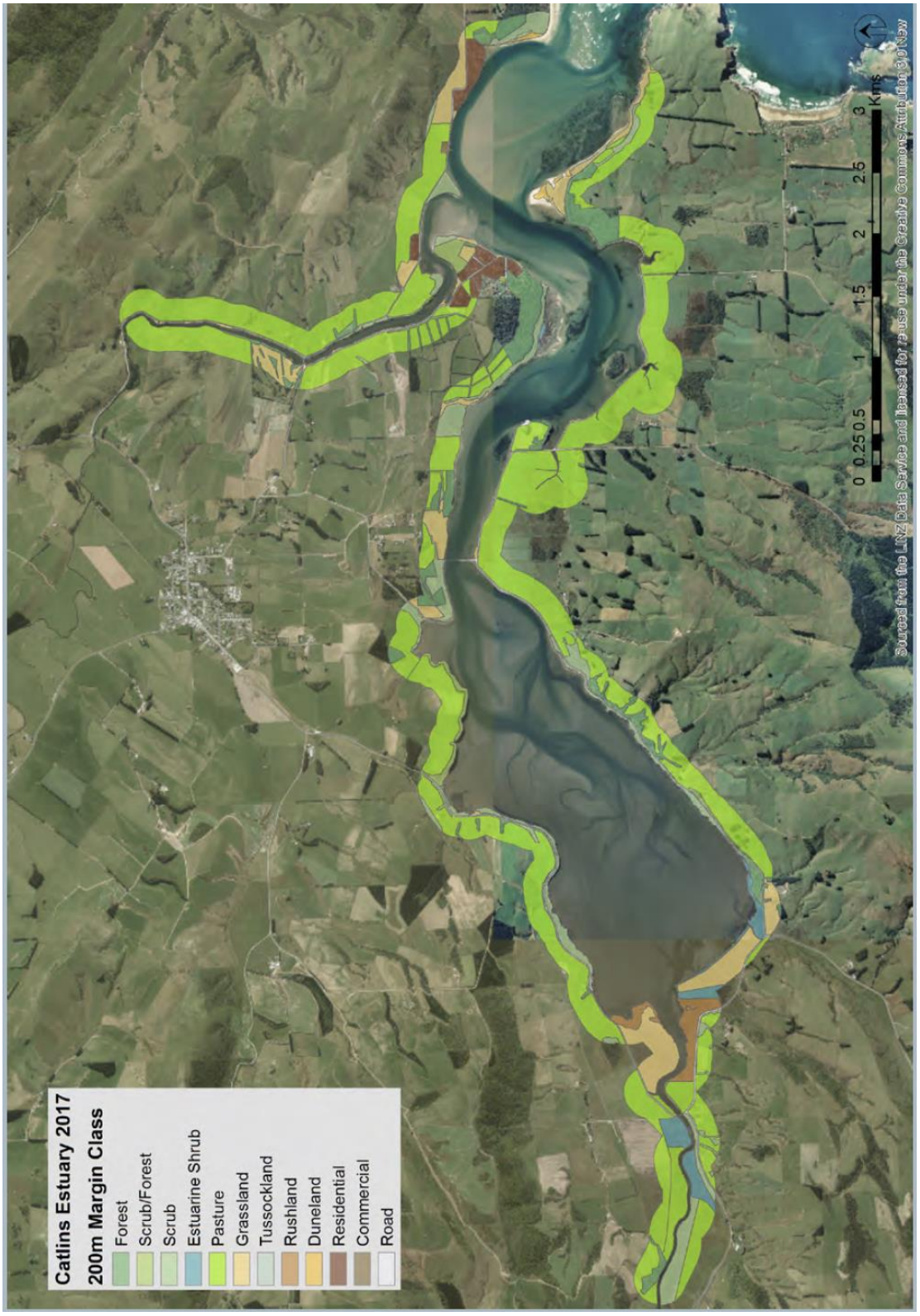

Figure 3.18: Map of 200m Terrestrial Margin depicting the dominant land cover, December, 2016 (Stevens and Robertson, 2017).

3.7.2. Erosion of Manuka Point and Cabbage Point

Landscape change is most prominent at the mouth of the Catlins and Owaka River's. Notably, the erosion of Manuka Point at the tidal entrance of the estuary (Figure 3.20). Manuka Point was in place during archaeological excavations during the 1950s and reports indicate that by 1979, 150 m of the spit had been eroded and a 22 m long, 3–4 m wide spit remained (Garland and Wadsworth, 2019; Hamel, 1977). Two years earlier in 1977, Manuka Point had been described as "37 m long, 5–9 m wide and 1.0–1.5 high covered with small totara trees." (Hamel, 1978, p. 3). Hamel wrote another letter describing the erosion "the trees are a factor in accelerating erosion when they are adjacent to over-steepened banks of loose sand, from wind working their roots like a crowbar." (Hamel, 1979, p. 2). A final archaeological dig took place in 1979, fears over erosion and the potential loss of undiscovered relics set the dig in motion. By 1985, the 22 m long area had eroded away and the Owaka River channel had been re-routed through what was previously Manuka Point (Figure 3.20).

Erosion at Manuka Point was a constant threat and attempts were made to slow erosion. Between 1933–1938 a 140 m groyne was built and rocks were placed surrounding Manuka Point (Otago Catchment Board Report, 1979). The groyne was built to prevent a breaching event that would separate the causeway and Manuka Point, detaching Manuka Point from the Pounawea Scenic Reserve. By 1955, the groyne had been breached and the protective rocks surrounding Manuka Point were scattered about the beach. Historical images did not show these protective measures. Manuka Point in the early 1900s was a dense vegetated forest (Figure 3.15 & Figure 3.19). Archaeologist Les Lockerbie, noted, in 1957, that parts of Manuka Point were submerged during high tide, indicating the low elevation of the area (Lockerbie, 1959). Aerial imagery (Figure 3.20) depicts the erosion process across 37 years. By 1967, a thin strip of forest remained, and by 1985 Manuka Point had eroded completely and the Owaka River outflow can be seen running through the former location of Manuka Point. The reduction in area of Manuka Point is shown in Table 3.2. This area is not as large as Cabbage Point, there is mention that Manuka Point had once been 650 m in length in 1865 (Garland and Wadsworth, 2019), therefore, it is likely that erosion had occurred for several decades before the first aerial photograph was taken. Local records and accounts indicate the erosion was natural, there is no mention of the area being cleared for timber production.

Figure 3.19: Catlins Estuary with Manuka Point in the centre, dated early 1900s. Picture courtesy of the Owaka Museum Collection.

Figure 3.20: Aerial images of Manuka Point and Cabbage Point from 1948 (left) and 1985 (right). Red and yellow polygons outline the edge of the forested area of Manuka Point in 1948 & 1967.

Cabbage Point is a coastal barrier, classified as a headland spit (Cowell and Thom, 1995) that once protected the Pounawea foreshore from storm surge. A flood tide delta behind and adjoining Cabbage Point driven by tidal currents and waves pushes sediment from the mouth of the estuary inland. The elevation of this flood delta is -0.2–0.3 m. The erosion of Cabbage Point has not resulted in the loss of this flood tide delta, meaning the sediment is still in the estuary system.

The size, shape and morphology of Cabbage Point has evolved over time. Cabbage Point has sustained extensive erosion over the last 75 years (Hamel, 1977). Cartographic maps (Appendix A, Figure A11 and Figure A12) and Figure 3.21 illustrate the boundary changes of Cabbage Point. In 1948 it was ~750 m long and covered an area of 200,301 m^2. As of 2019, Cabbage Point was ~250 m in length and covered 51,651 m^2. The erosion and subsequent movement of Cabbage Point is illustrated in Figure 3.21. Erosion occurred on the eastern edge between 1948 and 1967. The spit lost 60 m of width, the total erosion amounted to a loss of 38,362 m^2. This is a sizable loss but the overall shape of Cabbage Point remained stable. Significant erosion occurred between 1967 and 1985, a total of 92,616 m^2 was eroded, the width of the spit was reduced by a further 115 m (purple dashed line in Figure 3.21). The spit's length was reduced by over 500 m and no longer extended out onto the far reaches of the inter-tidal flats.

Catlins Estuary entrance is a dynamic environment, subject to erosion, sediment redistribution and tidal currents. Cabbage Point is part of this dynamic environment, reducing in size and shifting south-west towards the Catlins Estuary channel. A secondary channel has formed at the end of the vegetated spit (Figure 3.21). It may have been that after the erosion events of 1967–1985, waves may have propagated around the corner from an easterly swell direction. Sediment may have been eroded and transported through wave action, aeolian sediment transportation and tidal processes. The new channel may be a result of a combination of these processes occurring over several decades. The total area and area lost between images are found in Table 3.4. Erosion appears to have slowed down since 1997, roughly the same amount of area has eroded between 1985–1997 and 1997–2019. It has taken an extra ten years to erode the same amount of area that was lost between 1985–1997.

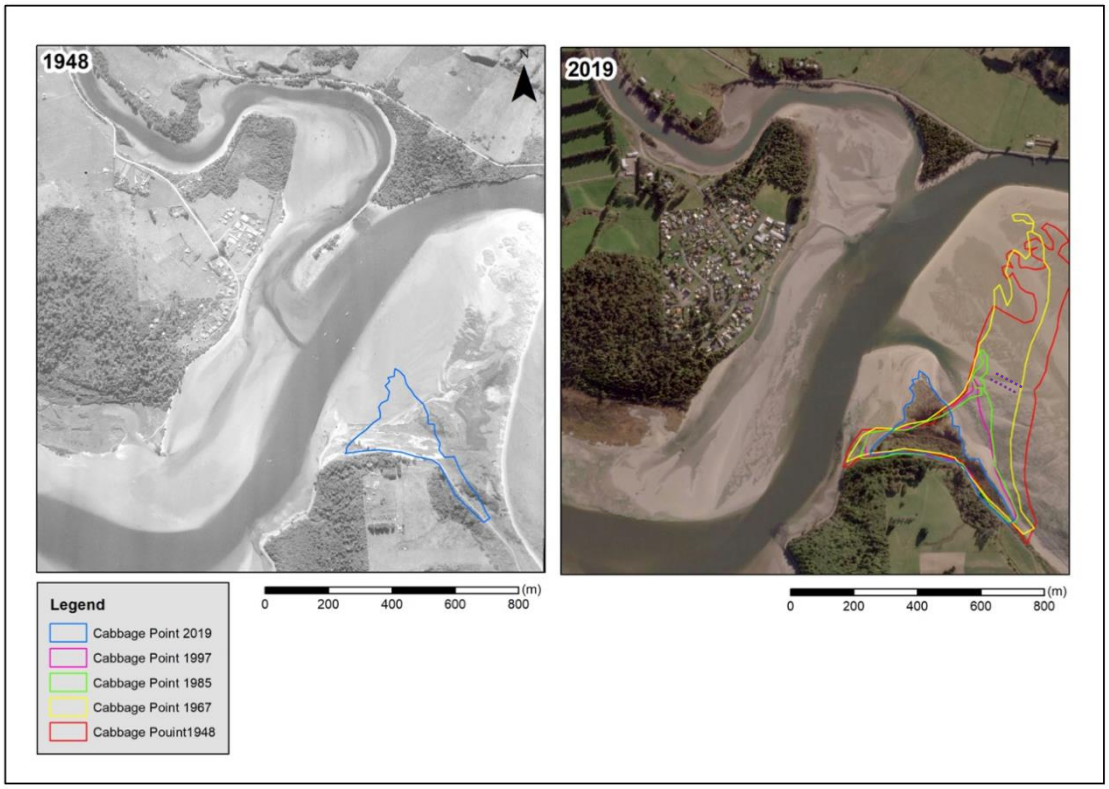

Figure 3.21: Cabbage Point erosion from 1948–2019.

Table 3.2: Total erosion area (m^2) of Manuka Point, 1948–1985.

Manuka Point	**Area (m^2)**	**Area lost (m^2) between images**
1948	2,434.48	0
1967	1,395.19	1,039.29
1985	0	1,395.19

Table 3.3: Cabbage Point 1948–2019 area (m^2) and loss of area between images.

Cabbage Point	**Area (m^2)**	**Area lost (m^2) between images**
1948	200,301.56	0
1967	161,939.91	38,361.65
1985	69,323.47	92,616.44
1997	60,402.09	8,921.38
2019	51,651.62	8,750.47

Cabbage Point likely acted as a protective barrier before being eroded. Pounawea could be considered a sheltered environment due to the protection from the prevailing south-west wind provided by the remnants of the podocarp forest at the southern end of the town. The erosion of Manuka Point and Cabbage Point may have exposed Pounawea to more severe storm-surge and north-east winds. These events coupled with low pressure and spring high tide could be devastating for the Pounawea foreshore. Manuka Point was once a densely vegetated spit as described above and seen in Figure 3.15 and Figure 3.19.

Erosion and flooding can occur quickly when the right conditions present themselves. In 2006, an erosion and flooding event took place at Pounawea. Spring high tide, a low-pressure system and strong south-south-east (SSE) winds caused damage to the Pounawea foreshore and wooden seawall. The seawall (Figure 3.22, e), was a simple wooden retaining wall, unfortunately, the conditions contributed to an erosion and flooding event. The event took place on April 26th, 2006. Spring high tides were forecast to peak on April 27th. Mean sea-level pressure data provided by *MetService* from Nugget Point climate station (10 km NE of Pounawea) was 1002.6 hPa on April 26th. The mean pressure of Pounawea was 1012 hPa, therefore, sea level would have been 10 cm higher than usual due to the inverse barometric effect (Pugh, 2004). Local wind data from Nugget Point climate station showed that peak wind speed occurred at the same time as high tide. This speed was recorded at 27.3 ms^{-1}, it is worth noting, the Nugget Point climate station sits atop of a steep cliff face therefore, it may be influenced by Bernoulli's principle (Hewitt, 2004). The wind speeds experienced at Pounawea may be less than those recorded at Nugget Point.

Local wind waves can be clearly seen in Figure 3.22 (e & f), soil saturation from wave overtopping may have stressed the wooden seawall, ultimately causing it to fail (Figure 3.22, c & d). Large boulders were used to fill the gaps of the eroded foreshore, by 2010 a rock seawall had been built and in 2017 the seawall was extended the length of the inhabited foreshore. A breakwater was also built near the remnant of Manuka Point, providing protection from waves propagating through the estuary mouth (Garland and Wadsworth, 2019).

Figure 3.22: Pounawea foreshore; (a) and (b) wind waves and wave overtopping on April 26th at high tide; (c) seawall collapse and erosion (looking north); (d) seawall collapse and erosion (looking south); (e) wooden seawall present before 2006 event; (f) rock seawall completed in May 2010. Photos taken by Mike Hilton.

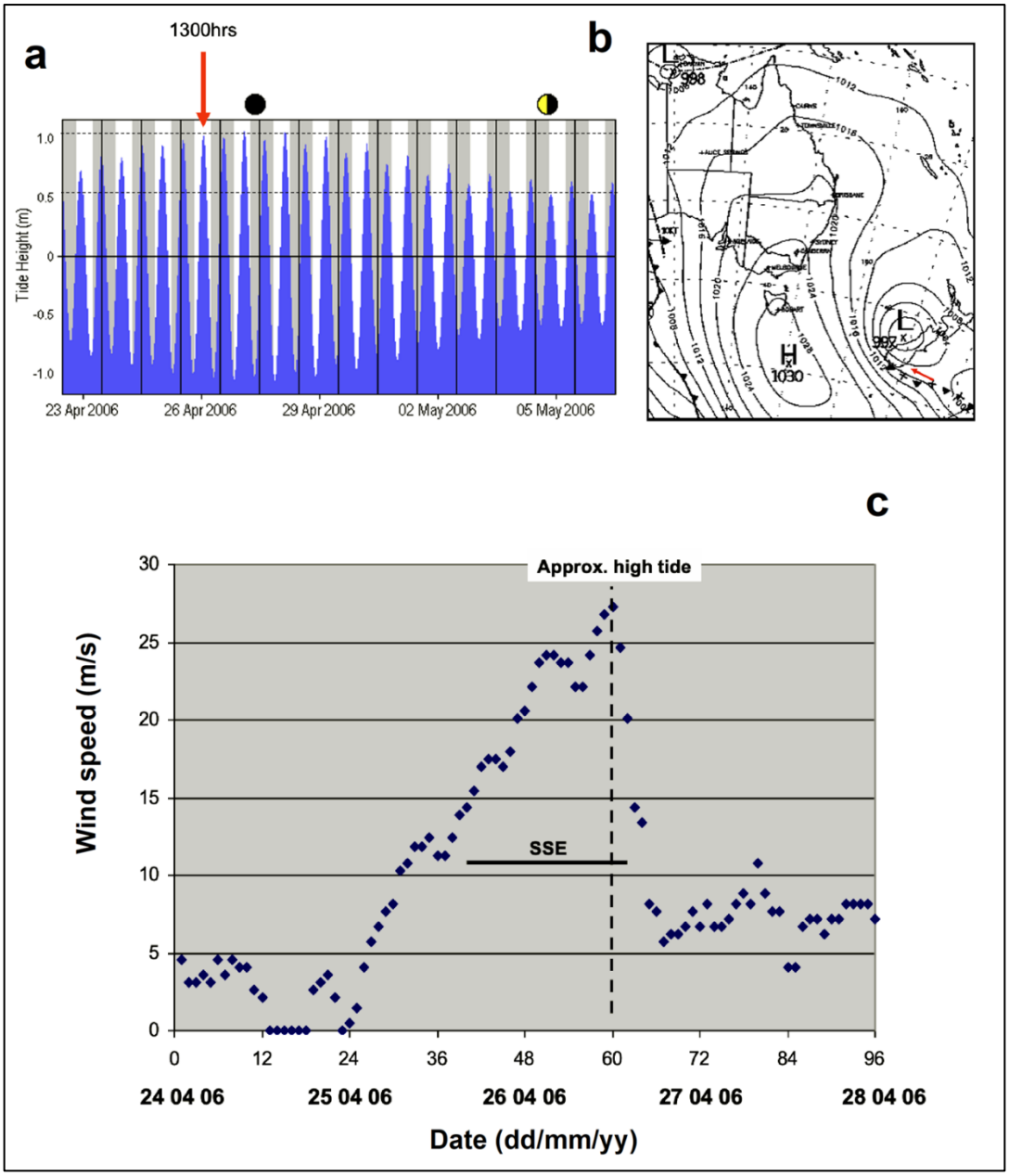

Figure 3.23: Climatic conditions present during the erosion event at the Pounawea foreshore & seawall, April 26th 2006. (a) local tide levels relative to MSL, red arrow indicates time of event; (b) synoptic MSL pressure analysis for noon April 26th, red arrow points to Pounawea; (c) wind speed (m/s) at Nugget Point, 24–28 April.

3.8. POUNAWEA WETLAND

3.8.1. Historic shoreline change

The shoreline edge consists of two different morphologies and a variable edge height. The wetland has a scarped and sloped edged. The scarp's height varies around the wetland. The maximum height is 0.7 m found at the western and eastern edges (Figure 3.26, a & d). The minimum is 0.2 m at the southern edge (Figure 3.36, b & d). The scarp is not continuous and is broken up by the sloped edge. The sloped edge appears at areas that only have a shell deposit. It is evident that the shoreline margin is periodically eroding (Figure 3.25). Erosion has occurred along every exposed shoreline edge except in one area (Figure 3.24). Sheltered from incoming waves and the prevailing south-west winds, the inlet edge eroded 2 m since 1948. The inlet edge is still exposed to southerly winds. The inlet is inundated in the mesotidal estuary during ebb and flood tides, water merely infills rather than washing against the marsh edge. Eastern and western edges have lost a significant amount of shoreline area. The western edge is exposed to south-westerly and westerly winds. Winds from the south-west would create fetch limited waves across the 650 m estuary, winds directly from the west would have 2000 m of fetch potential.

Table 3.4: Total area of Pounawea Wetland (square metres) and the area lost between aerial images

Year	**Area (m^2)**	**Area lost (m^2) between images**
1948	85,431	0
1967	77,178	8,253
1985	73,486	3,691
1997	69,758	3,779
2006	67,308	2,449
2015	62,626	4,682
2022	60,860	1,765

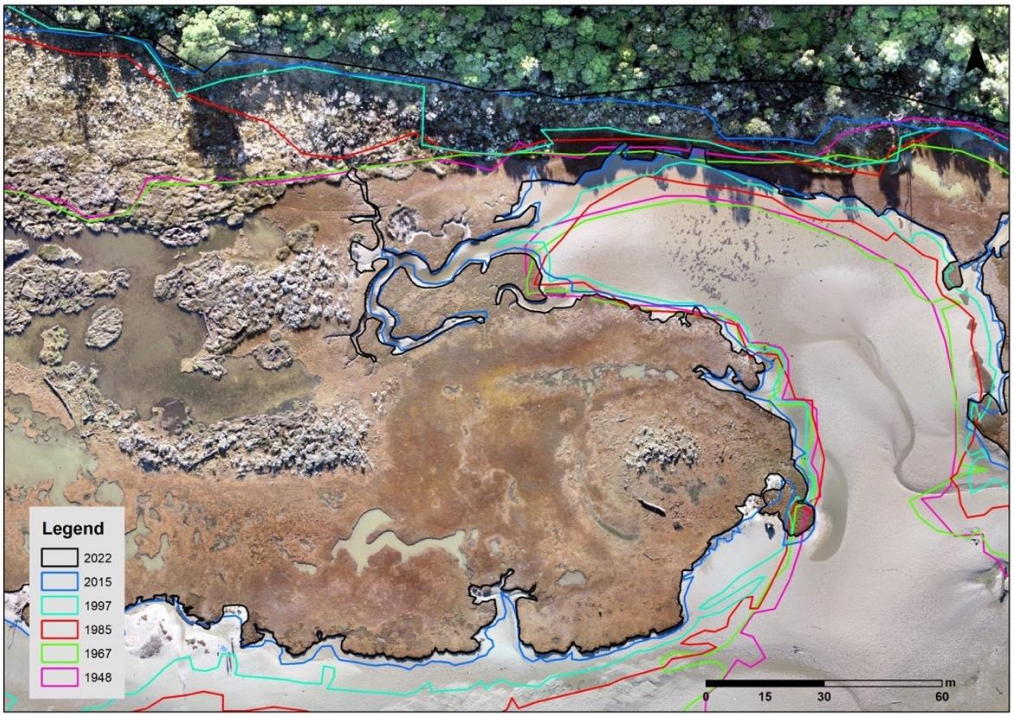

Figure 3.24: Close up view of the inlet area that has seen significantly less erosion than other parts of the wetland. This part of the inlet is the only north facing area on the wetland therefore not effected by wave or wind processes. Base image is from UAV flight on June 17th 2022.

Scarping, cliff toe erosion and wave action are more prominent on the western and eastern shorelines. These shoreline edges are close to the main estuary channel and the effects of the tidal cycle (inundation) reach these areas first. Furthermore, both shorelines are vulnerable to local wind waves. These two factors may be the cause of the erosion. The exposed margins suffer from wave undercutting and cliff-toe erosion. The base of the scarp is undercut and eroded by wave action, leading to scarp failure and large blocks of wetland collapsing. Large blocks of wetland have collapse from the east, south and western edges of the wetland (Figure 3.26, a. b, c). Block erosion is more commonly seen in the east and west nevertheless block erosion has been witnessed at the southern edge. The western edge had the largest overhanging scarp, an eroded part of the wetland is pictured on the intertidal mudflat (Figure 3.26, d). The western shoreline featured a significant proportion of the cliff-toe erosion.

The wetland area has decreased by 24,571 m^2 over the 72-year period from 1948–2022 (June). Table 3.4 illustrates the change in area of the wetland over time. This is an average yearly loss of 341 m^2. Landward transgression of the wetland contributed significantly to reducing the overall loss of wetland area. The boundary change resulted in a gain of ~7,079 m^2 of wetland between 1967–1985. This limited the losses suffered at the marsh edge where ~25 m of shoreline was eroded during the same period. The wetland still lost ~3,691 m^2 of total area between 1967–1985. Erosion rates increased during 2006–2015 comparative to 1997–2006, an additional 2,233 m^2 was eroded over the same length of time. The 2006 storm surge event discussed above (Figure 3.22) may have contributed to this acceleration. Additional large storms in 2007, 2009 and 2010 may have also contributed to accelerated erosion.

The wetland – podocarp forest boundary has shifted significantly since the first aerial photograph in 1948. The landward margin of the wetland in 1948 & 1967 was significantly further south than at any other time since (Figure 3.25 & Figure 3.8). It is with low to moderate confidence that we can assume that forest clearance has taken place between 1967–1985. The dense forest apparent in 1948 is no longer present, low lying shrubs remain. There is no documented evidence that indicate forest clearance but observations of the area and the clear depiction of dense forest in 1948 suggest some forest clearance occurred. A further explanation for the boundary change could be wetland transgression, and this scenario is explained in Chapter 6.

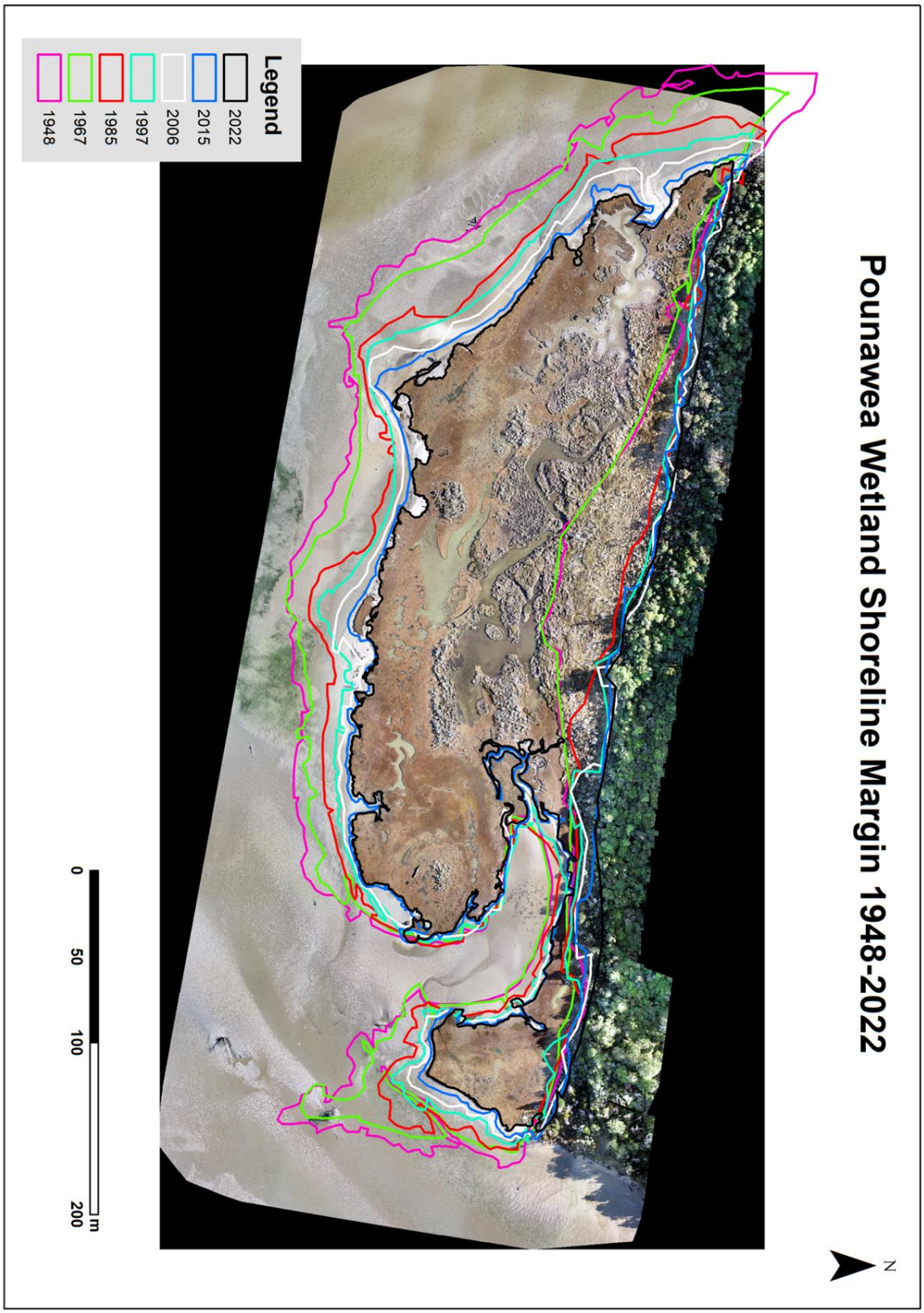

Figure 3.25: Pounawea Wetland boundary change over time, 1948–2022. Base photo is an orthomosiac image from a UAV survey completed on June 17th 2022.

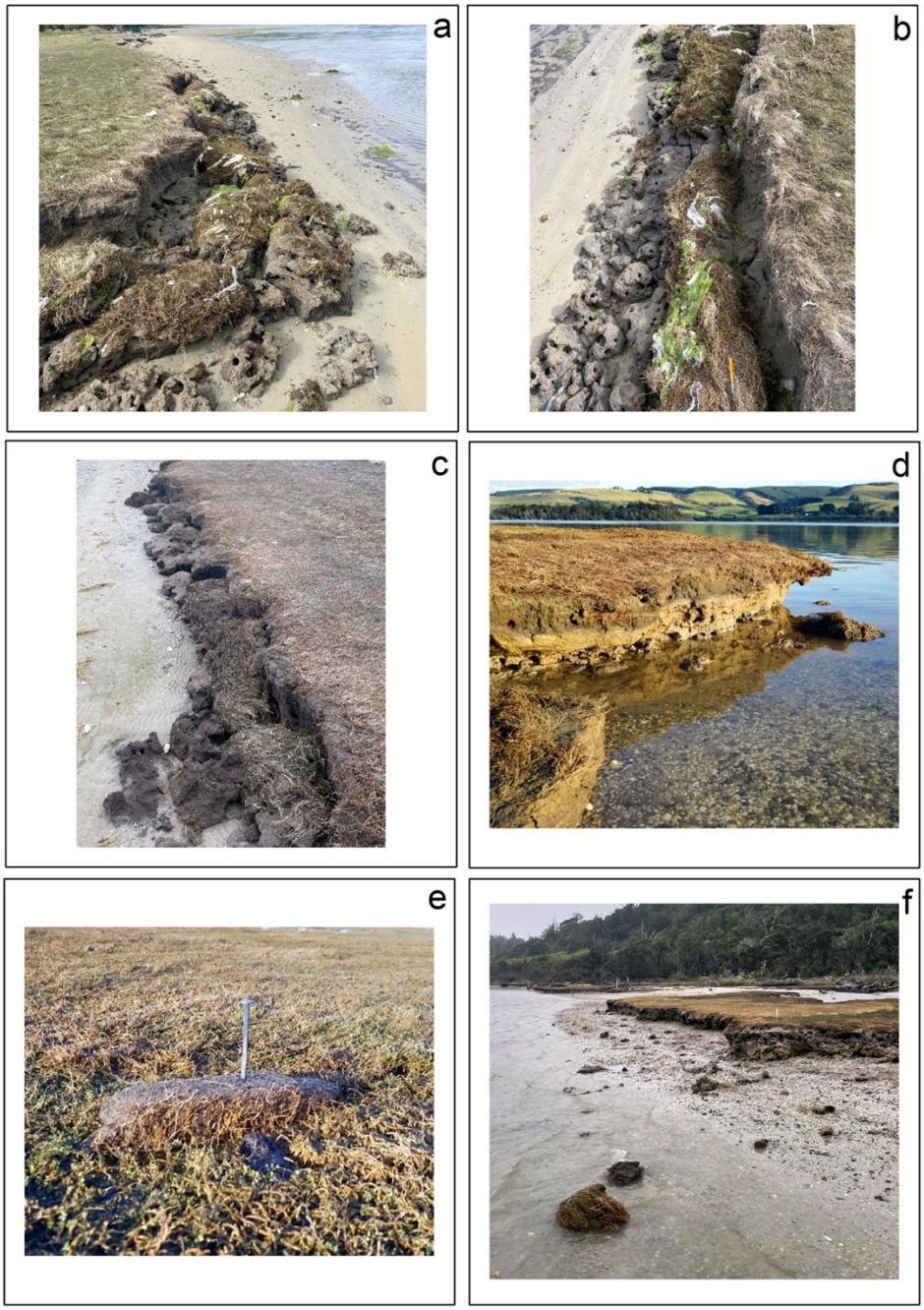

Figure 3.26: Pounawea Wetland erosion. Photos taken on different field trips; (a) and (b) eastern marsh edge block erosion, photos taken 30/10/21; (c) southern marsh edge, photo taken 09/04/22; (d) western marsh edge, cliff-toe erosion present and eroded material in on the intertidal mudflat, photo is looking south and taken on 17/06/22; (e) eroded marsh block re-deposited on the wetland platform during the recent spring high tide event, black peg used to for scale – peg is 150 mm long, photo taken 17/06/22; (f) western edge erosion, large blocks in the intertidal area had recently fallen away from the wetland, photo taken 19/05/22.

Digital Shoreline Analysis System

Net shoreline movement (NSM) is a calculation of the total shoreline movement through time. Shoreline movement from 1948–2022 across 11 shoreline transects is illustrated below (Figure 3.27). The southern shoreline illustrates the least amount of shoreline erosion. The three red transects seen in the inlet represent significant net shoreline movement, however, these transects passed through the eastern edge and DSAS assumes a linear movement through the transect. Thereby, DSAS has assumed that the eastern edge has eroded back to the inlet edge. This is one of the limitations of DSAS when using this tool on an irregularly shaped shoreline. The western shoreline features the highest concentration of yellow transects, representing 60–93 m of shoreline movement since 1948.

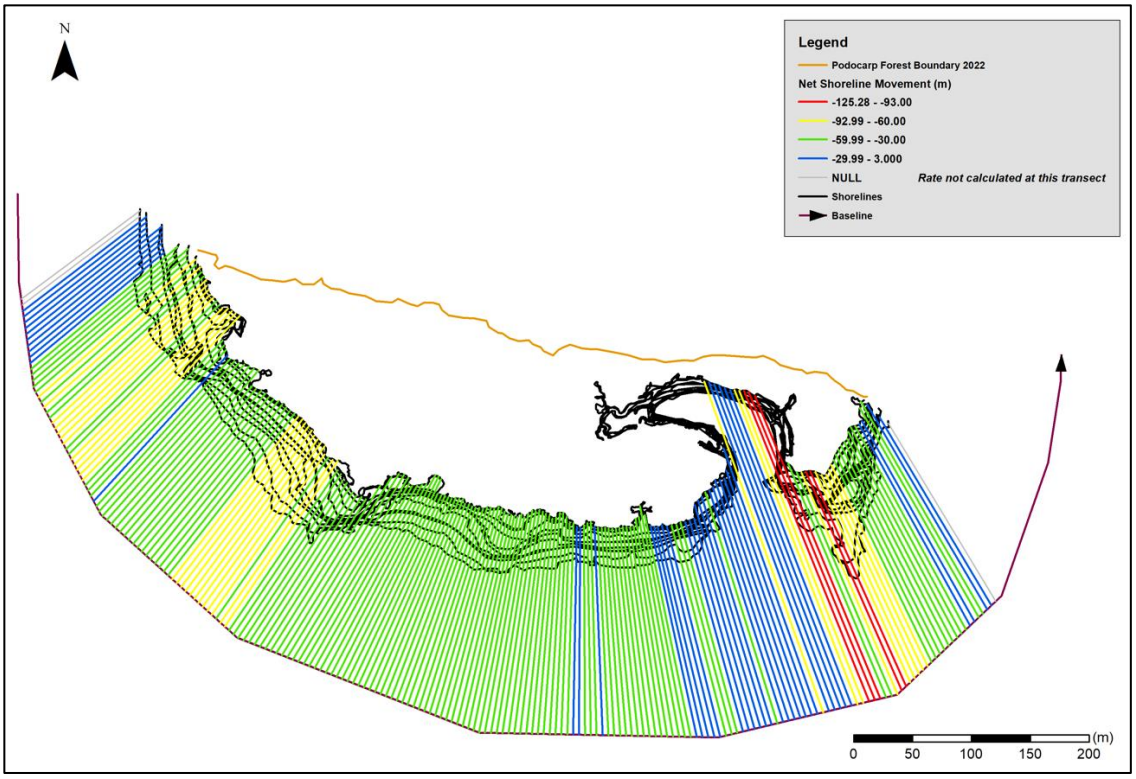

Figure 3.27: Net Shoreline Movement of the Pounawea Wetland calculated using DSAS, the legend indicates the amount of net shoreline movement in metres.

Shoreline erosion has occurred more rapidly along the western and eastern shorelines of the wetland. More than 65% of the western edge has eroded at a rate of -0.41 – -1.9 m/yr (Figure 3.28), this is expressed by the red, yellow and green transect lines. The southern margin is eroding at a rate of -0.41 – -0.88 m/yr (green lines). Lower rates of erosion can be found at the south-eastern shoreline (blue lines). Linear Regression Rates (LRR) >0.89 m/yr was not present on the southern edge.

Erosion within the inlet entrance is not an accurate reflection of historical rates of erosion. The blue lines (0.07– -0.299 m/yr) within the inlet are an accurate representation of LRR. Increased rates of erosion seen a few transect east (yellow and red lines) are depicted with LRR of -1.4 – -1.9 m/yr (Figure 3.28). This is not an accurate representation of erosion within the inlet. DSAS uses parallel transects for its calculations, the initial transect has passed through the eastern shoreline edge before continuing to the inlet edge. The eastern edge has interfered with the parallel transect and the LRR has been calculated at a significantly greater rate. The blue transects cast from the baseline were not interfered with and illustrate low LRR, therefore, the red transects should be rejected and the LRR ignored. The eastern edge features three out of the four categories of LRR (red transects have been ignored). Notably, several yellow transects are displayed, these transects intersect the large block of wetland that was eroded after 1967, the shoreline boundary is clearly seen in Figure 3.25. The grey transects labelled as 'NULL' found at very edges of the west and eastern edge were not able to be calculated because DSAS requires three shoreline profiles for LRR calculations. These two areas are only intersected twice.

One transect to the west of the inlet (purple transect) illustrates a positive LRR. This is likely to be a consequence of the transect layout as there is no indication in Figure 3.27 of any net gain in shoreline movement. There are 202 erosional transects and 97.04% have statistically significant erosion. The average rate of erosion is -0.67 ± 0.05 m. There is one transect that indicates shoreline accretion, however, the accretion is not statistically significant. DSAS's interpretation of accretion is that of progradation or horizontal accretion seaward, vertical accretion will be discussed in chapter 5.

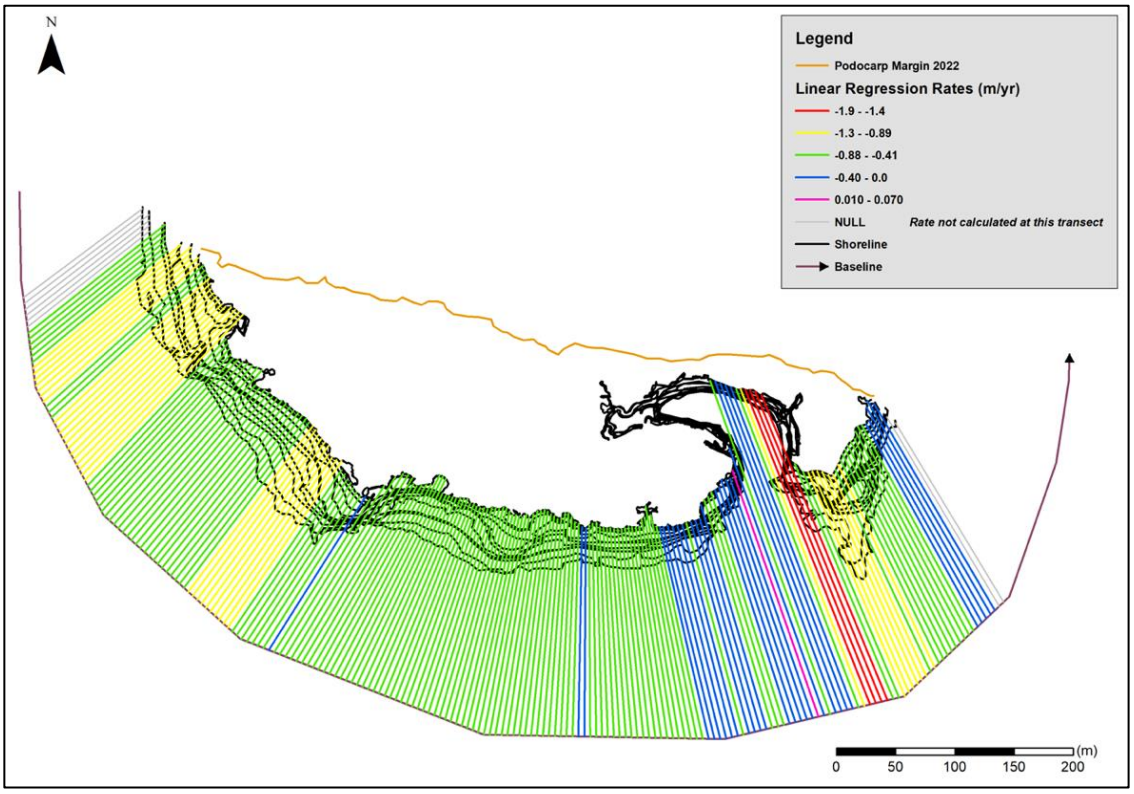

Figure 3.28: Linear Regression Rates (LLR) of erosion of the Pounawea Wetland shoreline. DSAS 5.0 was used to calculate the rates of erosion. LRR is measured in metres per year (m/yr).

The loss of Cabbage Point may have accelerated shoreline erosion through increasing the expose of the wetland to marine processes. The difference in LRR pre and post Cabbage Point is illustrated below (Figure 3.29 & Figure 3.30). Due to the limited aerial photography record, 1985 was used as the cut-off point. By 1985 Cabbage Point had significantly reduced in size (Table 3.3) and the period of time pre and post Cabbage Point is equal (37 years). The eastern margin has seen an increase in LRR represented by an increase in the number of green transects and the decrease in blue transects. The western edge features a similar pattern, increasing LRR with a greater number of green and yellow transects than blue transects (Figure 3.29). Both figures include transects that represent yearly progradation (pink). This value should be treated with caution as mentioned above. For the period 1948–1985, LRR was -0.62 ± 0.08 m, only 80.32% of the 186 transects featured erosion that was statistically significant. The LRR for 1985–2022 was -0.67 ± 0.05 m, 95.83% of the 166 transects featured erosion were statistically significant. It would be wrong to assume that the erosion of Cabbage Point is the primary reason for the increase in LRR. The morphodynamics of the east are

complex and are more exposed to marine processes than the west. The combination of an increasing exposure to marine processes likely increased after 1985 and could be the reason for the increase in LRR. The increasing rate of LRR seen in the west could be attributed to the lee effect of upwind trees and the removal of said trees. This will be analysed and discussed in the following chapter.

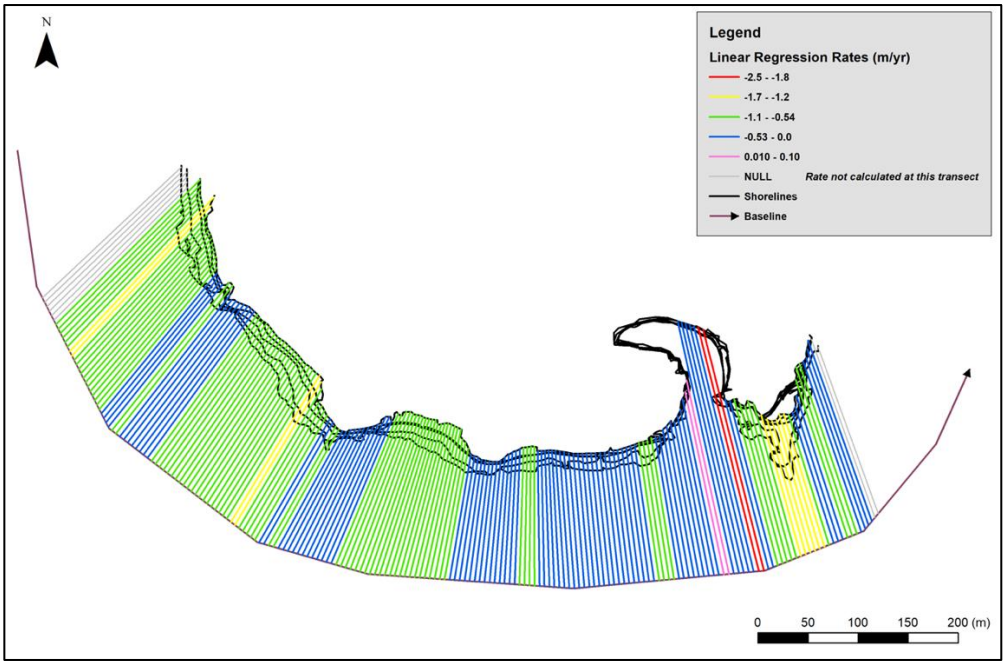

Figure 3.29: Linear Regression Rates 1948–1985.

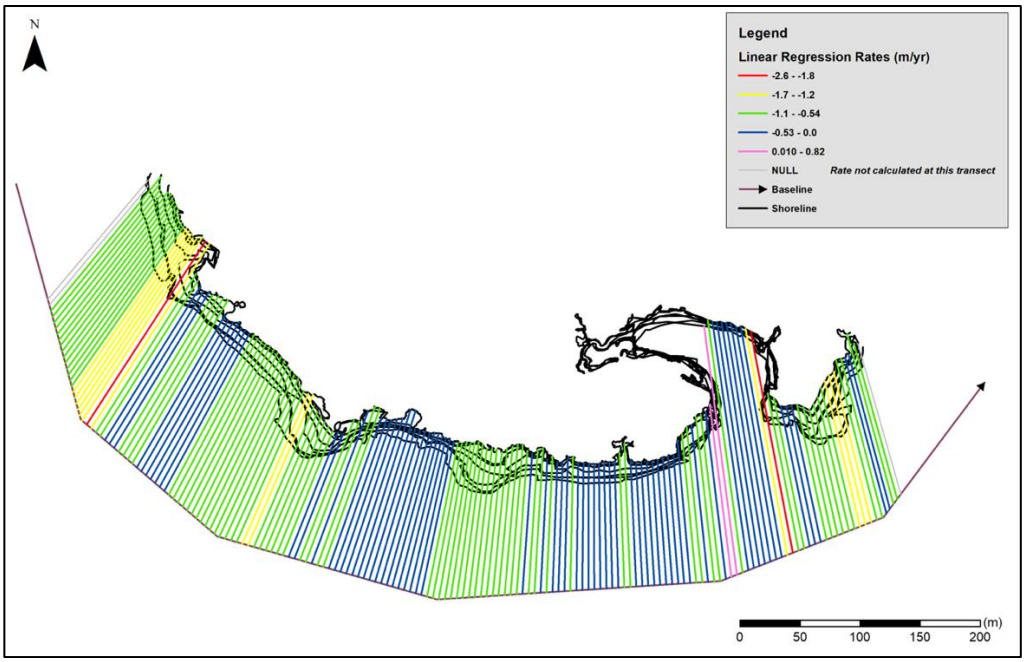

Figure 3.30: Linear Regression Rates 1985–2022.

DSAS uses statistical information and historical shoreline data to forecast the shoreline in 10 & 20 years. The shoreline forecasts depict continued erosion at all shoreline edges (Figure 3.31), most severely on the western edge. Once again due to the nature of the DSAS transect castings the inlet shoreline predictions and uncertainty bands should be ignored. The uncertainty bands (Figure 3.32) signify that this prediction should be treated with caution but they do illustrate the potential for significant erosion of the shoreline margin.

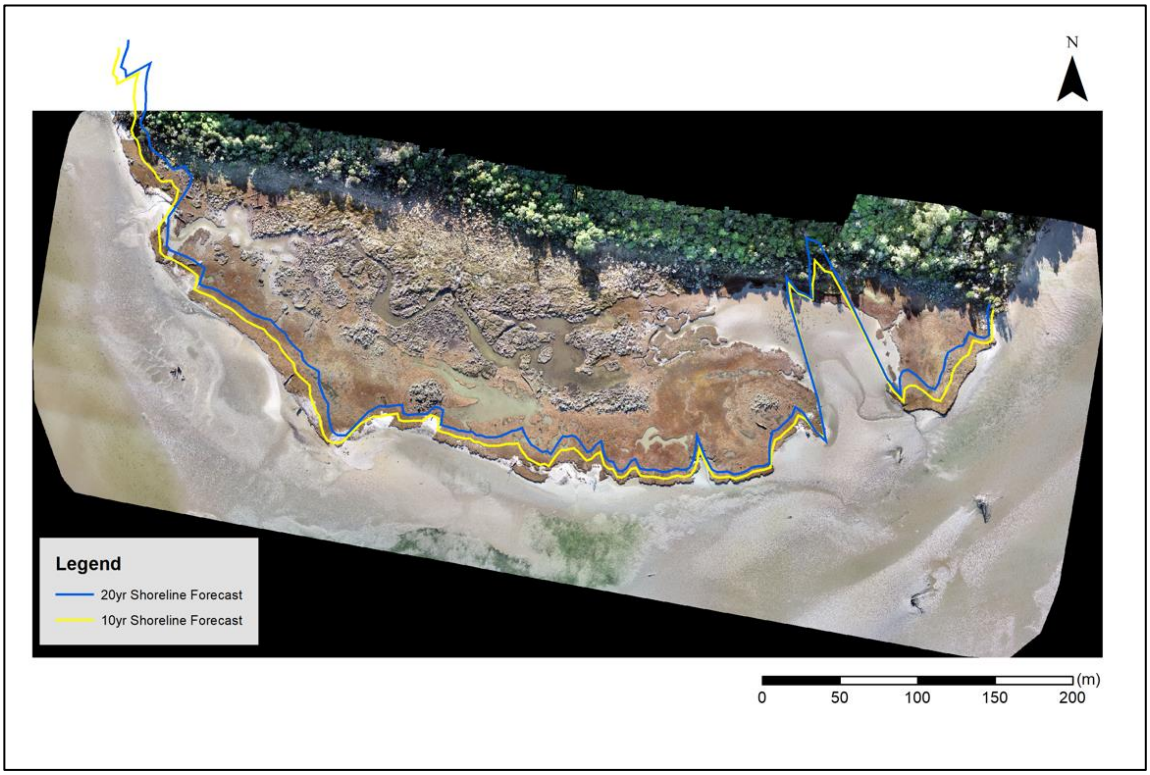

Figure 3.31: DSAS Beta Shoreline Forecasting using the Kalman filter for 10 & 20-year shoreline forecasts. Forecasts are overlain on the June 17th 2022 orthomosiac.

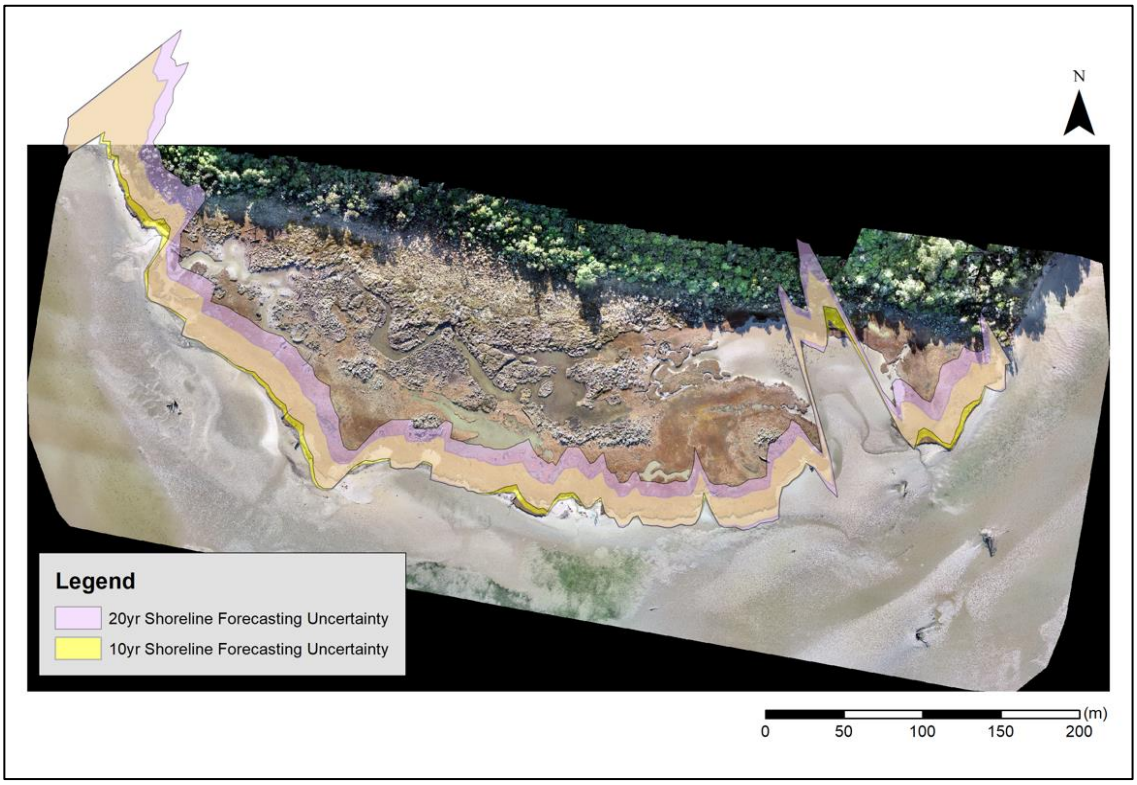

Figure 3.32: DSAS Beta Shoreline Forecasting uncertainty bands for 10 & 20-year shoreline forecasts.

3.8.2. Internal erosion & wetland morphology

The wetlands history is one of erosion, at the same time sections of the wetland are eroding as pools or depressions form. Internal erosion is an important part of the morphological change of the wetland because it will accelerate erosion rates. Internal erosion was not calculated in Figure 3.25 or included in Table 3.4. Internal erosion was not mapped in the majority of the historical aerial images. Erosion may have been present but poor image resolution restricted the ability to map these areas with confidence, therefore, only the latest UAV image from 2022 was used to display internal erosion.

One hypothesis for the formation of internal erosion areas is linked to the Tunnelling Mud Crab (*Austrohelice crassa)*. This endemic species is widespread across the intertidal mudflats and lower and middle marsh, borrowing into the wetland (Figure 3.37, f). The behaviour of these crabs is expressed in their name, they create tunnels on the intertidal sandflat and the wetland itself. Tunnelling on the wetland creates the 'honeycomb' exterior (Figure 3.37, d & e). Crab holes can be found throughout the wetland, the process by which the erosion is initiated is outside the scope of this thesis,

nor is rate of crab erosion or if they cause erosion. Work by Needham (2011) on the same species in the North Island discovered that "increasing burrow density reduced erodibility in cohesive mud, whereas in non-cohesive sand erosion was unimodal, being greatest at low borrow densities" (Needham, 2011, p. v). It is likely that crabs play a role in the morphological change within the wetland but beyond this generalisation their role is unknown and was not the focus of this research.

The presence of macroalgae on the wetland may be negatively affecting the lower marsh species. A second hypothesis for the development of internal erosion pools proposes that the presence of macroalgae on the wetland (Figure 3.14) could be responsible for the death of vegetation. Without vegetation the silty peat would be exposed and susceptable to sediment resuspension and erosion from inundation events. The exact reason for these internal erosion pools is unknown but they are likely to continue to develop and erode the wetland. Elsewhere, macroalgae (*Cladophora, Ulva*) has been known to smother wetland vegetation at the shoreline edge (McComb and Davis, 1993). A study on the relationship between a *Spartina alternifora* wetland and *Ulva* concluded that above and belowground biomass was decreased under high exposure to *Ulva*, whilst, low exposure resulted in only belowground biomass reductions (Watson *et al.*, 2015). Reductions in biomass can result in erosion, however, Pounawea Wetland is not a *Spartina alternifora* wetland so the results are not comparable.

Internal erosion could also be caused by the formation of brackish water ponds. Ponds form in wetlands during inundation. Poor drainage creates natural ponds that would saturate vegetation resulting in plant mortality and peat soil collapse (DeLaune *et al.*, 1994). Poor drainage at Pounawea means that ponds will stay inundated for long periods of time. The low elevation of Pounawea Wetland coupled with SLR, results in frequent inundation. Wetland inundation will be discussed in chapter 5.

The Pounawea Wetland exhibits internal erosion across the wetland (Figure 3.33). The majority of these areas are small (>15 m^2) but one large area exists, located parallel to the creek and ~ 20 m inland from the shoreline edge. This one erosion pool is 1,511 m^2, the total area of internal wetland erosion is 2,131 m^2. There are erosion pools east and west of the main eroded area. A further field observation regarding internal erosion was that areas void of vegetation and that were low lying were observed to be in the early stages of erosion.

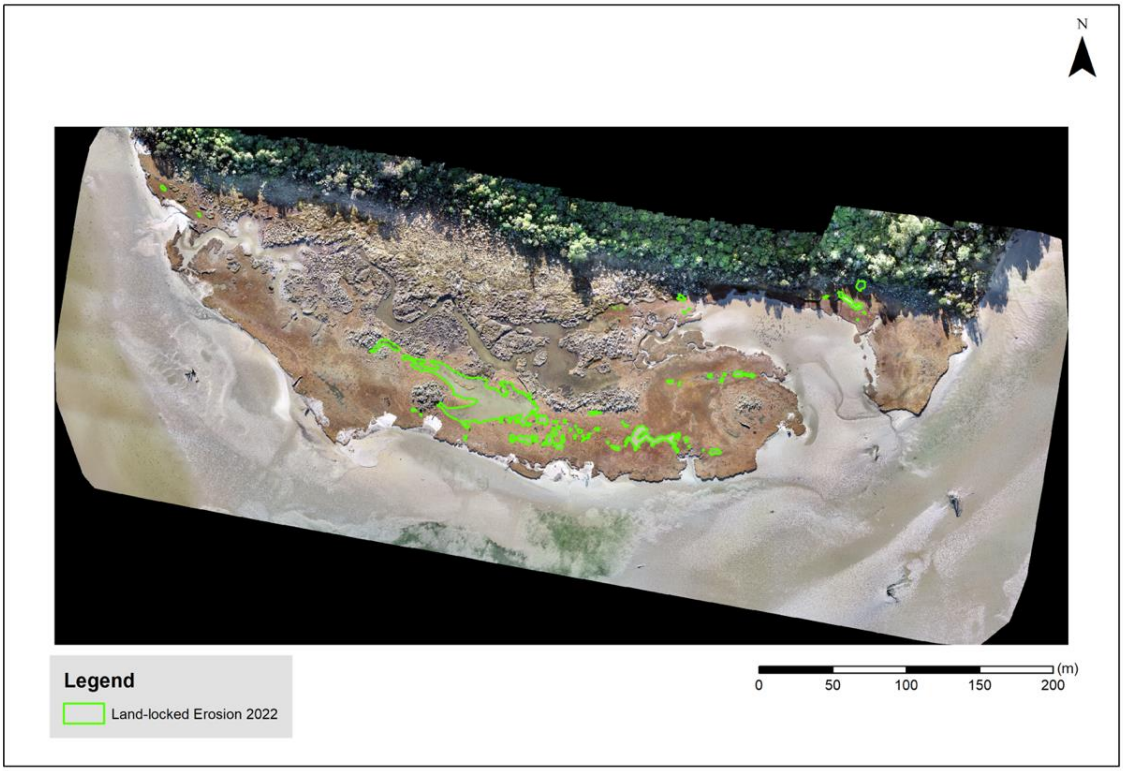

Figure 3.33: Land-locked erosion of Pounawea Wetland, areas that were not connected to the shoreline margin or creek/water were considered to be land-locked. Erosion has occurred internally through vegetation die off and crab erosion.

Pounawea Wetland features a tidal creek that meanders through the wetland (Figure 3.34). The creek's entrance is on the western side of the wetland, water exits the creek at the entrance. The ebb and flood of the tides fill and drain the creek daily. Over time the creek has expanded east, eroding the wetland from within. The entrance of the creek has not changed since 1948 nor has the pathway for water to flow, it has instead extended its flow further inland (Figure 3.34). The creek banks have become wider and a channel arm has developed. The end of the creek has significantly widened and a large pool of water can be observed during high tide. The creek bed is comprised of sand, silt and mud, the mud/silt can exceed depths of 0.3 m. If the creek continues its path east, eroding the wetland from within then it is likely to connect with western inlet sometime in the future. This will effectively divide the wetland laterally and may accelerate erosion.

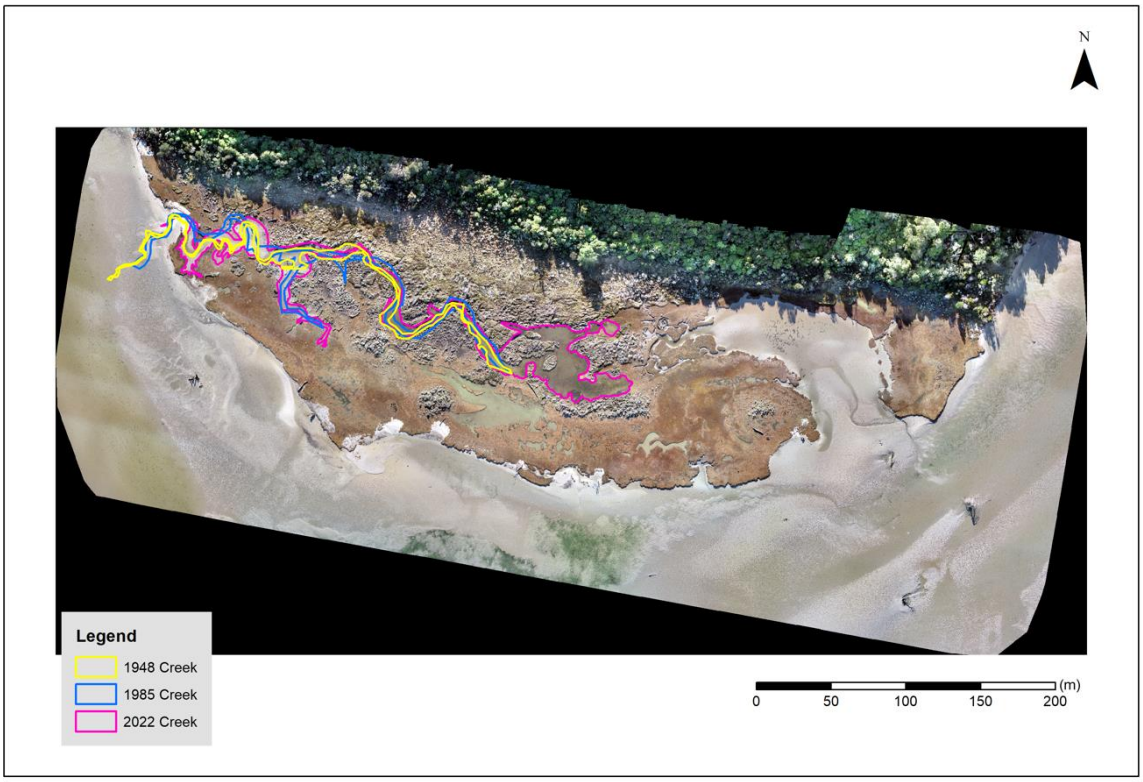

Figure 3.34: Pounawea creek development 1948–2022.

Inundation and storm surge can deposit large debris to areas inaccessible under normal conditions. A significant volume of woody debris, including large logs (1–15 m) partially block the channel pathway, however water is still able to flow through (Figure 3.35). The woody debris likely travelled up the creek channel or over the wetland during storm surges and spring high tide conditions. The ebb tide may not have had the energy to redirected the debris out of the creek and into the estuary. The logs blocking the channel cover 176 square metres.

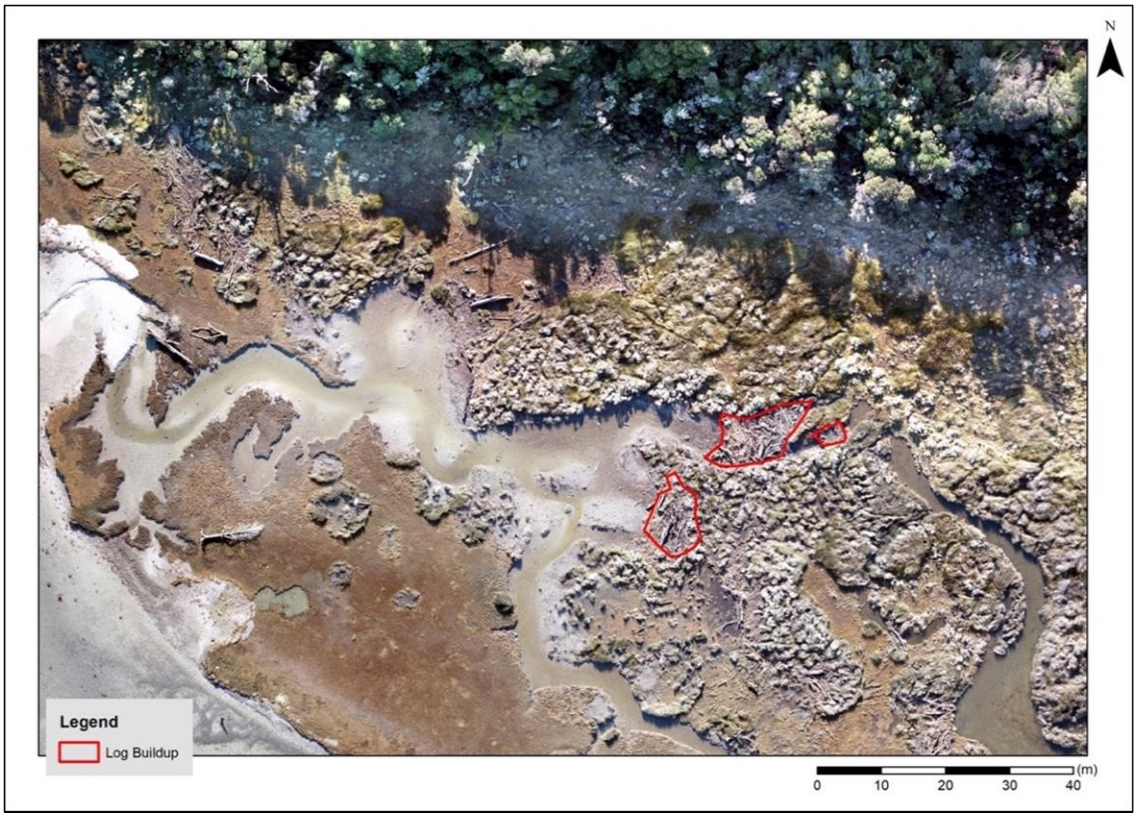

Figure 3.35: Log deposition obstructing the Pounawea creek channel.

3.8.3. Shell deposition

Depositional lobes of shell are a prominent feature of the wetland margins acting as an accretion force on the wetland all be it an imperfect representation of accretion. The development and movement of these depositional lobes has occurred as the wetland has undergone erosion. Shells are suspended during flood tides and storm surge events and deposited onto the wetland. At Pounawea it was common to find cockle shells on the wetland platform (Figure 3.36, b). These shells have been stranded during the November 2021 spring tide event. Several depositional areas since 1967 have been mapped using historical aerial photographs (Figure 3.37). It is difficult to say with certainty regarding the older images but the 2022 UAV orthomosaic shows the shell deposits at the shoreline margin. Upon site inspection the deposits were at the sloped shoreline edge and vegetation was not present. Shells are suspended and deposited and overtime the vegetation dies off due to an inability to photosynthesise because of shell deposition.

Shell banks appear in all historical images except the 1948 aerial image. There appears to be a distinct pattern to the deposition. The southern and western marsh edges feature shell banks throughout the years, the eastern edge does not. The dominant south-westerly wind flow is highly likely to have influenced the deposition of shell. Local wind waves from the south-west could have directed the shells whilst they were in suspension due to high tides. The ebbing tide moves water west to east and therefore could have also played a part in depositional events Between 1967 and 1985 the total area of shell deposits increased by 127% (Figure 3.38). A shell bank appears on the south-eastern edge in 1985. The shell banks have always remained on the shoreline edge, slowing encroaching landward but not once has there been a large deposition in the middle of the wetland. The encroachment is slow but it is occurring. Accretion of sediment and shells has been observed at one shell bank that backs onto an eroded pool (Figure 3.36, a), sediment and shells have been suspended and then deposited several metres inland.

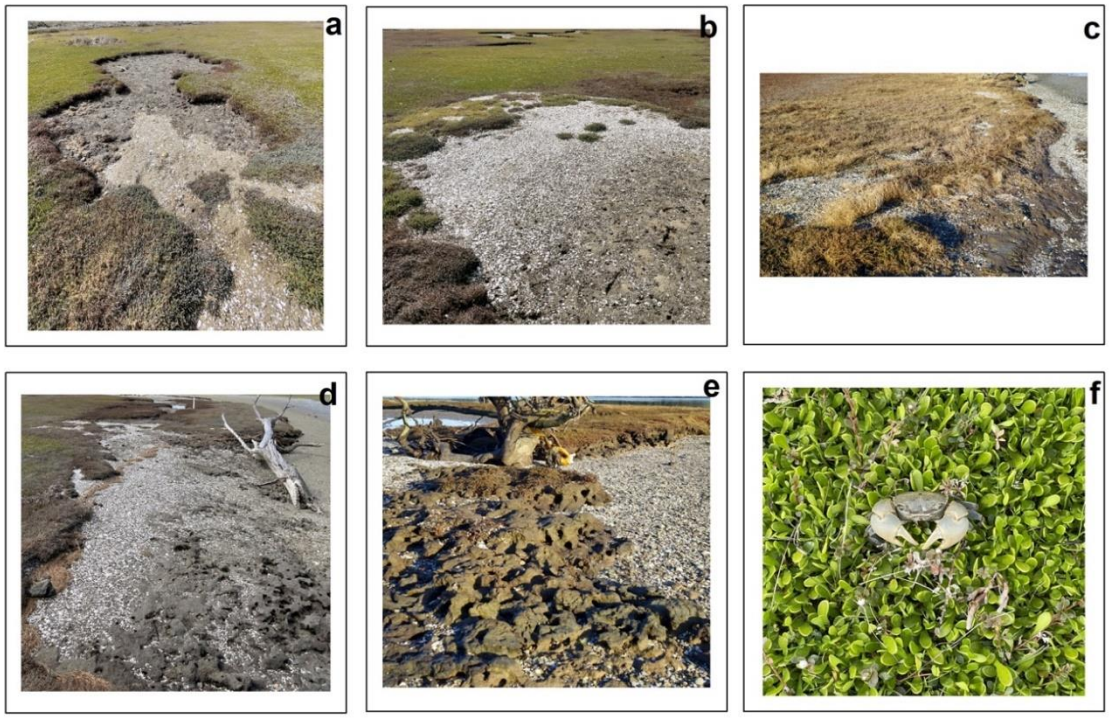

Figure 3.36: Shell accretion at Pounawea wetland; (a) shell and sediment accretion that has spilled into an eroded area at the shoreline; (b) shells banks on the southern shoreline edge, patches of vegetation can be seen throughout the shell bank; (c) shell deposition, shells have been uplifted from the intertidal flat onto vegetation; (d) shell deposition between honey combed marsh edge and vegetated marsh edge; (e) eroded shoreline with honeycomb erosion at the margin; (f) Tunnelling Mud Crab (*Austrohelice crassa*) moving across the dry *S. radicans* wetland area. Photos a, b, d, f was taken personally on the 18th March 2022, c & e were taken by Mike Hilton, 17th June, 2022.

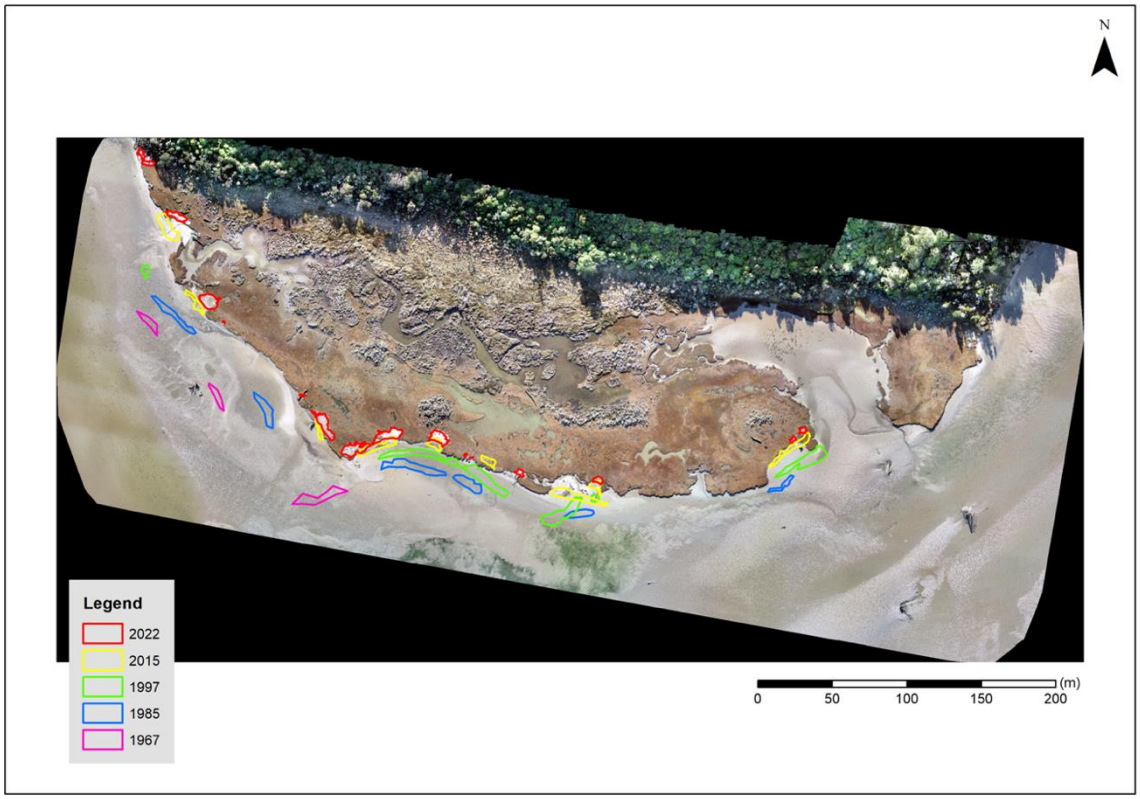

Figure 3.37: Shell over-wash areas of Pounawea Wetland 1967–2022. Highlighted areas are the boundary outlines of shell deposits observed in historical aerial imagery.

As the wetland edge continues to erode, the depositional lobes of shell appear to move at the same rate. The relationship between the wetland edge and shell deposits have remained constant. These shell deposits are similar to beaches, forming in areas of high sediment. Three shell banks have formed since 2015, all are located on the western shoreline. Two are small and one is medium sized and located at the most western edge of the wetland. The size of the shell deposits has varied over time. The 1985 and 1997 shell banks appear to be the largest across the historical analysis, some reaching 50 m in length. The clarity of aerial imagery in 2015 (Appendix A, Figure A9) and 2022 (Figure 3.25) enable a greater level of certainty regarding the boundaries of shell deposits. The boundary shift from tidal flat to shell bank and from shell bank to vegetation is not certain but the overall location and general size of shell deposit are displayed with confidence.

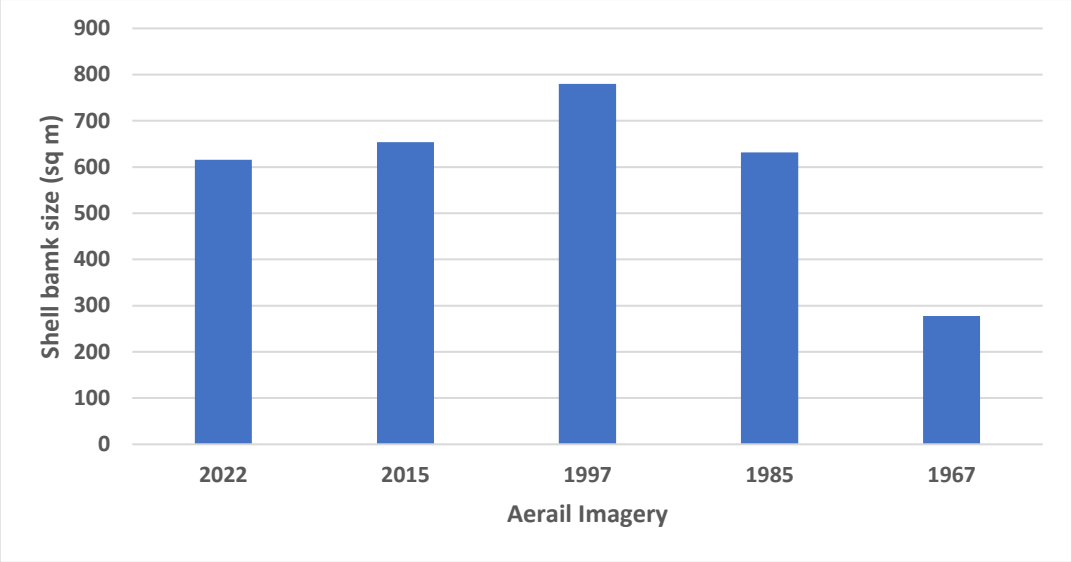

Figure 3.38: Total area of shell deposits since 1967 measured in square metres (sq m).

3.8.4. Human intervention

Today, the Pounawea Wetland is a protected area and recognised as a 'Regionally Significant Wetland' by the ORC (ORC, 2020b), this was not always the case. Species were introduced and structures were erected. *Spartina anglica (S. anglica)* was introduced to the Catlins Estuary in 1955 after being planted in the New River Estuary in Invercargill in the 1930s (Lee and Partridge, 1983). *Spartina anglica* invades sand flats, traps sediment and outcompetes the herbaceous vegetation. For this reason, it was removed in the 1970s through a spray and dig out program and is not present today. *Spartina anglica* is a prominent species in Europe and has been the focus of several studies of marsh erosion. It is widely seen as a species that could be used to re-stabilise wetland regions through sediment accretion and protect against erosion through wave attenuation (Balke *et al.*, 2012; van Eerdt 1985; van Loon-Steensma *et al.*, 2014). The spread of *S. anglica* is documented in Bascand (1970) and rates of accretion were measured in Lee & Partridge (1983). The Department of Conservation (DoC) has taken an active role in reducing its spread over the last 50 years (Brown and Raal, 2013). No documents could be found discussing the spray program that took place at Pounawea. Partridge (1984) mentioned digging out *S. anglica* with the removal of all plants except two by 1979 (Partridge, 1984). Today, *S. anglica* is present but is actively managed by DoC.

Structures once existed on the wetland, however, they were either removed or eroded. A Crown ranger and his family lived in old limeburner's hut on the eastern edge (Tyrrell, 2006). A limestone burner was also built, shells were melted down and used in construction (Tyrrell, 2006). Two Macrocarpa trees were planted to shelter the hut from the wind and one exists today in the estuary.

3.9. ENVIRONMENTAL CHANGE IN THE LOWER CATLINS ESTUARY

The historical boundary changes of the Catlins Estuary have likely contributed to the acceleration of shoreline erosion. Loss of protective barriers and forest clearance have increased the exposure of the wetland to fetch-limited local wind waves. If the current rate of shoreline erosion is to continue the wetland is going to significantly shrink, the western and eastern edges will be the worst affected. Mapping shoreline change over time has provided sufficient evidence to confidently state that based on historic shoreline erosion zones 2 & 3 of Pounawea Wetland will be completely eroded by the year 2150.

3.9.1. Cabbage Point and Manuka Point

The erosion of Cabbage Point resulted in an increase in the LRR. This erosion increased the exposure of the eastern shoreline to marine processes, furthering the acceleration of erosion. DSAS analysis pre and post erosion illustrated an increase in LRR after 1985 (Figure 3.29 & Figure 3.30). The erosion rate increased by 0.05 m/yr, this equates to an 8% increase in LRR, resulting in an additional loss of 1.85 m of shoreline due to the increase in LRR post Cabbage Point erosion. DSAS has been used as a tool to examine the data. The software is based on several assumptions and is by no means a precise analysis of complex shorelines, meaning that the results should be treated with caution. Inferences can be made that there has been a net increase in LRR since the erosion of Cabbage Point.

As outlined in section 3.7.2, Cabbage Point was a large vegetated sand spit, acting as a barrier island between the open coast and the Catlins Estuary. A storm in 1975 buried the vegetation in sand (Partridge, 1984) and this is likely the beginning of the significant transformation and erosion of the spit that took place between 1967–1985 (Figure 3.21).

GIS mapping of the spit boundary indicated significant loss of sand area. Today the spit is visible at low tide and inundated at high tide. This was not the case 40 years ago. The role of barrier protection for coastal erosion mitigation will be discussed in chapter 6.

The erosion of Cabbage Point and Manuka Island has increased the fetch potential of the Catlins Estuary mouth at high tide. Greater fetch would enable larger local wind waves to develop (Fagherazzi and Wiberg, 2009; Hunt *et al.*, 2015; Prahalad *et al.*, 2014). The statement that the erosion of the Pounawea foreshore was enabled by erosion of Cabbage Point and Manuka Point is made with low confidence. Nevertheless, the 2006 erosion event took place under spring tide conditions, coupled with an additional 10 cm of sea level due to the low pressure but ultimately it was the strong SSE wind that was the driving factor for erosion to occur.

The lack of wave data, surveying measurements and physical observations of Cabbage Point make it difficult to accurately interpret what the aerial images are showing. Furthermore, infrequent aerial imagery, specifically during 1948–1967 limits the ability to determine the rate of erosion or at what point it started to accelerate. It may have been the storm mentioned by Partridge (1984) that initiated the erosion or it might have been one of many during 1967–1985. Long- term survey and wave data would be needed to make accurate comparisons and conclusions. It is clear that land-use change, erosion and infrastructure development have all shaped the area. The 2006 erosion event illustrated that even under moderate storm surge erosion can occur.

3.9.2. Pounawea Wetland shoreline erosion

Shoreline erosion is an ongoing threat to the survival of Pounawea Wetland. The shoreline is eroding at a rate of -0.67 ± 0.05 m/yr. The results demonstrate that the western and eastern shoreline edge are eroding at a faster rate than the southern margin (Figure 3.28). The exposure to the south-west & north-east winds may have contributed to the generation of local wind waves and subsequent erosion (Prahalad *et al.*, 2014; Smith *et al.*, 2001). The importance of shelter from prevailing winds is illustrated within the inlet (Figure 3.24) and this will process is examined in the next chapter. The inlet has the slowest rates of erosion of anywhere on the wetland. Protection from the north-east wind from the podocarp forest and the south-west wind from salt meadow means that wave action is not likely within the inlet. Leonardi *et al.* (2016) discusses how marsh

erosion typically occurs under storm conditions with a return period of 2.5 months. Such conditions are rarely experienced within the inlet and therefore erosion has occurred at a significantly reduced rate. The eastern and western margins experience the prevailing winds regularly, increasing the likelihood of erosional events. The southern shoreline edge is not directly affected by the prevailing north-east wind. It is affected by the south-west wind but not as severely as the western edge and this may be why LRR are lower.

Beta Shoreline Forecasting is a useful tool to gauge how the wetland may develop in the future. It uses past rates of erosion and assumes constant environmental conditions, however, sea-level is rising and this will affect the wetland. There are other environmental and hydrodynamic processes that are not considered in the forecast. The forecast depicts continued shoreline erosion. The loss of more shoreline reduces salt meadow species habitat, specifically, *Samolus repens* and *Sarcocornia quinqueflora*. These two species occupy the shoreline edge due to their increased saline tolerance (Partridge and Wilson, 1988; Partridge and Wilson, 1989). If the upper margin of the 20 yr shoreline prediction band were to occur then the new shoreline would align with the large land-locked erosion pool (Appendix A, Figure A13). This would mean that the new shoreline would be the landward edge of the erosion pool, significantly decreasing the total area of the wetland.

The erosion pools are expanding and if they continue then wetland erosion will accelerate. How these erosion features form was not discussed in this research. Two external processes could be influencing the development of the pools. Firstly, crab borrowing and sediment shifting. Secondly, deposited macro-algae could provide excess fertilizer and decay the vegetation or it could help fuel vegetation growth. Further research would be needed to better understand the role of macro-algae on the wetland.

The results indicate that the southern podocarp forest boundary has not moved significantly in 40 years. This suggests that the upper marsh zone of shrubs may have reached its landward boundary. The inability for wetlands to transgress is often associated with coastal squeeze (Borchert *et al.*, 2018; Enwright *et al.*, 2016; Luisa Martínez *et al.*, 2014; Pontee, 2013; Silva *et al.*, 2020). Coastal squeeze occurs when wetlands are caught between rising sea levels and permanent development (seawall) or raised agricultural land. Whereby, the wetland is squeezed between the two and either adapts or is inundated and lost. Pounawea Wetland does not feature permanent features rather a native podocarp forest. From the historical evidence of landward transgression

(Figure 3.8) the upper marsh zone is more than likely to continue to transgress towards the forest. This transgression will reduce the size of the forest and have knock-on effects for biodiversity. The forest is under threat from SLR and frequent inundation, these impacts will be discussed in the next chapter.

3.10. SUMMARY

This chapter has detailed the morphodynamics and historical shoreline and vegetation change of Pounawea Wetland. A range of methods were used to document and analyse changes in boundary conditions, shoreline erosion and vegetation cover. The findings of this chapter are summarised below.

Shoreline erosion at Pounawea Wetland has been continuous since the first aerial photograph in 1948. DSAS cast 181 transects, 96.69% were statistically significant and the average rate of erosion per year was -0.67 ± 0.05 m. There were zero areas that showed statistically significant accretion. DSAS determined higher LRR at the western and eastern shoreline edges comparative to the southern edge. The exposure of these two areas to the prevailing winds, southwest and northeast, is likely to have increased the frequency and severity of fetch limited local wind waves, this hypothesis will be discussed in the following chapter. There has been a small increase in LRR post Cabbage Point erosion, from this we can infer that Cabbage Point was protecting the wetland from local wind waves and erosion.

Vegetation cover at zones 2 & 3 has decreased, the upper marsh boundary shifted landward, due to the recession of the podocarp forest. Zone 2 species (shrubs) have developed in lee of the receding forest margin. Salt marsh vegetation has declined because of shoreline erosion. Shoreline erosion will continue to decrease the area of viable habitat for salt marsh species. The effects of SLR and inundation will be discussed in chapters 4 & 5, respectively. The future of the wetland and its vegetation will be discussed in chapter 6.

The next chapter will analyse and discuss the role of vertical land movement, sea-level rise and climatic conditions in the potential erosion and inundation of the wetland.

Additionally, computational fluid dynamics will be used to illustrate the effect of an upwind podocarp forest and its effect on wind speed across the estuary.

4. Changing Boundary Conditions and their Effect on Pounawea Wetland

4.1. INTRODUCTION

The previous chapter discussed historic boundary changes and morphodynamics of the Catlins Estuary and Pounawea Wetland. The focus of chapter 4 will be on the changing boundary conditions and their effect on the wetland. Specifically, weather events resulting in erosion, sea level rise (SLR), vertical land movement (VLM) and the removal of a podocarp forest upwind of the wetland. Two research questions were formed; (1) is there any evidence of change in frequency or severity or nature of weather events that might impact the wetland? (2) how have boundary conditions have changed?

Understanding changing boundary conditions and the impact this might have on the environment is critical for understanding the environmental conditions of the wetland in the future. Understanding the historic weather events and identifying trends is important for developing an understanding of wetland inundation and erosion. Potential Erosion Events (PEE) occur when atmospheric pressure is <1000 hPa and wind speed is >7 ms^{-1} and from the south–west (180°–270°). Climate data (1972–2022) from Nugget Point was used for this analysis and SLR and VLM predictions taken from the *NZ SeaRise: Te Tai Pari O Aotearoa programme*.

The Catlins Estuary has undergone extensive land use change in the form of deforestation since European colonisation in 1860. The forest upwind of the wetland is likely to have sheltered the estuary from south-westerly winds. Computational Fluid Dynamics (CFD) was used to model wind speed over the estuary with and without the forest. Forests provide a leeward sheltering effect (Heisler and Dewalle, 1988; Markfort *et al.*, 2010). The sheltering effect can extend upwards of fifty times the height of the object providing the shelter (Heisler and Dewalle, 1988). Wave height is related to wind speed, fetch distance and water depth (Breugem and Holthuijsen, 2007).

This chapter will begin by discussing the methods for analysing climatic data and the development and implementation of the CFD simulations. Following this, the results section will examine how and if weather conditions have changed and the effect of forest

removal on wind speed across the estuary. The discussion will interpret and analyse the findings presented in the results. Finally, a summary of key findings is provided in section 4.5.

4.1.1. Sea-level change

Sea-level change is having a direct effect on wetland inundation and erosion. This section contextualises local sea-level change to build an understanding as to how SLR has affected Pounawea Wetland.

Sea-level is variable around the world leading to acceleration in rates of SLR for certain regions. The Tropical and Subtropical Pacific has seen an acceleration of SLR since 1993. Interdecadal Pacific Oscillation (IPO) and El-Niño Southern Oscillation (ENSO) are two drivers of this increase and future models have taken these processes into consideration when assessing future sea-level (Ackerley *et al.*, 2013). Hannah and Bell (2012) observed ±6 mm sea surface rises during La Niña and ±6 mm decreases during El Niño (Hannah and Bell, 2012). ENSO variability on a monthly scale of -0.10 m to +0.14 m was observed in Auckland (Bell and Goring, 1998; Hannah *et al.*, 2011). Tree ring records demonstrate an increase in the strength of ENSO during the twentieth century comparative to the last five centuries, indicating an increase in ENSO strength as temperatures warm (Fowler *et al.*, 2012). IPO can affect sea-surface by ± 5 cm further solidifying the dynamic nature of sea-level processes. Another influence on local sea-level is the Southland Front/Southland Current (Wunsch *et al.*, 2007). The reconstruction of sea-level using foraminifera in New Zealand and specifically at Pounawea Wetland reiterates a significant acceleration of SLR during the twentieth century (Gehrels *et al.*, 2008). Sea-level was increasing at 0.3 ± 0.3 mm/yr from AD 1500-1900 then sharply increases to 2.8 ± 0.5 mm/yr from 1900 – 1993 (Figure 4.1). The increase seen from 1900-1993 aligns with the long-term tide gauge records of Lyttelton, Dunedin and Bluff.

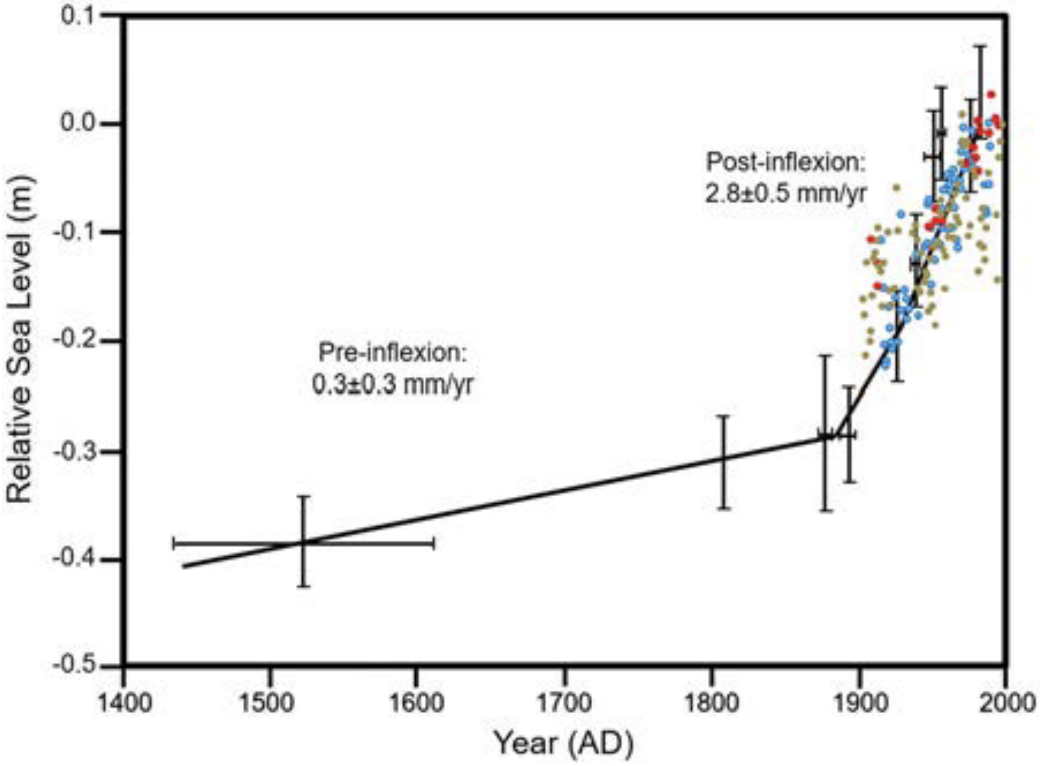

Figure 4.1: The relative sea-level curve derived from the Pounawea salt marsh by Gehrels *et al.* (2008), plotted with the annual sea-level data recorded at the Lyttelton (blue dots), Bluff (red dots), and Dunedin (green dots) tide gauges. Modified after Gehrels *et al.* (2008), with additional data from the Permanent Service for Mean Sea Level (Holgate et al. 2013). Figure and caption from King *et al.* (2020).

4.1.2. Dunedin sea-level

Dunedin mean sea-level has increased since records were established in 1899. In 2021 sea-level was 1.16 m, an increase of 0.233 m over 122 years (Figure 4.2). Variability year on year is common within sea-level records. A trendline has been inserted and illustrates an average sea-level in 2021 as 1.12 m (Figure 4.2). The Dunedin record is not complete, 15.4% of the record is missing, a five-year gap from 1991–1995 is present. Missing data has been inferred by LINZ, represented by the dashed lined. This long-term sea-level data provides insights into the trends of the South-eastern coastline of New Zealand.

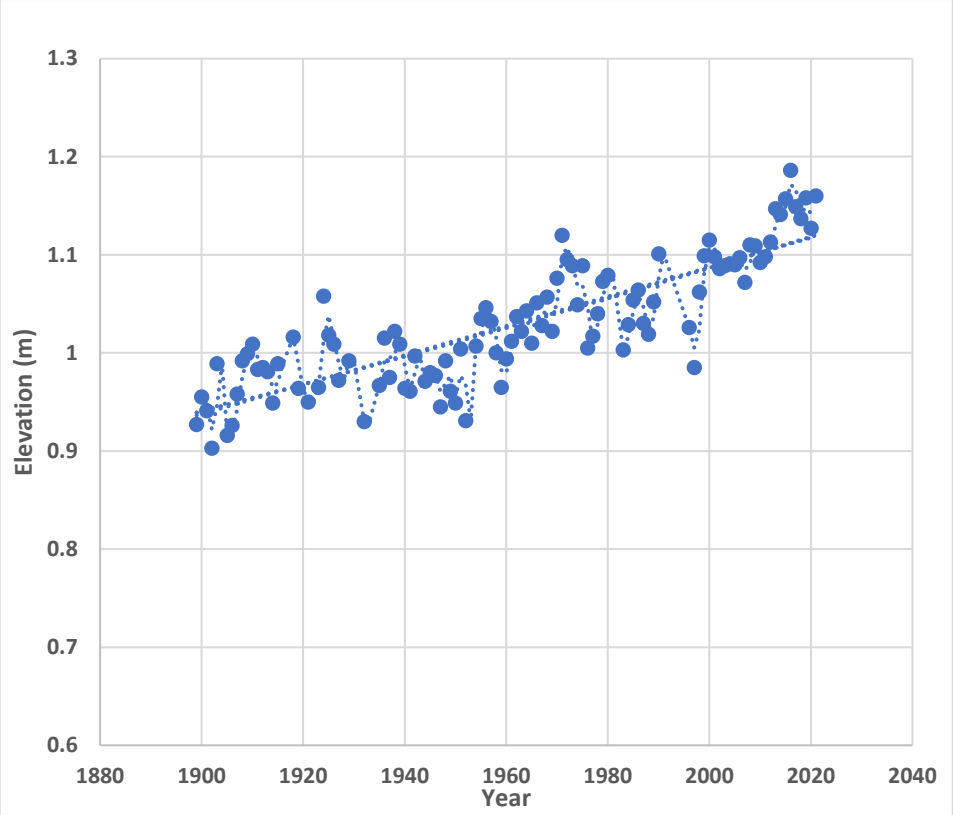

Figure 4.2: Dunedin sea-level record 1899-2021. Data courtesy of LINZ

4.2. METHODS

4.2.1. Sea-level rise and vertical land movement

Dunedin sea-level was derived from the Dunedin sea-level gauge (Hannah and Bell, 2012). Vertical Land Movement (VLM) measurements were calculated from the *NZ SeaRise: Te Tai Pari O Aotearoa programme*. The programme calculated and forecast VLM for every 2 km of New Zealand's coastline (King *et al.*, 2020). The two locations that were used in this research are shown below (Figure 4.3).

Figure 4.3: Locations of measurement for VLM for the *NZ SeaRise: Te Tai Pari O Aotearoa* programme. Red X's mark the locations of the North and South VLM indicators. VLM for the north is 1.06mm/yr, and the southern VLM is 1.67 mm/yr, the average of the two locations (1.37 mm/yr) was used for calculations.

4.2.2. Historic climate record

Climate data from 1972-2013 was provided by the National Climate Database (https://cliflo.niwa.co.nz/) and climate data from 2013 was obtained from *MetService*. The data was collected from instruments located at Nugget Point (Figure 1.1). Wind speed data from Nugget Point is not a direct reflection of the wind conditions at the Catlins Estuary. Nugget Point climate station is located on a peninsula and it is likely to record winds that have experienced significant topographic acceleration (in accordance with Bernoulli's principle, Hewitt, 2004). Wind re-direction is also an effect of topographic steering, therefore, recordings at Nugget Point may not represent wind direction accurately. Hourly records of atmospheric pressure (hPa) and average wind speed (m/s) and direction were used. Only records that had all three variables were used in the analysis for potential erosion events (PEE). Instances of instrument failure or missing data at Nugget Point resulted in the removal of pressure, wind speed and

direction data for that period. Pressure data was divided into four groups; extreme low pressure (960–979 hPa); low pressure (980–999 hPa); moderate pressure (1000–1019 hPa); and high pressure (>1020 hPa). Wind direction data was separated into three categories; (1): 0–180°; (2): 180–270°; (3): >270°. This was done to focus on wind from a south–west direction (180–270°) because the fetch potential is greatest and thereby wave development is likely to occur and effect the wetland shoreline. Pressure and wind data were categorised into decadal and yearly time periods. Data was available from 1972 but the data was only recorded once per day (9:00 am), this was increased to three times per day from 1978, then every three hours in 1980 and hourly records were available from January 1995. Weather observations have been sampled at these intervals which means that there are large differences in the number of events that have been recorded. The figures in section 4.3.2 use the absolute value of events. An event is one recorded climate observation, the combination of pressure and wind at one recording is still one event.

MatLab was utilised to interpolate wind and pressure data to determine potential erosion events (PEE). Missing data for either column (wind speed, direction and pressure) resulted in the entire row being deleted. Groupings were used in Microsoft Excel to classify the different variables and the function 'VLOOKUP' was used to order these variables. The class structure for wind direction remained the same. Pressure data was re-grouped into two classes; (1) >960>1000 hPa; (2) >1000 hPa. This was done to simplify the data. The combination of pressure and wind data was completed using 'IF' and 'AND' functions in Microsoft Excel. The requirements for erosion potential (EP) were, pressure > 1000 hPa, wind direction < 180° > 270° and wind speed > 7 ms^{-1}. If one of these requirements was not met then the recording was classed 'non-erosion event' (NEE).

Tidal data was not included in Figure 4.10. This chapter is not analysing how often inundation and subsequent erosion may have occurred, but rather it is analysing changing climatic boundaries. It is noted that SLR would have increased the tidal levels since 1972 and this is a changing boundary condition, an analysis of the frequency of inundation events will be discussed in the next chapter.

4.2.3. Computational fluid dynamic (CFD) modelling

Computational Fluid Dynamics (CFD) is a common tool used by researchers to investigate hypotheses related to fluid dynamics using the Naiver-Stokes equations (Smyth, 2016). Numerical algorithms are used to solve Navier-Stokes equations over a meshed computational domain (Smyth, 2016). Algorithms abide by conservation laws, where, mass can neither be created nor destroyed (conservation of mass). Momentum is conserved following Newton's second law and the conservation of energy is derived from the first law of thermodynamics (Smyth, 2016). Increasing the density of cells within the mesh improves the quality of the model output, however, the computing power and the time taken to solve the model increases significantly. CFD is a multi-disciplinary software tool that has become increasing popular in aeolian and fluid mechanics (Bauer and Wakes, 2022; Feichtner *et al.*, 2020). The ability to replicate environmental conditions, study site morphology and external inputs allows for a range of scenarios to be simulated in a cost-effective manner.

Model validation is an important part of CFD. Validation using field data allows for an accurate assessment of the efficacy of the models' outputs (Jiang *et al.*, 2013). Without validation, CFD results are merely theoretical and cannot be confirmed. Validation is important, however, the flexibility within CFD allows for environmental conditions to be simulated that cannot be replicated in the field. This contributes to the understanding of potential environmental outcomes, for example, sea-level rise and the effect of wave formation and erosion.

CFD was used to understand the sheltering effect of podocarp forest at Hinahina (Figure 4.11). Vegetation interrupts the momentum of airflow (Gillies *et al.*, 2006), causing decreases in wind speed. For this model, several assumptions were made due to the lack of historic and local wind data. Firstly, the drag co-efficient (Cd) of the forest was set at '0', '0.005', 0.009, 0.05, 0.1 and 0.15. The drag co-efficient represents the amount of resistance wind flow will experience as it passes through the forest boundary. The drag co-efficient (for the purpose of this research the drag co-efficient will be referred to as porosity) were selected based on literature focused on canopy flow modelling (Cedell, 2019; Jiang *et al.*, 2013; Jian *et al.*, 2018; Liu *et al.*, 2014). Secondly, tree height was set at 40 metres. Tree height is directly correlated with the length of the lee effect (Markfort *et al.*, 2010). Tree height was estimated from historical images (Figure 4.11). Other aerodynamic and hydrodynamic processes (Reynolds stress, Eddy

viscosity model, bottom shear stress and wave energy) that would influence wind flow and wave morphology were not considered during modelling.

Lack of physical data (local wind and wave records before and after forest removal) meant model validation was not possible, however, research literature provided a good base knowledge of what is to be expected from the model (Feichtner *et al.*, 2020; Jian *et al.*, 2018; Liu *et al.*, 2014; Mahgoub and Ghani, 2021; Ross and Baker, 2012). The model's purpose is to assess the effect of the forest on wind speed across the estuary and then inferring how wave height may have been influenced by the change in windspeed since the forest was removed.

Software ANSYS 20 was used to run the two-dimensional model. LiDAR data from a 2021 flight completed by Otago Regional Council (ORC) was used to construct the elevation profile used for the boundary conditions of the model. The LiDAR was processed in ArcGIS and exported to Excel. The effect of the topography on the wind speed and porosity of the forest is acknowledge but has been ignored (Ross and Baker, 2012). Furthermore, design modeller (where the CFD model is constructed) has a maximum domain length of 3 km, it is for this reason that the profile was reduced from 3500 m to 2800 m (Figure 4.12, c), reducing the effect of the Hinahina hills. To further simplify the model, a rectangle domain was used in place of individual tree structures or cylinders. This will impact the ability of this simulation to accurately represent the forest conditions, nevertheless, the porosity of the rectangle has been altered to reflect forest like conditions (Liu *et al.*, 2014; Mahgoub and Ghani, 2021). The height of the domains was set to 700 m, exceeding the requirements for airflow above the canopy surface (Mahgoub and Ghani, 2021).

The mesh was constructed using squares with a growth rate of 1.2, other statistics relating to the mesh can be found in Table 4.1. The mesh used for the simulation (Figure 4.4) and a close up view of the forest boundary (Figure 4.5) illustrates the denser mesh around the forest boundary. A dense mesh was used because the focus of the modelling centred on the relationship between wind speed and the surface, the denser mesh provided increased model accuracy.

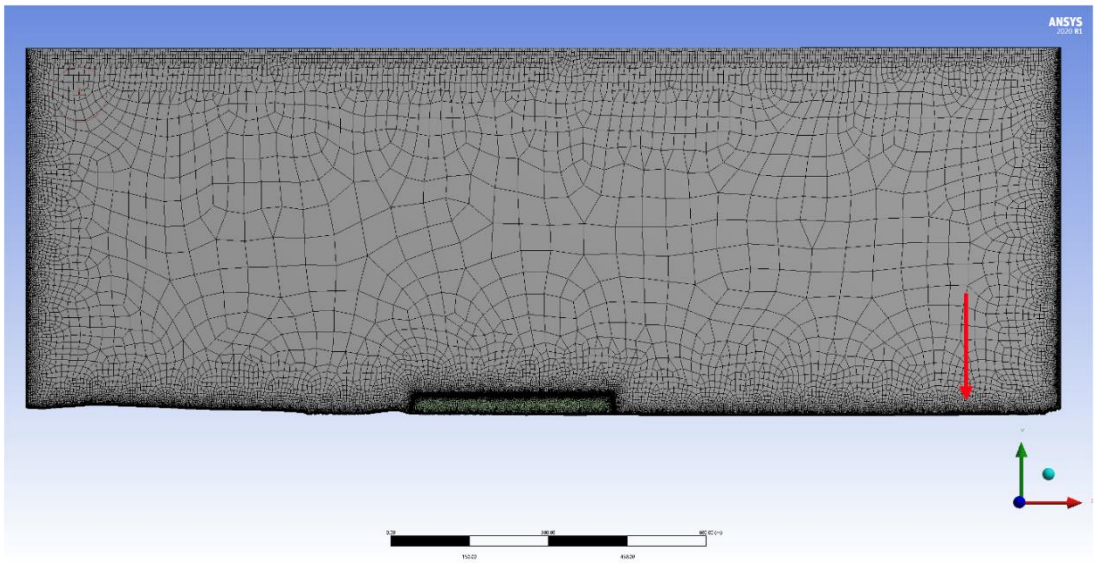

Figure 4.4: CFD mesh of forest model. Estuary margins outlined by orange lines; red arrow outlines the seaward edge of Pounawea Wetland.

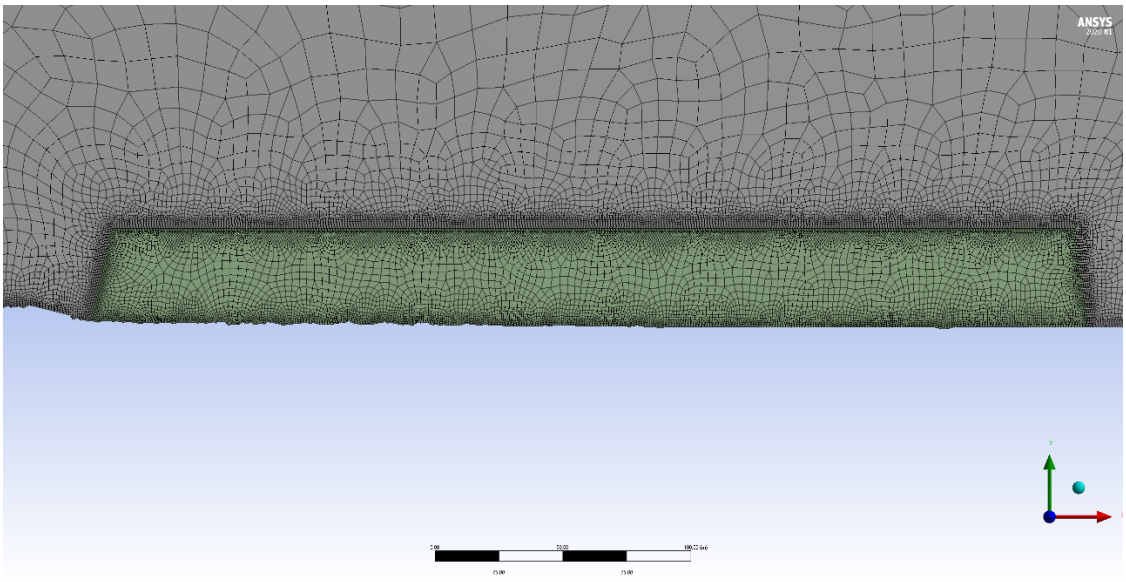

Figure 4.5: Close up of forest boundary mesh. The edges of the boundary and surface areas feature more elements and therefore are denser and results in greater accuracy.

Table 4.1: Mesh statistics

Nodes	64097
Elements	61160
Growth Rate	1.2
Maximum Aspect Ratio	0.272
Maximum Skewness	0.74779
Minimum orthogonal quality	0.4264

Wind Speed

Inlet wind speed was inputted as a code developed by Dr. Duc Nguyen. This code uses logarithmic calculations to output wind speed. Variations of the code were inputted to simulate different wind speeds. Input conditions were changed during the setup phase within ANSYS Parallel Fluent. The code used can be found in Appendix B. The model used the RNG k-ε method within ANSYS Fluent to simulate turbulence. Model parameters converged at a residual value of 1×10^{-4} as discussed in literature (Hesp and Smyth, 2021; Bauer and Wakes, 2022).

To calculate inlet wind speed, a velocity profile was erected 510 m before the forest boundary. By increasing or decreasing the wind speed the relationship between drag co-efficient and wind speed remains constant. Graphs depicting increased inlet wind speed can be found in Appendix B (Figure B1 and Figure B2).

Velocity profiles were created in CFD Post and extracted from four areas of the larger domain; forest edge (VP1); estuary 1 (VP2); estuary 2 (VP2); and wetland edge (VP4); each location is found in Figure 4.12. The velocity profiles were placed 200 m apart. The four locations were analysed individually and then a comparison for each porosity and wind speed simulation was undertaken. Each velocity profile was individually adjusted to begin recording data at levels associated with spring high tide, tide calculations were made assuming normal atmospheric conditions. Three profiles required adjustment, V2 (1.7 m), V3 (1.7 m) and V4 (0.8 m). The model parameters

remained constant, Cd was changed to simulate forest flow resistance. The maximum Cd was 0.15, this represents a dense, mature forest with limited flow capacity.

4.2.4. Calculating fetch limited waves

Fetch limited waves were calculated across the estuary using wind speed data generated from CFD models with and without the forest. The relationship between significant wave height and wind speed in shallow intertidal estuaries is complex and variable. Variations in wind speed, tidal water depth and surface roughness are contributing factors towards the development of fetch-limited wind waves (Smith *et al.*, 2001). Shallow water wave theory (Breugem and Holthuijsen, 2007) was used to calculate fetch-limited waves (Equation 1). This theory was also applied to the velocity profile outputs. The calculations for significant wave height (H_s) were executed using *eCoast* marine calculator (https://www.ecoast.co.nz/marine_calculators). The input variables required were; wind speed (ms^{-1}), fetch (km) and depth (m). The velocity profiles provided wind speed for three locations (V2, V3 and V4) at Y = 1 m. The fetch across the estuary was 0.6 km and the depth was averaged as 1.5 m. The outputs were; significant wave height (H_s), peak period (T_p) and time until fetch limited waves were developed (hours). Significant wave height (H_s) is the output of focus for this thesis, the others will not be included. Graphical outputs were also created using the *eCoast* marine calculator however, these were linear relationships and subsequently excluded.

Shallow wave theory calculates significant wave height as a linear relationship with wind speed. The inlet speed was ~12.47 ms^{-1}, classified as a 'strong breeze' on the Beaufort Scale (Monmonier, 2005). If wind speed is increased to ~20 ms^{-1} (Fresh gale), significant wave height would be 0.38 m (Breugem and Holthuijsen, 2007). Wind events exceeding 20 ms^{-1} are infrequent but they do happen during low pressure storm events.

Equation 1: Equations for fetch limited waves by (Breugem and Holthuijsen (2007) taken from the *eCoast* marine calculator. H_s = significant wave height; g = gravity (9.81 ms^{-1}); F = Fetch; Z = depth; u_{10} = wind speed.

$$H_{max} = \frac{0.24u_{10}^2}{g}$$

$$depth\_term = tanh\left(0.343\left(\frac{g * Z}{u_{10}^2}\right)^{1.14}\right)$$

$$fetch\_term = 0.000414\left(\frac{g * F}{u_{10}^2}\right)^{0.79}$$

$$H_s = h_{max} * \left(depth\_term \times tanh\left(\frac{fetch\_term}{depth\_term}\right)\right)^{0.572}$$

$$T_{max} = \frac{7.69u_{10}^2}{g}$$

$$depth\_term = tanh\left(0.1\left(\frac{g * Z}{u_{10}^2}\right)^{2.01}\right)$$

$$fetch_{term} = 0.0000\ 00277\left(\frac{g * F}{u_{10}^2}\right)^{0.187}$$

$$T_p = T_{max} * \left(depth\_term \times tanh\left(\frac{fetch\_term}{depth\_term}\right)\right)^{0.572}$$

$$time\_to\_develop = \frac{77.23F^{0.67}}{u10^{034} * g^{0.33}}$$

4.3. RESULTS

4.3.1. Vertical land movement

New Zealand is located on the edge of the Pacific Rim of Fire and at the collision zone of the Pacific Plate and Indo-Australian Plate (Okaya *et al.*, 2007). New Zealand has experienced rapid vertical uplift caused by earthquakes. Most recently, the 2016 M_w 7.8 Kaikoura earthquake which saw areas north of Kaikoura uplifted by 6 m and areas south of Kaikoura subside by -2.5 m (Xu *et al.*, 2018). The movement of land through earthquakes is hard to predict but important to understand. Natural forces can quickly alter the environmental boundary conditions of an area. Uplift will cause a net decrease in SLR and land subsidence will have a net increase in SLR. Dunedin has had two significant earthquakes in historic times, 1st September 1945 and 12th October 1979, M_w 7.4 and 7.3 respectively (Denys *et al.*, 2020). However, at the Puysegur Subduction Zone in Fiordland, where the Australian Plate is subducting under the Pacific Plate, the effects of this subduction could result in changes in VLM and SLR at a regional scale. Understanding how these changes occur globally is beyond the scope of this research, however, understanding the impact of land movement locally is important when discussing and forecasting for SLR.

Vertical land movement (VLM) is a significant factor in the acceleration of SLR. Local land movements can alter the rate at which SLR will affect coastlines. Vertical uplift at a rate faster than projected SLR (3 mm/yr) will result in a net decrease in SLR. Land subsidence will result in a net increase in SLR. The inclusion of VLM for all local SLR predictions throughout New Zealand has recently been calculated and voiced (King *et al.*, 2020). Satellite GPS data has provided the ability to accurately measure vertical uplift and has been used to validate long term tide gauge data (Denys *et al.*, 2020; King *et al.*, 2020).

VLM is regionally variable, there can be areas of uplift and subsidence with one region. Vertical uplift from earthquake events from the Puysegur Subduction Zone and even more locally at the Akatore fault have lessened the significance of this uplift over the last 100 years (Denys *et al.*, 2020). The effect of these earthquakes on Dunedin is difficult to measure and Denys *et al.* (2020) concludes that any VLM projections note the uncertainty of the vertical contribution of earthquakes (Denys *et al.*, 2020).

The coastline North and South of the Catlins River mouth was mapped and analysed as part of the *NZ SeaRise: Te Tai Pari O Aotearoa programme*. VLM on the northern side is estimated to be -1.07 mm/yr and -1.65 mm/yr on the south. The additional effect on of VLM can be substantial across 150 years as depicted in Figure 4.6. Furthermore, the additional 0.58 mm/yr of subsidence at the southern side of the Catlins Estuary equates to an additional 80 mm of net sea-level gain across 130 years. The shaded areas represent the uncertainty within the model, greater uncertainty arises further into the future. In Figure 4.6 (c & d) the effect of SSP3-7.0 on predicted SLR and VLM can be observed. Under this scenario, sea-level would be 1.27 m above 2006 levels, with VLM, the North would have 1.44 m and the South 1.52 m. These models do not account for a potential acceleration or deceleration of the rate of VLM (Denys *et al.*, 2020).

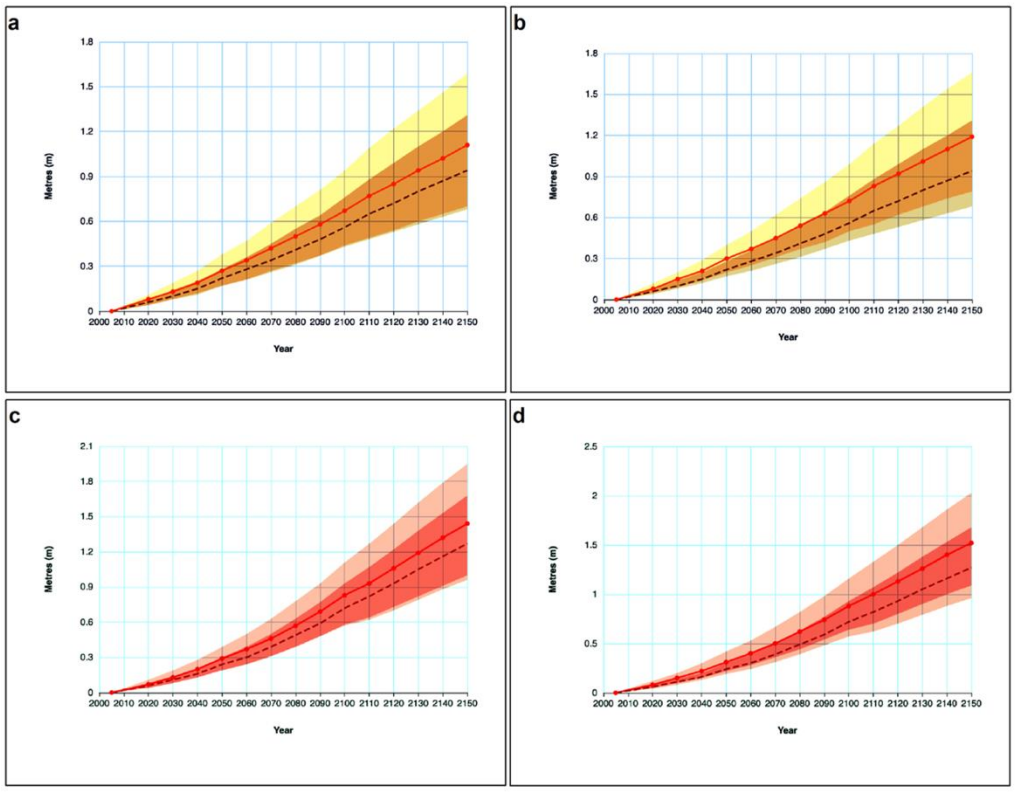

Figure 4.6: SLR and VLM forecast for the Northern & Southern Catlins Estuary taken from the *NZ SeaRise: Te Tai Pari O Aotearoa* programme; (a) Northern SLR & VLM under SSP2-4.5; (b) Southern SLR & VLM under SSP2-4.5; (c) Northern SLR & VLM under SSP3-7.0; (d) Southern SLR & VLM under SSP3-7.0. The dashed line represents SLR, the solid line represents SLR + VLM, shaded areas illustrate the uncertainty within the models.

4.3.2. Changing climate

There is evidence that the frequency and magnitude of global extreme weather events has been increasing and will continue to do so in the future (Marcos *et al.*, 2011). Whilst others argue that the return period of storms has decreased but the severity of their impact is likely to increase in the future (Cid *et al.*, 2015). Locally, a statistically significant increase in storm surge intensity (SSI) was found by Adam *et al.* (2020) but when applying cross correlation of SSI to ENSO and the Southern Annular Mode (SAM) there was no detectable relationship (Adam *et al.*, 2020).

Pressure (hPa) events has remained relatively constant since 1972 (

Figure 4.7). The results are illustrated as absolute values for the decade. The number of pressure recordings is significantly reduced during 1972–1990 compared to all other years. A small increase in extreme low-pressure events (960–979) can be observed from 1995-2021 (Figure 4.8). As explained in section 4.2.2, data collection during the 1970-1980 period amounted to once per day, comparatively, hourly records (1995-present) have the potential to capture 24 events in the same timeframe. Similarly, the 1980–1990 record where recordings were taken every three hours would not capture an equal number of events as hourly recordings. Furthermore, the 60 events observed during 2020–2022 may not be a representative figure when comparing with 2000–2010 and 2010–2020 because the 2020–2022 data amounts to one quarter of each of the other two decades. For these reasons, data from 1995-2021 was used in Figure 4.8.

The orange bars represent low pressure (980–999 hPa) and high pressure is represented by yellow bars (

Figure 4.7). There have been more high-pressure events than low pressure events. The average pressure for Nugget Point is 1012 hPa, this is exemplified by the significant number of hourly recordings between 1000–1020 hPa (grey bars) accounting for 61–65% off all pressure recordings since 1972. There is no clear increase or decrease of atmospheric pressure during this time.

The number of extreme low-pressure events (960–970 hPa) peaked in 2012 (Figure 4.8). Zero extreme low-pressure events took place in 1996 and 2016. The removal of data (failure to record wind direction, speed or pressure) could be the reason for zero events

in 1996 and 2016. In 2005, one hour of extreme low pressure occurred and in 2020, two hours of extreme low pressure occurred. The number of hours of extreme low pressure during these two years was unusually low in comparison to other years. La Niña conditions could also explain the lack of low-pressure events.

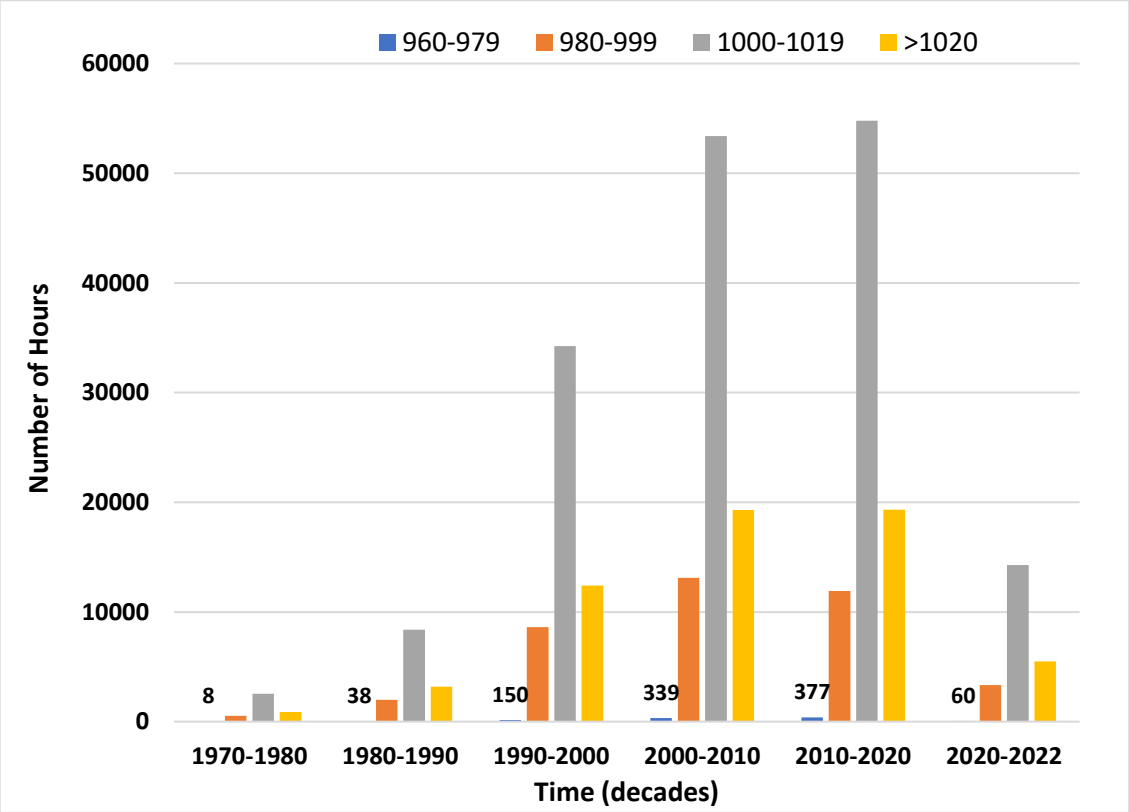

Figure 4.7: Nugget Point pressure (hPa) record 1972-2022. Data sampling rates are not consistent through the decades, however, the ratio of for each pressure level has remained relatively constant.

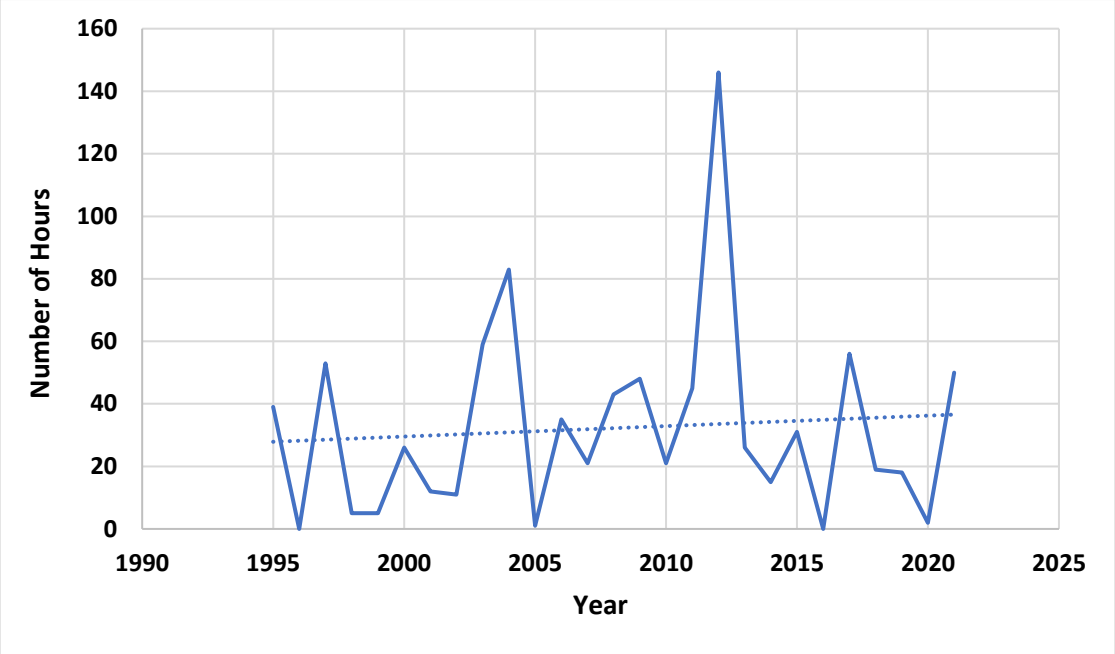

Figure 4.8: The number of hours characterised by pressures below 979 hPa from 1995–2022.

The majority of wind events at Nugget Point occur between 0°–270° (Figure 4.9). Figure 4.9 illustrates three wind direction classifications, this thesis is focused on winds from a south-west direction (180°–270°) represented by the orange bars. The number of S–W wind hours increased from 1,491 in 1972–1980, to 35,015 in 2000–2010, before decreasing to 33,444 in 2010–2020 and 8,717 in 2020–2022. The number of S–W events peaked during 2000–2010. Similar to the pressure data from the 1970s, the wind data is subject to only one then three recordings per day. Wind direction is highly variable throughout the day especially at the coast therefore the early data is not a fair representation of the direction of wind at Nugget Point.

The number of potential erosion events (PEE) has increased since 1972. PEE occur when wind speed exceeds 7 ms^{-1}, wind direction was between 180°–270°, and pressure was less than 1000 hPa. There has been a total of 10,153 PEE recorded, out of 268,708 recordings, this equates to 3.78%. There are three distinct peaks; 1997; 2003–2004; and 2017 (Figure 4.10). The number of recordings has also increased, the number of PEE from 1995 (hourly data period) does not indicate an increase in the overall trend.

Nugget Point data indicates an increase in extreme low pressure (960-980 hPa) events since recordings began in 1972. There has not been a significant change to the wind direction since records began (Figure 4.9). Increases in PEE align with the increase to hourly recordings from the Nugget Point climate station in 1995.

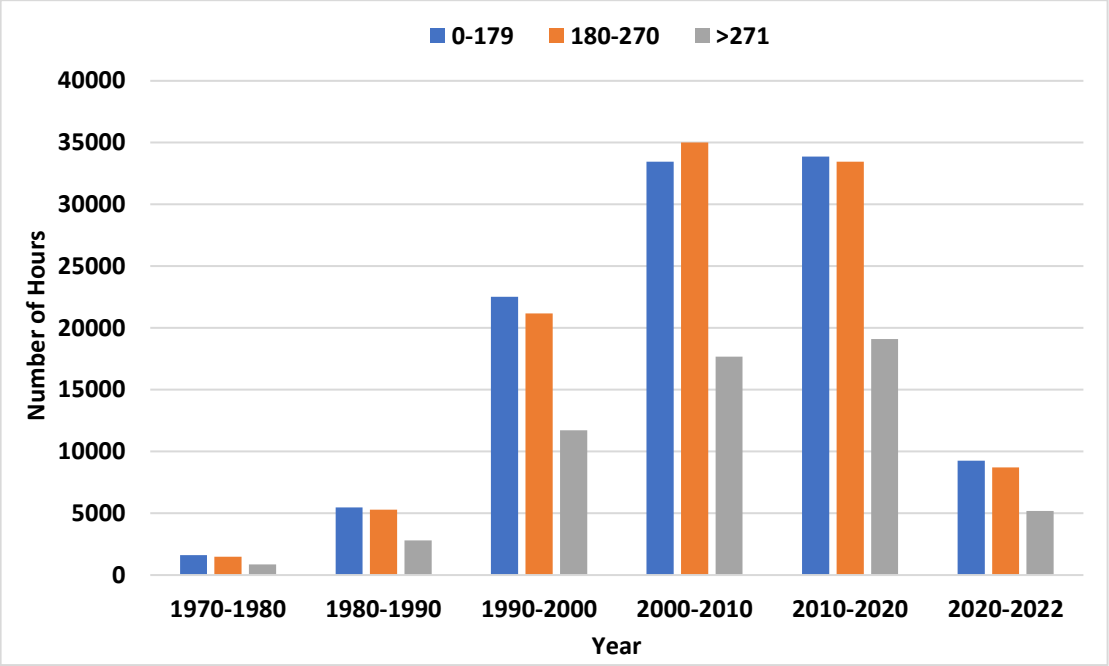

Figure 4.9: Wind directions recorded at Nugget Point 1972-2022, categorised by decades and wind angle; 0-179°; 180-270°; >271°

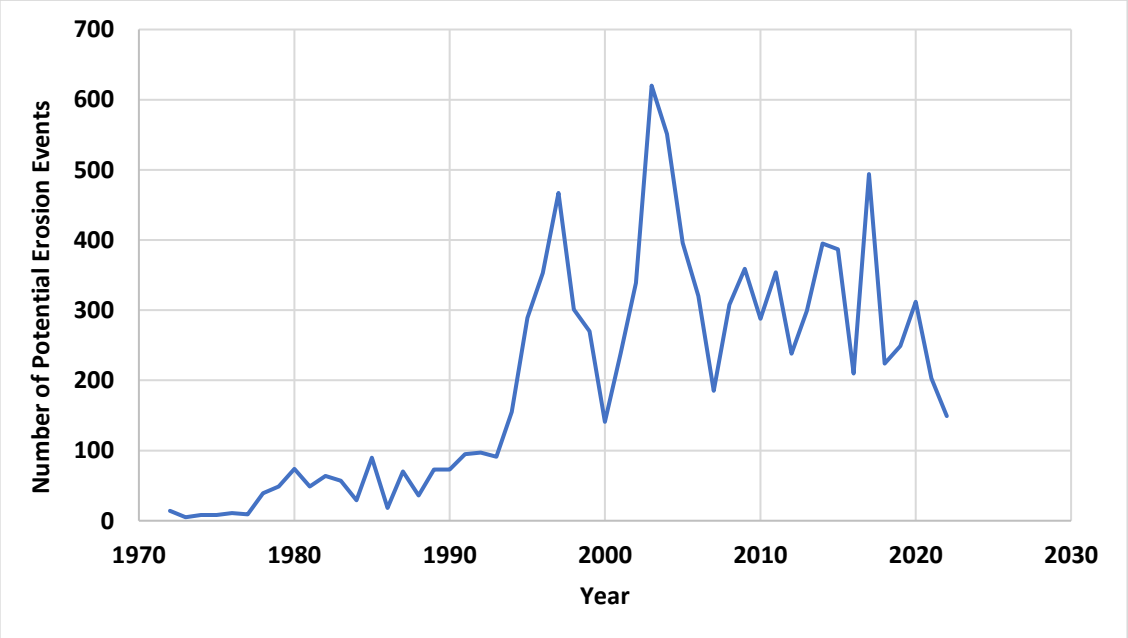

Figure 4.10: Number of Potential Erosion Events (PEE) between 1972-2022.

4.3.3. Forest cover

Forest cover upwind of the Catlins Estuary and Pounawea Wetland has significantly decreased since European colonisation affecting fetch-limited waves propagating across the estuary. As described in chapter 3 and illustrated below (Figure 4.11), the Catlins Estuary catchment was densely forested until 1967. In 1906, areas of tree felling and bare ground can be seen as well as large trees at shoreline edge (Figure 4.11). The removal of this forest may have exposed the estuary to increased wind speed and frequency of wave potential events.

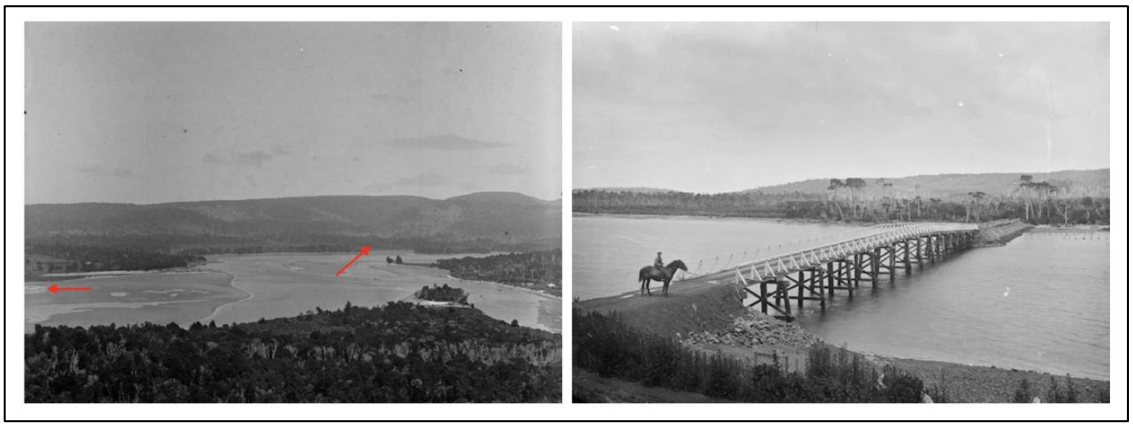

Figure 4.11: Forest cover at Hinahina. Photo of the left is from 1906, dense native forest coverage with patches of felled trees. Red arrow on the left points to where Cabbage Point is located in 1906, red arrow on the right is the forest located to the east of Hinahina Island. The image on the right is Hinahina Bridge in 1926, tall trees are seen on the foreshore, before logging commenced these trees would have been a common sight along the Catlins Estuary.

ANSYS 20R was used to demonstrate the effect of forest cover removal on wind speeds across the estuary. Results indicate that wind speeds in the lee of the forest increased following forest clearance. This decrease resulted in smaller fetch-limited waves occurring across the estuary. The decrease in wind speed, illustrated by the blue colouration of Figure 4.12 and Figure 4.13.

Changes in the porosity of the model (for the purpose of this research Cd is the inverse of porosity, thereby, decreasing the porosity equates to increasing the drag co-efficient) have a direct effect on wind speed. By decreasing the porosity, the resistance

or drag within the forest boundary increases and wind speed is affected. The decrease in wind speed as a result of the lee effect is depicted by blue/dark blue shading on the lee of the forest boundary (Figure 4.12, b). As the porosity decreases (Figure 4.13), wind speed reduces, represented by dark blue tones (Figure 4.12, Figure 4.13). When Cd = 0 (no forest), light blue/green colouring can be seen closer to the surface, indicating <12 ms^{-1} wind speed. Without the forest there is a continuous flow of wind and no change in colouration (Figure 4.12, a).

Wind speed decreased within the forest boundary and in the lee of the forest. As the porosity is reduced, wind speed decreased but it did not decrease evenly across the forest. The leeward end of the forest decreases at a faster rate than the windward side. The windward upper boundary of the forest edge is the last area to transition from green to light blue to dark blue (Figure 4.13).

Increases in wind speed are correlated with elevation. This is evident in Figure 4.12 and Figure 4.13. This is the effect of the log profile of the input wind speed code as well as a frictionless environment where wind speed can remain constant.

An increase in wind speed above the wetland (<1800 m, Figure 4.12, c) can be observed in Figure 4.12 (b). This increase is likely caused by the end wall of the model. Wind flow is likely to be reflecting off the end wall of the model and re-circulating above the wetland. The re-circulation is not affecting wind flow over the estuary and does not affect significant wave height across the estuary.

The lee effect provides sheltered conditions across the estuary. Vertical lines (black pillars, Figure 4.12, Figure 4.13) were inserted and wind speed profiles (VP) were extracted to assess the effect of forest boundary and different drag co-efficient. Data was extracted from the vertical lines equivalent to the spring high tide surface (Y= 1 m). Wind speed data for each Cd simulation can be found in Appendix B (Table B1).

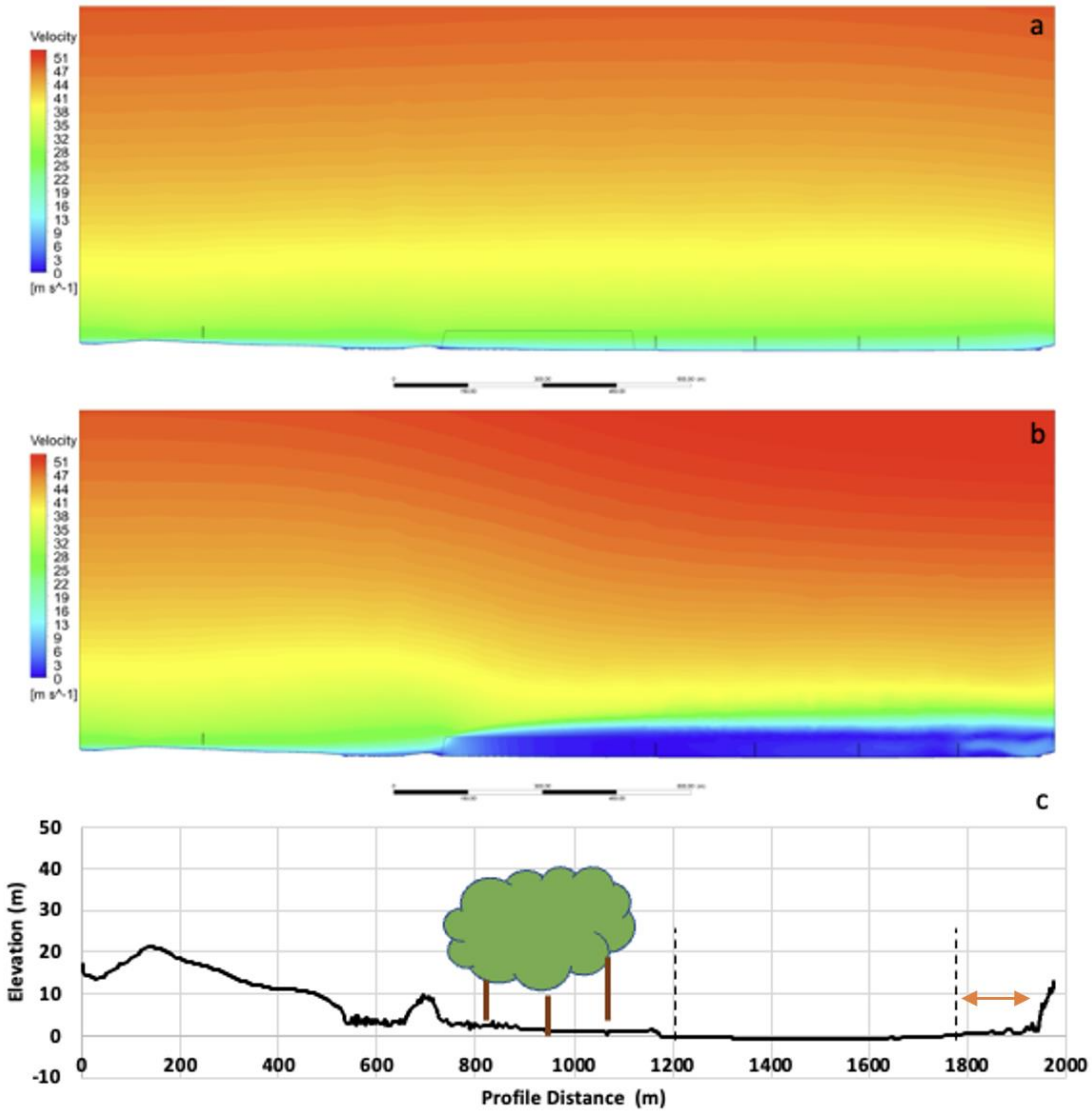

Figure 4.12: Wind speed (ms^{-1}) across the estuary, with and without the forest. (a) wind speed without the forest (Cd =0), rectangle in the centre represents the forest boundary, wind speed does not decrease as it passes through. Black pillars represent speed profiles VP0-VP4 (left to right); (b) wind speed under forested conditions (Cd = 0.15); (c) vertically exaggerated (14x) surface profile, dashed lines mark the estuary boundary, green bubble and brown vertical lines represent the forest boundary, orange arrow represents the wetland area.

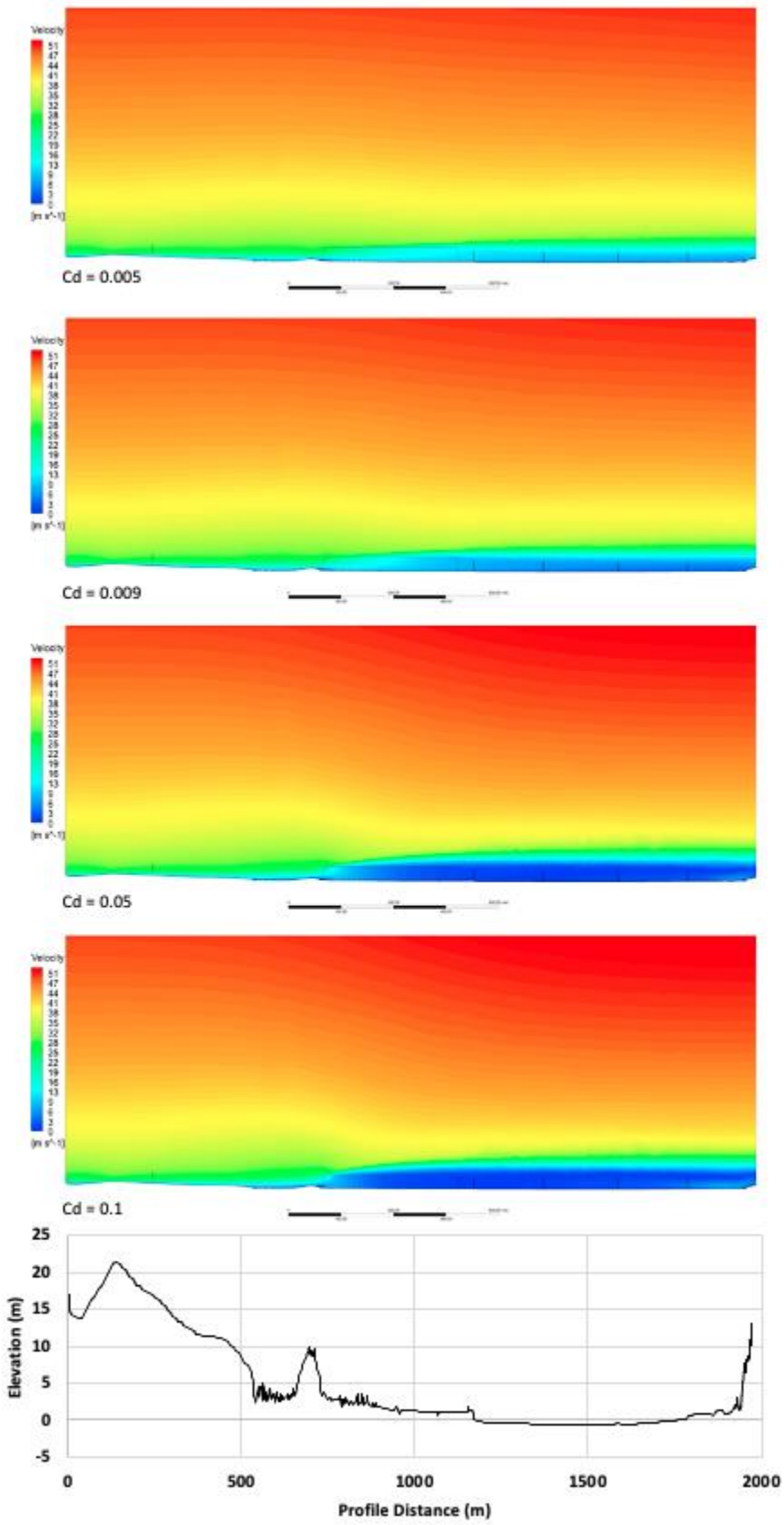

Figure 4.13: Wind speed across four drag co-efficient (Cd); (a) 0.005 Cd; (b) 0.009 Cd; (c) 0.05 Cd; (d) 0.1 Cd; (e) Profile transect

Wind speed across the estuary is not linear. Wind speed data from VP1–VP4, using four drag co-efficient simulations is illustrated below (Figure 4.14). Inlet wind speed was 12.47 ms^{-1}. This measurement was calculated 490 m upwind of the forest and 17.5 m elevation (1 m above the surface). Inlet wind speed was consistent under all Cd simulations. Inlet wind speed increased as the elevation above the surface increased, reaching 30 ms^{-1} at Y = 50 m.

Without the forest (Cd = 0), VP1, VP2 and VP3 have increasing wind speeds at Y = 1 m, 12.41 ms^{-1}, 13.9 ms^{-1} and 14.11 ms^{-1} respectively, before decreasing to 11.26 ms^{-1} for VP4 (Appendix B, Table B1). VP2 and VP3 have increased wind speed above the inlet wind speed (12.47 ms^{-1}).

The effect of the Cd = 0.005 (Figure 4.14, b) depicts a significant decrease in the wind speed across the estuary. Wind speed at Y = 1 m decreased by ~50%, from 12–14 ms^{-1} to 5–7 ms^{-1}. Wind speed is 2 ms^{-1} greater at Y = 5 m at the forest edge (VP1) than at the same height of the other velocity profiles.

Increasing (Cd) to 0.05 (Figure 4.14**,** c) has a significant effect on the wind speed across the estuary. Notably, the wind speed significantly decreased, indicating a reduction in wind speed across the estuary. VP1 is shaped like a 'hockey stick' with wind speed increasing in the first four metres before flattening out at 1.3 ms^{-1}, wind speed increases at Y = 20 m. VP2 depicts a near vertical profile until Y = 10 m. Wind speed at the surface was 0.03 ms^{-1}.VP3 depicts a decreasing speed profile as elevation increases. VP4 increases with elevation initially before decreasing at Y =10 m.

Wind speed across the estuary (VP2, VP3, VP4) decreases as the drag co-efficient is increased to Cd = 0.15 (Figure 4.14, d). VP1 is vertical with a speed of 0.02 ms^{-1} at 1 m. VP2 and VP3 are vertical profiles, 0.85 ms^{-1} and 1.97 ms^{-1}, respectively. VP4 is increasing but it is not smooth and the effect of air re-circulation may have influenced the profile.

Increases in wind speed occur at the height of the forest (Y = 40 m). Wind speed increases across the estuary (Figure 4.13, a & b). Decreases in the lee effect is most notable in simulations with lower flow resistance (Cd = 0.005, Cd = 0.009). When the resistance of the forest is increased (Figure 4.13, c & d) the decrease in wind speed is less noticeable and is occurring at a higher elevation.

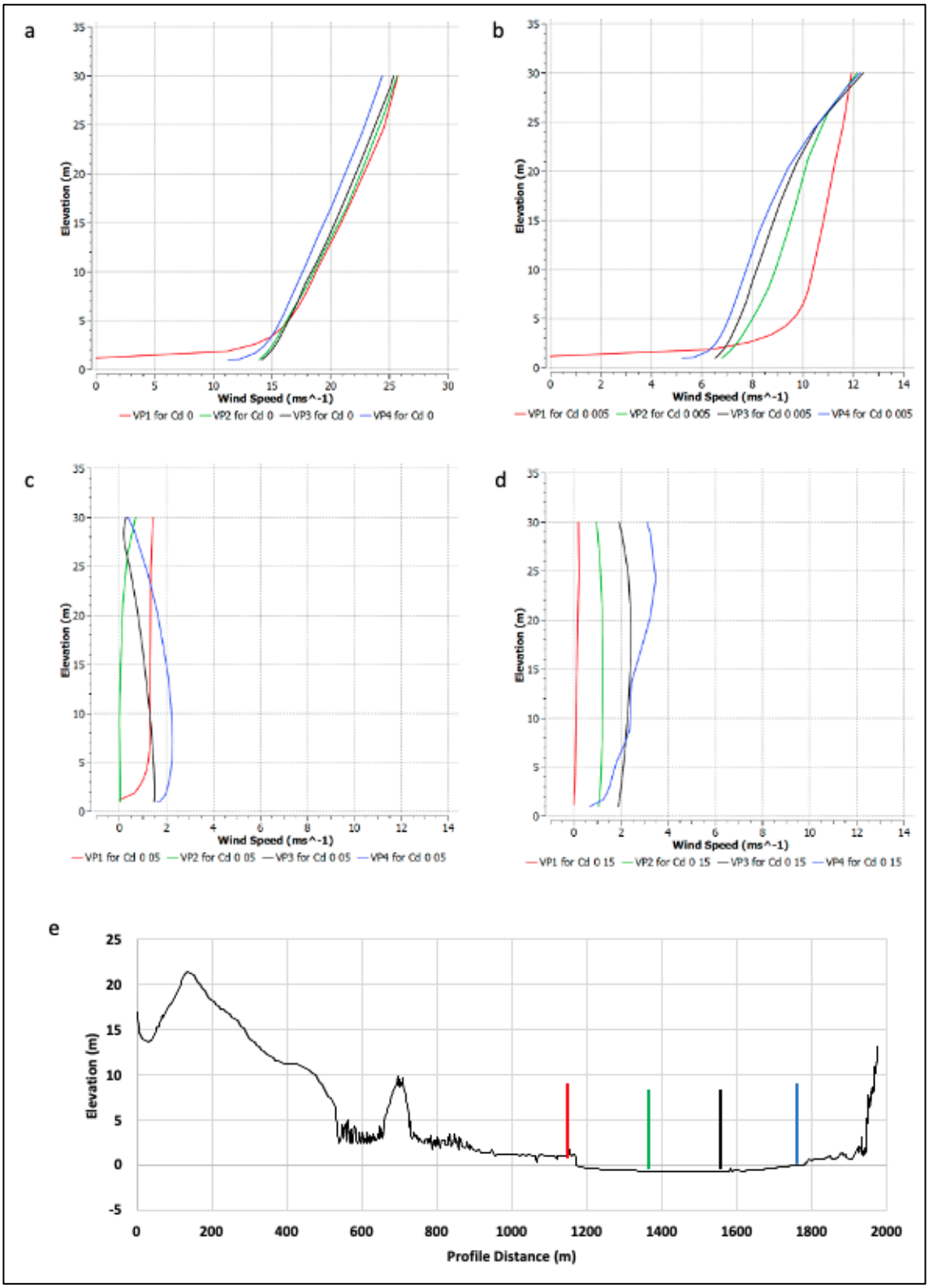

Figure 4.14: Wind speed across the estuary profile under four Cd simulations, (a) Cd = 0 (different x axis scale) VP ; (b) Cd = 0.005; (c) Cd = 0.05; (d) Cd = 0.15; (e) CFD profile model, vertical lines represent VP profiles; red = VP1; green = VP2; black = VP3; blue = VP4

Significant wave height (H_s) is strongly associated with wind speed. Wind speed decreases across the Catlins Estuary for 75% of Cd simulations (Figure 4.15). Reduced wind speed results in decreased significant wave height. The largest decrease in H_s is modelled for the Cd = 0 (blue line, Figure 4.15), a 6 cm decrease in H_s from V3 to V4. Wave height under Cd = 0.005 decreases by 3 cm from VP2 to VP4. Both Cd = 0.05 and Cd = 0.15 increase significant wave height by 2cm from VP2 to VP3, Cd = 0.05 remains constant and Cd = 0.15 decreases 1 cm from VP3 to VP4 (Figure 4.15). Velocity Profile 1 was not included in Figure 4.15 and Table 4.1 because the profile data was recorded on land. Wind speed on land does have an effect on wind speed across the estuary however since waves are not present at V1 it has been ignored.

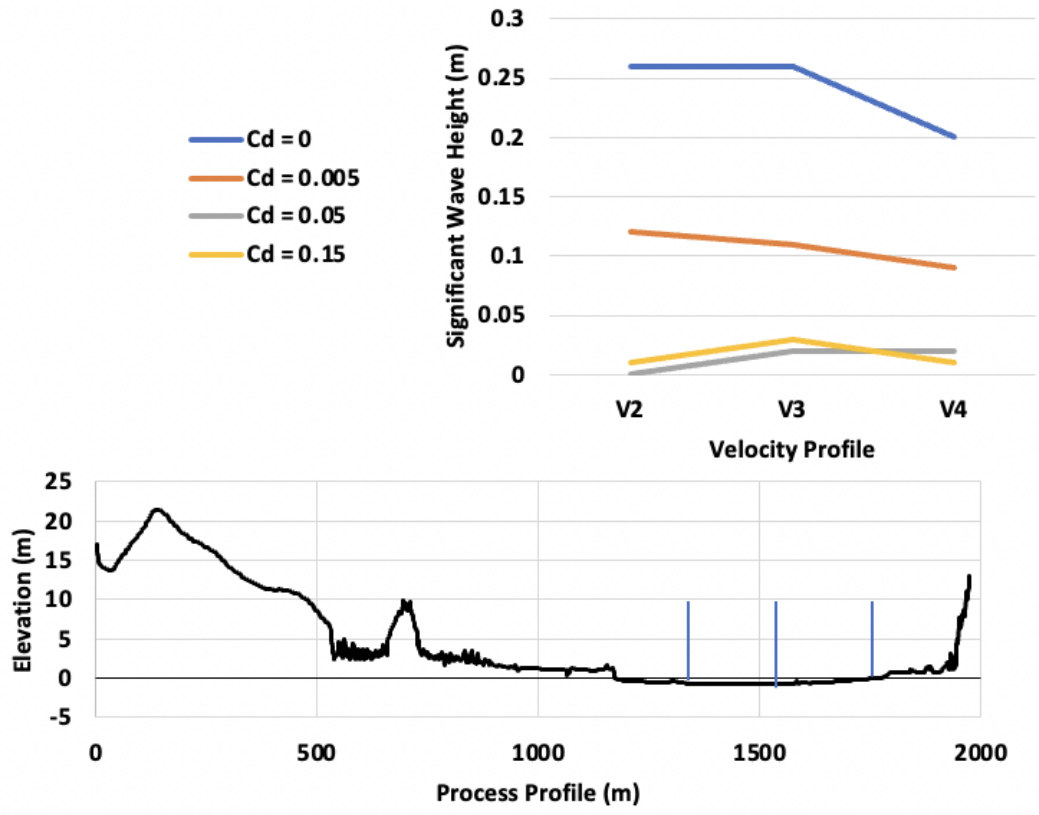

Figure 4.15: Significant wave height (H_s) across the Catlins Estuary and intertidal sandflat. Data extracted from VP2, VP3 and VP4 (blue lines on the profile, left to right) from four drag co-efficient simulations.

Table 4.2: Wind speed and significant wave height across three velocity profiles (VP) and drag co-efficient at Y = 1 m

Cd = 0	VP	Wind Speed (m/s)	H_s (m)
	V2	13.9	0.26
	V3	14.10	0.26
	V4	11.26	0.2
Cd = 0.005			
	V2	6.78	0.12
	V3	6.53	0.11
	V4	5.22	0.09
Cd = 0.05			
	V2	0.03	0
	V3	1.48	0.02
	V4	1.60	0.02
Cd = 0.15			
	V2	1.04	0.01
	V3	1.88	0.03
	V4	0.67	0.01

Wind speed is important for understanding wave formation and subsequent shoreline erosion potential. Simulations using decreased inlet wind speed produced velocity profiles identical in shape, the speed across the wetland was decreased. The decrease in wind speed was expected. These graphs were not included in this chapter but can be seen in Appendix B alongside the changes to the inlet wind speed code.

4.4. DISCUSSION

Two research questions were posed at the start of this chapter: (1) is there any evidence of change in frequency or severity or nature of weather events that might impact the wetland and (2) how have boundary conditions changed during the period of 50 years?

Pounawea Wetland has been affected by three processes separated into primary and secondary factors. Firstly, the removal of the forest boundary upwind of the wetland has likely contributed to the acceleration of shoreline erosion. The secondary factors of SLR and VLM enable increased opportunity for inundation and erosion of the wetland shoreline. SLR and VLM are changing boundary conditions, the effects of SLR and VLM will continue long into the future. Climate data has shown no significant trends of increasing frequency or severity of weather events; therefore, climatic events are not a changing boundary condition.

4.4.1. Changes in extreme weather events

Weather events at Pounawea Wetland have not changed in severity or frequency since 1972. Analysis of wind (speed and direction) and pressure data from Nugget Point climate station since 1972 did not show any significant trends for increases or decreases in low pressure events or potential erosion events. Weather events (wind and pressure) varied year to year. The effects of ENSO (El Niño Southern Oscillation) in Southern New Zealand was studied, findings indicated stronger south-westerly winds during El Niño conditions (Godoi *et al.*, 2018). The cycle between La Niña and El Niño could explain the fluctuations in events year to year.

Weather events have not changed, intensified or become more frequent since 1995. Adam *et al.* (2020) investigated the frequency and magnitude of storm surge events in Southern New Zealand and found no significant increase in either the frequency or magnitude of events. The authors note the significant difficulty of examining storm surge frequency and magnitude through time. Oceanographic teleconnections effecting ENSO and IPO and changes to the mid-latitudes prevailing westerly flow as a result of fluctuations in climate circulations were noted as problems for accurately predicting storm surge frequency (Adam *et al.*, 2020). Adam *et al.* (2020) provides further evidence

that climatic conditions in Southern New Zealand have not increased in severity or frequency, these results are reiterated in the analysis of the climatic conditions at Nugget Point (

Figure 4.7, Figure 4.9, Figure 4.10).

Climate change is predicted to result in the decrease of low pressure events in New Zealand (Gibson *et al.*, 2016). Using SSP8.5 scenario which denotes no change in climate policy or technological innovation to reduce carbon emission, Gibson *et al.* (2016) has modelled the changes in synoptic patterns for New Zealand in the 21st century. They predict substantial increases in the frequency of anticyclone conditions and widespread decreases in low pressure (Gibson *et al.*, 2016). The decrease in pressure and increase in frequency of light winds associated with anticyclones could reduce the number of potential erosion events, contrary to the trends discussed in this chapter (Figure 4.8, Figure 4.10).

Eustatic sea level rise will result in more frequent inundation of the wetland. Currently, at spring high tide (1 m MSL) under average pressure (1012 hPa) the wetland is inundated. Increases in sea-level will enable more frequent tidal and storm surge-related inundation. For example, if sea-level was 20 cm higher, a pressure event with 1010 hPa would have the same effect on wetland inundation as a 990 hPa event. Pressure events of 1000–1020 hPa are very common and occur more than any other category (

Figure 4.7), thereby creating the opportunity for potential erosion events to increase. SLR will also increase the length of time inundation occurs across the wetland. This will impact the vegetation and species that inhabit the wetland. Inundation will be discussed at length in the next chapter.

VLM will also result in a net-gain in sea level due to the on-going subsidence of the region (1.06–1.67 mm/yr). There is the possibility for vertical uplift either directly from an earthquake in the area or from an uplift event in Fiordland (King *et al.*, 2020). Whilst an uplift event is plausible, a sudden shift in sea-level relative to vertical movements on land is unlikely to affect Pounawea Wetland. Vertical uplift would result in a net-loss in sea level relative to the wetland. A vertical uplift event could slow the rate of shoreline erosion and reduce the frequency of inundation events. A decrease of 50 cm in relative sea-level caused by an uplift event would inundate the wetland when an extreme low-pressure event (<975 hPa) and spring high tide coincided. If a 20 cm uplift

event took place, inundation of the wetland would not occur under spring high tide and average pressure conditions (1012 hPa). The rate of lateral erosion may decrease but without inundation the wetland is unlikely to vertically accrete, rates of vertical accretion will be discussed in the following chapter.

The recorded data provided by *NIWA* and *MetService* contained gaps over the 50-year period. As discussed earlier, the recordings only became hourly in 1995. Given the nature of weather systems and how quickly they can change course it should be expected that many potential erosion events were missed due to changing sampling rates, especially from 1972 to 1990. Low pressure events can last for hours or days. Hourly climate recordings would record multiple hours for the same low-pressure system whereas, daily recordings might only capture the event three times. Therefore, data from 1972–1995 underrepresents the number of hourly events compared to 1995–2022.

Potential erosion events were identified using three variables (atmospheric pressure, wind speed and direction). If one variable was missing or invalid, all recorded data for that time period was deleted. More than 25,000 data entries were removed. The large amount of missing data does represent a significant amount of time in which erosion events may have occurred.

4.4.2. Forest removal and its effect on boundary conditions

This study presents the first analysis of wind flow across an estuary upwind of an eroding wetland where wave size is related to upwind porosity. Forest removal at the Catlins Estuary southern shoreline has allowed wind from the southwest an unobstructed pathway across the estuary. When wind flow is unobstructed fetch limited waves can form (Smith *et al.*, 2001). Shoreline erosion of wetlands can be accelerated when fetch limited waves increase in size (Prahalad *et al.*, 2014). The removal of the forest took place from 1860 until 1967. (Wilson, 1993) and there is no historical wind data to measure the effect of forest sheltering across the estuary.

CFD modelling has been employed here to examine the potential effects of wind sheltering in the lee of the Hinahina forest cover. This section will discuss the results of the CFD simulations and the implications of forest removal. The relationship between wind speed and porosity and the implications on significant wave height is discussed below. Results show a significant increase in wind speed under a non-forested simulation.

The increase in wind speed increases the potential for local wind waves to occur. Forest cover is a changing boundary condition and primary factor that has affected estuary conditions and wetland edge erosion.

The removal of the podocarp forest has been modelled and the results indicate an increase in wind speed across the Catlins Estuary. The modelling completed in this chapter re-affirms overseas research on wind sheltering in the lee of a forest (Heisler and Dewalle, 1988; Markfort *et al.*, 2010). The forest would have reduced wind speed across the estuary and potentially decreased erosion caused by fetch limited waves during S–W wind events. Without the forest, the frequency of fetch limited waves propagating across the estuary is likely to have increased. These waves might be small (<0.2 m) but they are occurring at a higher frequency now that the forest is removed. Small and consistent waves can contribute to shoreline erosion (Leonardi *et al.*, 2016).

The CFD model used was simplified in comparison to other wind speed forest canopy studies (Dalpé and Masson, 2008; Desmond *et al.*, 2014; Jian *et al.*, 2018; Jiang *et al.*, 2013). Field data was not collected or used to validate the model. Validation is a critical part of CFD modelling, nevertheless, the models illustrate the sheltering effect of the Hinahina forest before deforestation. By changing the flow resistance (Cd) the model depicts potential conditions as the forest was cleared in blocks (Figure 4.11). Removal of trees would have likely increased porosity thereby increasing wind speed across the estuary (Cd = 0.005, 0.009, 0.05, 0.1, 0.15) compared to complete removal (Cd = 0).

Wind sheltering decreases as distance away from the object increases (Markfort *et al.*, 2010). Increases in wind speed are visible in the low resistance models (Figure 4.13, a & b). Increases in wind speed are at their highest <20 m above the wetland. At the surface (1 m), only Cd = 0.05 illustrated an increase in wind speed from V3 to V4. This increase could be caused by topographic steering. The increase in speed occurs because air flow is constricted by the topography causing it to accelerate and change direction (Walker *et al.*, 2006). The influence of topographic steering across the estuary and wetland is beyond the scope of this thesis.

Decreasing the porosity of the forest appears to decrease wind speed outside the forest boundary, specifically, above the forest (Figure 4.13, c & d). The decrease in wind speed above the forest boundary could be caused by a redirection of wind flow as it enters the boundary of resistance. Wind redirection would decrease the speed of the surrounding

areas (Cedell, 2019) (Figure 4.13, c & d). There is no quantitative evidence to support this theory of wind redirection.

The significant wave height (H_s) of fetch limited waves at the Catlins Estuary has increased because of the removal of the upwind podocarp forest. The increase in wind speed indicates that significant wave height would have increased due to short wave theory. Differences in wave height between the models was observed (Table 4.2, Figure 4.15), providing evidence of the lee effect of the forest.

CFD modelling has been used to demonstrate that the removal of the podocarp forest has changed the boundary conditions of the Catlins Estuary. Simulations have shown that wind speed would have increased upon the removal of the forest. Increased wind speed is associated with increases in significant wave height.

4.5. SUMMARY

This chapter has examined the changing boundary conditions and their potential effect on the Pounawea Wetland. Storm conditions are not increasing in frequency or severity. SLR and VLM are boundary conditions that are going to continue to change in the future. Forest removal has affected the Catlins Estuary catchment and this has been modelled using CFD. It is likely that the primary reason that the wetland is eroding is the loss of forest cover and the complete change in the wind environment across the estuary and the potential for waves to generate. There are other secondary factors, vertical land movement and sea-level rise that have changed the environmental conditions of the estuary but the primary factor is deforestation.

SLR and VLM will inevitably affect the wetland in the future. The Pounawea area is subsiding by 1.07−1.65 mm/yr, resulting in a net increase in sea-level of 1.07−1.65 mm/yr. The acceleration of SLR is highly dependent on the socioeconomic pathway of the future. A continuation of current carbon emissions will result in increased rates of SLR. A swift transition away from fossil fuels will still result in sea-level increases, all be it at a slower rate. SLR is also going to affect the wetland and this will be discussed in the following chapter.

Historic climate data (atmospheric pressure, wind speed and direction) from the Nugget Point climate station does not indicate that there has been a change in weather conditions in the last 50 years. The inconsistency of data from 1970 until 1995 reduces the certainty of this statement, however, data from 1995 does not suggest a trend of increasing erosion potential events. Variability and seasonality within the data is to be expected.

CFD modelling was used to illustrate the potential effects of forest removal on wind speed across the estuary. The CFD simulations indicate that wind speed across the estuary would be lower if the forest was still present. This outcome is to be expected given what is known about wind sheltering in the lee of objects. An increase in wind speed across the estuary since forest removal could have led to an increase in the frequency of fetch limited waves propagating across the estuary.

5. Processes of Wetland Inundation, Erosion and Sedimentation

5.1. INTRODUCTION

Chapter 3 examined the environmental change and morphodynamics of Pounawea Wetland. Chapter 4 focused on changing boundary conditions, specifically, sea-level rise (SLR), vertical land movement (VLM) and the removal of an upwind forest on wind speed across the Catlins Estuary. This chapter details the processes of wetland inundation, erosion and sedimentation at Pounawea Wetland. The chapter will discuss how, where and when sediment is being deposited on the wetland. The relationship between tides and atmospheric pressure is detailed and the effect of sea-level rise on future inundation is discussed. Finally, the effect of increasing water level on wall shear at the scarp edge using computational fluid dynamics (CFD) is discussed. Wall shear is the force per unit area exerted by a solidary boundary on a fluid in motion (Katritsis *et al.*, 2007). This chapter analyses the historical relationship between sea-level and atmospheric pressure and makes predictions regarding the future of the wetland.

Two research aims were developed for this chapter: (1) to determine the spatial patterns and rate of sediment deposition during inundation events; and (2) to determine how sea-level rise will affect processes of erosion at the scarp.

The methods used to collect sediment, calculate sediment depth, observed and record wetland inundation and model wall shear stress using CFD are first outlined. Following this, the results will be described to explain when, where and how sediment is deposited on the wetland as well as how inundation occurs and the effects of water level on wall at the scarp. Finally, the discussion will describe and relate the findings to the research questions, a summary of the chapter's findings will conclude the chapter.

5.2. METHODS

5.2.1. Sediment mats

Artificial grass mats were used to trap sediment from inundation events. This method has been employed globally to measure sedimentation in flood plains with success (Asselman and Middelkoop, 1995; Baborowski *et al.*, 2007; Kronvang *et al.*, 2017). Initially, the mats were 50 x 50 cm (Asselman and Middelkoop, 1995) but there were difficulties rinsing the sediment from such large mats so they were reduced in size by 50%. Artificial mats were used instead of Modified Wilson and Cook (MWAC) contraptions (Goossens *et al.*, 2018) or other sediment trapping methods (sediment paper) because mats are low lying, blend in with the wetland so they would be less likely to be disturbed by humans or other species (sea lions, birds) and are similar to the vegetation of the wetland.

Artificial grass mats cut to 25 x 25 cm squares with 3 cm long blades were placed on different transects along the wetland. Two areas of focus were established, firstly, the scarp edge transect (Figure 5.1). Four mats (a, b, c, d) were placed along this transect at 5 m intervals. The second area of focus is the sloped shoreline edge (Figure 5.1). This location was chosen because it faced south-southwest (dominant wind direction) and two different edge morphologies were present (scarp and slope). The artificial mats (e, f, g, h) were placed ~5m apart and the vegetation that was below and surrounding the mat was noted. It was hypothesised that the wetland edge will experience a greater volume of sediment deposition than the landward margin.

Mats were placed at low tide and then collected again at low tide. During the summer months (November–February) mats were swapped out every tidal cycle, in winter (May–June), the lack of light and timing of the tides meant that mats were not able to be collected and would be re-inundated during the next high tide. This could not be avoided as health and safety would not approve working in the dark near water. Therefore, sediment results from the May–June field excursions should be treated with caution as they do not follow the same methodology as summer fieldwork. There is sufficient data from the winter fieldwork to treat these results separately without the need for comparison to the summer fieldwork. By using the same mats for two tidal cycles per day it was difficult to associate which incoming tide had produced the most sediment.

Results could be inferred from the hourly wind record at Nugget Point, where higher winds during high tide would likely result in more sediment accumulation on the wetland compared to low winds and high tide.

Sediment mats were carefully placed in ziplock bags and transported to the laboratory where they were rinsed with 3L of distilled water into a 15L container. Each sediment sample was then transferred to an 8L container for at least 10 days to settle (revised version of Stokes' law (Church and Ferguson, 2004)). Upon settlement, a pump powered hose was used to extract the excess water before the sediment buckets were placed in the oven at 40°C for five days. The dried sediment was then gently worked through 2mm and 64µm sieves to separate the sand from the silt. Sand and silt fractions were weighed and the sediment stored.

Black plastic particles that originate from the base of the mats were dislodged when the sediment mats were washed and rinsed. Large pieces were removed with tweezers but the majority were too small (Figure 5.2). This plastic may have increased the total weight of the sediment sample. No other methods for sediment capture were tried but filter paper was considered but storm conditions could damage the paper and the risk of losing sediment was too high.

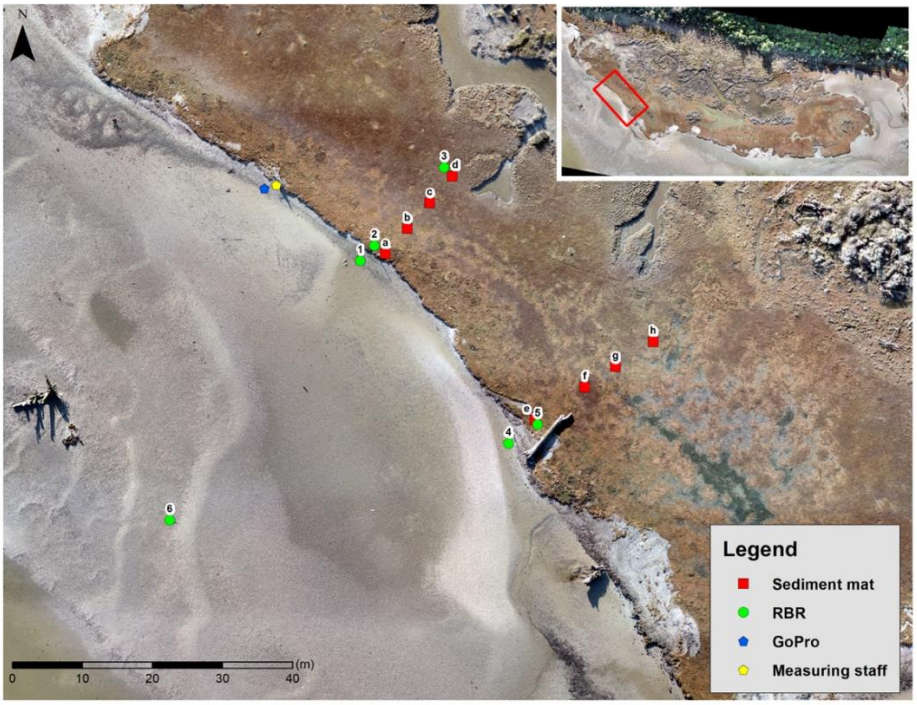

Figure 5.1: Location of sediment mats, RBRs, GoPro and measuring staff.

Figure 5.2: Left: 25 x 25 cm sediment mat after inundation event; right: black plastic particles from mat.

5.2.2. Sediment depth

Sediment depth per unit area was calculated from the sediment collected on the mats from each field trip. Data from the winter field trips (May-June) will be used because a range of tidal and pressure conditions were covered and the methodology was consistent throughout, unlike the summer fieldtrips. Sediment mats were left for two tidal cycles due to an inability to retrieve and replace the mats as explained above.

Equation 1 will solve for volume (cm^3). One assumption has been made for this equation, the material density is equivalent to quartz (2.65 g cm^{-3}). The area value used in Equation 2 is equal to 625 cm^2 (25 cm x 25 cm, mat size). Calculations and graphs were made in Microsoft Excel.

Equation 2:

Volume (cm^3) = Mass (g) / Material density (g cm^{-3})

Equation 3:

Depth (cm) = Volume (cm^3) / Area (cm^2)

5.2.3. Sediment budget

The sediment budget of the Catlins Estuary catchment was calculated using modelling and outputs created by (Hicks *et al.*, 2019) and located on the website https://koordinates.com/from/data.mfe.govt.nz/layer/103686/. The work by Hicks *et al.* (2019) enables a theoretical sediment budget of the catchment to be calculated. Furthermore, it shows how the accumulation of sediment changes through the catchment. A map of the catchment from https://koordinates.com/from/data.mfe.govt.nz/layer/103686/ is shown below , each blue line has a modelled sediment budget, both historic (pre-human, pre-European) and current, the red areas highlight the three zones of focus, Catlins Lake, wetland and estuary mouth.

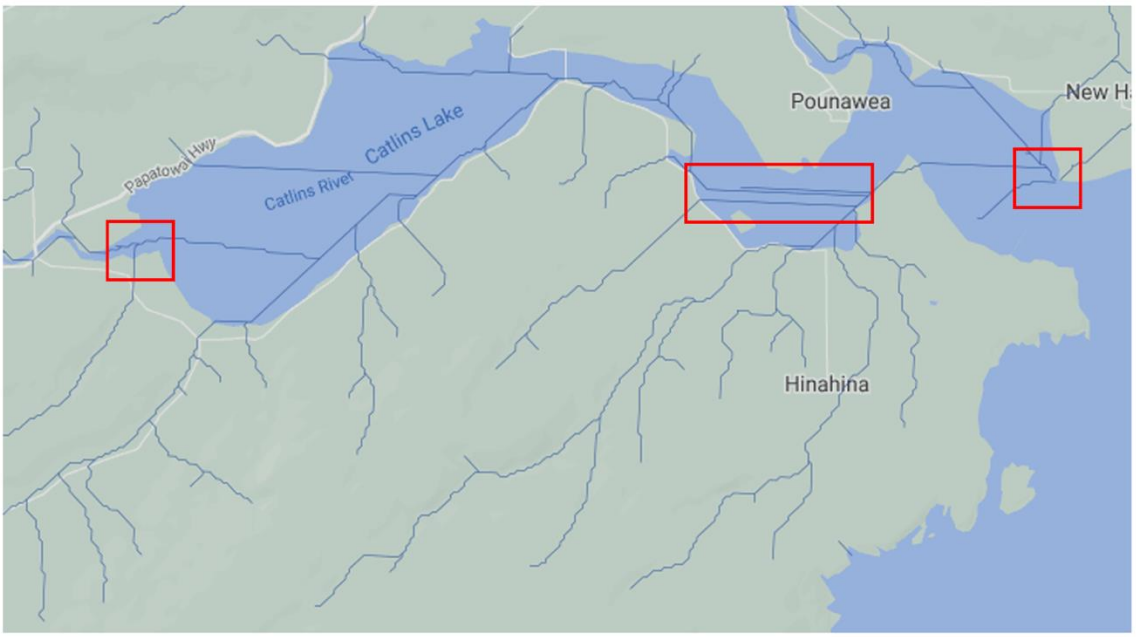

Figure 5.3: Sediment inputs of the Catlins Estuary catchment, blue lines represent sedimentary inflows, red boxes indicates the areas of focus for this thesis. Image from https://koordinates.com/from/data.mfe.govt.nz/layer/103686/

5.2.4. Wetland inundation

A time-lapse camera (GoPro) was set up to capture images of the incoming tide along the wetland edge. Images were taken once per minute for about two hours. A measuring staff was placed in the foreground to gauge water level and asses the rate of tidal inundation. Estimations of sea-level and wave heights were possible but poor lighting decreases the certainty of results. The GoPro did not have enough battery life to capture the outgoing tide and only one battery was brought on the field trip.

RBR pressure transducers were placed on the wetland and intertidal zone. The RBRs were set to measure pressure at a rate of 4 Hz continuously. The RBRs were encased in steel tubes and staked into the wetland or intertidal sandflat. Each RBR was surveyed with the RTK-GPS before each deployment. At the end of the deployment the RBRs were rinsed and dried before the data was extracted using RUSKIN software. The data was then exported as a *csv* file to Excel where it needed to be pressure adjusted. The pressure of the RBRs was set to 1012 hPa at the time of deployment. Local pressure data was obtained from MetService and calculations to adjust the recorded pressure were undertaken. If local pressure was below 1012 hPa then 1 cm of sea-level was added to the RBR data as per the Inverse Barometric effect (Pugh, 2004).

The effect of wetland inundation coupled with SLR was modelled using code developed by Dr Douglas Fraser, the code can be found in Appendix C. The code uses the DEM and point mesh cloud created by Pix4D to reconstruct the wetland environment. Inputs that were able to be changed included: year, rate of SLR, pressure range and tidal range. SLR and VLM were added together and equate to a net rise in sea-level of 3.16 mm/yr (1.8 mm/yr for SLR and 1.36 mm/yr for VLM).

The depth of water over the wetland was calculated using the RBR pressure transducers. The sample size was reduced from four samples per second to one sample per minute. This was done to simplify the presentation of the graph and for data processing convenience. MatLab was used and the code can be found in Appendix C.

The amount of wetland inundation in 2021 using tide level and pressure was calculated using the 'IF' and 'AND' functions in Excel. Hourly tidal and atmospheric pressure data was used to calculate the number of inundation hours there were in 2021. There are 8760 hours in one year, due to data collection error within the data set, 57 hours were removed. This left 8703 hours for tidal inundation. Four scenarios were chosen to

illustrate how the alignment of tides and pressure are critical for inundation. The scenarios used were; (1) pressure<1012 hPa and tide>0.9 m; (2) pressure<990 hPa and tide>0.7 m; (3) pressure<1000 hPa and tide>0.8 m; (4) pressure<980 hPa and tide>0.6 m.

5.2.5. Computational fluid dynamic modelling

ANSYS 20.R was used to construct the CFD models for this chapter. CFD modelling was used because it illustrates how wave processes interact with the wetland edge. Changes to wave dynamics (wave height and wave length) can also be modelled to demonstrate a variety of conditions that may not be observed in the field. For this study, wave parameters from an RBR were used, changes to wave parameters were not undertaken. Wave height was set to 0.0718 m and wave length was 8.152 m.

Model domains were created using surveyed profiles of the wetland from the RTK-GPS. Initially, two models were run using different equations for computation; k-omega and k-epsilon were chosen for their suitability towards fluidic dynamics. Mesh size and domain parameters were kept constant for both models. Once water stabilization occurred (160 seconds into the simulation) data was extracted to excel and compared using root mean square error (RMSE) to determine the best suited equation with the lowest error. The k-epsilon model recorded a lower RMSE and was used. The mesh and model parameters for the scarp and slope simulations are detailed in Table 5.1. Figures illustrating the model geometry and mesh are in Appendix C (Figure C2).

Table 5.1: Mesh statistics

Nodes	3381206
Elements	6748776
Growth Rate	1.2
Maximum Aspect Ratio	1.65
Maximum Skewness	0.26
Minimum orthogonal quality	0.82

The model was setup using the standard method employed by Nguyen *et al.* (2021). Models were pressure orientated and set to simulate in time transient mode. Viscous (laminar) flow and the k-epsilon model were used. Water depth at the inlet, wave height and period were all inputted from the RBR data collected on the 19th May 2022. Roughness was set to 0.01 m for the intertidal and 0.25 m for the wetland surface. Residuals were set $1x10^{-4}$ (Nguyen *et al.*, 2021) and maximum iterations was 20. Coordinates for the RBR's were inputted and data was exported for comparison between simulations and field data.

The effect of the morphology for each simulation was closely examined. Water depth was the key parameter under investigation. Understanding how water depth is affected by different morphologies was used to infer how sediment might be deposited onto the wetland.

5.2.6. Shear wall stress

CFD was used to quantify the amount of wall shear stress exerted on the scarp edge under different water level scenarios. Wall shear stress as defined by Katritsis *et al.* (2007) is "*the force per unit area by a solid boundary on a fluid in motion (and vice-versa) in a direction on the local tangent plane"* (Katritsis *et al.*, 2007, p. 307). Seven water levels were tested (0.2, 0.4, 0.6, 0.8, 1.0, 1.2, 1.4 m) using ANSYS Fluent. All other variables remained constant during testing. Wave height was set to 0.0718 m and wave length was 8.1512 m. Wall shear stress was calculated at the bottom, middle and top of the scarp from RTK-GPS survey data of the profile. The coordinates for the middle point were calculated using Equation 4. The range in wall shear (Pa) was plotted against water level. The wall shear of each location (top, middle, bottom) and water level are illustrated below (Figure 5.4).

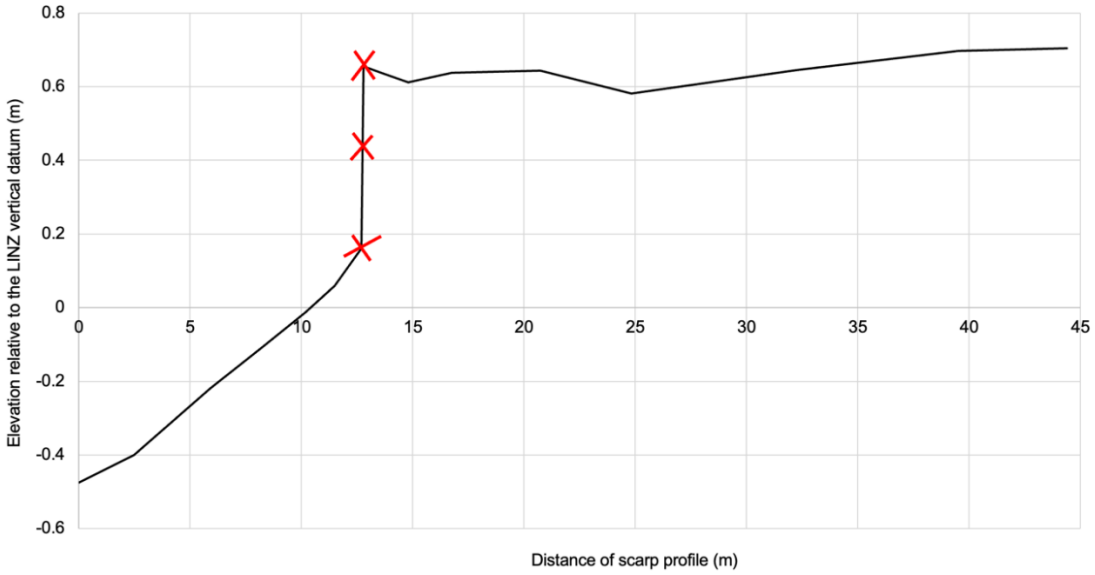

Figure 5.4: Top, middle and bottom wall shear locations extracted using CFD post.

Equation 4: Midpoint coordinates (m) calculation, x_1 = x coordinate of scarp top, x_2 = x coordinate of bottom scarp, y_1 = y coordinate of scarp top, y_2 = y coordinate of bottom scarp.

$$M = \frac{x_1+x_2}{2}, \frac{y_1+y_2}{2}$$

'CFD Post' was used to graph the results of the 150–300 second time transient model. To assess the differences between wall shear across five water levels, the average and range of wall shear was used. Average stress was calculated as the average of shear stress under water stabilization. Water stabilization was necessary, the first 100 seconds of the model saw wave impacts at the scarp edge and spill over before inundation eventuated. The average shear stress and range was found between 140 seconds and 300 seconds. The shear stress at the top, middle and bottom was analysed at different water levels. Wall shear was plotted against water level in excel and graphs were produced illustrating the range and average wall shear at different water levels.

5.3. RESULTS

5.3.1. Historic sediment accretion

Sediment accretion rates at Pounawea Wetland indicate that the wetland is vertically accreting faster than SLR. Long term accretion experiments were not possible for this thesis. The stratigraphic analysis of Pounawea Wetland (Gehrels *et al.*, 2008) was used to infer rates of sediment accretion since 1880 and up to 2006. Pollen analysis (palynology) identifies the introduction of *Pinus Radiata* into New Zealand in 1880 (Figure 5.5). This introduction marks a known boundary from where sediment accretion rates can be calculated. The amount of silty peat accumulated on the wetland calculated from the introduction of *P. radiata* is estimated to be 27 cm (Figure 5.5). This equates to 0.214 cm/yr of sediment accretion since 1880.

There is a large peak in the charcoal levels in 1935 (Figure 5.5), which probably accumulated during the Catlins' Bush Fire (Wilson, 1993). This event is another marker in time from which sediment accretion rates can be calculated. It is estimated that 15 cm of sediment has deposited onto the wetland after the Catlins Bush Fire. This equates to 0.211 cm/yr, confirming the steady rate of accretion since 1880. A spike in the Pb/Sc level in 1991 (Figure 5.5) provides a final opportunity to calculate sediment accretion. Since 1991, 3 cm of accretion has occurred, indicating an accretion rate of 0.2 cm/yr.

When calculating sediment accretion using Gehrels *et al.* (2008) stratigraphic analysis an assumption that sediment accumulated at a constant rate was made. It should be acknowledged that sediment accretion may not be constant across the 126 years, it could have accelerated, stopped or slowed. Sediment accretion is likely to be variable and environmental conditions or events may have affected the rate of vertical accretion. The data is insufficient to provide an accurate assessment of sediment accretion; however, it does allow for inferences to be made that provide an indication of the potential rates of sediment accretion at Pounawea Wetland.

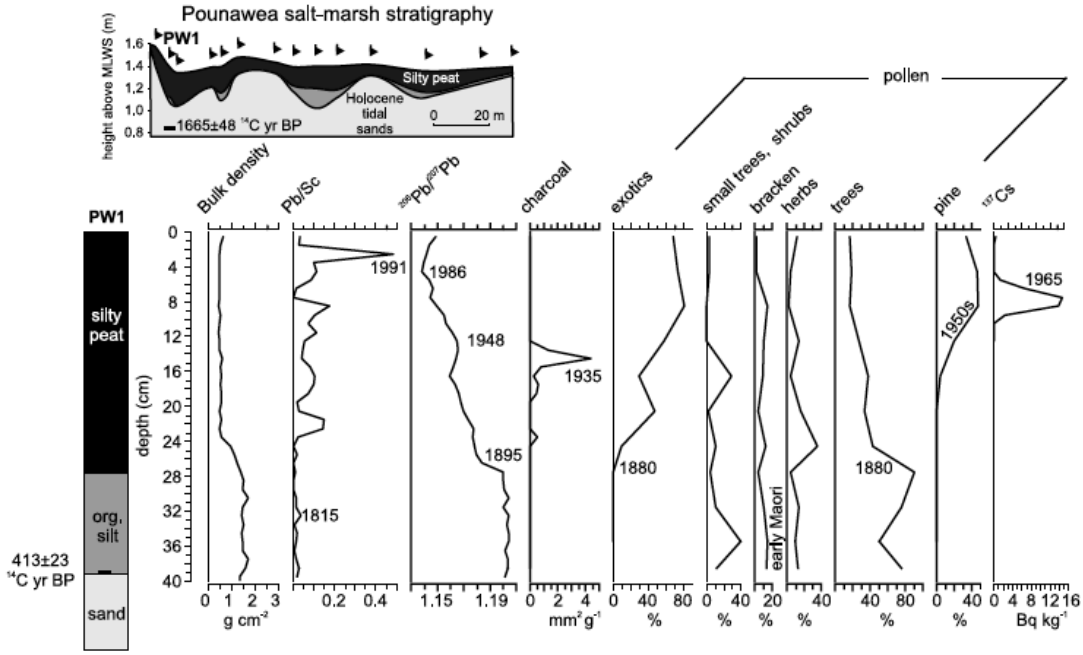

Figure 5.5: Pounawea Wetland stratigraphy (figure provided by Gehrels *et al.* (2008), appears in chapter 3 as Figure 3.7).

5.3.2. Sediment deposition

Sediment deposition is the main process in wetland accretion. Course sediment and shells are largely deposited at the shoreline edge (Figure 5.6). Sediment accumulation decreased across the RBR transect (a–d, Figure 5.1) whereas sediment accumulation at the slope transect (e-h, Figure 5.1) featured a significant decline from 'e' to 'f' before plateauing. The total sediment accumulated at each sediment mat across six tidal cycles is illustrated below (Figure 5.6). Of the sediment that was deposited, the vast majority was >63μm, in the silt and clay fraction. Sediment mat 'a' was the only mat to capture sediment >1 mm. This occurred during the June 13-14 spring high tide under storm conditions where the average wind speed was 20 ms^{-1} and the significant wave height could have been 0.38 m (calculated using short wave theory (Breugem and Holthuijsen, 2007)). Sediment distribution of silt (<63μm) is greater at mat 'b' than mat 'a'. Silt sediment at the slope follows the pattern of distribution for larger sediment, greater volume at the shoreline before plateauing across the profile (Figure 5.6). These processes of sediment deposition location and sediment size are portrayed conceptually in Figure 5.7.

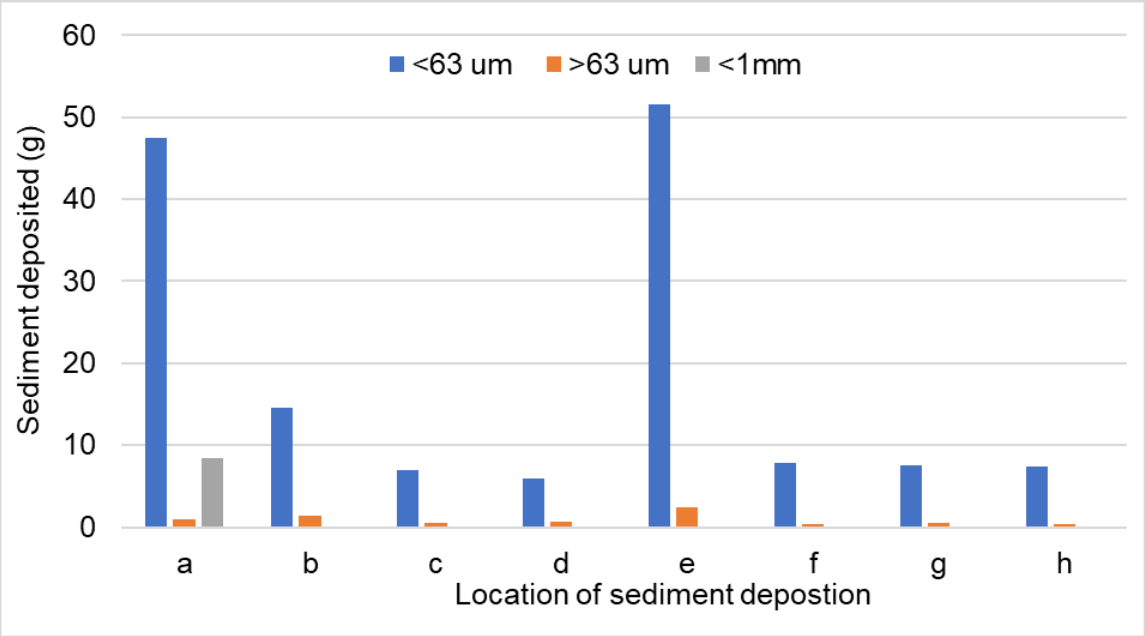

Figure 5.6: Total sediment and size of sediment deposited at two sediment transects over three field trips (18-21 May, May 31–2 June, 13-14 June).

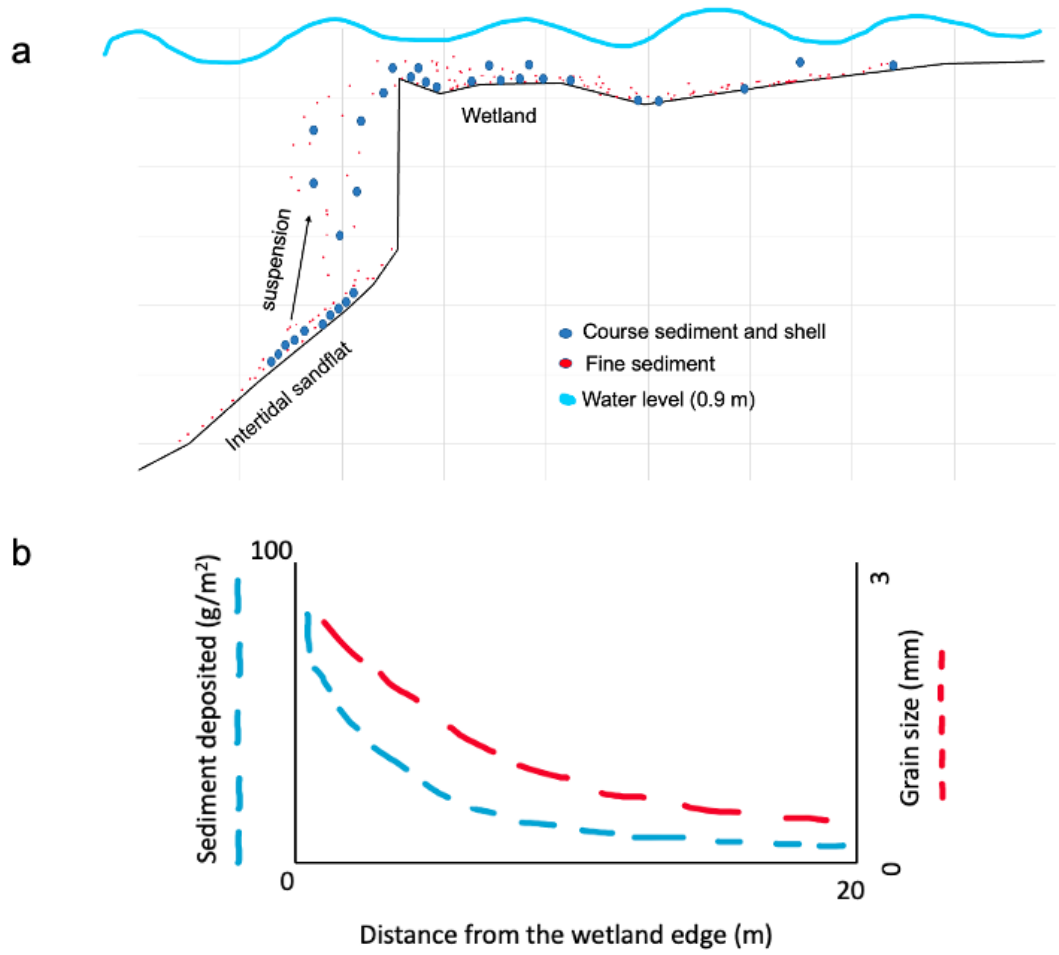

Figure 5.7: (a) conceptual model of sediment suspension and settlement illustrating larger sediment predominantly settles at the wetland edge; (b) conceptual model of sediment deposited (g/m^2) and grain size change from the wetland edge inland.

Sediment deposited on the wetland is mostly mineral and terrestrial sands, rocks, shells and quartz (Figure 5.8). The mineral sands and quartz are between 0.1–0.3 mm. Rock and shell fragments are between 0.5–3 mm. The vast majority of accumulated sediment on the wetland is inorganic, thereby contributing to the accretion of the wetland. Organic material (wooden stick) can be seen in Figure 5.8 (a) on the left-hand side. This material will eventually decompose.

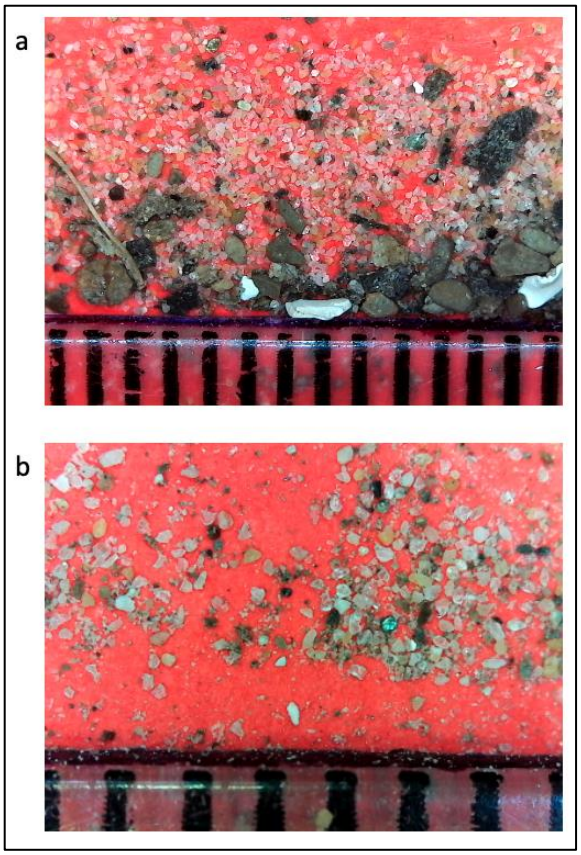

Figure 5.8: Sediment size from ‘mat a’ (Figure 5.1); (a) 13-14th June; (b) 20-21st May; note the ruler at the bottom of each image, the gap between the lines represents 1 mm.

For sediment to be deposited on the wetland storm conditions or tidal inundation are required. Sediment deposition through tidal inundation alone is significantly lower when there is no wind or wave action. Six tidal deployments (Figure 5.9) depict the cumulative sediment from eight artificial mats. Results show a significant amount of sediment was deposited onto the wetland between 13th–14th June. More sediment was deposited on the wetland during this period than all other periods combined. The four-day deployment (18–21 May) displays a steady increase in the amount of sediment deposited each day. Less than 10 g of sediment was deposited each day across eight mats between 31st May and 1st June (Figure 5.9).

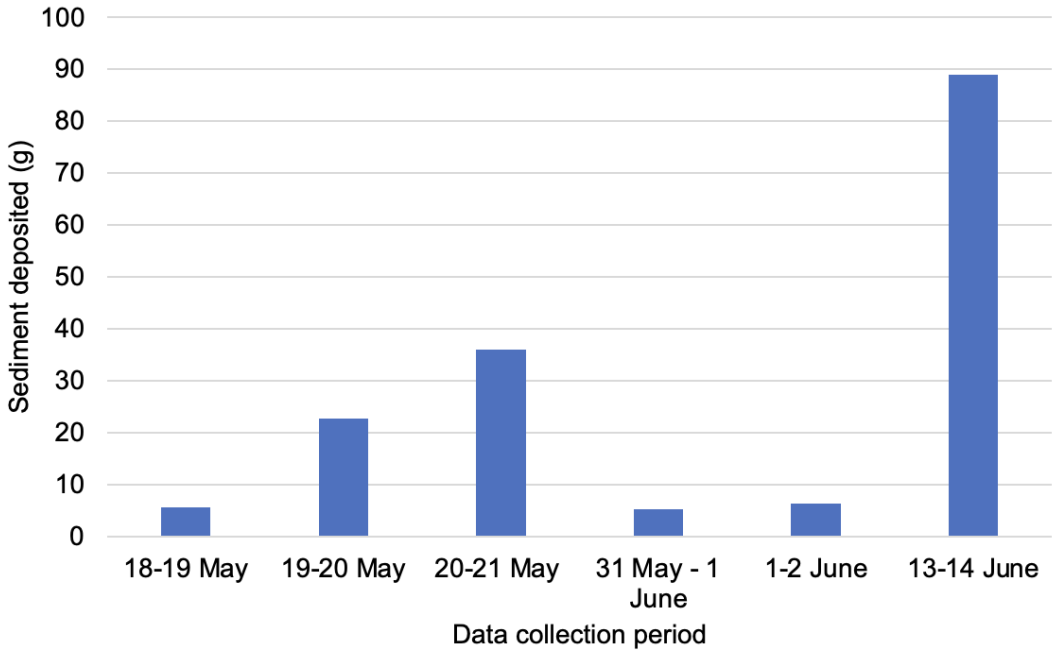

Figure 5.9: Total sediment deposited during each tidal cycle (one tidal cycle = two high and low tides).

Wind speed is associated with significant wave height in shallow fetch limited environments. This statement was discussed in chapter 4 and it is important to reiterate. The following figure depicts the relationship between average wind speed (m/s) and significant wave height (m). Significant wave height and wind speed are correlated (Figure 5.10). Increases in wind speed (18th–21st May) are reflected by an increase in significant wave height, similarly, the decreases in wind speed (31st May–1st June) also demonstrate a decrease in significant wave height. Where there are increases in significant wave height this is largely to do with an increase in wind speed. The maximum wave height across the estuary is 0.61 m, this calculation assumes depth (1.5 m) and wind speed (35 m/s) are constant (Breugem and Holthuijsen, 2007).

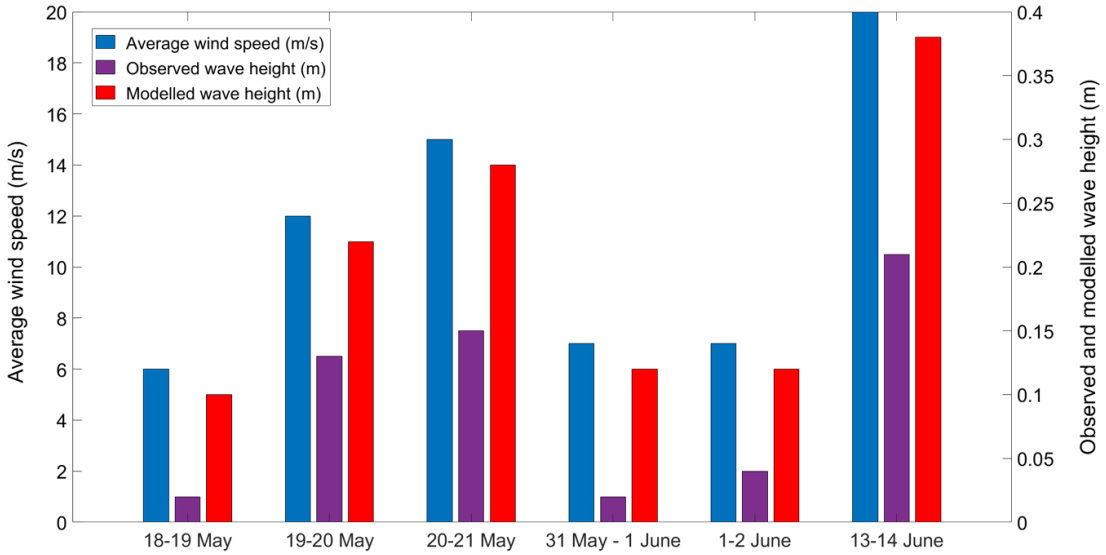

Figure 5.10: Average wind speed (left axis) and significant wave height (right axis) over the six mat deployments.

Sediment deposition on the wetland was related to significant wave height measured on the wetland (Figure 5.11). During the 18th – 21st May deployment there is an increase in the amount of sediment each day as well as an increase in the significant wave height, this trend is also seen in Figure 5.10. All deployments except June 13th – 14th have a higher modelled wave height relative to the amount of sediment that has been deposited (Figure 5.11). Wind velocity data was obtained from Nugget Point climate station and may not accurately represent the local wind conditions at Pounawea Wetland. Significant wave height during 31st May – 1st June is shown to be 0.12 m (Figure 5.11), however, photos from the wetland at high tide depict flat, calm conditions with no wave action present (Figure 5.12).

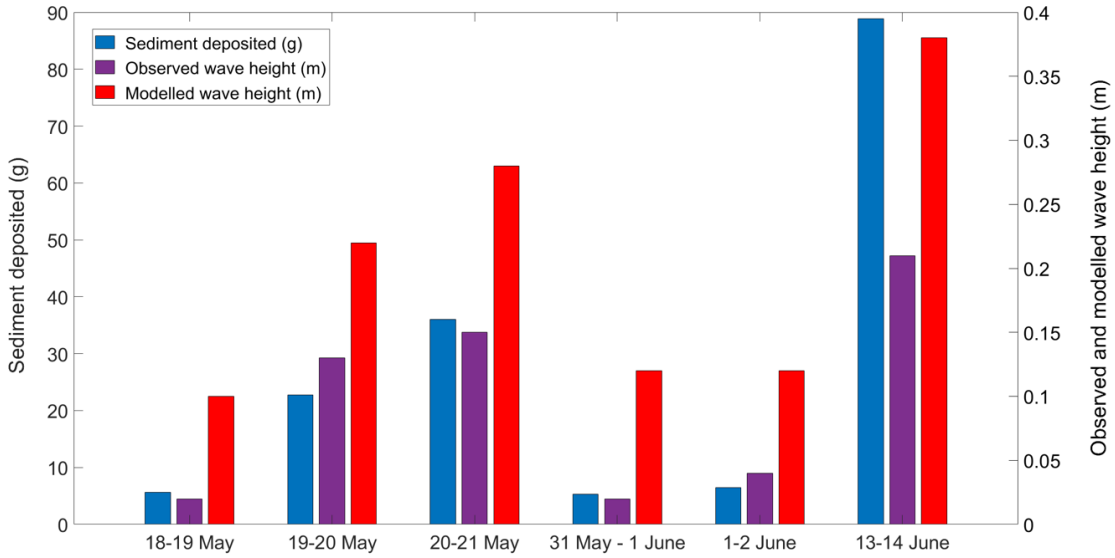

Figure 5.11: Sediment deposited and significant wave height across the six deployments.

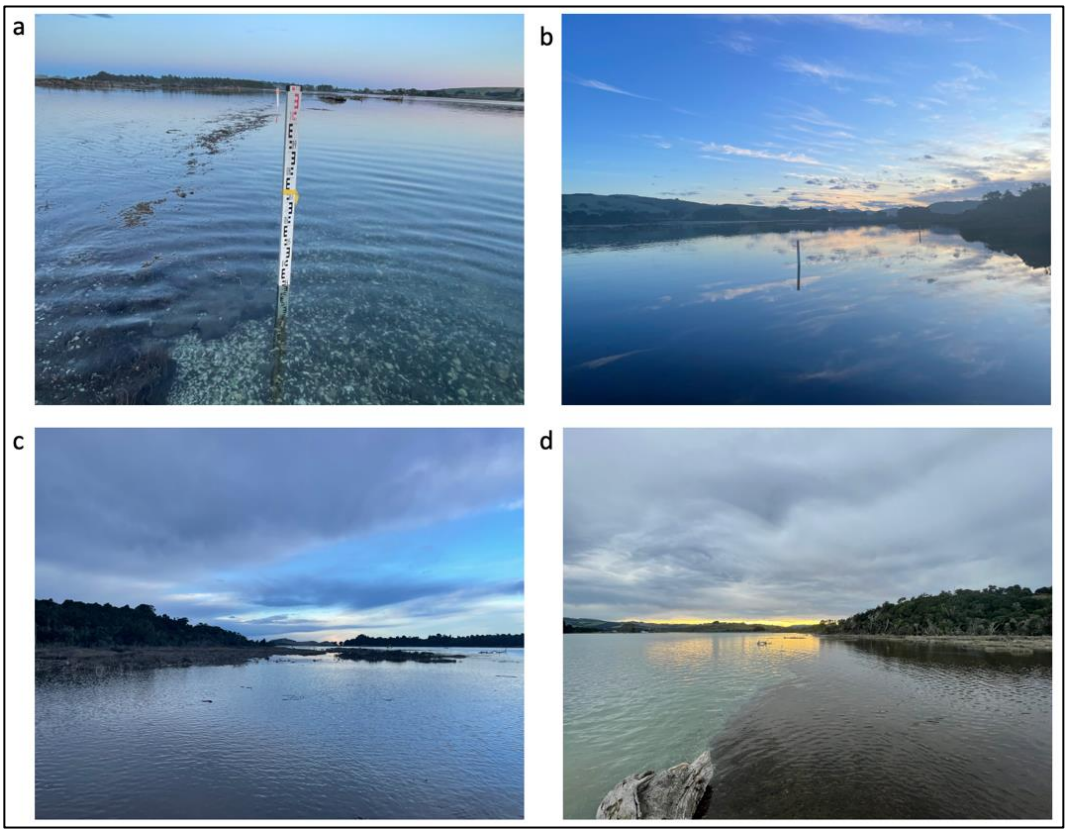

Figure 5.12: Pounawea Wetland 31st May – 1st June; (a) shoreline edge looking south east on 31st May, ripples were made from personal movement; (b) wetland in the foreground shoreline edge marked by the post in the centre, photo is looking west 31st May; (c) inundated wetland on June 1st looking north east; (d) inundated shoreline edge on June 1st looking west.

There is no clear trend in the relationship between atmospheric pressure and sediment deposition. The low sample size (6) of events is not representative of the yearly conditions of Pounawea Wetland. If the study was extended, it could be expected to see a winter and summer trend in the relationship between pressure, wave formation and sedimentation.

Low pressure (1-2 June, 13-14 June) does not mean large sediment deposition as depicted by 1-2 June data (Figure 5.13). Sediment deposition is driven by significant wave height and wind velocity, low pressure events (i.e. storm fronts) can increase wind velocity therefore increase significant wave height. Low pressure can develop in the area before the front of wind is present. Atmospheric pressure and wind data from Nugget Point climate station on the 3rd June show an average pressure of 997 hPa and 22 m/s, peaking at 37 m/s. The low pressure and minimal sediment deposition observed on the 2nd June was likely the precursor to the south-westerly front rolling through the following day with strong winds.

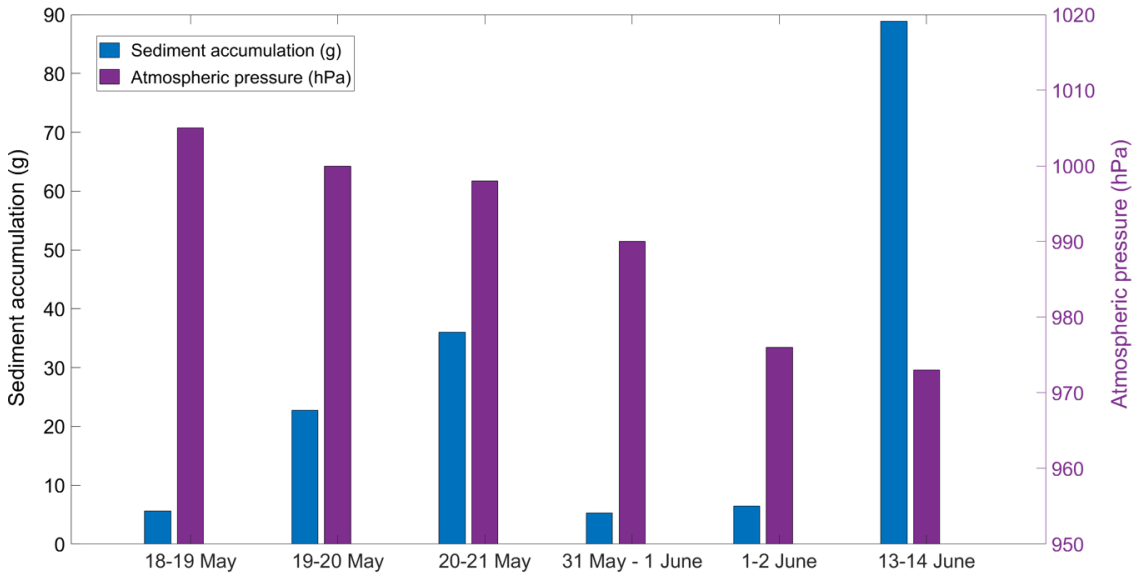

Figure 5.13: The relationship between sediment deposition and atmospheric pressure across six deployments

5.3.3. Sediment depth

The amount of sediment deposited on the wetland is not evenly distributed, a large proportion is deposited at the shoreline edge. The relationship between significant wave height and sediment deposition has been shown above (Figure 5.11) but what this figure fails to show is where the sediment is deposited. Three deployments have been used in Figure 5.14, the deployments vary in total sediment accumulation and conditions. The depth of sediment for all deployments and locations is found in Appendix C (Table C1). Landward sediment mats (b, c, d, f, g, h, Figure 5.1) were totalled together and averaged because of the low sediment yield for individual mats. Furthermore, by grouping landward mats together it illustrates the disproportionate distribution of sediment across the lower wetland, heavily focused at the shoreline edge. Sediment depth for the 1st–2nd June deployment shows greater depth of sediment at the landward mats comparative to the shoreline edge. This deployment coincided with no wave action. Flat, calm conditions were present during inundation (Figure 5.12). June 13-14 was the only event to deposit <1 mm sediment (shells) at the wetland edge, this is another indication of the intensity of the storm.

The rate of accretion per year at Pounawea over the period 1880 to 2006 was 0.2 cm/yr (Gehrels *et al.*, 2008). To reach this level of accretion, sediment deposition events at the shoreline similar to 13–14 June would need to happen ten times per year and for the landward mats there would need to be 114 events per year. In contrast, if the amount of sediment deposited at the shoreline edge during 1-2 June was deposited every day for one year it would equate to a depth of 0.1489 cm, ~0.05 cm less than the accretion rate identified by Gehrels *et al.* (2008). For sediment depth to reach 0.2 cm/yr there would need to be 25 shoreline and 210 landward sediment events similar to the one measured during May 20–21 (Figure 5.14).

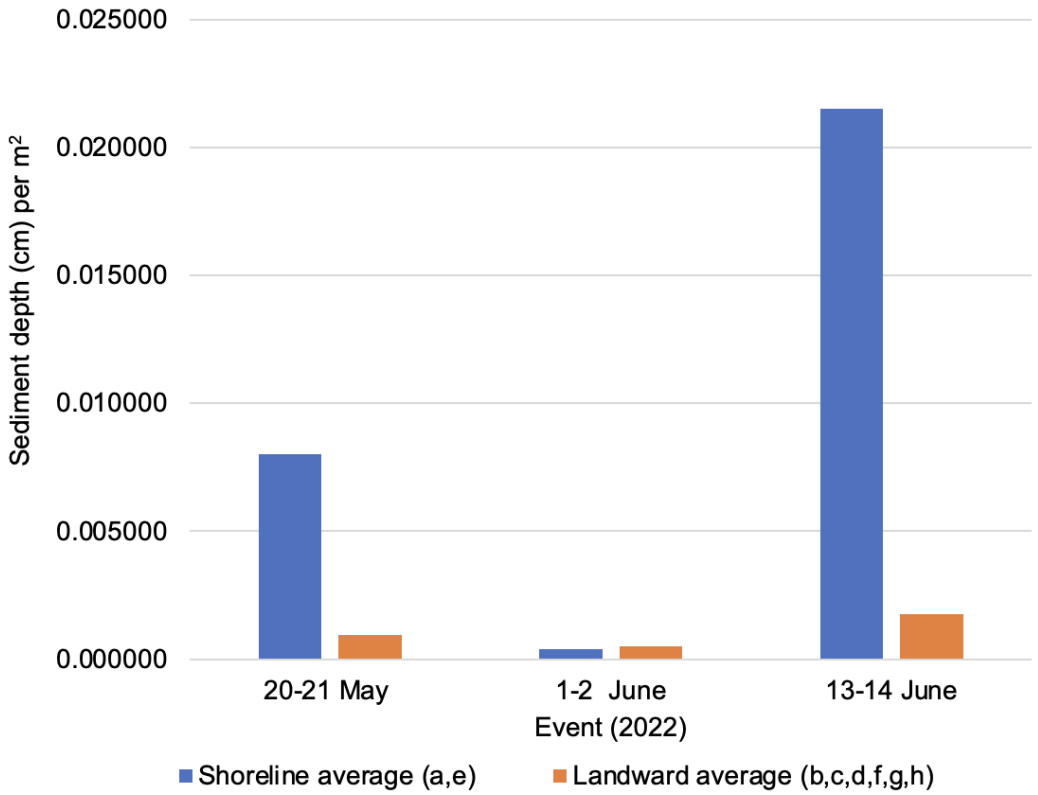

Figure 5.14: Depth of sediment at the shoreline edge (blue) and inland (orange) mats. The inland mats are the summed average of the three mats.

The rate of sediment accretion at the Pounawea Wetland was calculated for the area of the polygon in Figure 5.15. The location of mats and the events recorded enables high confidence of the accretion rates in this area. Expanding this method to the southern and eastern wetland edge reduces the confidence of the results because of differences in wind fetch and sediment supply and scarp height.

The average depth per m^2 per day for all mats (a-h) across the three deployments (May 18-21; May 31 – June 1; June 13-14) was 0.002075 cm. Yearly deposition at this rate would equate to 0.75 cm of accretion per m^2.

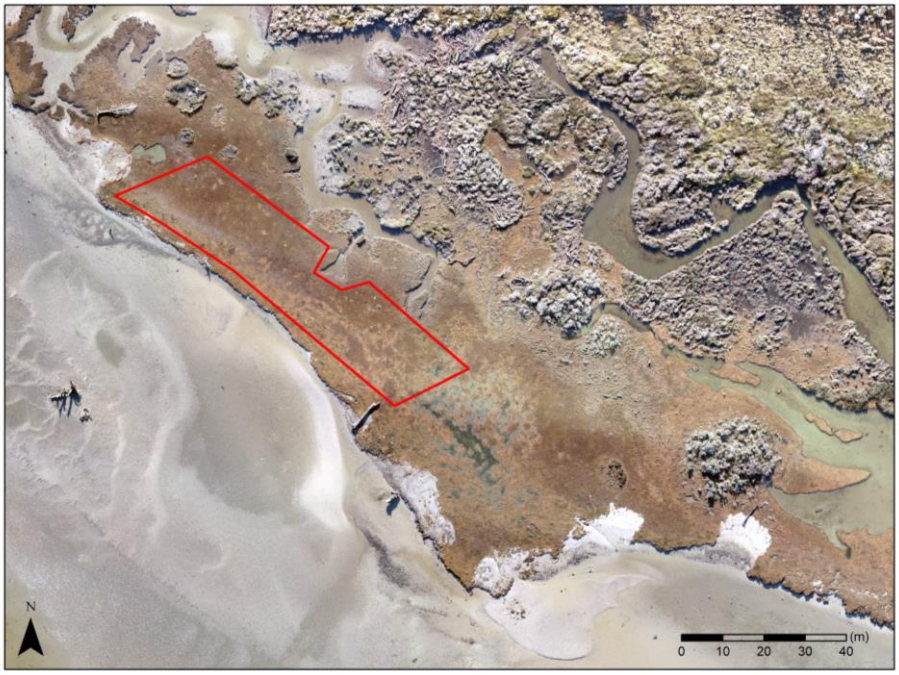

Figure 5.15: Polygon area of sediment accretion zone, polygon area is 1515 m^2.

5.3.4. Sediment budget

The Catlins Estuary catchment has two sediment inputs, the tributary rivers that flow into Catlins Lake and the beach zone at the mouth of the estuary. Sediment inflows at Catlins Lake and the estuary mouth have increased since European colonisation but have decreased near the wetland (Figure 5.16). The rivers and streams that flow into the entrance of Catlins Lake contribute 17,446 tonnes/yr. Sediment accumulation near the wetland is 114 tonnes/yr and at the mouth of the estuary it is 15,308 tonnes/yr (https://koordinates.com/from/data.mfe.govt.nz/layer/103686/). Significant sediment is present at the entrance and exit of the Catlins Estuary catchment but not near the wetland. The significant decrease in sediment near the wetland could be explained by the Catlins Lake acting as a sediment sink, where sediment enters the lake and settles instead of being transported downstream. Sediment inflows at Catlins Lake and estuary mouth have increased by ~4000 tonnes/yr and ~6000 tonnes/yr since pre-European models (https://koordinates.com/from/data.mfe.govt.nz/layer/103686/). Sediment accumulation has decreased by 700 tonnes/yr at the wetland over the same time period.

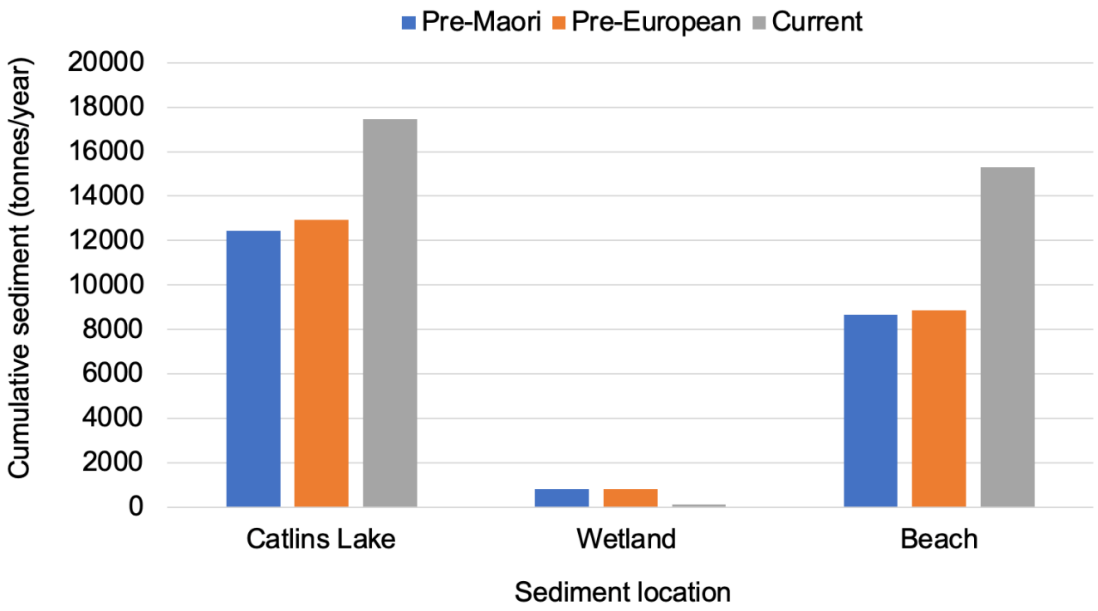

Figure 5.16: Historic and current sediment accumulation (tonnes per year) from three areas of the Catlins Estuary catchment, source: https://koordinates.com/from/data.mfe.govt.nz/layer/103686/

5.3.5. Wetland inundation

Wetland inundation is determined by tidal cycle and atmospheric pressure. Pounawea Wetland is low lying and adjacent to the Catlins Estuary, but it is only inundated or nearly inundated at spring high tide. Low atmospheric pressure is a key factor for determining inundation and depth of inundation across the wetland. Under mean pressure conditions (1012 hPa), spring high tide (1 m) would inundate the wetland by 0.3 m, the wetland edge rises to 0.7 m. The effect of low pressure can significantly increase the rates of inundation of the wetland. A range of tidal conditions can inundate the wetland if the pressure is low enough. As sea-level rises the need for low pressure decreases and the wetland becomes more susceptable to inundation. The following section will illustrate observed and modelled effects of pressure and tidal conditions, how SLR and VLM has changed these processes historically and their effect in the future.

Wetland inundation occurs both internally and at the shoreline. Waves propagate across the estuary and push water onto the wetland when the tide is high. As the tide increases, crab holes (‘honeycombed’ exterior) become saturated with water, bubbling to the surface (Figure 5.18). Time lapse footage captured on a GoPro illustrates the inundation process (Figure 5.17). Pools of water form inland from the edge (Figure 5.17,

c, d, e), initially, the pools are isolated but as the tide increases the pools become connected. Pools of water formed through water bubbling (Figure 5.18). Surface bubbles were prominent on calm days.

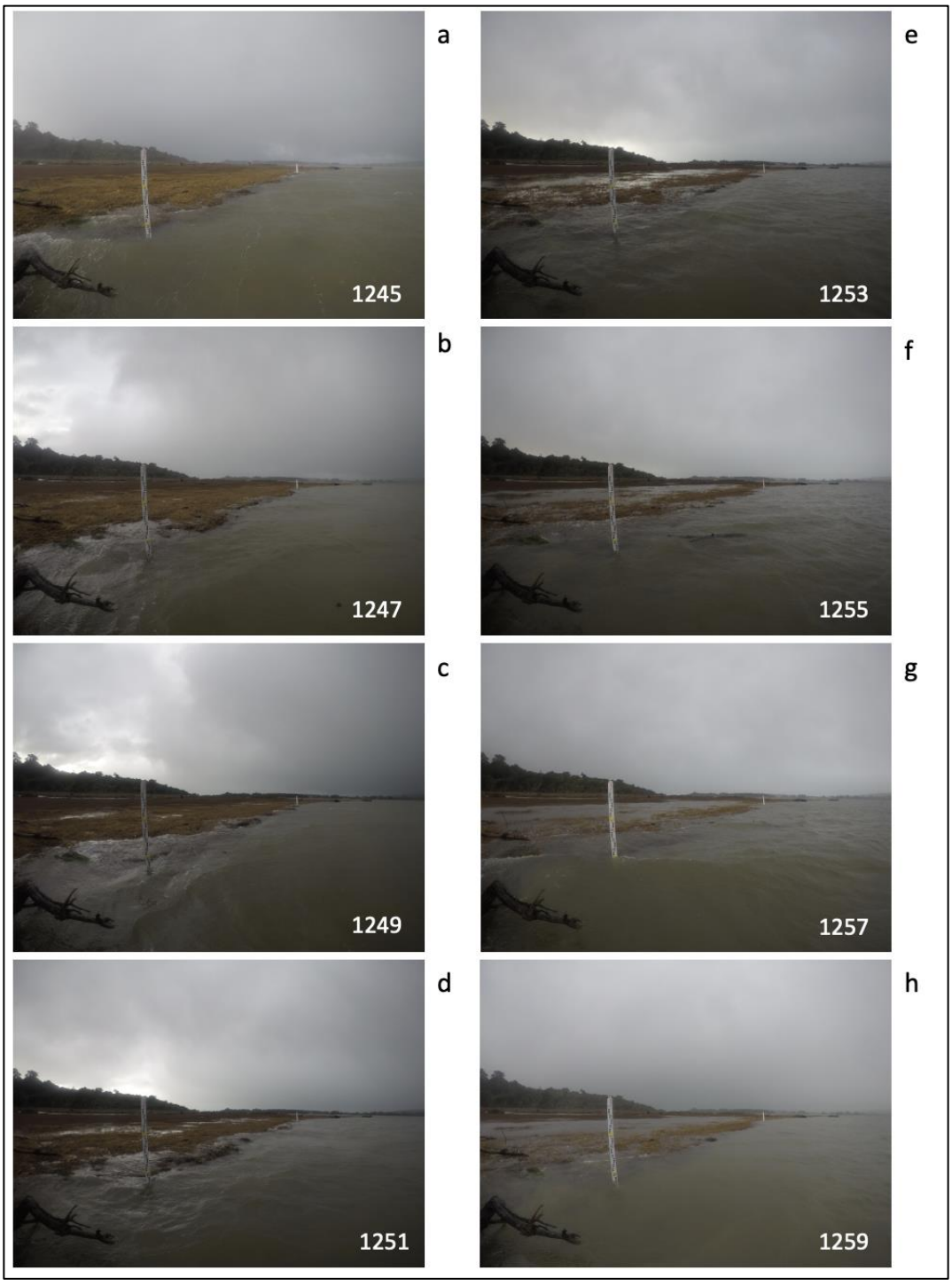

Figure 5.17: Time-lapse photographs from a GoPro camera on June 14th 2022. Images are two minutes apart.

Figure 5.18: Pool of water inland of the wetland edge with air escaping from crab holes (bubbles). Photo taken on 30th May 2022.

Inundation of the wetland does not occur frequently. In 2021, the wetland was only inundated for 112 hours of 8703. For inundation to occur the tide and atmospheric pressure must align. The alignment of tides > 0.6 m and pressure < 980 hPa or tides > 0.9 m and pressure < 1012 hPa are just two examples of potential alignments. An analysis of tide and pressure from 2021 indicates how often these events might take place. A single year comprises of 8760 hours; and the data used for this analysis amounted to 8703 hours, 57 hours of data was not recorded and therefore could not be analysed. Of the 8703 hours, 112 hours of wetland inundation occurred when tides > 0.9 m and pressure < 1012 hPa, this equates to 4.7 days out 362.6 (8703 hours). The number of hours (112) does not reflect the time the wetland was inundated. When the wetland is inundated it can take up to three hours for the tide to fully recede, soil saturation and water pooling is present after inundation (Figure 5.19). Pressure and tide conditions shown in Table 5.2 illustrate the number of hours inundation would have occurred at Pounawea Wetland in 2021.

Table 5.2: Number of inundation hours during 2021 using a combination of tidal conditions and atmospheric pressure.

	<1012 hPa >0.9 m	<1000 hPa >0.8 m	<990 hPa >0.7 m	<980 hPa >0.6 m
Wet	112	57	33	13
Dry	8591	8646	8670	8690

Figure 5.19: Pools of water across Pounawea Wetland after the morning tide on June 17th 2022. Photo taken by Mike Hilton.

The effect of 3 mm/yr of SLR and 1.36 mm/yr of VLM movement will increase inundation events in the future. Historic modelling indicates that SLR and VLM have increased net sea-level by ~32 cm every 100 years. The model does not account for yearly variations, instead it assumes continuous increases in sea-level each year. An increase of 32 cm per 100 years is not accurate, the Dunedin sea-level record illustrates an increase of 24 cm since 1900 (Figure 4.2). Modelling indicates a pressure event of 1012 hPa in 2000 would have resulted in a water level of 0.93 m. In 1900, the same water level (0.93 m) was modelled during a 980 hPa event (Table 5.3). The relationship between pressure, tides and water level seen in Table 5.3 is illustrated in Figure 5.20 (Appendix C, Figure C3, for years 1900, 2100, 2300). There is a 100-year lag between water level and the two pressure scenarios. This means that mean pressure (1012 hPa) events in 2100 will have the same water level as a low pressure (980 hPa) event of 2000. Mean pressure events occur more often and therefore, it 2100, inundation events are likely to be more frequent because of higher mean sea-level.

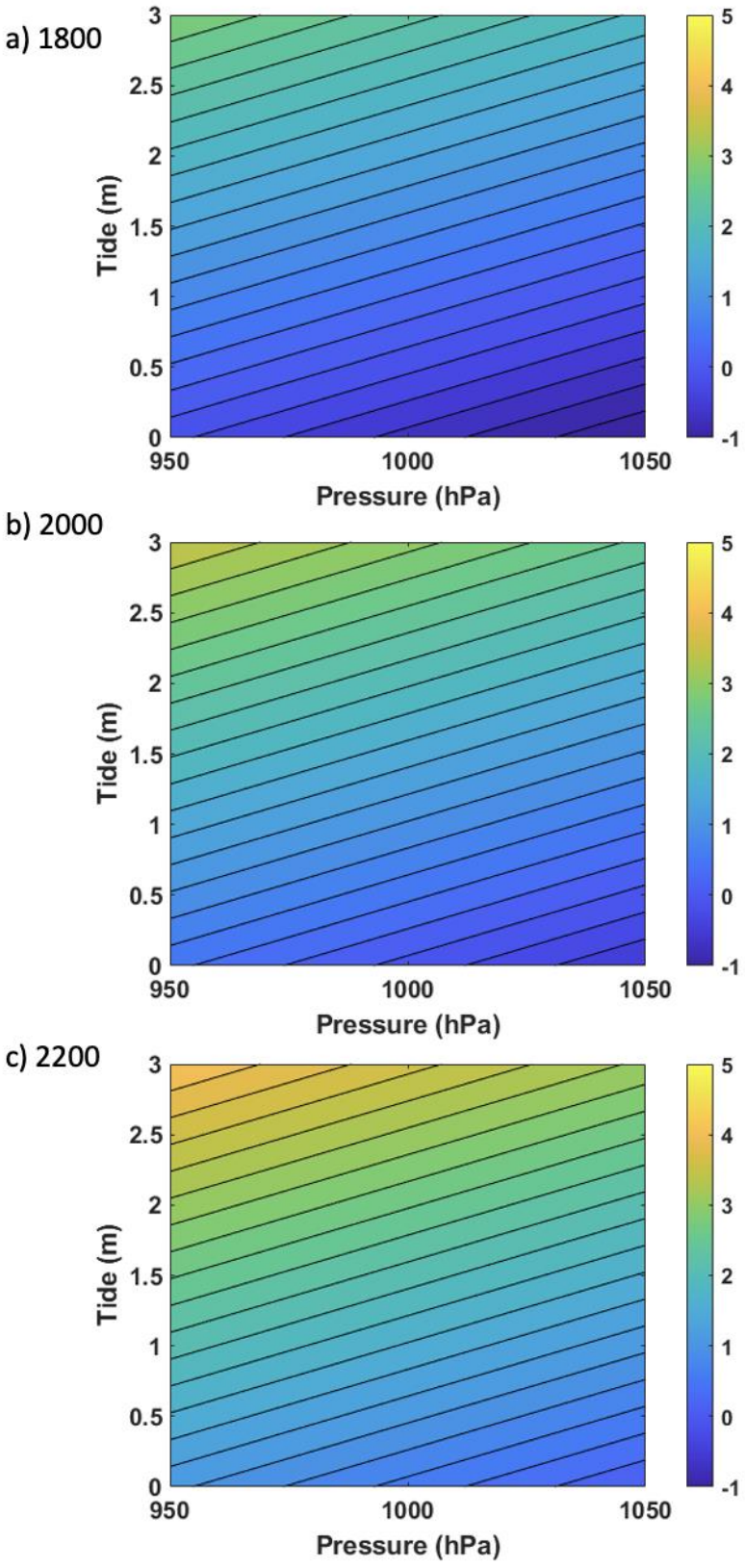

Figure 5.20: The modelled effect of tide, pressure on water level past, present and future; a: 1800; b: 2000; c: 2200. Water level is in metres (right hand bar), the wetland edge is 0.7 m.

Table 5.3: Past and future water level using two pressure scenarios. SLR and VLM have been included in the calculations of water level.

Year	Pressure (hPa)	Water Level (m)	Pressure (hPa)	Water Level (m)
1800	1012	0.29	980	0.62
1900	1012	0.61	980	0.93
2000	1012	0.93	980	1.25
2100	1012	1.25	980	1.56
2200	1012	1.56	980	1.88
2300	1012	1.88	980	2.19

In 1800, the water level during a 1012 hPa event was modelled to be 0.29 m (Figure 5.21, a), relative to the height of the wetland today (~0.7 m). The intertidal sandflat areas are not inundated due to their natural elevation. Complete inundation of Pounawea Wetland is modelled using a tide of 0.93 m (Figure 5.21, c). This level of inundation would only occur in low pressure conditions (<980 hPa) in 1900. In 2000, this level of inundation would occur during a 1012 hPa event (Table 5.3).

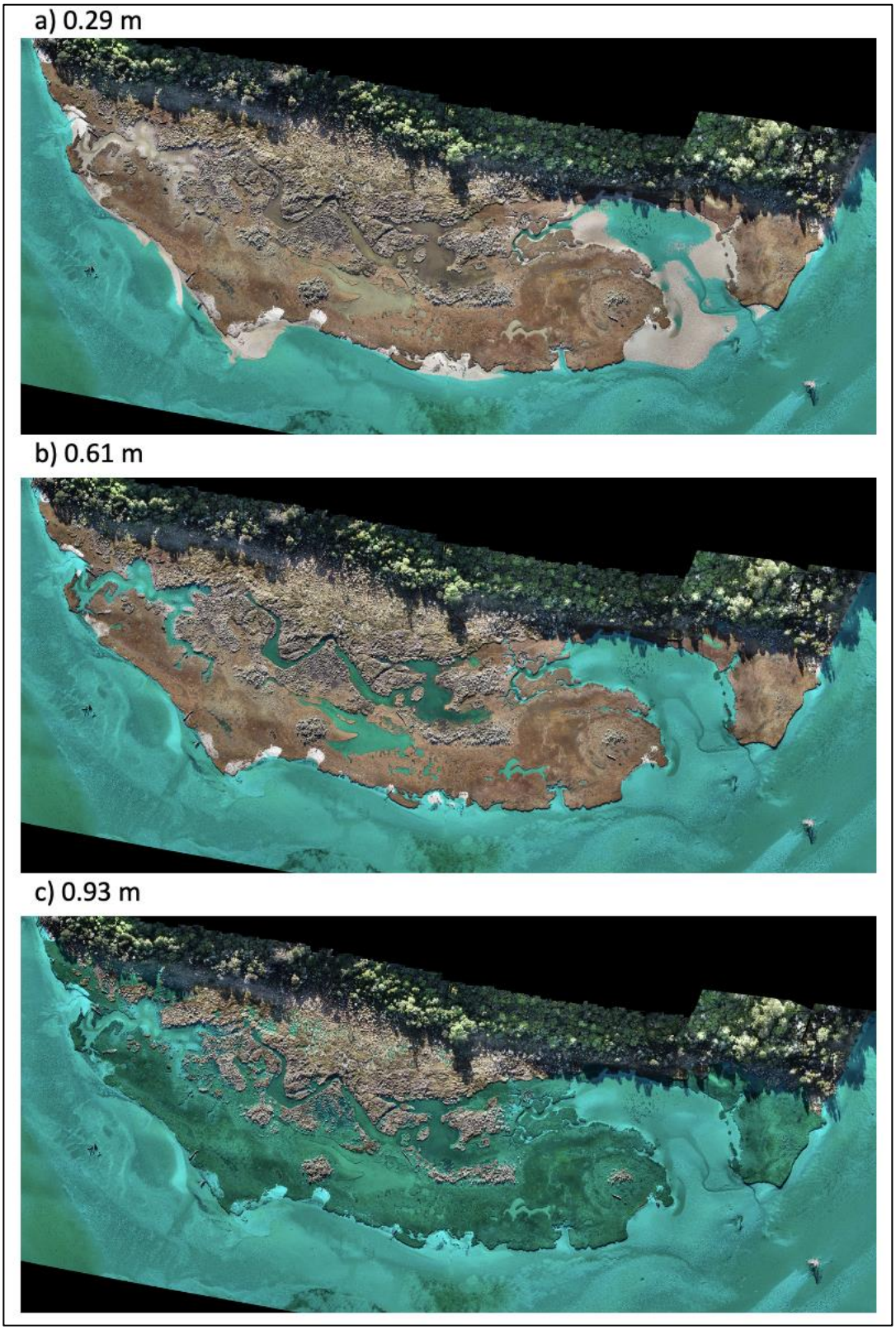

Figure 5.21: Wetland inundation under three water levels (relative to the height of the wetland (0.7 m); (a) 0.29 m; (b) 0.61 m; (c) 0.93 m. Water levels are relative to the LINZ vertical datum.

SLR will increase the frequency of wetland inundation in the future. At the same time the width of the wetland is decreasing due to marginal erosion (Chapter 3). Shoreline erosion has occurred at a rate of -0.67 ± 0.05 m/yr since 1948. The shoreline is likely to be 18 m, 52 m and 85 m inland of its current position by 2050, 2100 and 2150, respectively (Figure 5.22). It should be noted that these setbacks do not incorporate SLR or VLM. Under normal pressure (1012 hPa) and 1 m spring tide (tide level from 2022) would inundate the shoreline edge in 2100 and partly inundate the 2150 edge.

Figure 5.22: Pounawea Wetland inundated with 1 m tide, dashed lines indicate predicted shoreline edge using LRR (-0.67 ± 0.05 m/yr).

The level (or depth) of inundation during events is dependent on the tide and pressure conditions during the inundation event. The depth of water over the wetland at the shoreline edge of the wetland (Figure 5.1, a) is illustrated below (Figure 5.23). The recorded pressure and predicted tidal level are shown in Table 5.4. Predicted tidal level is higher during the day than at night (Table 5.4), Maximum water depth for all deployments took place in the afternoon (Figure 5.23). Inundation during wind events is illustrated by the length and density of the lines. A clear difference can be seen between the evening inundation events on the 18th and 19th May (Figure 5.23).

A very low pressure (974 hPa) event coinciding with a neap high tide on June 1st 2022 resulted in 0.25 m of inundation over the entire wetland. The predicted tide level was 0.77 m. Eleven days later (June 13th), during spring high tide (1.02 m), the same

pressure was recorded (974 hPa). The combination of spring high tide and extreme low pressure on this occasion resulted in 0.48 cm of inundation over the wetland. On June 14th, the predicted tide level was 8 cm higher (1.1 m) than June 13th and pressure was also higher, 990 hPa, compared to 974 hPa. In theory, this should have resulted in lower inundation across the wetland because the increase in tide level is less than the increase from the change in pressure. The increase in water level could be explained by the presence of waves over the RBR. Strong westerly (260°) winds were recorded at Nugget Point during high tide, measuring 25 ms^{-1}. High winds were recorded during the June 13-14 deployment as seen from the increased range in water level over the wetland (Figure 5.23). The increase in range represents fetch limited waves.

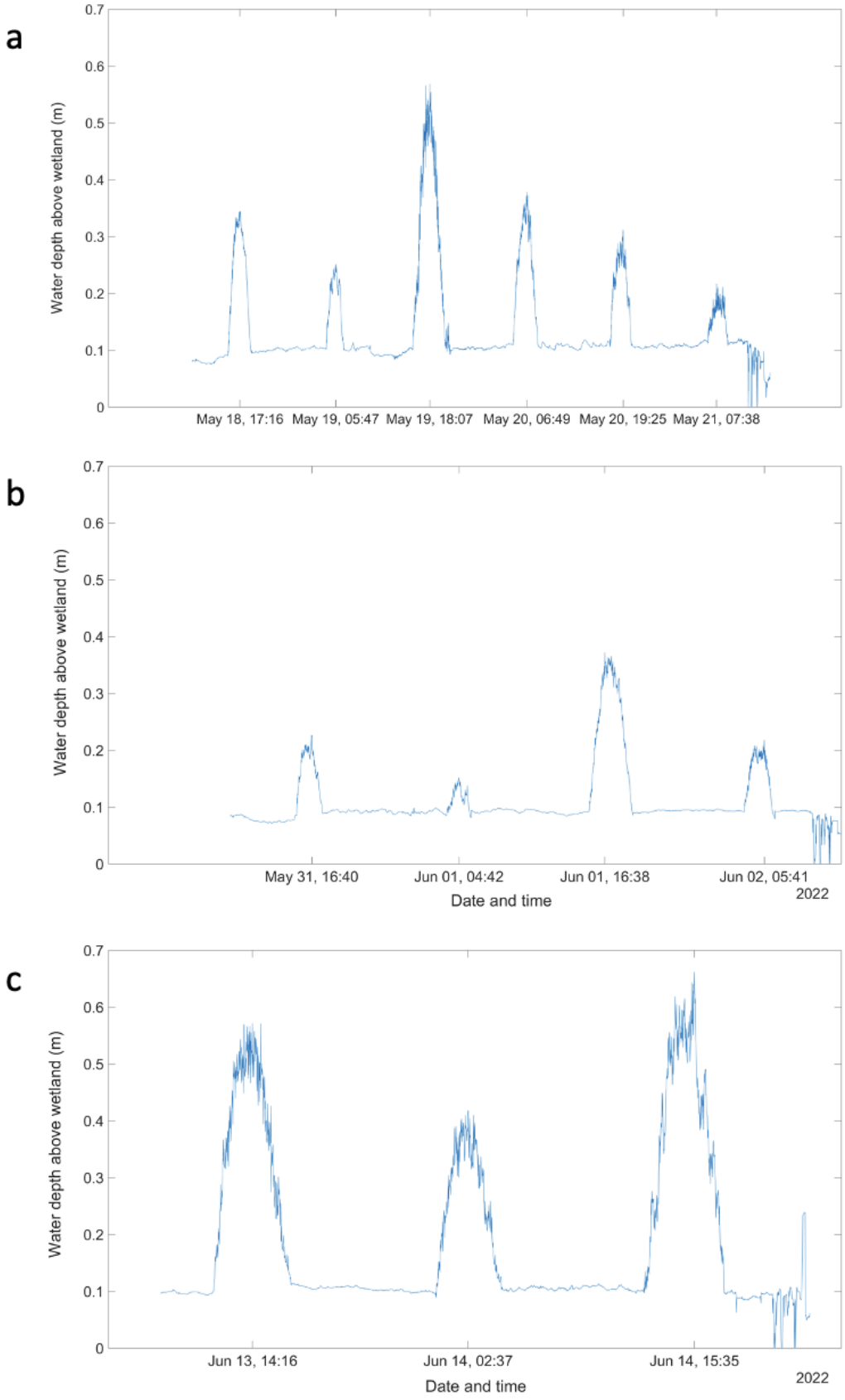

Figure 5.23: Water depth over the wetland during 2022 inundation events; (a) May 18–21; (b) May 31 – June 2; (c) June 13–14.

Table 5.4: Predicted tide level for field experiments and observed pressure from Nugget Point climate station. Cells in *italics* are not illustrated in Figure 5.23 because the RBRs were not deployed. Cells in **bold** correlate to the peaks seen in Figure 5.23.

AM	Tide	Pressure	PM	Tide	Pressure
18-May	*0.94*	*1007*	18-May	1.08	1005
19-May	0.9	996	**19-May**	**1.05**	**990**
20-May	0.85	995	20-May	1	1002
21-May	0.8	999	21-May	0.94	1002
31-May	*0.7*	*989*	31-May	0.78	989
1-Jun	0.67	981	**1-Jun**	**0.77**	**974**
2-Jun	0.63	979	2-Jun	0.74	990
13-Jun	*0.88*	*969*	**13-Jun**	**1.02**	**974**
14-Jun	0.93	985	**14-Jun**	**1.1**	**990**

5.3.6. Wall shear stress and water level

Wall shear stress at the scarp edge is not a constant force across the height of the scarped edge. The top, middle and bottom of the scarp are affected by different values of shear stress under the same water level conditions. Water level is a further determinant of the amount of shear stress exerted on the wetland edge. This section will outline how increasing water level will affect the scarp edge with respect to wall shear stress.

The level of shear stress (Pa) is at its maximum at the top of the scarp. The top of the scarp recorded 10 times the amount of shear stress than the middle section and 5000-7000 times more than the base under all water level conditions, except for water level 0.2 m. The exact position of where the measurements were extracted from is illustrated in Figure 5.4.

Shear stress at the top of the scarp is significantly lower at 0.2 m water level. Shear stress at the scarp edge peaked at 0.5 Pa. Waves are breaking at the base and middle of the scarp (Figure 5.24, a) noted by the increase in wall shear at 0.2 m comparative to other water levels. These breaking waves are not reaching the top of the scarp and thereby not exerting any pressure on this part of the wetland when 0.2 m water level is present.

As water level increases wall shear at the top of the scarp increases, peaking at 10 Pa with 0.6 m water level. Wall shear decreases from 0.6 m to 0.8 m before levelling out for 1 m water level. The wall shear range is narrowed at 0.8 m before widening again at

1 m water level. The range of wall shear at 0.2 m water level is significantly restricted whereas at 0.4 m and 0.6 m the range is equally wide (Figure 5.24, a). Wall shear stress decreases again as water level is increased to 1.2 m and 1.4 m.

Wall shear at the middle of the scarp illustrates an inverse representation of the top of the scarp. Wall shear peaks at 0.2 m water level and then decreases as water level increases (0.4 m & 0.6 m) before levelling off once again at 0.8 m and 1 m water level (Figure 5.24, b). A sharp decrease in wall shear is observed between 0.4 m and 0.6 m. Wall shear at middle of the scarp is significantly lower than the top of the scarp as denoted by the y axis scale (Figure 5.24, a & b). The middle of the scarp experiences a wide range of wall shear stress under 0.2 m and 0.4 m, 0–0.75 Pa and 0–0.61 Pa, respectively. The range of wall shear for 0.8 and 1 m are narrowed, 0.12–0.31 Pa and 0.1–0.31 Pa, respectively. Wall shear at the middle of the scarp decreases as water level is increased.

Wall shear stress at the base of the wetland is very low (Figure 5.24, c) comparative to the middle and top of the scarp. The scale of the y axis for the bottom of the scarp is ~200 times smaller than that of the middle. The amount of wall shear experienced under 0.2 m was significantly higher (150 x) than other base measurements, for this reason it could not be directly compared to other wall shear levels at the base and had to be excluded (Figure 5.25). Wall shear peaks at 0.2 m (0.6 Pa) then decreases significantly at 0.4 m (0.0004 Pa) before increasing again at 0.6 m. A steep decline in wall shear from 0.6 m to 0.8 m is observed as well as a narrow and very low wall shear at 0.8 m (0.000125 Pa). At 1 m, wall shear increases to a range of 0–0.0013 Pa. All water levels at the base of the scarp have ranges that include ‘0’ Pa.

Wall shear under all water levels peaks in the first 50 seconds of each water level model (Appendix C, Figure C4-C10). Wave breaking against the scarp edge increased the wall stress. Wall stress decreases as inundation of the wetland occurs. The 0.2 m model does not inundate the wetland and therefore wall shear stress is greater at the base and middle of the scarp.

The amount of time the scarp edge is ‘attacked’ with waves or water was estimated using the GoPro time-lapse footage from June 13th & 14th. Water propagated against the scarp edge for up to 40 minutes before complete inundation occurred (Figure 5.26).

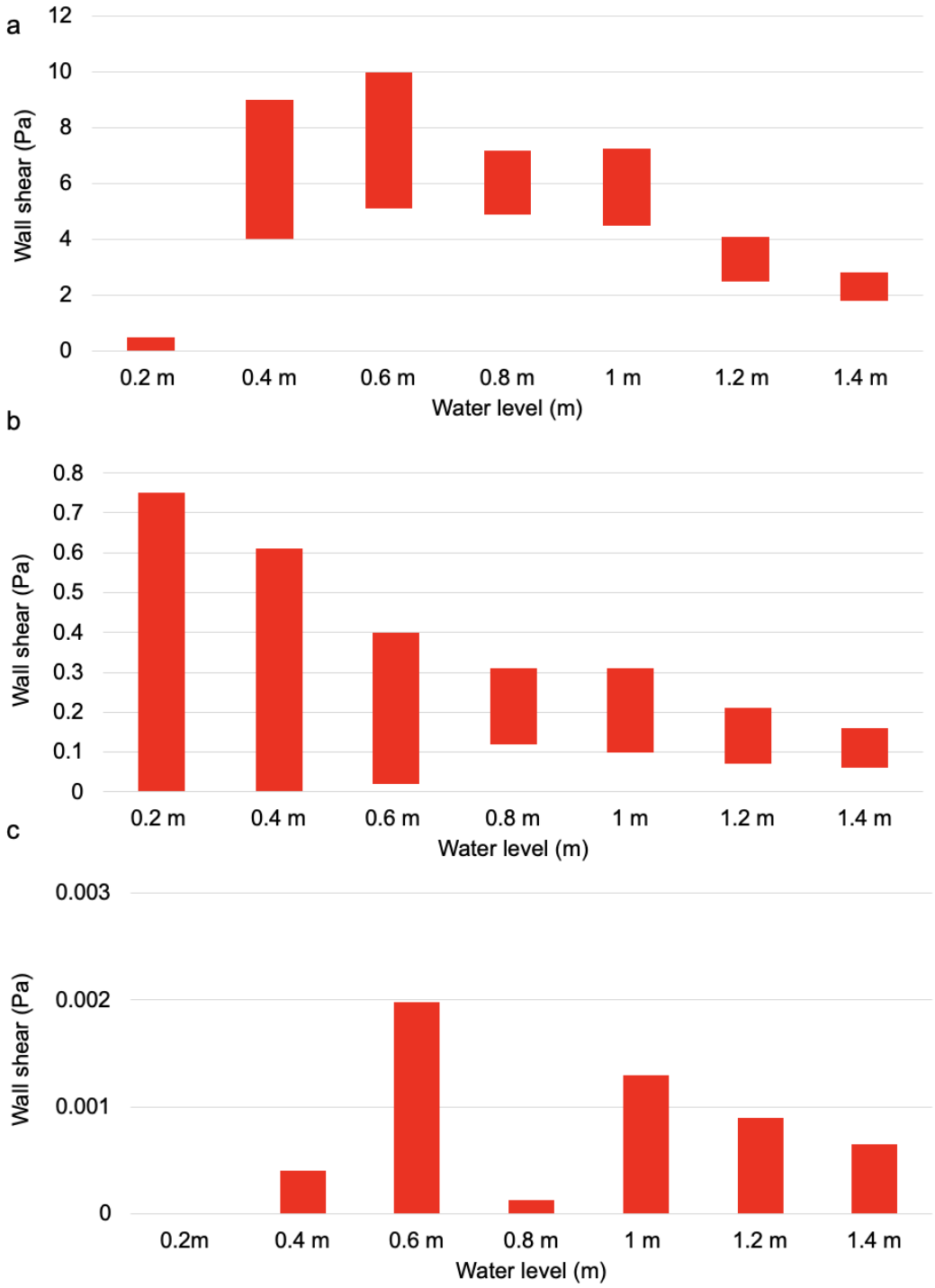

Figure 5.24: Wall shear stress (Pa) at the top (a), middle (b) and bottom (c) of the scarp edge of the wetland using seven water level scenarios with wave height of 0.0718 m and wave length of 8.1512 m. Note the differences in y axis (Pa) scale for a, b and c.

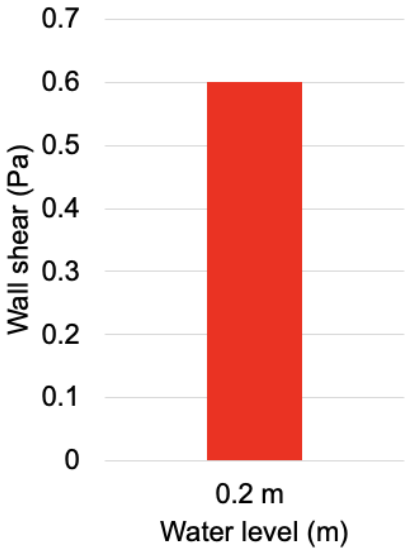

Figure 5.25: Shear wall stress at the base of the scarp under 0.2 m; scaling is significantly different from Figure 5.24 and therefore needed to be separated.

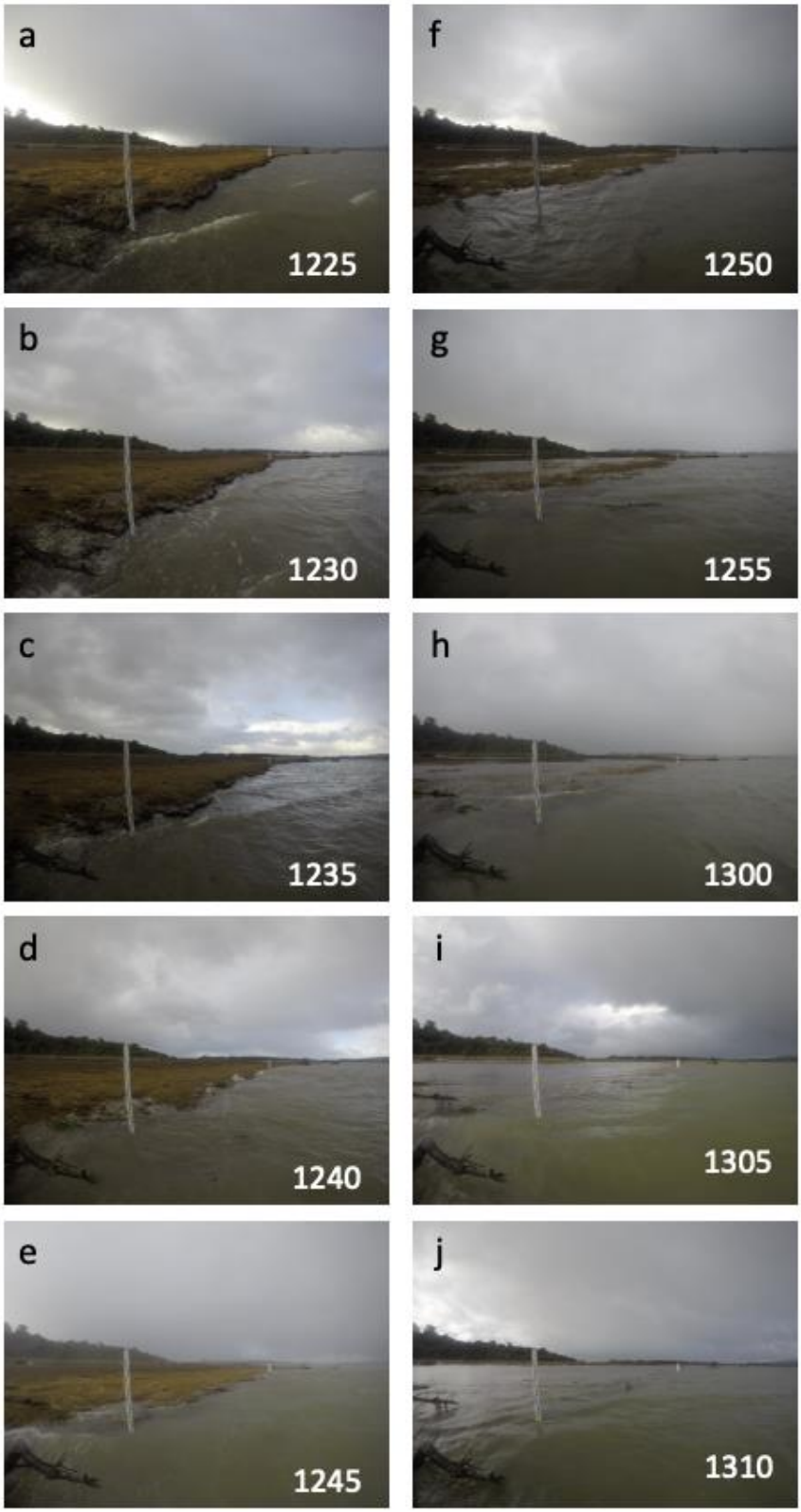

Figure 5.26: Time-lapse of wetland inundation on June 14th; five-minute intervals were used to illustrate the length of time the wetland edge experiences wall shear stress before being completed inundated.

5.4. DISCUSSION

5.4.1. Sediment accumulation

Sediment accumulation on the surface of the Pounawea Wetland is associated with high onshore winds and wave action. Increases in wind speed form larger shallow water waves (Breugem and Holthuijsen, 2007). Such waves have greater turbulence and energy to suspend sediment (Fredsøe and Diegaard, 1992). For sediment to accumulate on the wetland, inundation or partial inundation must occur. Wave action against the wetland edge resulting in water spray onto the wetland could deposit sediment. The results (Figure 5.11 & Figure 5.14) clearly show the association between sediment accumulation and significant wave height.

Sediment deposited on the wetland during inundation is contributing to the vertical accretion of the wetland. Deposited sediment made up of quartz, mineralised sands, shells and organic matter all contribute to the vertical accretion of Pounawea Wetland (Figure 5.8). The combination of these deposits over time develop into silty peat and then finally peat, this is the morphology of the Pounawea Wetland (Gehrels *et al.*, 2008). Vertical accretion is a key part of wetland adaptation (Kirwan *et al.*, 2016; Nolte *et al.*, 2013).

Organic material decomposes and compacts limiting its ability to significantly increase the relative height of the wetland by itself. Marine and terrestrial sands are essential for vertical accretion. These sands made up the majority of sediment deposited on the wetland (Figure 5.6). The combination of organic material and course and fine sand is present within the wetland (Figure 5.5). Gehrels *et al.* (2008) illustrates that the top layer of the Pounawea Wetland is made up of silty peat, a combination of decomposed organic material and sediment. Turner *et al.* (2006), Neubauer (2008) and Morris *et al.* (2016) attest to the importance of organic matter in vertical accretion of wetlands, arguing that it is the principal method of vertical accretion. The processes of below ground biomass and the contribution to vertical accretion is acknowledged but is outside the scope of this thesis and field experiments were not completed to understand the function of below ground biomass at Pounawea Wetland. Morris *et al.* (2016) recognises the low availability of sediment limits vertical accretion (Morris *et al.*, 2016).

Sediment availability is the primary driver of vertical accretion (Weston, 2013). Sediment availability is limited at Pounawea Wetland and has decreased since European

colonisation, whereas upstream and downstream sediment availability has increased over the same time period (Figure 5.16). The Catlins Estuary catchment is sediment rich, however, upstream, the Catlins Lake acts as a sediment sink reducing the flow of sediment downstream.

Without sufficient sediment, wetlands will not be able to vertically accrete faster than rising sea-levels. The rate of sediment accumulation at the wetland edge is greater than the rate of SLR (Figure 5.14). The large majority of sediment deposited on the wetland settles at the edge, a small levee has formed at the wetland edge. During inundation the landward portion of the wetland is inundated before the edge (Figure 5.17, g) indicating higher elevation at the edge. Transect profiles (Figure 3.4, 3.5 and 3.6) and the DEM (Figure 3.3) illustrate a small rise in elevation at the wetland edge. The increase in elevation is the result of sediment deposited in higher concentrations near the sediment source (estuary).

The spatial distribution of sediment deposited during inundation events at Pounawea Wetland is disproportionate and is likely to result in the loss of the wetland due to lateral erosion at the edge where sediment is being deposited. The weight of sediment accumulated on each landward mat is significantly lower than the shoreline edge mats. The rate of sediment accumulation remains constant or decreases further inland (Figure 5.6). This is likely a result of minimal wave action occurring inland. Sediment is resuspended from the intertidal sandflat and then settles at the edge as wave energy is reduced from the interaction with the scarp edge. The amount of sediment deposited inland annually does not equate to 0.2 cm/yr (0.2 cm/yr was calculated using Gehrels *et al.* (2008) stratigraphic analysis). The amount of sediment deposited at the shoreline edge aligns with Gehrels *et al.* (2008) however, the shoreline edge is eroding at rate of -0.67 ± 0.05 m/yr. This means the majority of sediment accumulated at the wetland edge during inundation events is likely to be eroded away each year. This poses a significant issue for the wetland and its ability to vertically accrete faster than SLR. If sediment is not evenly distributed across the wetland then lateral erosion of the wetland edge will continue to erode the areas of highest accretion (wetland edge).

It was hypothesised that the wetland edge would experience a greater volume of sediment deposition compared with the landward margin, because this area is effected by wave breaking. This hypothesis is supported by the results outlined in this chapter.

Sediment deposition during inundation events is higher near the wetland edge, compared with sites 5–20 m landward (Figure 5.6).

There is sufficient sediment supply within the Catlins Estuary to keep pace with SLR, however, the wetland would need to be inundated every day of the year and sediment would need to be deposited further inland. Daily inundation would equate to 0.75 cm of sediment accretion per year. This is more than three times the amount of sediment accretion estimated from Gehrels *et al.* (2008) stratigraphic analysis. Wetland inundation does not happen every day, however, by 2100 daily inundation is likely and landward areas of the wetland are unlikely to have accreted at the same rate as SLR. For now, wetland inundation is dependent on high tide and low pressure.

Sediment accumulation during calm inundation events is constant across the wetland (Figure 5.14). This highlights the role of significant wave height in contributing to the suspended and transportation of sediment onto the wetland, even if the majority of sediment is deposited at shoreline edge. Under calm conditions, the wetland would need to be inundated for 500 days to accumulate enough yearly sediment (0.2 cm/yr). Waves are key drivers of sedimentation, only 10 events per year equivalent to that of June 13-14 would be needed for 0.2cm/yr accretion. This shows that low pressure wind events aligned with high tides are of critical importance for vertical accretion at Pounawea Wetland.

This chapter has shown that there is sufficient sediment deposition onto the wetland to maintain the 0.2 cm/yr rate (Gehrels *et al.*, 2008) which is faster than the rate of SLR. However, the majority of sediment is deposited adjacent to the wetland edge. As discussed in chapter 3, the wetland edge is periodically eroding at a rate of -0.67 ± 0.05 m/yr. Sediment is being eroded laterally before it can contribute to the vertical accretion of the wetland.

5.4.2. Inundation

Wetland inundation is associated with events characterised by low atmospheric pressure and high astronomical tides. Increases in net sea-level driven by SLR and VLM have increased the likelihood of inundation. However, even with increases in sea-level, the alignment of tides and pressure is critical for inundation at Pounawea Wetland. Results from tide and pressure data from 2021 (Table 5.2) demonstrate only 13 hours of inundation occur under extreme low pressure (<980 hPa) and high tide conditions (>0.6 m). Historical and future models (Figure 5.21 & Figure 5.22) illustrate how SLR and VLM have decreased the need for low pressure to obtain higher sea-level. The implications of SLR and VLM will result in increased frequency of inundation events enabled by relative mean sea level and high-pressure events (Figure 4.7).

It was hypothesised that wetland inundation is dependent on the tidal cycle and that spring high tide conditions are necessary for wetland inundation. This hypothesis is partially supported by the results of this chapter. Inundation is dependent on the tidal cycle; however, atmospheric pressure is a significant factor in wetland inundation. Furthermore, spring high tide is not essential for inundation to occur. The alignment of a high tide (>0.6 m) and extreme low pressure (<980 hPa) will result in wetland inundation.

Inundation will apply increasing pressure on wetland vegetation species. The increase in frequency of inundation caused by SLR and VLM will result in a wetland that is more saline. Less tolerant species will be under increasing stress and will likely decay, possibility resulting in poorer soil stabilization which could accelerate erosion at the wetland edge as illustrated in wetlands overseas (Bouma *et al.*, 2014). Inundation of salt meadow environments was not common in the 1990s. Thannheiser and Holland (1994) noted that salt meadow environments in Otago are seldom reached by spring tides, instead they are only flooded during storm tides (Thannheiser and Holland, 1994). The situation today is very different to what Thannheiser and Holland (1994) have described and in another 30 years the wetland is likely to look and behave differently from today.

The amount of pressure exerted on the scarp edge is not equal and the area of wave impact and relative water level are determining factors for wall shear. At the top of the scarp wall shear increases as water level rises to the point of inundation before decreasing (Figure 5.24). Increases in wall shear can be linked to the amount of turbulence created when wave impact occurs at the scarp, indicating erosion (Leonardi *et al.*, 2016). Decreases in shear stress are correlated with increases in water depth (Mariotti and

Fagherazzi, 2013; Li *et al.*, 2019). Significant differences in the scale of wall shear were observed at the top, middle and bottom of the scarp. This is likely because the bottom and middle of the scarp were inundated with water under all simulations and pressure on the wetland scarp was already present. The top of the scarp did not have an external force applied until waves broke against the surface. As inundation occurs less pressure is applied to the scarp, this energy is transferred across the wetland platform.

Future inundation of the wetland (2100+) will likely result in less wall shear at the scarp edge. Results indicate that higher water level (0.8, 1, 1.2 and 1.4 m) produce less wall shear at the top and middle of the scarp than 0.4 m and 0.6 m water level. Erosion at the wetland edge will decrease once inundation of the wetland has occurred because waves will pass over the wetland edge and dissipate inland. However, rising sea-level will increase the frequency of tidal and wave events against the scarp edge. This would increase wall shear at the scarp as seen under 0.4 m and 0.6 m water level (Figure 5.24, a), leading to an increase in lateral erosion of the scarp edge. Ironically, it is wave events that resuspend sediment onto the wetland that enables vertical accretion. The propagation of waves causes bed shear turbulence which resuspends estuarine sediment (Shi *et al.*, 2012; Li *et al.*, 2019). As discussed in section 5.4.1, storm events deposit sediment onto the wetland, unfortunately, the majority of this sediment is deposited at the wetland edge which is periodically eroding at a rate of -0.67 ± 0.05 m/yr.

The duration of wave impact at the wetland edge is unlikely to change under SLR when inundation is certain (low pressure & high tide). Instead, the frequency of wave impacts will increase when tidal and pressure conditions do not align. As sea-level increases, the tidal requirements to reach the wetland edge will decrease. This will result in wave action occurring under lower tidal conditions. Inundation of the wetland may not occur but the ebb and flood tides will reach the wetland edge. Leonardi *et al.* (2016) demonstrated that marsh erosion occurs between light air and a fresh breeze (Figure 2.7). Climate data from Nugget Point illustrates that fresh breezes are prominent (Figure 1.3) and the fetch across the estuary enables fetch-limited wind waves up to 0.61 m to develop (Breugem and Holthuijsen, 2007). Therefore, even under light wind conditions, erosion of the wetland margin is going to continue. Eventually, SLR will reach a point where the wetland will be inundated throughout the tidal cycle, it is likely that by this time (2150) the lower and middle marsh zones would be eroded (Figure 5.22).

5.5. SUMMARY

This chapter has described sediment deposition on the wetland and the relationship between tides and atmospheric pressure required for wetland inundation at Pounawea. Field observations and CFD modelling have enabled a comprehensive understanding of the relationship between sea-level and wall shear at the scarp edge as well as a knowledge of sediment accumulation in the lower marsh area.

Sediment accumulation at the wetland edge is sufficient to outpace the relative increases in sea-level caused by SLR and VLM. Sediment deposited on the wetland is mostly mineral sands, rocks, shells and quartz. Results indicate that sediment deposition on the wetland is heavily focused at the wetland edge, the same area that is periodically eroding (-0.67 ± 0.05 m/yr). Accumulation of sediment is also associated with significant wave height, the same process contributing to wetland edge erosion. Pounawea Wetland is likely to erode before sufficient sediment is deposited to outpace SLR and VLM.

Wetland inundation at Pounawea is reliant on the alignment of tides and atmospheric pressure. Future SLR and VLM are going to cause more frequent inundation. The necessity for extreme low pressure for inundation is going to reduce. Low and medium pressure (981−1020 hPa) in combination with high tides (>0.6 m) will inundate the wetland. This will directly affect the wetland edge erosion and vegetation. Wall shear at the scarp increases until the water level inundates the wetland, at this point it decreases. This means that the scarp edge will be under increasing pressure at lower tidal levels, likely accelerating erosion but at the same time bed shear stress increases and sediment resuspension will increase contributing to the vertical accretion of the wetland.

6. Mitigation Strategies

6.1. INTRODUCTION

Pounawea Wetland has eroded at a rate of -0.67 ± 0.05 m/yr since 1948. This chapter reviews the drivers of environmental change identified in the previous chapters and examines the potential for nature-based options for mitigating this erosion. Environmental solutions will be categorised into short and long-term solutions. Within these two categories, the associated benefits of each management option will be discussed. The purpose of this chapter is not to determine the feasibility of the solutions proposed, rather it is to demonstrate an understanding of the environmental drivers and how specific solutions, or a combination of solutions, could be implemented to mitigate present and future threats to Pounawea Wetland.

6.1.1. Key thesis findings

Pounawea Wetland is under significant threat of lateral. Pounawea Wetland is clearly vulnerable to sea-level rise (SLR) and lateral erosion. The low-lying elevation of the wetland and proximity to Catlins Estuary make the wetland suspectable to SLR, coastal flooding or storm events. Erosion of the wetland edge has been documented since the first aerial photograph in 1948. The linear regression rate (LRR) of erosion was calculated to be -0.67 ± 0.05 m/yr since 1985. Before the erosion of Cabbage Point in 1985, LRR was calculated to be -0.62 ± 0.08 m. This small change in LRR is possibly the result of the erosion of Cabbage Point.

Lateral erosion of the wetland edge has reduced the area of habitat for lower marsh species. The upper marsh boundary shifted landward in association with recession of the podocarp forest from 1985. This highlights the ability of wetland vegetation to adapt and transgress when habitable space becomes available.

Land use change of the surrounding estuary catchment, particularly forest removal upwind of the wetland, has increased the wind speed across the estuary during south–west wind events; which has subsequently increased significant wave height at the

wetland margins. Computational fluid dynamics (CFD) simulations were used to model the changes in wind speed before and after forest removal. Results indicated a significant increase in wind speed across the estuary after forest removal and it is likely that the removal of the forest upwind of the wetland resulted in an increase in the size and frequency of fetch-limited waves that accelerated erosion of the wetland edge.

The Pounawea area is subsiding at a rate of 1.07–1.65 mm/yr (King *et al.*, 2020). This subsidence, coupled with projected SLR (3 mm/yr), will result in a relative rise in sea-level of at least 4 mm/yr. Vertical accretion at the wetland edge is sufficient to outpace the relative rise in sea-level caused by SLR and VLM. However, 67% of sediment deposited during inundation events occurs along the edge of the wetland (Figure 5.6), within 2 m of the scarp. This margin of the wetland is eroding at a rate of -0.67 ± 0.05 m/yr. Sediment deposition appears to be associated with significant wave height (Figure 5.11) During wind events (>7 m/s) at high tide (>0.6 m water level) fetch limited wind waves propagate across the estuary and create turbulence, resuspending sediment which is deposited on the wetland during episodes of inundation.

Wetland inundation is associated with tides and atmospheric pressure. Sea-level rise will increase the frequency of inundation during higher pressure events. Wetland inundation no longer requires extreme low pressure (<980 hPa) and spring tides (>0.9 m). As water level rises wall shear at the scarp increases; once inundation of the wetland has occurred wall shear stress at the scarp decreases. This means that there is more force exerted on the scarp as water level rises as opposed to when the scarp is fully inundated.

6.1.2. Drivers of change

Wetland morphodynamics and erosion can be linked to two central processes: (1) land use change; and (2) sea-level rise and vertical land movement. Land use change within the Catlins Estuary catchment has been extensive since European colonisation. The loss of Cabbage Point as a sand spit at the entrance of the estuary and the deforestation of the surrounding landscape have resulted in loss of the wind sheltering effect of forests and wave reflection and attenuation from sand spits. Indirectly, land use change has been a driving force of increased erosion of the wetland. Increased wave exposure due to deforestation has been identified as the primary consequence of land use change. A secondary consequence resulting in increased wave exposure is the loss of

Cabbage Point. The second driver is SLR and VLM. Changes in sea-level are associated with more frequent inundation which directly effects wetland vegetation. SLR and VLM are historical drivers of wetland change but these two processes will continue to change the wetland in the future. It should be noted that solutions to resolve SLR and VLM are not possible at a local scale. The subsidence of this area of the Catlins is the result of the Australian Plate subducting under the Pacific Plate (Denys *et al.*, 2020). SLR is a global issue driven by increases in greenhouse gas (GHG) emissions causing temperatures to increase and result in higher sea-level (Fox-Kemper *et al.*, 2021). These are global processes that are not going to be solved. At best, the rate of SLR can be slowed, but forecasts indicate 1.8–3 mm of sea-level rise per year until at least 2100 and likely further into the future (Fox-Kemper *et al.*, 2021).

6.2. METHODS

The methods of this chapter are focused on case studies from around the world relating to different mitigation strategies. The literature of salt meadow wetlands, erosion of these wetlands and mitigation strategies specifically focused on this type of wetland is extremely limited. For this reason, literature pertaining to the erosion and protection of coastal wetlands has been used. Literature from open coast wetlands, estuarine and lagoon wetlands in low and high energy environments was analysed. *Spartina alterniflora* (cordgrass) wetlands were predominantly used as case studies for literature from the United States. The tall, stiff grass is unlike the herbaceous species found at Pounawea. Literature associated with shelterbelts and sand renourishment did not focus on wetland erosion but the effects (wind sheltering and wave attenuation) can be inferred and applied to wetland erosion.

6.3. SHORT TERM ENVIRONMENTAL MANAGEMENT SOLUTIONS

6.3.1. Do nothing

To do nothing to protect Pounawea Wetland would leave it vulnerable to erosion from tides and storms. Pounawea is a relic salt meadow environment, consisting of a lower, middle and upper marsh and a native podocarp forest at the marsh boundary. As outlined above (section 6.1.1), the wetland faces a range of threats that will ultimately result in the loss of the wetland. Pounawea Wetland is recognised as a regionally significant wetland and noted as having Kai Tahu cultural and spiritual values in the Otago Regional Plan (ORC, 2020b). The wetland is also an important habitat for fisheries and waterfowl. Wetland conservation was established by the Ramsar Convention in 1971. New Zealand became a signatory in 1976 and while Pounawea Wetland does not come under the protection of the Ramsar Convention it is worth noting that wetland environments are recognised internationally for their high biodiversity and ecological function (Gardner and Davidson, 2011).

Erosion of the wetland margins will continue if no management action is taken. The historic rate of erosion is of -0.67 ± 0.05 m which would mean the wetland would erode to the internal creek (85 m inland from the 2022 wetland edge) by 2150 if these rates are maintained. The rate of erosion could accelerate as sea-level increases, as demonstrated through wall shear (section 5.3.6). The predicted shoreline of Pounawea Wetland was illustrated in Figure 5.20. This showed the wetland edge location in 2050, 2100 and 2150, with the latter illustrating the wetland edge would be where the upper marsh zone is today. In 128 years, the lower and middle marsh zones would be lost to erosion.

Eustatic sea-level rise and land subsidence cannot be mitigated at a local scale. The effects of SLR, such as an increase in wave activity on the wetland could be mitigated. By 2150, the wetland will be inundated daily by mid (0.4 m) and high tides (0.6 m). This would be detrimental to the species that inhabit the area. Lower and middle marsh species at Pounawea (*Selliera radicans, Samolus repens* and *Sarcocornia quinqueflora*), while salt tolerant, are not hydrophytes (aquatic plants) and they would likely decay. Landward transgression of wetland species is not uncommon and has taken place at Pounawea in the past. The ‘roll-back’ of the podocarp Forest (Figure 3.8) and the encroachment of the

upper marsh zone between 1948 and 1985 could have been initiated by repeated tidal inundation and soil saturation, leading to reduced forest growth and decay. Repeated inundation would cause the back margins of the wetland to become more saline, instigating wetland soil development and wetland vegetation (Fagherazzi *et al.*, 2019). Inundation of brackish-water creates osmotic stress and sulphide toxicity which may lead to the decay of forest species (Brinson *et al.*, 1995; Kozlowski, 1997). Carr *et al.* (2020) discusses that wetland transgression across the forest boundary is influenced by slope, water level, forest recovery and the timing and frequency of extreme events (floods) (Carr *et al.*, 2020). Given that the slope of Pounawea Wetland is minimal, the frequency of inundation events and the rate of SLR are significant drivers of wetland transgression. There is ~ 0.15 m of elevation change from the lower marsh to the upper marsh, this is an opportunity for lower marsh species (*S. repens, S. radicans & S. quinqueflora*) to migrate landward. If lower marsh species cannot transgress then changes to the wetland environment are an opportunity for more saline tolerant species, like hydrophytes to colonise the inundated areas.

The costs associated with doing nothing vary. Monetarily, there is no cost. Biophysically, New Zealand loses one of the best examples of a southern salt meadow wetland. The species that inhabit the lower and middle marsh zones will likely be lost, however, *Selliera radicans* and *Salicornia quinqueflora* may naturally migrate landward.

Doing nothing signifies the failure of policy set up to protect vulnerable environments and mitigate coastal hazards. Politically, not doing anything sets a precedent regarding environmental management of low-lying coastal wetlands. The question then becomes, what does constitute protection and why? Understandably, the line needs to be drawn at some point in time, since not all environments can be protected from SLR. The New Zealand Coastal Policy Statement 2010 (NZCPS) outlines the need to avoid and mitigate adverse effects on coastal wetlands as well as promoting the restoration and rehabilitation of coastal wetlands (New Zealand Government, 2010). The policy also acknowledges the potential for coastal wetlands to act as a natural defence against coastal hazard. This illustrates the government's commitment to protecting coastal wetlands, but in reality, there are many wetlands and or coastal environments that are facing the same stresses as Pounawea Wetland.

Wetlands enhance the natural landscape adding social value to an area. Pounawea Wetland is no different. To measure the social value of Pounawea Wetland a social value

evaluation index system could be implemented. A study by Ye and Sun (2021) showed how to conduct the evaluation using a range of indicators to better understand how wetlands are viewed by society and their value (Ye and Sun, 2021). Applying this method to Pounawea could provide insight into the perceived value of the wetland and aid decisions regarding how to approach environmental management solutions for the eroding wetland.

Culturally, wetlands are important to Māori, both spiritually and for food gathering (kaimoana). Māori believe that the environment is an interconnected part of the wider social order. Te Ao Māori, recognises that all elements of creation both living and spiritual are interrelated, this is governed by whanaungatanga (kinship) (Harmsworth and Awatere, 2013). Therefore, degradation or loss of an area is seen as failure of society. Doing nothing is not likely to be an appropriate outcome for Māori given the importance of whanaungatanga.

The drivers of environmental change at Pounawea will continue uninterrupted if the do-nothing approach continues. Erosion and inundation of the wetland will continue either at the same rate or at an increased rate. New Zealand will lose a rare salt meadow wetland and the Catlins Estuary ecosystem will change.

6.3.2. Oyster reefs

The removal of forest upwind of Pounawea Wetland has increased the frequency and size of waves breaking against the wetland edge at high tide. Oyster reefs are a natural mechanism for wave attenuation (Scyphers *et al.*, 2011; Wiberg *et al.*, 2018). The construction of hybrid infrastructure to protect the coast is becoming increasingly popular and oyster reefs are regularly used. They have become popular because they offer additional ecosystem services (Figure 6.1) and have low maintenance costs. Oyster reefs can be built in a number of ways (Figure 6.2). Located on intertidal mudflats, oyster reefs mitigate shoreline erosion by attenuating waves and stabilizing wetland sediment which contributes to wetland accretion (Meyer *et al.*, 1997; Pontee *et al.*, 2016; Salvador de Paiva *et al.*, 2018; Scyphers *et al.*, 2011; Wiberg *et al.*, 2018). The potential to use oyster reefs at Pounawea will be explored in the following paragraphs.

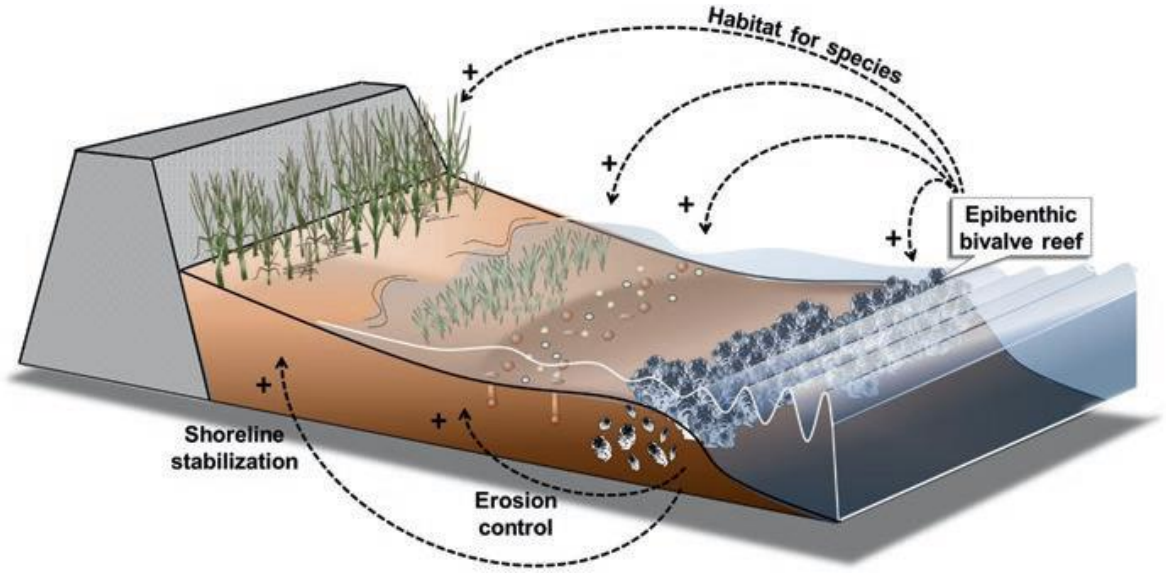

Figure 6.1 Conceptual model of ecosystem services provided by epibenthic bivalve reef (oyster reef), services include; erosion control; shoreline stabilisation; and habitat creation (Ysebaert *et al.*, 2019).

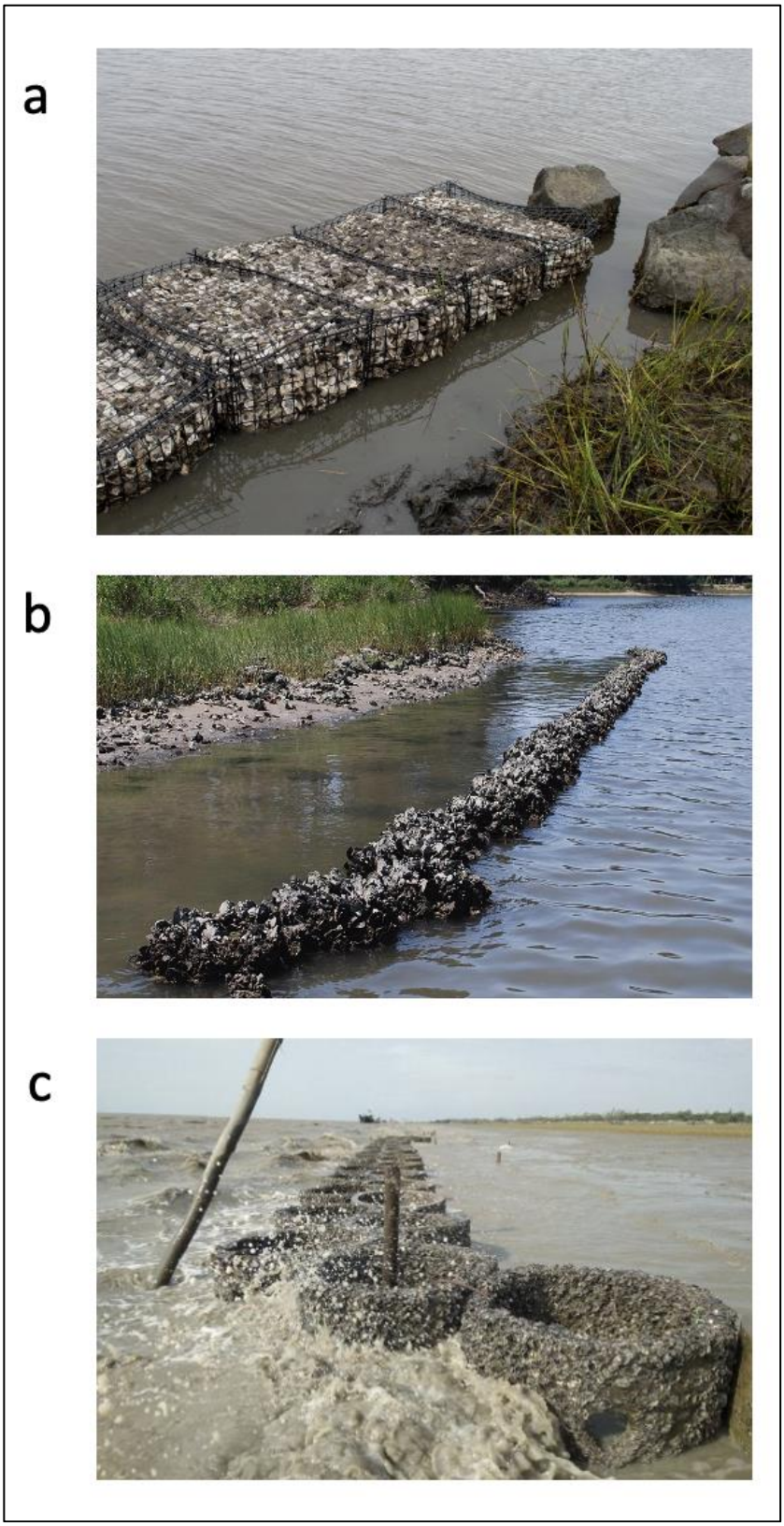

Figure 6.2: Constructed oyster reefs: (a) oyster reefs grown within a gabion basket (Williams, 2019); (b) oyster reef on concrete blocks (Drake, 2021); (c) hexagon concrete oyster reef structures (Chowdhury, 2019).

Oysters reefs can be arranged in two ways (Figure 6.3) - isolated or overlapping oyster reefs. Isolated oyster reefs could be used to directly protect the wetland from the predominant wind (southwest) or if costs were an issue. A limited number of oyster reefs could be implemented in the most affected areas. Overlapping oyster reefs would protect the wetland from all angles but could be expensive. The structure of oyster reefs is dependent on the type of reef implemented. Hybrid structures such as gabion baskets and hexagonal concrete oyster reefs (Figure 6.2, b & c) that can be interlinked and act as a oyster habitat and a breakwater for waves can be arranged in a manner to suit the environment and dominant wave direction.

Oyster reefs are permeable, meaning, water flows through the structure instead of being reflected (Scyphers *et al.*, 2011). Wave energy is dissipated and silt and fine sediments can pass through and settle on the wetland. Reducing wave height and wave energy would limit the erosion effect.

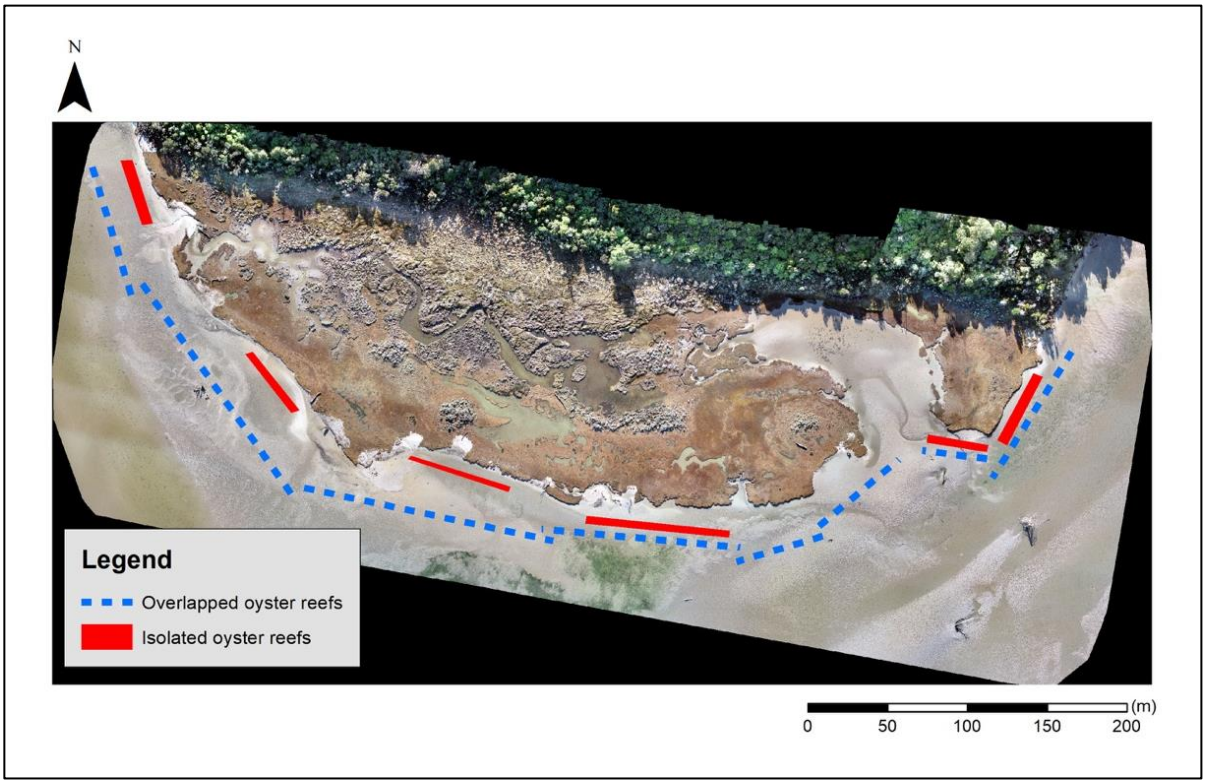

Figure 6.3: Potential oyster reef layouts, overlapped (blue) and isolated (red).

As sea-level increases the effectiveness of oyster reefs may be reduced. A recent study by Morris *et al.* (2021) showed that wave attenuation by oyster reefs significantly decreased when oyster reefs were inundated >50% of the time (Morris *et al.*, 2021). This study focused on living shorelines, using low lying oyster reefs on beach shorelines and estuary sandflats. Oyster reefs were used to protect the shoreline but one case study in Louisiana focused on mitigating marsh erosion adjacent to the oyster reefs (Morris *et al.*, 2021). Oyster reefs were effective at reducing the rate of marsh erosion compared to non-protected areas but both areas continued to erode (Morris *et al.*, 2021). Gabion baskets would enable taller oyster reefs to be constructed which could offer greater protection under SLR.

Pounawea Wetland presents itself as a unique opportunity to apply a nature-based solution (oyster reef) to an eroding wetland edge. A study could be undertaken to assess the effectiveness of *Tiostrea chilensis* (Bluff oyster) oyster reefs at Pounawea. *T. chilensis* grow in sheltered environments in depths up to 35 m (Jeffs and Creese, 1996). *T. chilensis* grow in Bluff harbour so water temperature is no issue. Gabion baskets (Figure 6.2, a) are easily constructed and can be filled and place in the desired position. A comparison between an oyster protected shoreline and an unprotected shoreline could be completed. McClenachan *et al.* (2020) demonstrated how the DSAS tool in ArcGIS can analyse the rate of change of shoreline movement (McClenachan *et al.*, 2020). This analysis would accurately assess the difference between the wetland edge sheltered by oyster reefs and areas that are not, furthermore, CFD modelling could be used to test different oyster reef structures to determine the most effective for wave attenuation. Carter *et al.* (2015) tested 9 artificial oyster reefs built at MSL with crest widths ranging from 2.4–3 m. CFD measured average transmission coefficient (Kt), average reduction in wave power (%), Shoreline change reduction (m/yr), and cost ($) per ft of shoreline change reduction (Carter *et al.*, 2015). The 9 options were then ranked on their relative effectiveness. The results demonstrated the importance of modelling different oyster reef structures to ensure the right design is implemented. CFD modelling could be undertaken at Pounawea Wetland and then following this a trail could be set up to test the model before full scale implementation.

The costs and benefits associated with oyster reefs are outlined in Table 2.2 and Figure 2.10. The average cost of oyster reef construction is NZD \$218.46 m^2 (Narayan *et al.*, 2016). Based on this cost, the isolated oyster reefs in Figure 6.3 would cost

$363,133 NZD to implement (these costs are based on Narayan *et al.,* 2016, and have not been adjusted for inflation; conversion from USD to NZD was undertaken using 2022 currency exchange rates; $1 USD to $1.61 NZD).

The ecosystem services of an oyster reef would enhance biodiversity and the social and cultural value of the wetland. Oyster reefs improve estuarine water quality through filtration of suspended sediment; provide habitat for epibenthic invertebrates; augment fish production; stabilise the shoreline; and increase the diversification of the landscape (Gedan *et al.*, 2014; Grabowski and Peterson, 2011). Mitigating the effects of erosion at the shoreline using oyster reefs has the potential to slow the rate of erosion and potentially improve sediment accumulation across the wetland.

Constructed oyster reefs could be a permanent solution if successful in reducing wetland edge erosion. Oyster reefs can vertically accrete, meaning they can keep pace with SLR and continue to act as natural barrier (Grabowski *et al.*, 2012; Rodriguez *et al.*, 2014). For oyster reefs to be effective they need to be inundated more than 50% of the time (Scyphers *et al.*, 2011), meaning that the reefs would need to be nearer to the estuary channel to begin with and as sea level rises they could be relocated closer to the wetland edge. However, Wiberg *et al.* (2018) demonstrated that wave attenuation decreased with water depth. For the experiment, oyster reef crest elevation were 0.3-0.5 m below MSL and when water depth exceed 1.5 m there was < 10% reduction in wave height, whereas, for water depth 0.5-1 m there was a 30-50% reduction in wave height (Wiberg *et al.*, 2018). This means that there is a fine balance between effective wave attenuation and the height of oyster reefs relative to mean sea level. This was demonstrated by Servold *et al.* (2015) in a low energy wave environment (wave height<0.1 m). Six 125 m long and 0.61 m crested oyster reefs were placed 30 m offshore for one month and there was no statistically significant decrease in wave height leeward of the oyster reefs (Servold *et al.*, 2015). This result led Servold *et al.* (2015) to the conclusion that crest height is a determining factor of wave attenuation.

Overseas examples provide a good foundation for understanding of how oyster reefs can be used but each oyster reef site is unique and adaptation for hydrodynamic processes and the surrounding environment are likely needed (Howie and Bishop, 2021). The length, width, height, oyster density and hydrodynamic processes should all be considered with each oyster reef constructed (Fitzsimons *et al.*, 2020). Research by Allen and Webb (2011) illustrated that increasing the width of oyster reefs improved wave

attenuation and species richness (Allen and Webb, 2011). Further work by Webb and Allen (2015) modelled wave transmission through artificial oyster reef breakwaters in a laboratory environment. Froude scaling of 1:5 was used and the dimensions of the oyster reef was 0.61 x 0.30 x 0.25 m (length, height, crest width). A range of water depths (0.2-0.41 m), wave heights (0.05-0.2 m) and wave lengths (1-3 seconds) were tested (Webb and Allen, 2015). Results indicated that wave transmission decreased as structure height increased relative to water depth (Webb and Allen, 2015), meaning, there is a clear dependence on structure height for wave attenuation to be effective. The unscaled values of water depth (1–2.05 m) and wave period (5–15 s) used in Webb and Allen (2015) have similarities to conditions observed at Pounawea; and the lower range of wave height (0.2–1 m) is also reflective of conditions observed at Pounawea.

Scyphers *et al.* (2011) demonstrated that shoreline retreat decreased by 40% when oyster reefs were implemented. The reefs were 25 x 5 x 1 m (length, width, height), constructed on geo-textile fabric to reduce subsidence on the intertidal and were placed slightly above Mean Lower Low Water (MLLW) (Scyphers *et al.*, 2011). The capacity for wave attenuation diminished over time because wave energy exceeded the strength of the geotextile mats that oysters were attached to. This study took place on the open coast in the Gulf of Mexico which experiences hurricanes and deep water waves (Scyphers *et al.*, 2011). Wave height and energy in the Gulf of Mexico is higher than the fetch-limited shallow water waves typical of Pounawea Wetland.

Piazza *et al.* (2005) discussed how small fringing reefs (25 x 1 x 0.7 m) would be suitable for low energy environments and less effective in high energy environments such as hurricanes or severe storm surge (Piazza *et al.*, 2005). Pounawea Wetland is exposed to strong south-westerly winds but the limited water depth (1-2 m) means that large waves (>1 m) do not occur and it is likely a low energy environment suitable for oyster reefs. Several reefs could be constructed using Scyphers *et al.* (2011) model (25 x 5 x 1 m) and place offshore where the depth of water during spring high tides would not exceed 1 m to ensure effective wave attenuation (Wiberg *et al.*, 2018).

Oyster reefs can begin as community led projects and be scaled up to cover large areas where the ecosystem services are more evident. Projects in Sydney started small as ‘proof of concept’ ideas and slowly grew larger as public awareness and the positive impacts were observed. The potential to use oyster reef restoration as an education and hands on learning experience in schools was demonstrated in Australia (Fitzsimons *et*

al., 2020). Incorporating the local community and businesses through initiates such as 'Shuck Don't Chuck' where restaurants and seafood wholesalers pass on their discarded shells to oyster restoration projects. The Bluff Oyster festival and local restaurants in Owaka, Balclutha and Catlins areas could be included in the initiative. Creating community engagement and investment will improve the outcome of the project (Fitzsimons *et al.*, 2020).

6.3.3. Sand nourishment of Cabbage Point

Sand spits are a natural protective barrier that can attenuate wave energy and form an effective habitat for flocking birds to nest within the vegetation at high tide (Hanley *et al.*, 2014). Cabbage Point was once a long (~750 m) and wide (~200 m) sand spit that protected the estuary entrance and wetland from north easterly storms. The dynamic movement of the spit and subsequent erosion was discussed in section 3.7.2. Re-establishing Cabbage Point could decrease the rate of wetland erosion by limiting wave propagation from the easterly swells as well as increase biodiversity as a migratory and native species habitat.

The movement away from hard structures at the coast refocuses attention on the natural process of sand nourishment. Sand nourishment is not a new concept and has been used in the past to replenish beaches from storms, improve pedestrian access to water or as a by-product of marina or development dredging (Healy *et al.*, 1990; Bird and Lewis, 2014). More recently, the re-nourishment of a sandspit in Japan after the 2011 Tsunami. The Naruse River mouth was once protected by a sandspit but after the Tsunami this spit was washed away and waves were able to propagate through the river entrance (Nguyen *et al.*, 2019). Wave propagation through the river mouth meant that sediment was transported upstream or into the nearby canal due to wave diffraction. After seven years, the sandspit had not naturally recovered due to insufficient sediment supply and work began on re-nourishment (Figure 6.4).

Figure 6.4: Aerial images of during and after sand nourishment of the sandspit at Naruse River, Japan (Nguyen *et al.*, 2019).

Cabbage Point in 1948 was a 750 m long, 200 m wide vegetated sandspit (Figure 6.5). Re-establishing this landscape could reduce wetland erosion through wave attenuation and wind sheltering from the north easterly storms. Re-nourishing Cabbage Point to an elevation above mean high water spring (MHWS) and planting vegetation could restore the spit. Native dune vegetation could be planted. Planting *Ammophila arenaria* (marram grass) would result in a relatively steep and densely vegetated foredune (Figure 6.6) (Hesp, 2002). *A. arenaria* is a sand-binding species often planted to stabilise dune systems (Darke *et al.*, 2016; Hesp, 2002). The use of *A. arenaria* to build up and stabilise Cabbage Point, while effective, does not align with the work to remove this species in favour of the native dune species, *Ficinia spiralis* (pīkao) (Hilton and Konlechner, 2010). *F. spiralis* are relatively low dunes systems with a hummocky

morphology (Figure 6.6) (Konlechner *et al.*, 2015). This morphology should increase biodiversity and the atheistic value of Cabbage Point. Wave attenuation or the response to inundation is not well studied in relation to pīkao dune systems.

The re-establishment of Cabbage Point could be a two-phase process. Firstly, nourish the spit with sand and plant *A. arenaria*. Planting marram grass would likely provide the spit with the best chance to retain sediment and build a dune landscape that could survive an inundation event. The second phase would see the removal of marram grass using a spray program similar to that undertaken in Mason Bay and Doughboy Bay and planting pīkao (Hilton and Konlechner, 2010; Konlechner *et al.*, 2015). These spray programs have been successful in re-establishing pīkao foredunes.

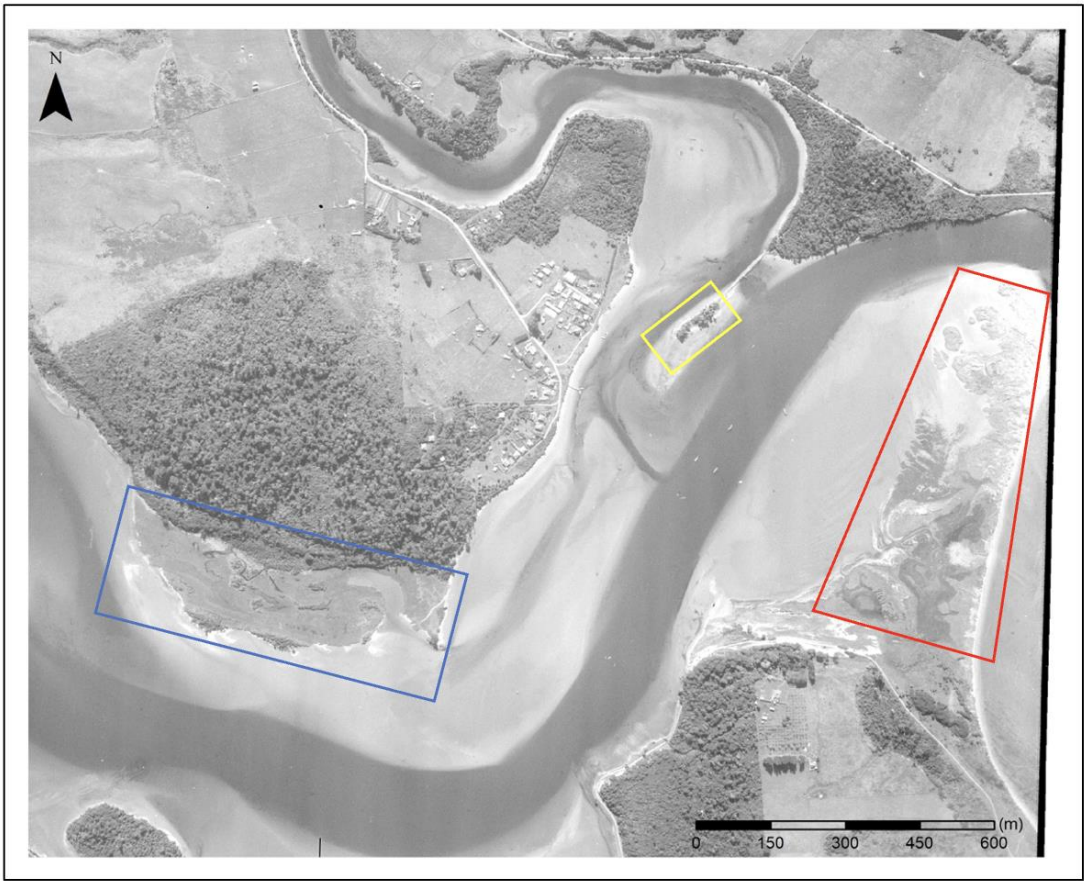

Figure 6.5: Pounawea Wetland (blue), Manuka Point (yellow) and Cabbage Point (red) in 1948. Cabbage Point is vegetated and extends across the intertidal area to the estuary channel.

Figure 6.6: left: *Ammophila arenia* (marram grass) foredune at Mason Bay, Stewart Island in 2007 (Hilton and Konlechner, 2021); right: *Ficinia spiralis* (pīkao) foredune at Doughboy Bay, Stewart Island in 2021 (photo from Maddie Brown).

Cabbage Point is exposed to easterly swells and north-east winds, the combination of these events would likely contribute to erosion of the sandspit. The scope of this chapter is to discuss solutions that address the drivers of environmental change, however, the feasibility of these solutions is beyond the scope of this thesis. Re-nourishment without the planting sand-binding dune species would likely result in the erosion of Cabbage Point. Extreme low pressure, strong winds coupled with spring tides would likely erode parts of Cabbage Point. Successive erosion events could result in the loss of Cabbage Point again. To avoid the potential of erosion events, climate data analysis and modelling could be completed to determine when calm conditions would be more frequent, similar modelling was done by Kühn (2021) to reduce the risk of erosion during nourishment (Kühn, 2021).

If a storm were to occur during sand nourishment then it is likely that the sand would be eroded. The formation of a foredune by sand nourishment, depositing sand in the presence of a sand binder, a primary colonising species (*A. arenria*) should result in a foredune. Marram grass seeds are buried within the foredune and can be viable from depths of up to 4 m (Hilton *et al.*, 2019). The excavation and redistribution of marram grass would likely save valuable time that would otherwise be spent on waiting for *A. arenaria* to germinate and bind sand together to form a foredune.

Culturally and socially, nourishing Cabbage Point with sand would likely been seen as an improvement to the estuary catchment given the events of the 2006 storm (section

3.7.2). It is inferred that the removal of Cabbage Point exacerbated the erosion and flooding seen at the Pounawea foreshore (Figure 3.22).

Re-nourishing Cabbage Point could potentially decrease the rate of lateral erosion of the wetland whilst increasing biodiversity habitat for birds by providing a refuge for nesting and a migratory pathway. A sandspit and dune system could shelter the wetland from north-east winds and swells. The native dune landscape of pīkao could provide refuge for flocking birds or a nesting area. Sand nourishment should be used in conjunction with another management solution (oyster reefs or sandbags). Historical erosion of Cabbage Point would indicate that the possibility for it to occur again is likely. Investing and relying on one method of mitigation is not a viable solution, a combination of management initiatives is likely needed.

6.3.4. Sandbags

Protecting the wetland edge from waves is a crucial factor in limiting erosion at Pounawea. Sandbags are an effective short-term mechanism to reflect and absorb wave energy (Christianen *et al.*, 2013). They are low cost (Figure 2.10) and effective for shoreline protection (Martinelli *et al.*, 2011). The structure, size and location of the sandbag are important to achieve meaningful wave attenuation (Moreira *et al.*, 2016). Sand bags can contribute to the protection of the wetland but they do not add social or biophysical value, there are not any ecosystem services benefits aside from reducing wetland edge erosion.

Sandbags were used in conjunction with oyster reefs during an experimental test by Dunlop *et al.* (2017) at Manly Lagoon, NSW, Australia. Sandbags were placed landward and on the crest of oyster reef structures, preventing displacement. The experiment concluded that sandbags were an effective addition to oyster reefs but the structure of sandbag placement (height and width) were important parameters for wave attenuation (Dunlop *et al.*, 2017). This means that, for more exposed areas where waves are larger, the height and width of the sandbags should be increased.

The monetary cost would likely be low compared to other management options (re-nourishment or hard structures). The structure and layout of the sandbags would have a large impact on the costs (Martinelli *et al.*, 2011). Sand could be collected locally at the estuary mouth, reducing costs associated with transportation. If the sandbags were

ineffective at reducing the rate of lateral erosion or decreased the rate of sediment deposition onto the wetland they could be removed. The removal will not affect the ecology and morphology of the salt meadow.

Aesthetically, sandbags are unattractive and devalue the natural landscape. They are also associated with natural disasters (flooding, cyclones). Socially, sandbags would increase the longevity of the wetland which is a positive outcome for people that use and value the wetland. Sandbags could be used temporarily while other mitigation strategies have time to establish.

Land use change is the driving force of erosion at the wetland edge. Sandbags would provide wave attenuation capabilities and protect against erosion, thus mitigating the effects of land use change. The effects of SLR related to inundation would not be resolved by sand bags. Unlike oyster reefs, sand bags are less permeable and therefore sediment is unlikely to accumulate on the wetland. Sands bags would protect against lateral erosion but hinder the vertical accretion of the wetland.

6.4. MEDIUM TO LONG TERM INTERVENTIONS

6.4.1. Wind shelterbelt

Land use change is a key driver of erosion at Pounawea Wetland. The loss of the upwind forest located at Hinahina has increased wind speed across Catlins Estuary which has likely increased the frequency and size of fetch limited waves during strong southwest winds. Planting a shelter belt upwind of the wetland should decrease wind speed across the estuary.

Shelterbelts are regularly used by farmers to shelter crops and or livestock from wind (Gregory, 1995). Planted in east-west lines to provide shade to the south side, shelter belts are typically only one row of trees. The use of poplar species is most common in New Zealand since they can be pruned to improve air movement (Gregory, 1995)

The effectiveness of a windbreak is correlated to the porosity of the windbreak, the number of rows of trees and the spacing between the trees (Wan *et al.*, 2005). A windbreak utilizing a medium-porous design is optimal for wind speed reduction

(Středová *et al.*, 2012). Wind speed is not significantly reduced when using a high porosity windbreak, whereas, low porosity results in a significant decrease in wind speed in the lee of the shelter break, but over a relatively short downwind length (Středová *et al.*, 2012). Designing the optimal windbreak would require more detailed modelling of the surrounding area. Understanding local wind direction and frequency is crucial but also how this might change in 15–30 years when the shelter belt is actively reducing wind speed.

Preliminary CFD modelling illustrates the effect of a 100 m, 50 m and 10 m wide shelter belts on wind speed across the estuary (Figure 6.7 to 6.10). The same model setup from chapter 4 was used, only the width of the forest was changed, the height remained at 40 m. As the drag co-efficient increases wind speed across the estuary decreases. Widening the shelterbelt appears to decrease the wind speed, however, the drag coefficient (Cd) is a product of shelterbelt width using the equation 1/m. This means that as the length of the shelterbelt increases the effect of the Cd increases and wind speed decreases. This is illustrated by the increase in darker colouring (dark blue) as the Cd increases as the shelterbelts are widened (Figure 6.7 to 6.9). The lee effect produced by the shelterbelt extends across the estuary under Cd=0.1 and Cd=0.5. The lee effect is correlated with the height (H) of the forest, and this effect can extend 6–15 H (Jian *et al.*, 2018; Markfort *et al.*, 2010). The sheltering effect decreases from ~10 H, illustrated by the darker blue seen over the wetland in Figure 6.7 (b).

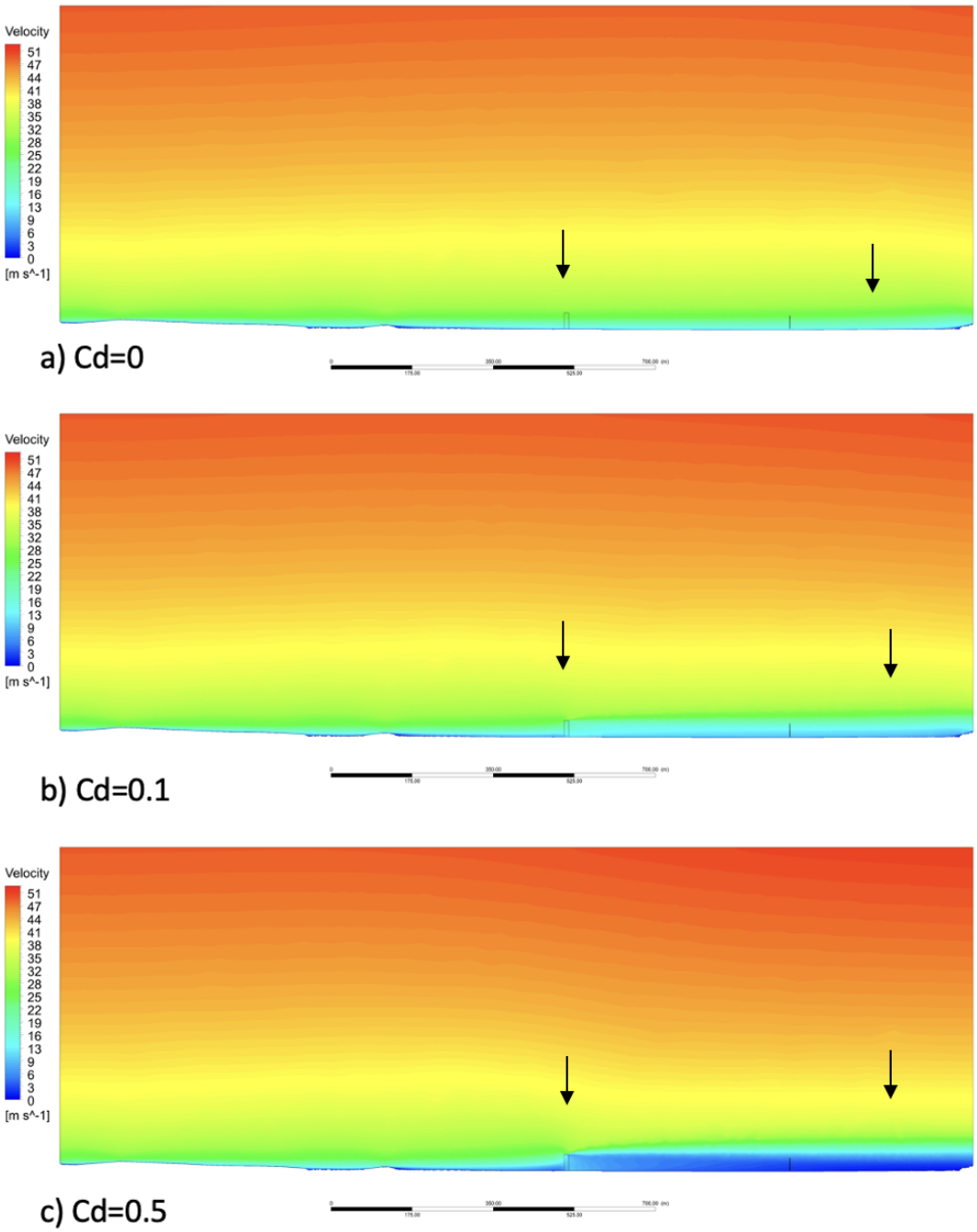

Figure 6.7: Wind speed across Catlins Estuary using a 10 m shelter belt, black arrows mark shelter belt and wetland edge, black line between arrows is the velocity profile marker.

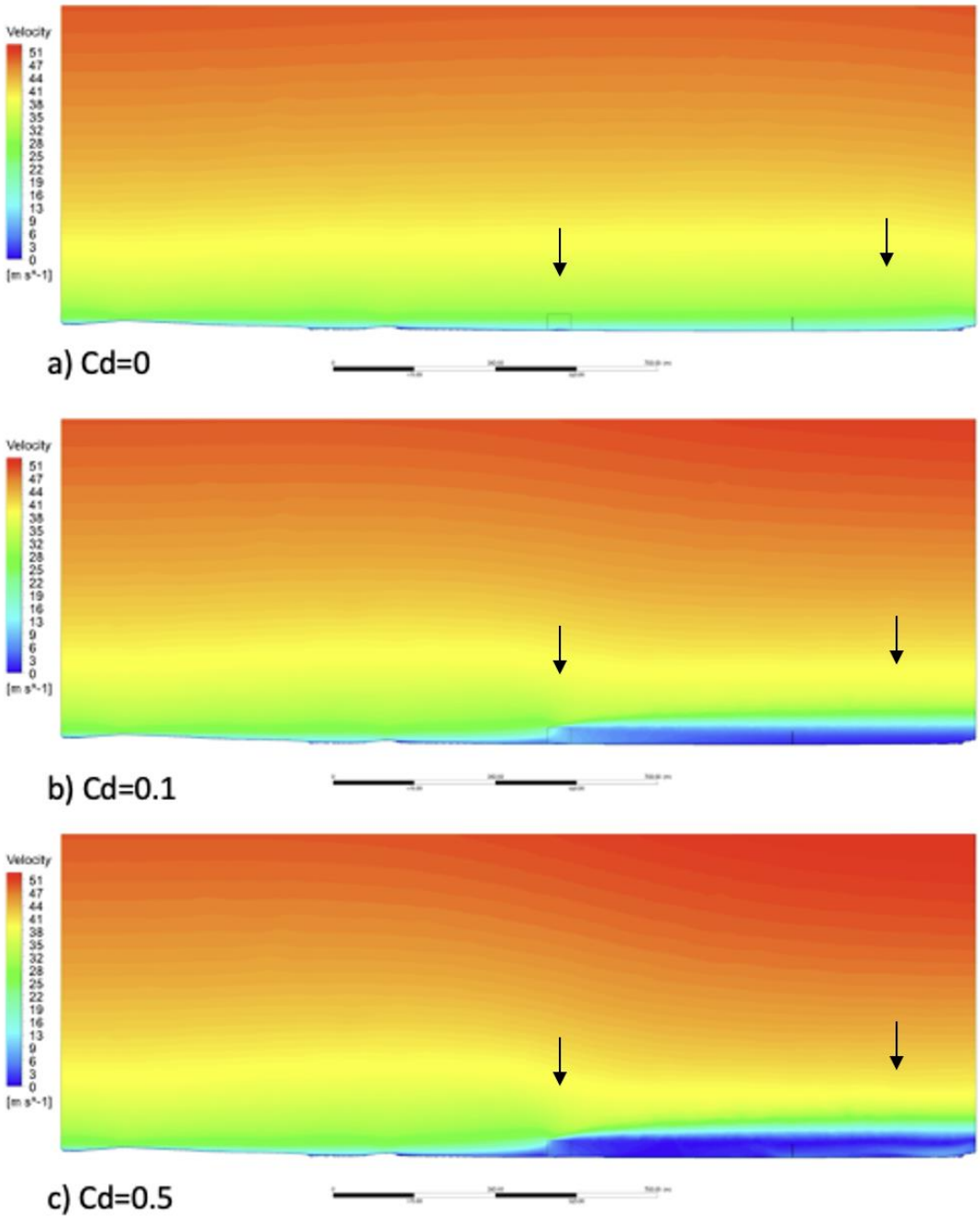

Figure 6.8: Wind speed across Catlins Estuary using a 50 m shelter belt, black arrows mark shelter belt and wetland edge, black line between arrows is the velocity profile marker.

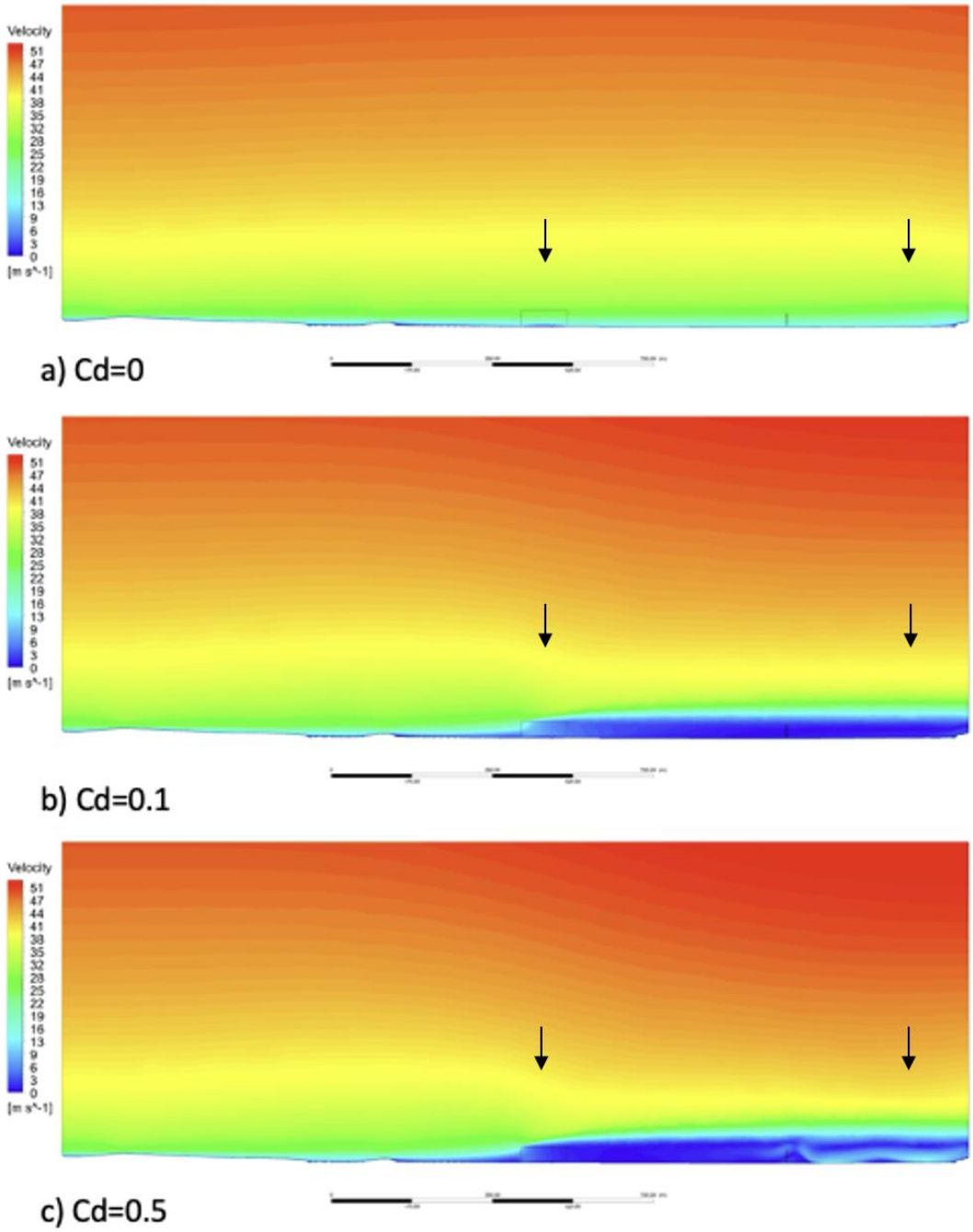

Figure 6.9: Wind speed across Catlins Estuary using a 100 m shelter belt, black arrows mark shelter belt and wetland edge, black line between arrows is the velocity profile marker.

Drag coefficients (Cd) of 0, 0.1 and 0.5 Cd were tested for each shelterbelt width and the decrease in wind speed caused by the increase in Cd is evident (Figure 6.10). Wind speed at Y = 1 m is reduced as the width of the shelterbelt is increased (Figure 6.10), as discussed above this could be caused by the relationship between Cd and forest width, rather than solely the response of widening the shelterbelt.

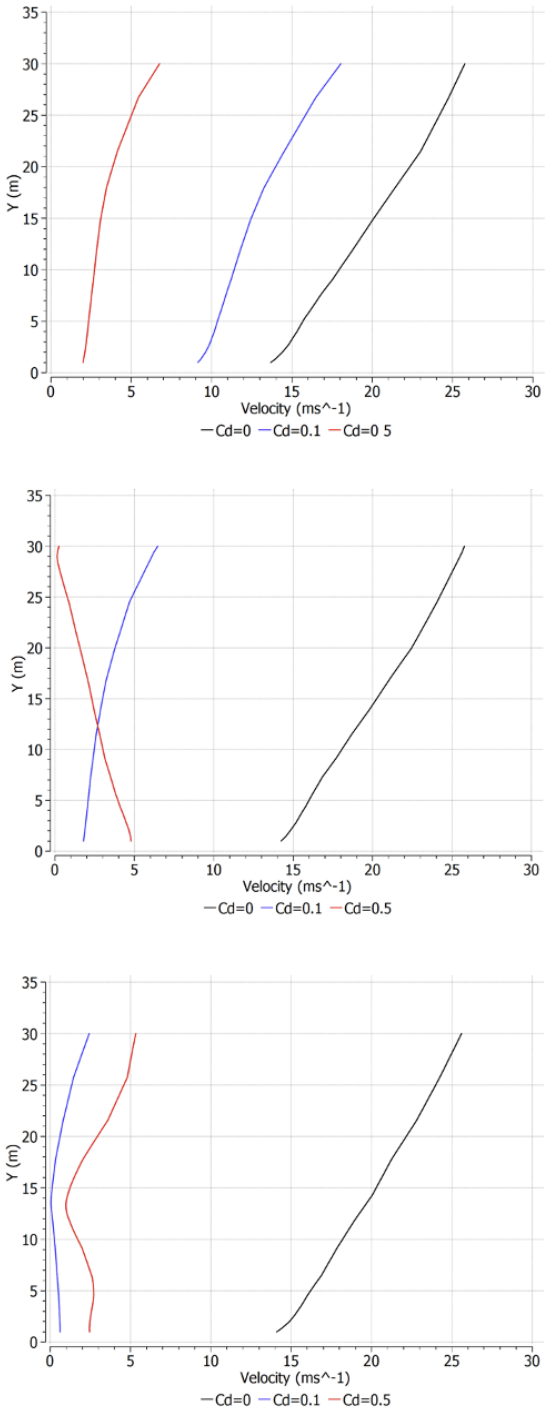

Figure 6.10: Velocity profiles for (a) 10 m wide; (b) 50 m wide; (c) 100 m wide shelter belts. The three drag coefficients are outlined below each graph. Y (m) is the elevation relative to MSL.

The right species of tree and layout of the trees are important considerations for shelterbelts (Gregory, 1995). Native species that once existed in this area should be planted again, including matai (*Prumnopitys taxifolia*), miro (*Prumnopits ferruginea*), totara (*Podocarpis totara*), kahikatea (*Dacrycarpus dacrdioides*) and rimu (*Dacrydium cupressinum*) (Stevens and Robertson 2017). These species reach heights of up to 35 m and will shelter the wetland from south−west winds nearing maturity (75 + years). These native species grow slower than other exotic species (*Eucalyptus nitens* and *Pinus radita*) but it is important to plant a range of species to improve biodiversity, planting a monoculture of trees could lead to maladaptation (Seddon *et al.*, 2020).

A shelter belt could be planted in two stages simultaneously. At the seaward edge, *Eucalyptus nitens (E. nitens)*, on the windward side; and native forest (matai, miro, tōtara, kahikatea and rimu) to the lee of the exotic plantings. *E. nitens* have been planted and cultivated in Southland in the 1990s and grow at a rate of 1−1.5 m/yr (Hay *et al.*, 1999). This fast growth rate means *E. nitens* could shelter the wetland from south−west winds and reduce the height of propagating waves across the estuary within 20 years, well before the native trees. Once the native trees have matured *E. nitens* could be cut down and sold as firewood or given away. Purchasing the land or co-operating with the land owner would be the prerequisite step before planting.

Shelter belts are not a quick fix. Trees take time to grow and mature before they can make a meaningful impact on wind speed. The wetland is over 600 m north of the proposed shelter belt, meaning that tall trees are necessary to have an effect on reducing wind speed near the wetland. Mature trees, 30 m or taller would be ideal, but this could take at least 50 years. The slow development of a shelter belt means this environmental solution should be used in conjunction with a short-term solution. Additionally, windbreak nets could be installed to provide immediate sheltering across the estuary. Windbreak nets are used on orchards to protect crops. They are relatively cheap and easy to install (Ushiyama, 2009). Empirical science on the effect of different net materials, porosity, height, mesh size and durability are not well studied (Castellano *et al.*, 2008). Literature on large windbreak nets (>10 m) could not be found.

Figure 6.11: Potential shelter belt locations at Hinahina. Shelter belt is ~100 m wide and would reduce wind speed from south and south-westerly winds.

The conversion of pasture land to a native tree shelter belt would improve the biodiversity of the estuary catchment by increasing habitat for bird species such as the Tui, Kereru, Korimako (bellbird), Piwakawaka (Fantail) and the Ruru (Morepork).

If the shelter belt proves to be a success then more native species should be planted within the boundary of the shelter belt to increase biodiversity. The podocarp forest behind Pounawea Wetland should be replicated at Hinahina within the confines of the shelter belt boundary.

6.4.2. Hard infrastructure – breakwater

Breakwaters are used to attenuate waves in high density areas such as harbour entrances or coastal townships (Firth *et al.*, 2014; Schoonees *et al.*, 2019). They are expensive to build and maintain, do not provide additional ecosystem services but they can be highly effective at mitigating wave energy (Morris *et al.*, 2018; Narayan *et al.*, 2016).

Two breakwaters could be constructed within the Catlins Estuary catchment. The first could be built on the subtidal sand bar where Cabbage Point used to extend to. The second could be placed in parallel to the south and west wetland edge, similar to the overlapping oyster reefs (Figure 6.3).

The Pounawea foreshore is protected by a rock revetment, established after the collapse of the wooden seawall in 2006. Damage in 2010 saw the installation of a rock revetment extend the length of the foreshore. The need for a breakwater at Cabbage Point is an unnecessary cost that the local community probably cannot afford. The breakwater would protect against storm surge events; however, this is a large cost for events that are unpredictable. Furthermore, the mobility of the sand bar could undermine the structural integrity of the breakwater, interlocking tetra blocks (Figure 6.12) have been used overseas to great effect and could be implemented.

Figure 6.12: Tetrapod blocks forming a breakwater offshore of Ogimi Village on the north eastern side of Okinawa Island, Japan (Masucci *et al.*, 2019).

Offshore breakwaters would reduce storm surge and limit wetland edge erosion. This solution does not limit wind speed across the estuary unlike the shelter belt, instead it allows waves to propagate across the estuary and attenuates them offshore of the wetland. This solution does not solve the root cause of the environmental driver (land use change), rather it attenuates waves that are a result of deforestation upwind of the wetland.

Breakwaters are not going to reduce the tidal rise in sea-level caused by SLR. Breakwaters are likely to effect the sedimentation processes in the lee of the barrier (Palinkas *et al.*, 2017). Modelling indicates that breakwaters are an obstacle for sediment transport and will impact sediment deposition in the lee of the breakwater (Vona *et al.*, 2020). Sediment deposition is critical for wetland accretion to maintain or outpace the rate of SLR.

Breakwaters are costly and add little to no ecosystem services to the area. From a cultural perspective, hard infrastructure interferes with the surrounding ecosystem and is an unnatural solution that does not align with Te Ao Māori values.

Pounawea Wetland epitomises the opportunity to move away from hard structures and towards nature-based solutions to mitigate erosion and SLR. The options laid out in the above sections are likely to be more beneficial environmentally, socially, financially and culturally then a breakwater for Pounawea Wetland. The breakwater is only going to reduce wetland edge erosion whilst limiting the ability for the wetland to accrete, essentially allowing the wetland to be inundated by SLR. The costs of resource consents, materials, construction and maintenance are likely too high for a small community like Pounawea.

6.5. DISCUSSION

Pounawea Wetland is a low-lying coastal wetland under threat from lateral erosion and SLR. The geomorphology and ecology of this wetland is sensitive and any environmental management solutions are likely to change and effect the wetland in some way. There is no certainty that the outcomes seen in other parts of the world will occur at Pounawea. Each environment is different and salt meadow wetlands are no exception. Salt meadow wetlands are not well studied and management of such environments is not documented. However, the current study provides a basis for further consideration of the options identified.

Identifying the drivers of environmental change and engaging with stakeholders are fundamental steps in coastal hazard management. These parameters are the foundation for coastal hazard management for local governments as outlined in the 10-step decision cycle (Figure 6.13). This 10-step decision cycle has five key questions, the

first of which asks ‘what is happening?’. Chapters 3, 4 and 5 and section 6.1.1 have outlined the issues of lateral erosion, land use change, sedimentation and inundation as a consequence of SLR and VLM. Catchment morphodynamics and historical land use change have been used to describe and explain why these issues have occurred. Historical analysis of the issue and relative parameters is important for understanding what needs to change and how that change can be implemented.

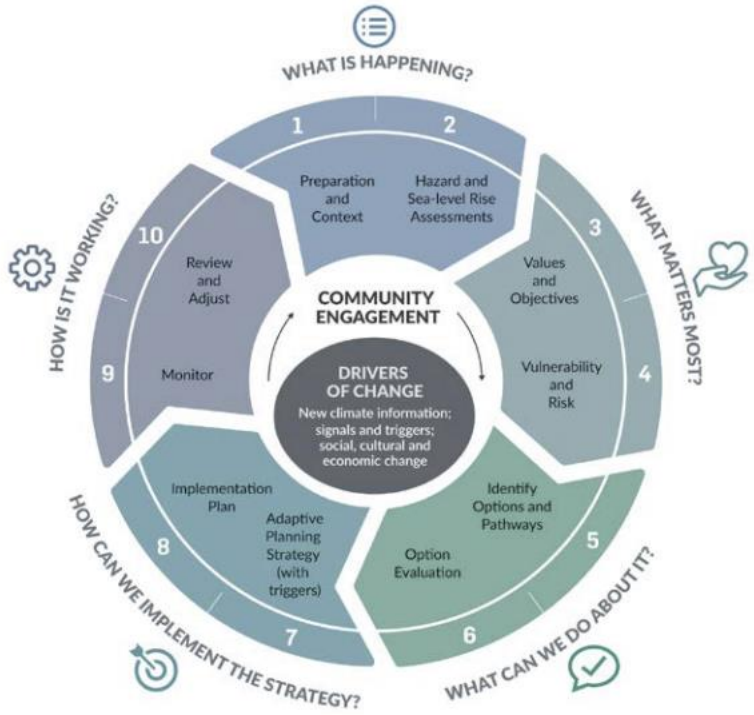

Figure 6.13: 10-step decision cycle on managing coastal hazards and climate change for local government (Bell *et al.*, 2017).

The second question asks ‘what matters most?’, this is where community engagement is important for understanding the value of the wetland. Engaging with the community improves understanding of the issues at hand and provides alternative perspectives of the issue that may go unnoticed (Allen *et al.*, 2018; Evans *et al.*, 2017; Gillgren *et al.*, 2018; Jurjonas and Seekamp, 2018; Lawrence *et al.*, 2018). Implementing a social value evaluation index system (Ye and Sun, 2021) could be an effective way to understand the social value of the wetland. The more information and engagement from those affected should better inform decision makers to ensure the appropriate

management solutions are implemented (Gillgren *et al.*, 2018; Jurjonas and Seekamp, 2018).

The third question asks ‘what can we do about it?’. The environmental solutions discussed within this chapter acknowledge the two drivers of change (land use change and SLR) and work to address these central issues. Evaluations of each solution should be undertaken as well as consultation with local iwi, community groups, residents and relevant experts. Consultation is an important part of coastal resilience and ensuring that it is done correctly is important (Miller *et al.*, 2010).

The fourth question asks ‘how can we implement the strategy?’. Comprehensive management plans and modelling should be undertaken to ensure the most effective methods are selected. The issues facing Pounawea Wetland are complex and will likely need a multidisciplinary approach, meaning, more than one management strategy should be implemented. Implementing a shelterbelt is a long-term solution that will not be effective in the short term. A secondary solution such as oyster reefs could also be implemented to improve coastal resilience and reduce lateral erosion whilst allowing for sediment accretion to continue. The combination of short and long-term solutions is critical for addressing the drivers of environmental change.

The fifth question asks ‘how is it working?’. Wetlands are dynamic environments that adapt to environmental change naturally. Therefore, when implementing a strategy that will affect the wetland it is important to frequently monitor the environmental parameters to ensure the strategy is working effectively. Reviewing and adjusting strategies can be difficult and expensive if hard infrastructure is used. Nature-based solutions are adaptive by nature and are likely to be less destructive and less costly to change if they prove ineffective (Narayan *et al.*, 2016).

The management solutions outlined in this chapter recognise the primary drivers of environmental change affecting the Pounawea Wetland – local deforestation, eustatic sea-level rise and the loss of a protective late-Holocene coastal barrier (Cabbage Point). However, SLR is a global issue that cannot be resolved with a localised solution, unlike land use change. The acceleration of SLR is likely to continue for at least 50 years even if global emissions reduction targets are achieved (Fox-Kemper *et al.*, 2021; IPCC, 2021a). The acceleration of SLR is going to significantly affect the morphology and environmental conditions of the wetland. Solutions outlined in this chapter have

acknowledged the challenges posed by increases in sea-level and how management solutions are likely to become ineffective once SLR inundates Pounawea Wetland daily. Continued monitoring and reassessment of the effectiveness of management solutions will be imperative for wetland survival. Future innovation and technology may provide solutions that alleviate the stresses of SLR on low-lying coastal communities. However, management plans for worst case scenarios should be developed to ensure that endemic and critically important species are protected, either assisted in landward transgression or relocated.

The challenges of SLR and likely eventuality of complete inundation can be overwhelming and the option to 'do nothing' appears to make sense. The question of 'why would you spend money on an area that is likely to be significantly affected by SLR in 100 years?' is a fair question. The rebuttal to this question is "why not?" Low-lying salt meadow wetlands like Pounawea are rare and should be protected or actively managed to preserve the environment for as long as possible. Doing nothing is not logical given the proposed solutions outlined in this chapter. Nature-based solutions are cost effective, adaptable and improve ecosystem services (Arkema *et al.*, 2013; Morris *et al.*, 2018; Narayan *et al.*, 2016; Sutton-Grier *et al.*, 2015; Temmerman *et al.*, 2013). Implementation of these solutions should be encouraged; local government and communities should evaluate how SLR will affect management strategies but they should not let it dictate if a strategy should be implemented in the first place.

Shelterbelts are an effective mechanism to reduce wind speed downwind (Jian *et al.*, 2018; Markfort *et al.*, 2010). Preliminary modelling has illustrated that the height of the forest is the determining parameter for wind shelter aligning with conclusions found in the literature (Desmond *et al.*, 2014; Jian *et al.*, 2018; Markfort *et al.*, 2010; Smyth, 2016). The width of the shelterbelt whilst important is not a defining factor for wind reduction. Modelling indicates that a 10 m shelter belt would reduce wind speed across the estuary (Figure 6.7 and Figure 6.10). This means that a large shelterbelt (50 and 100 m) whilst beneficial for increasing biodiversity and ecosystem services, are not necessary for wind sheltering. This reduces the financial cost of this strategy and potentially increases the likelihood of cooperating with the landowner. The deforestation of the surrounding hills is the key driver of land use change that has resulted in the acceleration of wetland edge erosion. Shelterbelts are a simple, yet effective management strategy to

mitigate the effects of wind speed across Catlins Estuary and reduce the frequency and size of fetch-limited waves propagating across the estuary and eroding the wetland edge.

Environmental management is an investment in the future and decisions related to mitigation strategies can be expensive to implement and costly to change, especially, hard infrastructure (Sutton-Grier *et al.*, 2015). Breakwaters can be effective for wave attenuation but large storms can overtop these structures causing them to fail (Oumeraci, 1994). The solution is often to build several breakwaters or make them taller and more robust (Firth *et al.*, 2014). But at what point, do they become too big and decrease the recreational value of a beach or coastline. At what cost are they too expensive? If sea-walls are constructed to protect the coast, each successive seawall is built further into the dynamic zone of the coast. The seawall at St Clair, Dunedin, New Zealand, is a perfect example of this failure to see the bigger picture. Each new seawall has been built further out to sea, restricting the natural process of the sediment (Register, 2004), refracting wave energy alongshore and decreasing the usability of the beach for residents. The continued use of sea-walls at St Clair has resulted in two options; continue to build new sea-walls that are larger and further out to sea or to retreat. The modification to the coastal zone has gone too far for there to be an intermediate option. This is why for areas that can avoid hard infrastructure and assess the long-term implications of mitigation strategies, issues experienced at St Clair can be avoid.

Nature-based solutions have attracted attention for their potential to protect the coast and improve biodiversity. Turning this attention into action is a challenging process. The politics of environmental management is effecting the implementation of nature-based solutions at the larger scale (Cohen-Shacham *et al.*, 2019). NBS is relatively new and has limited application in large scale environments and there is little long-term data to assess the efficacy of these solutions (Nesshover *et al.*, 2017; Seddon *et al.*, 2020). Moreover, assessing the efficacy is difficult because NBS exhibit non-linearity towards coastal protection, meaning that ecosystem services vary over time and space due to these protection methods growing and developing (Koch *et al.*, 2009). This creates difficulties for large scale NBS protection to receive funding for implementation (Möller, 2019). Whereas, hard infrastructure have an established record of protecting the coast (Dewidar and Frihy, 2008; Pranzini *et al.*, 2015), all be it at a significant financial and ecological cost (Schoonees *et al.*, 2019).

Decision makers are hesitant to implement NBS because there is a lack of long term data (Kabisch *et al.*, 2016). Without the monetary funding to implement NBS at the scale needed for widespread coastal protection this method will not become established. Hard structures will remain and the degradation of coastal environments downdrift of these structures will continue (Rangel-Buitrago *et al.*, 2018). The literature expressively signals that hard infrastructure results in negative ecological consequences and have failed to protect coasts from erosion as SLR and storm surge have increased (Dewidar and Frihy, 2008; Firth *et al.*, 2014; Narayan *et al.*, 2016; Rangel-Buitrago *et al.*, 2018; Schoonees *et al.*, 2019), however, there is an unwillingness to try new management solutions at a larger scale (Möller, 2019). This is the politics of environmental management, repetitive solutions (hard structures) for coastal hazard management expecting a different result, knowing full well there are other options available but unwilling to utilised them due to fear of the unknown.

6.6. SUMMARY

This chapter has outlined the drivers of environmental change, summarised key scientific findings of the thesis and discussed short and long-term environmental management options to mitigate wetland erosion. The use of the 10-step decision cycle from "Coastal Hazards and Climate Change: Guidance for Local Government" (Bell *et al.*, 2017) was used to illustrate how the solutions provided in this chapter align with the principles of the government document.

Two key drivers of change were identified and management options were assessed. The effects of land use change are a localised problem that can be resolved or mitigated. SLR is a global issue that is likely to continue to stress the resiliency of coastal environments. Short and long-term management options were described and discussed. The use of these management strategies is likely needed for successful wetland erosion mitigation. Nature-based solutions are adaptative, cost effective and improve ecosystem services. The growing body of literature and implementation of nature-based solutions across the world is a testament to their success and resilience in the face of climate change and sea-level rise.

7. Conclusion

7.1. INTRODUCTION

Coastal wetlands are an important ecosystem at risk of erosion and inundation as a consequence of sea-level rise and environmental change. These wetlands are low-lying, vulnerable and often overlooked in pursuit of protecting beaches or coastal developments. This is the first study addressing environmental change and erosion at Pounawea Wetland, the best remaining example of this wetland type in southern New Zealand. Understanding how and why the wetland is eroding is important for implementing the right strategy to mitigate future erosion. Coastal protection has long been associated with hard infrastructure (sea walls, breakwaters). Recently, nature-based solutions have gained recognition as an effective mitigation strategy for coastal erosion, wave attenuation and flood events all the while improving ecosystem services for the wider environment.

Chapter 1 introduced the concepts of coastal wetland erosion, land use change, sea-level rise and outlined the research aims of this thesis. Chapter 2 summarised key literature on coastal wetlands, salt marsh vegetation and erosion, sea-level rise, hydrodynamics processes, coastal resilience and nature-based solutions. Chapter 3 discussed environmental change and the morphodynamics of Pounawea Wetland. Chapter 4 examined the frequency and severity of changing boundary conditions and how deforestation upwind of the wetland had affected wind speed and consequently significant wave height across the estuary. Chapter 5 examined the spatial patterns of sediment accumulation and how SLR would affect scarp erosion. Chapter 6 summarised key findings associated with the two key drivers of environmental change and mitigation strategies were proposed that addressed these key drivers. The following chapter will address each of the research aims, discuss the limitations of this study and outline the potential for future research related to Pounawea Wetland.

7.2. RESEARCH AIMS

7.2.1. Document environmental change and morphodynamics of Pounawea Wetland

Pounawea Wetland is a low-lying salt meadow adjacent to the Catlins Estuary. The elevation of the wetland is 0.7 m (relative to the LINZ vertical datum) and the topography is almost flat. There is a 10 cm increase in elevation from the top of the wetland edge to the podocarp forest boundary. Three distinct vegetation zones comprise the wetland. The lower marsh zone is dominated by *S. radicans, S. repens* and *S. quinqueflora*. The middle marsh is occupied by shrubs and grasses, mostly *Leptocarpus similis*, *Coprosma propinqua* and *Plagianthus divaricatus*. The upper zone is the marginal podocarp forest (*Podocarpis totara*, *Dacrycarpus dacrdioides* and *Prumnopitys taxifolia*). The spatial boundaries of these zones have changed concomitant to the wetland and wider catchment.

Erosion of the wetland edge, on average 80 m between 1948 and 2022 has significantly reduced the area of lower marsh. It was not a focus of this thesis but it appears there has been colonisation of the middle marsh by lower marsh species. Subsequently, the middle marsh species have colonised the podocarp forest. Between 1967 and 1985 the podocarp forest transgressed 10–56 m, which allowed middle marsh species (shrubs) to colonise higher elevations, it is not clear why the rollback occurred. Species zonation evolves and adapts to changes in environmental conditions. Shoreline erosion and tidal inundation are two threats to wetland vegetation at Pounawea. The lower marsh species are halophytes and can tolerate increases in salinity, however, SLR will inundate the wetland more frequently in the future and by 2100 the wetland will likely be submerged during incoming tides. This will affect all vegetation because of the low elevation and relatively flat topography of the wetland.

The Pounawea Wetland is eroding at a mean rate of -0.67 ± 0.05 m/yr. Aerial photographs, satellite imagery and UAV drone surveys were analysed to assess shoreline change and the *Digital Shoreline Analysis System* (DSAS) extension used through ArcGIS calculated the linear regression rate and net shoreline movement of the wetland

edge from 1948–2022. The western and eastern edges of the wetland eroded by more than 80 m since 1948. These areas experienced increased rates of erosion as well. This is because these areas are exposed to westerly and easterly winds that propagate waves across the estuary and against the wetland edge. Cliff toe erosion and wave undercutting were also more prevalent at the west and eastern edge. The morphology of the wetland continues to change concomitant to the eroding shoreline. The tidal creek within the wetland widened and lengthened from 1948. Internal erosion has also increased with the largest erosion pool expanding more than 1500 m^2. The bioturbation of the Tunnelling Mud Crab (*Austrohelice crassa*) could be a factor for the increase.

Erosion is a common theme within the Catlins Estuary. Cabbage Point and Manuka Island have eroded by 75% and 100% since 1948. Cabbage Point would have attenuated waves from easterly storms and swell. After Cabbage Point eroded in 1985, the Pounawea foreshore was exposed to storm waves and in 2006 a low-pressure storm coincided with spring high tide which inundated the foreshore and damaged the wooden seawall (Figure 3.22). The loss of Manuka Island and Cabbage Point likely changed the morphodynamics of the wetland.

7.2.2. The frequency and severity of storm wave and inundation events

The frequency and severity of potential erosion events (PEE) has not significantly changed in the last 50 years. Historic climate data (pressure, wind speed and direction) from 1972-2022 was analysed to identify trends in climate events. Data from 1995-2022 was a central focus, because hourly data was available for this period. Whereas, before 1995, climate data was recorded daily (1972-1978), 3 x per day (1978-1989) and then every 3 hours (1989-1995). The variance in data collection posed difficulties in accurately reflecting the changing climate conditions and fast-moving climate events might not have been recorded. Climate data was processed and outputs related to potential erosion events (PEE) were determined. A potential erosion event was likely to have occurred when wind speed > 7 ms^{-1}, wind direction was between 180°–270°, and atmospheric pressure < 1000 hPa. Of the 268,708 hours of climate data from 1972-2022, only 3.78% (10,153) were PEE. There was no indication of an increase in these events

across the 50-year period. However, there was an increase in PEE for years 1997, 2003-2004, and 2017.

Sea-level rise and vertical land movement are changing boundary conditions. The rate of SLR is currently 1.8 mm/yr and this is predicted to increase to 3 mm/yr (IPCC, 2021a). VLM at Pounawea is between 1.07–1.65 mm/yr. VLM increases the relative sea-level and will negatively impact the wetland by increasing the frequency of inundation events. A sudden uplift event (earthquake) whilst unlikely is plausible and would benefit the wetland. The elevation of the wetland would have increased relative to the water level and therefore the frequency of wetland inundation would decrease.

Deforestation of the Hinahina areas, the forest upwind of the wetland, has likely increased wind speed across the Catlins Estuary. The lee effect of the former forest probably extended across the estuary, or at least six times the height of the forest (Heisler and Dewalle, 1988; Markfort *et al.*, 2010). Computational fluid dynamics (CFD) was used to model variations in wind speed across the estuary with, and without, an upwind forest. The results indicate a significant decrease in windspeed across the estuary when forest porosity is decreased. A range of forest porosities were tested. The less porous the forest the greater the decrease in wind speed. The results of the CFD modelling align with published research on the effects of wind sheltering from forests (Heisler and Dewalle, 1988; Markfort *et al.*, 2010).

Forest clearance may be the primary cause of wetland erosion. The removal of the forest appears to have resulted in an increase in wind speed across the estuary. Wind speed and significant wave height are associated in fetch-limited shallow water environments. The increase in wind speed likely resulted in an increase in the frequency of fetch-limited waves propagating across the estuary. The increase in wind speed likely increased significant wave height resulting in the acceleration of lateral erosion at the wetland edge.

7.2.3. The spatial patterns and rate of sediment deposition during inundation events and how sea-level rise will affect processes of erosion at the wetland edge

Sediment deposition across the Pounawea Wetland during inundation events is not evenly distributed. A disproportionate amount of sediment is deposited within 2 m of the wetland edge during inundation events. This pattern of sediment accumulation is exacerbated during inundation events with increasing wave heights. Chapter 4 argued that increases in significant wave height are associated with increases in sediment accumulation across the wetland, with the largest increases occurring within 2 m of the wetland edge. The accretion results indicate that sediment deposition at the wetland edge during inundation events is sufficient to enable the wetland to accrete faster than SLR. However, the wetland edge is laterally eroding at a rate of -0.67 ± 0.05 m/yr, meaning, a significant proportion of the sediment deposited onto the wetland each year does not contribute to vertical accretion and wetland mass. The wetland is eroding faster than it is accreting.

Breaking waves increase the amount of wall shear stress exerted on the scarp edge. As water level increases above the wetland edge (>0.7 m) wall shear stress decreases. This is because wave energy is passing over the wetland edge and is dissipated across the wetland, whereas, during lower water levels (<0.7 m) wave energy was being dissipated against the scarp edge, specifically at the top of the scarp where wave breaking took place. The amount of wall shear stress modelled on the face of the wetland edge differed significantly. The middle of the scarp recorded 10 times less than the top and the bottom recorded 5000-7000 less than the top of the scarp. A time-lapse camera depicted the wetland edge being ‘attacked’ for 35-45 minutes before inundation occurred and wave energy was transferred across the wetland.

Wall shear stress will likely decrease as inundation increases due to SLR. By 2100, water levels of 1, 1.2 and 1.4 m will be regular occurrences and under these water level scenarios modelling illustrates a decrease in wall shear stress at the top of the scarp. This is because waves will pass over the scarp and dissipate further inland across the wetland. However, rising sea levels will also increase the duration of wave impacts when tides are lower (>0.6 m). The relative sea-level will be higher which will result in lower high tides

and more of the tidal cycle (mid tide) reaching the wetland edge. This would likely result in more lateral erosion, however, as sea-level rises and the frequency of inundation increases the potential for sediment deposition also increases.

7.3. CONCLUDING REMARKS

This study has shown how the Pounawea Wetland has changed since 1948, the processes by which it has changed, how it will continue to change and indicated potential mitigation strategies to alleviate the drivers of environmental change. Wetlands are dynamic environments subject to changing environmental conditions. Deforestation of the surrounding hillsides has accelerated wetland edge erosion. Previously the forest sheltered the wetland from south–westerly winds, however, upon removal of this forest, CFD modelling indicates that wind speed across the estuary has increased and therefore significant wave height and likely the frequency of fetch-limited shallow water waves also increased. Deforestation has been the primary driver of wetland erosion and replanting the forest or a shelterbelt is a long-term mitigation strategy that will reduce wind speed across the estuary and subsequently reduce significant wave height and lateral erosion of the wetland.

Eustatic sea-level rise will inundate the wetland daily by 2150. There is sufficient sediment within the Catlins Estuary system but this sediment is not deposited evenly across the wetland and therefore the wetland will not accrete faster than SLR. The rise in net sea-level from SLR and VLM will drown the wetland and New Zealand will lose one of the last remaining salt meadow environments. Wetlands are resilient and adaptable and vegetation transgression towards higher elevation may increase the longevity of the wetland. The effects of climate change and SLR are going to continue to affect vulnerable low-lying coastal wetlands, beaches and infrastructure. The implementation of nature-based solutions could help mitigate the effects of SLR and coastal erosion whilst improving ecosystem services for the wider environment. The methods undertaken within this thesis could be applied to other salt meadow environments to build a comprehensive understanding as to why salt meadow wetlands are eroding or vulnerable to sea-level rise and what mitigation strategies could be implemented to improve coastal resilience.

7.4. RESEARCH LIMITATIONS AND FUTURE RESEARCH

7.4.1. CFD modelling

The simulations of wind speed through the forest boundary using various drag-co-efficient values to simulate the lee effect has been effective. However, several variables were not included in the analysis due to limited field data, so that model validation could not be completed. Canopy density and leaf size are crucial variables that should be included when investigating the effect of wind flow through a forest canopy (Cedell, 2019; Jian *et al.*, 2018; Jiang *et al.*, 2013). Validating the model requires field data or physical simulations (wind tunnel experiments using a scale model), without validation the CFD models can only illustrate the potential effects of wind flow through a forest boundary. Validation of the models would enable conclusive findings regarding the effect of wind flow across the estuary.

The boundary dimensions of the forest were a further limitation of the model. The forest height was an estimate based on historical images (Figure 4.11) and an assumption that the podocarp forest located behind the Pounawea Wetland would have been similar in height to the forest across the estuary at Hinahina.

CFD is a powerful tool to simulate past, present and future environmental conditions. Future research could focus on wave dynamics and set up under various climatic conditions (storm events) and sea-level projections. Fetch limited waves are correlated to wind speed and understanding how waves form and propagate across the estuary could provide insight to the shoreline erosion occurring at Pounawea Wetland. Research could also focus on validating the models constructed in this thesis. The podocarp forest behind the wetland could be used as a data collection site for wind speed through a forest canopy. Leaf size and canopy density could from Pounawea forest could also be used in model validation.

7.4.2. Sediment deposition

The artificial mats used to trap sediment were effective, however, the mats do not mirror all the attributes of lower marsh species. Lower marsh vegetation (*S. radicans, S. primrose, S quinqueflora*) is 3–10 cm in height, whereas, the artificial mats are a uniform ~ 3 cm high. The mats are uniform in size and shape whereas the lower marsh area can have all three species intertwined, more commonly two species grouped together (Figure 2.5). Artificial grass mats with longer (7 cm) grass blades should have been used as this would better reflect lower marsh vegetation (*S. radicans, S. primrose, S quinqueflora*).

Mat deployment covered a 24-hour tidal cycle instead of a 12-hour cycle due to health and safety concerns (working at night). Sediment resuspension during the second incoming tide may have reduced the amount of sediment that was deposited on the mats depending on the environmental conditions at the time.

A further limitation was the absence of local wind data. Nugget Point climate station located ~10 km north-east of Pounawea was used for wind and pressure data. The pressure of the two areas was likely to be the same, however, wind speed and direction could be different. A 6 m wind mast set up in November 2021 would have recorded local wind strength and direction which may have improved the understanding of the relationship between wind speed and wave height across the Catlins Estuary. Sediment accumulation could be assessed against local wind events to understand what wind speed produced the most sediment deposition. The wind speed and direction data could have been used to compare winds at Nugget Point to Pounawea and allow for more accurate assessment of historical wind trends from Nugget Point that were discussed in chapter 4.

Future research on sediment transport and deposition onto the wetland could aid in understanding wetland accretion. One arm of this future research could examine the movement of sediment either through suspension and settlement during receding tides. The second part could examine sediment transport along the surface of the wetland. Sediment is not reaching inland areas of the wetland and understanding how sediment is transported onto and across the wetland during different events (storm surge verses calm spring tide inundation) could be valuable for the protection of salt meadow environments.

7.4.3. Erosion

The Pounawea Wetland is eroding but exactly what processes and species are contributing is not certain. Future research could investigate the relationship between wave energy at the estuary mouth and wave energy at the wetland shoreline. Understanding how much wave energy is making its way to the shoreline edge from the estuary mouth may help explain the rates of erosion under certain weather conditions. Further research is required into understanding the behaviour and potential erosional effect of the Tunnelling Mud Crab (*Austrohelice crassa*). The internal erosion of Pounawea Wetland is quite significant and has been steadily increasing over time. Understanding the role of this species on the wetland and whether it is actively eroding the wetland internally and at the shoreline edge could influence mitigation strategies.

References

ACKERLEY, D., BELL, R. G., MULLAN, B. A. & MCMILLAN, H. 2013. Estimation of regional departures from global-average sea-level rise around New Zealand from AOGCM simulations. *Weather and Climate,* 33**,** 2-22.

ADAM, R. J., HILTON, M. J., JOWETT, T. & STEPHENSON, W. J. 2020. The magnitude and frequency of storm surge in southern New Zealand. *New Zealand Journal of Marine and Freshwater Research***,** 1-16.

ALLEN, R. J. & WEBB, B. M. Determination of wave transmission coefficients for oyster shell bag breakwaters,. Coastal Engineering Practice 2011 San Diego, California. 684-697.

ALLEN, S. K., BALLESTEROS-CANOVAS, J., RANDHAWA, S. S., SINGHA, A. K., HUGGEL, C. & STOFFEL, M. 2018. Translating the concept of climate risk into an assessment framework to inform adaptation planning: Insights from a pilot study of flood risk in Himachal Pradesh, Northern India. *Environmental Science & Policy,* 87**,** 1-10.

ALLEY, R. B., CLARK, P. U., HUYBRECHTS, P. & JOUGHIN, I. 2005. Ice-Sheet and Sea-Level Change. *Science* 310**,** 456-460.

ARKEMA, K. K., GUANNEL, G., VERUTES, G., WOOD, S. A., GUERRY, A., RUCKELSHAUS, M., KAREIVA, P., LACAYO, M. & SILVER, J. M. 2013. Coastal habitats shield people and property from sea-level rise and storms. *Nature Climate Change,* 3**,** 913-918.

ARKEMA, K. K., VERUTES, G. M., WOOD, S. A., CLARKE-SAMUELS, C., ROSADO, S., CANTO, M., ROSENTHAL, A., RUCKELSHAUS, M., GUANNEL, G., TOFT, J., FARIES, J., SILVER, J. M., GRIFFIN, R. & GUERRY, A. D. 2015. Embedding ecosystem services in coastal planning leads to better outcomes for people and nature. *Proc Natl Acad Sci U S A,* 112**,** 7390-5.

ARTHUR, F. S. 1971. *A history of the Catlins,* Dunedin, Francis S. Arthur.

ASSELMAN, N. E. M. & MIDDELKOOP, H. 1995. Floodplain sedimentation: Quantities, patterns and processes. *Earth Surface Processes and Landforms,* 20**,** 481-499.

AUSSEIL, A., CHADDERTON, L., GERBEAUX, P., STEPHENS, R. & LEATHWICK, J. 2011. Applying systematic conservation planning principles to palustrine and inland saline wetlands of New Zealand. *Freshwater Biology,* 56**,** 142-161.

BABOROWSKI, M., BÜTTNER, O., MORGENSTERN, P., KRÜGER, F., LOBE, I., RUPP, H. & TÜMPLING, W. V. 2007. Spatial and temporal variability of sediment deposition on

artificial-lawn traps in a floodplain of the River Elbe. *Environmental Pollution,* 148**,** 770-778.

BALKE, T., HERMAN, P. M. J., BOUMA, T. J. & NILSSON, C. 2014. Critical transitions in disturbance-driven ecosystems: identifying Windows of Opportunity for recovery. *Journal of Ecology,* 102**,** 700-708.

BALKE, T., KLAASSEN, P. C., GARBUTT, A., VAN DER WAL, D., HERMAN, P. M. J. & BOUMA, T. J. 2012. Conditional outcome of ecosystem engineering: A case study on tussocks of the salt marsh pioneer Spartina anglica. *Geomorphology,* 153-154**,** 232-238.

BALKE, T., SWALES, A., LOVELOCK, C. E., HERMAN, P. M. J. & BOUMA, T. J. 2015. Limits to seaward expansion of mangroves: Translating physical disturbance mechanisms into seedling survival gradients. *Journal of Experimental Marine Biology and Ecology,* 467**,** 16-25.

BALSON, P. 2000. Accomodation space and estuarine evolution. Modelling Estuary Morphology and Process, Phase 1 final report of the research by the EMPHASYS Consortium for the MAFF project FD1401.

BARAL, R., PRADHAN, S., SAMAL, R. N. & MISHRA, S. K. 2018. Shoreline Change Analysis at Chilika Lagoon Coast, India Using Digital Shoreline Analysis System. *Journal of the Indian Society of Remote Sensing,* 46**,** 1637-1644.

BATEMAN, M. D., MCHALE, K., BAYNTUN, H. J. & WILLIAMS, N. 2020. Understanding historical coastal spit evolution: A case study from Spurn, East Yorkshire, UK. *Earth Surface Processes and Landforms,* 45**,** 3670-3686.

BAUER, B. O. & WAKES, S. J. 2022. CFD simulations of wind flow across scarped foredunes: Implications for sediment pathways and beach–dune recovery after storms. *Earth Surface Processes and Landforms,* 47**,** 2989-3015.

BEEFTINK, W. G. 1977. Salt-marshes. *In:* BARNES, R. S. K. (ed.) *The Coastline.* John Wiley & Sons Ltd.

BELL, R., LAWRENCE, J., ALLAN, S., BLACKETT, P., STEPHENS, S., HANNAH, J., SHAND, T., THOMSON, P., GLAVOVIC, B., BRITTON, R., DICKSON, M., QUILTER, P., HUDSON, N. & DAVIES, K. 2017. Coastal Hazards and Climate Change: Guidance for Local Government.

BELL, R. G. & GORING, D. G. 1998. Seasonal Variability of Sea Level and Sea-surface Temperature on the North-east Coast of New Zealand. *Estuarine, Coastal and Shelf Science,* 46**,** 307-318.

BELL, R. G., GORING, D. G. & DE LANGE, W. P. 2000. Sea-level Change and Storm Surges in the Context of Climate Change. *Transactions of the Institution of Professional Engineers New Zealand: General Section,* 27**,** 1-10.

BENGTSSON, L., HODGES, K. I. & KEENLYSIDE, N. 2009. Will extratropical storms intensify in a warmer climate? *Journal of Climate,* 22**,** 2276-2301.

BERGIN, D., MILLER, E., ROTORUA, E., LESLIE, J. & JAMIESON, P. 2007. PERFORMANCE OF INDIGENOUS SAND-BINDERS PLANTED ON A RESHAPED FOREDUNE AT OAKURA BEACH, NEW PLYMOUTH. New Plymouth

BERTNESS, M. D. & EWANCHUK, P. J. 2002. Latitudinal and climate-driven variation in the strength and nature of biological interactions in New England salt marshes. *Oecologia,* 132**,** 392-401.

BIRD, E. & LEWIS, N. 2014. *Beach Renourishment* Springer.

BORCHERT, S. M., OSLAND, M. J., ENWRIGHT, N. M., GRIFFITH, K. T. & ROHR, J. 2018. Coastal wetland adaptation to sea level rise: Quantifying potential for landward migration and coastal squeeze. *Journal of Applied Ecology,* 55**,** 2876-2887.

BOUMA, T. J., VAN BELZEN, J., BALKE, T., ZHU, Z., AIROLDI, L., BLIGHT, A. J., DAVIES, A. J., GALVAN, C., HAWKINS, S. J., HOGGART, S. P. G., LARA, J. L., LOSADA, I. J., MAZA, M., ONDIVIELA, B., SKOV, M. W., STRAIN, E. M., THOMPSON, R. C., YANG, S., ZANUTTIGH, B., ZHANG, L. & HERMAN, P. M. J. 2014. Identifying knowledge gaps hampering application of intertidal habitats in coastal protection: Opportunities & steps to take. *Coastal Engineering,* 87**,** 147-157.

BREUGEM, W. A. & HOLTHUIJSEN, L. H. 2007. Generalized shallow water wave growth from Lake George. *Journal of waterway, port, coastal, and ocean engineering,* 133**,** 173-182.

BRINSON, M. M., CHRISTIAN, R. R. & BLUM, L. K. 1995. Multiple states in the sea-level induced transition from terrestrial forest to estuary. *Estuaries,* 18**,** 648-659.

BROWN, I., JUDE, S., KOUKOULAS, S., NICHOLLS, R., DICKSON, M. & WALKDEN, M. 2006. Dynamic simulation and visualisation of coastal erosion. *Computers, Environment and Urban Systems,* 30**,** 840-860.

BROWN, K. & RAAL, P. 2013. Is eradication of Spartina from the South Island feasible? Wellington: Department of Conservation.

CAHOON, D. R., HENSEL, P. F., SPENCER, T., REED, D. J., MCKEE, K. L. & SAINTILAN, N. 2006. Coastal Wetland Vulnerability to Relative Sea-Level Rise- Wetland Elevation Trends and Process Controls. *Ecological Studies,* 190**,** 271-292.

CAHOON, D. R., LYNCH, J. C., ROMAN, C. T., SCHMIT, J. P. & SKIDDS, D. E. 2018. Evaluating the Relationship Among Wetland Vertical Development, Elevation Capital, Sea-Level Rise, and Tidal Marsh Sustainability. *Estuaries and Coasts,* 42**,** 1-15.

CARR, J., GUNTENSPERGEN, G. & KIRWAN, M. 2020. Modeling Marsh-Forest Boundary Transgression in Response to Storms and Sea-Level Rise. *Geophysical Research Letters,* 47.

CARTER, J., FENICAL, S., HARTER, C. & TODD, J. 2015. CFD Modeling for the Analysis of Living Shoreline Structure Performance. *In:* WALLENDORF, L. & COX, D. (eds.) *Coastal Structure and Solutions to Coastal Disasters Joint Conference* Boston, Massachusetts: American Society of Civil Engineers

CASTELLANO, S., SCARASCIA MUGNOZZA, G., RUSSO, G., BRIASSOULIS, D., MISTRIOTIS, A., HEMMING, S. & WAAIJENBERG, D. 2008. Plasitc Net in Agriculture: A General Review of Types and Applications. *Applied Engineering in Agriculture,* 24**,** 799-808.

CASTRO, P. & FREITAS, H. 2011. Linking Anthropogenic Activities and Eutrophication in Estuaries: The Need of Reliable Indicators. *Eutrophication: Causes, Consequences and Control*. Springer.

CEDELL, P. 2019. Forest Simulation with Industrial CFD Codes. Stockholm, Sweden: Royal Institute of Technology, KTH Mechanics.

CHAGUÉ-GOFF, C. & GOFF, J. 2003. Long- and short-term envirnomental changes in coastal wetlands *The New Zealand Coast*

TE TAI O AOTEAROA. Palmerston North: Dunmore Press.

CHARLIER, R. H., CHAINEUX, M. C. P. & MORCOS, S. 2005. Panorama of the History of Coastal Protection. *Journal of Coastal Research,* 211**,** 79-111.

CHIROL, C., HAIGH, I. D., PONTEE, N., THOMPSON, C. E. & GALLOP, S. L. 2018. Parametrizing tidal creek morphology in mature saltmarshes using semi-automated extraction from lidar. *Remote Sensing of Environment,* 209**,** 291-311.

CHOWDHURY, M. S. N. 2019. *Ecological engineering with oysters for coastal resilience: Habitat suitability, bioenergetics, and ecosystem services.* PhD, Wageningen Unversity

CHRISTIANEN, M. J., VAN BELZEN, J., HERMAN, P. M., VAN KATWIJK, M. M., LAMERS, L. P., VAN LEENT, P. J. & BOUMA, T. J. 2013. Low-canopy seagrass beds still provide important coastal protection services. *PLoS One,* 8**,** e62413.

CHURCH, J. A. & WHITE, N. J. 2006. A 20th century acceleration in global sea-level rise. *Geophysical Research Letters,* 33**,** n/a-n/a.

CHURCH, M. & FERGUSON, R. I. 2004. A SIMPLE UNIVERSAL EQUATION FOR GRAIN SETTLING VELOCITY. *Journal of Sedimentary Research,* 74**,** 933-937.

CID, A., MENÉNDEZ, M., CASTANEDO, S., ABASCAL, A. J., MÉNDEZ, F. J. & MEDINA, R. 2015. Long-term changes in the frequency, intensity and duration of extreme storm surge events in southern Europe. *Climate Dynamics,* 46**,** 1503-1516.

CIRIA 2013. *The international levee handbook,* London, CIRIA.

COHEN-SHACHAM, E., ANDRADE, A., DALTON, J., DUDLEY, N., JONES, M., KUMAR, C., MAGINNIS, S., MAYNARD, S., NELSON, C. R., RENAUD, F. G., WELLING, R.

& WALTERS, G. 2019. Core principles for successfully implementing and upscaling Nature-based Solutions. *Environmental Science & Policy,* 98**,** 20-29.

COHEN-SHACHAM, E., WALTERS, G., JANZEN, C. & MAGINNIS, S. 2016. Nature-based Solutions to address global societal challenges. Gland, Switzerland.

COSTA, C. S. B., MARANGONI, J. C. & AZEVEDO, A. M. G. 2003. Plant zonation in irregularly flooded salt marshes relative importance of stress. *Journal of Ecology,* 91**,** 951-965.

COSTANZA, R., D'ARGE, R., DE GROOT, R., FARBER, S., GRASSO, M., HANNON, B., LIMBURG, K., NAEEM, S., O'NEILL, R. V., PARUELO, J., RASKIN, R. G., SUTTON, P. & VAN DEN BELT, M. 1998. The value of the world's ecosystem services and natural capital. *Ecological Economics,* 25**,** 1-15.

COSTANZA, R., GRAUMLICH, L. & STEFFEN, W. 2007. Sustainability or Collapse: Lessons from Integrating the History of Humans and the Rest of Nature. *In:* COSTANZA, R., GRAUMLICH, L. & STEFFEN, W. (eds.) *Sustainability or Collapse: An Integrated History and Future of People on Earth.* Cambridge: MIT Press.

COWELL, P. J., ROY, P. S. & JONES, R. A. 1992. Shoreface translation model- Computer simulation of coastal-sand-body response to sea level rise. *Mathematics and Computers in Simulation* 33**,** 603-608.

COWELL, P. J. & THOM, B. G. 1995. Morphodynamics of coastal evolution. *Coastal Evolution.*

DALPÉ, B. & MASSON, C. 2008. Numerical study of fully developed turbulent flow within and above a dense forest. *Wind Energy,* 11**,** 503-515.

DARKE, I. B., WALKER, I. J. & HESP, P. A. 2016. Beach-dune sediment budgets and dune morphodynamics following coastal dune restoration, Wickaninnish Dunes, Canada. *Earth Surface Processes and Landforms,* 41**,** 1370-1385.

DEEGAN, L. A., JOHNSON, D. S., WARREN, R. S., PETERSON, B. J., FLEEGER, J. W., FAGHERAZZI, S. & WOLLHEIM, W. M. 2012. Coastal eutrophication as a driver of salt marsh loss. *Nature,* 490**,** 388-92.

DELAUNE, R. D., NYMAN, J. A. & PATRICK, W. H. 1994. Peat Collapse, Ponding and Wetland Loss in a Rapidly Submerging Coastal Marsh. *Journal of Coastal Research,* 10**,** 1021-1030.

DENYS, P. H., BEAVAN, R. J., HANNAH, J., PEARSON, C. F., PALMER, N., DENHAM, M. & HREINSDOTTIR, S. 2020. Sea Level Rise in New Zealand: The Effect of Vertical Land Motion on Century-Long Tide Gauge Records in a Tectonically Active Region. *Journal of Geophysical Research: Solid Earth,* 125.

DESMOND, C. J., WATSON, S. J., AUBRUN, S., ÁVILA, S., HANCOCK, P. & SAYER, A. 2014. A study on the inclusion of forest canopy morphology data in numerical

simulations for the purpose of wind resource assessment. *Journal of Wind Engineering and Industrial Aerodynamics,* 126**,** 24-37.

DEWIDAR, K. & FRIHY, O. 2008. Pre- and post-beach response to engineering hard structures using Landsat time-series at the northwestern part of the Nile delta, Egypt. *Journal of Coastal Conservation,* 11**,** 133-142.

DRAKE, L. 2021. *OYSTER RESTORATION TO PROTECT NANSEMOND RIVER SHORELINES* [Online]. Chesapeake Bay Foundation. Available: https://www.cbf.org/how-we-save-the-bay/programs-initiatives/virginia/oyster-restoration/oyster-restoration-to-protect-nansemond-river-shorelines.html [Accessed November 11 2022].

DUARTE, C. M., LOSADA, I. J., HENDRIKS, I. E., MAZARRASA, I. & MARBÀ, N. 2013. The role of coastal plant communities for climate change mitigation and adaptation. *Nature Climate Change,* 3**,** 961-968.

DUNLOP, T., FELDER, S., GLAMORE, W. C., HOWE, D. & COGHLAN, I. R. Optimising Ecological and Engineering Values in Coastal Protection via Combined Oyster Shell and Sand Bag Designs. Coasts & Ports 2017 Conference, 2017 Cairns

DYMOND, J. R., SABETIZADE, M., NEWSOME, P. F., HARMSWORTH, G. R. & AUSSEIL, A.-G. 2021. Revised extent of wetlands in New Zealand. *New Zealand Ecological Society,* 45**,** 1-8.

ENWRIGHT, N. M., GRIFFITH, K. T. & OSLAND, M. J. 2016. Barriers to and opportunities for landward migration of coastal wetlands with sea-level rise. *Frontiers in Ecology and the Environment,* 14**,** 307-316.

EVANS, A. J., GARROD, B., FIRTH, L. B., HAWKINS, S. J., MORRIS-WEBB, E. S., GOUDGE, H. & MOORE, P. J. 2017. Stakeholder priorities for multi-functional coastal defence developments and steps to effective implementation. *Marine Policy,* 75**,** 143-155.

FAGHERAZZI, S., ANISFELD, S. C., BLUM, L. K., LONG, E. V., FEAGIN, R. A., FERNANDES, A., KEARNEY, W. S. & WILLIAMS, K. 2019. Sea Level Rise and the Dynamics of the Marsh-Upland Boundary. *Frontiers in Environmental Science,* 7.

FAGHERAZZI, S. & FURBISH, D. J. 2001. On the shape and widening of salt marsh creeks *Journal of Geophysical Research,* 106**,** 991-1003.

FAGHERAZZI, S. & WIBERG, P. L. 2009. Importance of wind conditions, fetch, and water levels on wave-generated shear stresses in shallow intertidal basins. *Journal of Geophysical Research,* 114.

FEAGIN, R. A., LUISA MARTINEZ, M., MENDOZA-GONZALEZ, G. & COSTANZA, R. 2010. Salt Marsh Zonal Migration and Ecosystem Service Change in Response to Global Sea Level Rise- A Case Study from an Urban Region. *Ecology and Society,* 15.

FEICHTNER, A., MACKAY, E., TABOR, G., THIES, P. R., JOHANNING, L. & NING, D. 2020. Using a porous-media approach for CFD modelling of wave interaction with thin perforated structures. *Journal of Ocean Engineering and Marine Energy,* 7**,** 1-23.

FENSTER, M. S., DOLAN, R. & ELDER, J. F. 1993. A New Method for Predicting Shoreline Positions from Historical Data. *Journal of Coastal Research,* 9**,** 147-171.

FINOTELLO, A., MARANI, M., CARNIELLO, L., PIVATO, M., RONER, M., TOMMASINI, L. & D'ALPAOS, A. 2020. Control of wind-wave power on morphological shape of salt marsh margins. *Water Science and Engineering,* 13**,** 45-56.

FIRTH, L. B., KNIGHTS, A. M., BRIDGER, D., EVANS, A., MIESZKOWSKA, N., MOORE, P., O'CONNOR, N. E., SHEEHAN, E., THOMAS, R. C. & HAWKINS, S. J. 2016. Ocean sprawl- challenges and opportunities for biodiversity management in a changing world. *Oceanography and Marine Biology,* 54**,** 189-262.

FIRTH, L. B., MIESZKOWSKA, N., THOMPSON, R. C. & HAWKINS, S. J. 2013. Climate change and adaptational impacts in coastal systems: the case of sea defences. *Environ Sci Process Impacts,* 15**,** 1665-70.

FIRTH, L. B., THOMPSON, R. C., BOHN, K., ABBIATI, M., AIROLDI, L., BOUMA, T. J., BOZZEDA, F., CECCHERELLI, V. U., COLANGELO, M. A., EVANS, A., FERRARIO, F., HANLEY, M. E., HINZ, H., HOGGART, S. P. G., JACKSON, J. E., MOORE, P., MORGAN, E. H., PERKOL-FINKEL, S., SKOV, M. W., STRAIN, E. M., VAN BELZEN, J. & HAWKINS, S. J. 2014. Between a rock and a hard place: Environmental and engineering considerations when designing coastal defence structures. *Coastal Engineering,* 87**,** 122-135.

FITZSIMONS, J. A., BRANIGAN, S., GILLIES, C. L., BRUMBAUGH, R. D., CHENG, J., DEANGELIS, B. M., GESELBRACHT, L., HANCOCK, B., JEFFS, A., MCDONALD, T., MCLEOD, I. M., POGODA, B., THEUERKAUF, S. J., THOMAS, M., WESTBY, S. & ZU ERMGASSEN, P. S. E. 2020. Restoring shellfish reefs: Global guidelines for practitioners and scientists. *Conservation Science and Practice,* 2.

FLESTER, J. A. & BLUM, L. K. 2020. Rates of Mainland Marsh Migration into Uplands and Seaward Edge Erosion are Explained by Geomorphic Type of Salt Marsh in Virginia Coastal Lagoons. *Wetlands,* 40**,** 1703-1715.

FOWLER, A. M., BOSWIJK, G., LORREY, A. M., GERGIS, J., PIRIE, M., MCCLOSKEY, S. P. J., PALMER, J. G. & WUNDER, J. 2012. Multi-centennial tree-ring record of ENSO-related activity in New Zealand. *Nature Climate Change,* 2**,** 172-176.

FOX-KEMPER, B., HEWITT, H. T., XIAO, C., AÐALGEIRSDÓTTIR, G., DRIJFHOUT, S. S., EDWARDS, T. L., GOLLEDGE, N. R., HEMER, M., KOPP, R. E., KRINNER, G., MIX, A., NOTZ, D., NOWICKI, S., NURHATI, I. S., RUIZ, L., SALLÉE, J.-B., SLANGEN, A. B. A. & YU, Y. 2021. Ocean, Cryosphere and Sea Level Change. *In:*

MASSON-DELMOTTE, V., ZHAI, P., PIRANI, A., CONNORS, S. L., PÉAN, C., BERGER, S., CAUD, N., CHEN, Y., GOLDFARB, L., GOMIS, M. I., HUANG, M., LEITZELL, K., E.LONNOY, MATTHEWS, J. B. R., MAYCOCK, T. K., WATERFIELD, T., YELEKÇI, O., YU, R. & ZHOU, B. (eds.) *Climate Change 2021: The Physical Science Basis. Contribution of Working Group I to the Sixth Assessment Report of the Intergovernmental Panel on Climate Change.* Cambridge, United Kingdom New York, NY, USA.

FREDSØE, J. & DIEGAARD, R. 1992. *Mechanics of Coastal Sediement Transport,* Singapore, World Scientific Publishing Co. Pte. Ltd.

GANJU, N., KIRWAN, M., DICKHUDT, P., GUNTENSPERGEN, G., CAHOON, D. & KROEGER, K. 2015. Sediment transport-based metrics of wetland stability. *Geophysical Research Letters,* 42**,** 7992-8000.

GARDNER, R. C. & DAVIDSON, N. C. 2011. The Ramsar Convention. *In:* LEPAGE, B. (ed.) *Wetlands.* Dordrecht: Springer.

GARLAND, J. & WADSWORTH, T. 2019. An Archaeological Survey of Catlins Lake and Estuary, Southland. *Archaeology in New Zealand***,** 27-38.

GEDAN, K. B., KELLOGG, L. & BREITBURG, D. L. 2014. Accounting for Multiple Foundation Species in Oyster Reef Restoration Benefits. *Restoration Ecology,* 22**,** 517-524.

GEDAN, K. B., KIRWAN, M. L., WOLANSKI, E., BARBIER, E. B. & SILLIMAN, B. R. 2010. The present and future role of coastal wetland vegetation in protecting shorelines: answering recent challenges to the paradigm. *Climatic Change,* 106**,** 7-29.

GEHRELS, W. R., HAYWARD, B. W., NEWNHAM, R. M. & SOUTHALL, K. E. 2008. A 20th century acceleration of sea-level rise in New Zealand. *Geophysical Research Letters,* 35.

GIBB, J. G. & COX, G. J. 2009. Patterns & Rates of Sedimentation within Porirua Harbour.

GIBSON, P. B., PERKINS-KIRKPATRICK, S. E. & RENWICK, J. A. 2016. Projected changes in synoptic weather patterns over New Zealand examined through self-organizing maps. *International Journal of Climatology,* 36**,** 3934-3948.

GILLGREN, C., STØTTRUP, J. G., SCHUMACHER, J. & DINESEN, G. E. 2018. Working together: collaborative decision making for sustainable Integrated Coastal Management (ICM). *Journal of Coastal Conservation,* 23**,** 959-968.

GILLIES, J. A., NICKLING, W. G. & KING, J. 2006. Aeolian sediment transport through large patches of roughness in the atmospheric inertial sublayer. *Journal of Geophysical Research,* 111.

GITTMAN, R. K., FODRIE, F. J., BAILLIE, C. J., BRODEUR, M. C., CURRIN, C. A., KELLER, D. A., KENWORTHY, M. D., MORTON, J. P., RIDGE, J. T. & ZHANG, Y.

S. 2017. Living on the Edge: Increasing Patch Size Enhances the Resilience and Community Development of a Restored Salt Marsh. *Estuaries and Coasts,* 41**,** 884-895.

GODOI, V. A., BRYAN, K. R. & GORMAN, R. M. 2018. Storm wave clustering around New Zealand and its connection to climatic patterns. *International Journal of Climatology,* 38**,** e401-e417.

GOFF, J. R., NICHOL, S. L. & ROUSE, H. L. 2003. *The New Zealand Coast TE TAI O AOTEAROA,* Palmerston North, Dunmore Press.

GÖNNERT, G., DUBE, S., OLDEN, J., BRUNO, J. & MD, B. 2001. Global storm surges: theory observation and application. *Die Küste*.

GOOSSENS, D., NOLET, C., ETYEMEZIAN, V., DUARTE-CAMPOS, L., BAKKER, G. & RIKSEN, M. 2018. Field testing, comparison, and discussion of five aeolian sand transport measuring devices operating on different measuring principles. *Aeolian Research,* 32**,** 1-13.

GRABOWSKI, J. H., BRUMBAUGH, R. D., CONRAD, R. F., KEELER, A. G., OPALUCH, J. J., PETERSON, C. H., PIEHLER, M. F., POWERS, S. P. & SMYTH, A. R. 2012. Economic Valuation of Ecosystem Services Provided by Oyster Reefs. *BioScience,* 62**,** 900-909.

GRABOWSKI, J. H. & PETERSON, C. H. 2011. Restoring Oyster Reefs to Recover Ecosystem Services. *In:* CUDDINGTON, K., BYERS, J. E., WILLSON, W. G. & HASTINGS, A. (eds.) *Ecosystem Engineers: Plants to Protists* San Diego, California Academic Press.

GRACIA, A., RANGEL-BUITRAGO, N., OAKLEY, J. A. & WILLIAMS, A. T. 2018. Use of ecosystems in coastal erosion management. *Ocean & Coastal Management,* 156**,** 277-289.

GREGORY, N. G. 1995. The role of shelterbelts in protecting livestock: A review. *New Zealand Journal of Agricultural Research,* 38**,** 423-450.

GUERRY, A. D., POLASKY, S., LUBCHENCO, J., CHAPLIN-KRAMER, R., DAILY, G. C., GRIFFIN, R., RUCKELSHAUS, M., BATEMAN, I. J., DURAIAPPAH, A., ELMQVIST, T., FELDMAN, M. W., FOLKE, C., HOEKSTRA, J., KAREIVA, P. M., KEELER, B. L., LI, S., MCKENZIE, E., OUYANG, Z., REYERS, B., RICKETTS, T. H., ROCKSTROM, J., TALLIS, H. & VIRA, B. 2015. Natural capital and ecosystem services informing decisions: From promise to practice. *Proc Natl Acad Sci U S A,* 112**,** 7348-55.

HAIGH, I. D., ELIOT, M. & PATTIARATCHI, C. 2011. Global influences of the 18.61 year nodal cycle and 8.85 year cycle of lunar perigee on high tidal levels. *Journal of Geophysical Research,* 116.

HAMEL, G. E. 1977. *Prehistoric Man and His Environment In The Catlins, New Zealand.* University of Otago.

HAMEL, G. E. 14 November 1978 1978. *RE: The excavation of the archaeological site of Manuka Point, Pounawea*

HAMEL, G. E. 28th January 1979 1979. *RE: Manuka Point* Type to GLEAVE.

HANLEY, M. E., HOGGART, S. P. G., SIMMONDS, D. J., BICHOT, A., COLANGELO, M. A., BOZZEDA, F., HEURTEFEUX, H., ONDIVIELA, B., OSTROWSKI, R., RECIO, M., TRUDE, R., ZAWADZKA-KAHLAU, E. & THOMPSON, R. C. 2014. Shifting sands? Coastal protection by sand banks, beaches and dunes. *Coastal Engineering,* 87**,** 136-146.

HANNAH, J. 2004. An updated analysis of long-term sea level change in New Zealand. *Geophysical Research Letters,* 31.

HANNAH, J. & BELL, R. G. 2012. Regional sea level trends in New Zealand. *Journal of Geophysical Research: Oceans,* 117.

HANNAH, J., BELL, R. G. & PAULIK, R. Auckland- A Case Study in the Regional Assessment of Long-Term Sea Level Change. Bridging the Gap Between Cultures, 18-22 May 22011 2011 Marrakech, Morocco.

HARMSWORTH, G. R. & AWATERE, S. 2013. Indigenous Māori knowledge and perspectives of ecosystems. *In:* DYMOND, J. (ed.) *Ecosystem services in New Zealand – Conditions and trends.* Lincoln, New Zealand: Manaaki Whenua Press.

HAY, A. E., KIMBERLEY, M. O. & KAMPFRAATH, B. M. P. 1999. MONTHLY DIAMETER AND HEIGHT GROWTH OF YOUNG EUCALYPTUS FASTIGATA, E. REGNANS, AND E. SALIGNA. *New Zealand Journal of Foresty Science,* 29**,** 263-273.

HAYWARD, B. W., GRENFELL, H. R., SABAA, A. T., SOUTHALL, K. E. & GEHRELS, W. R. 2007. FORAMINIFERAL EVIDENCE OF HOLOCENE SUBSIDENCE AND FAULT DISPLACEMENTS, COASTAL SOUTH OTAGO, NEW ZEALAND. *Journal of Foraminiferal Research,* 37**,** 344-359.

HEALY, T. R., KIRK, R. M. & DE LANGE, W. P. 1990. Beach Renourishment in New Zealand. *Journal of Coastal Research,* 6**,** 77-90.

HEISLER, G. M. & DEWALLE, D. R. 1988. Effects of windbreak structure on wind flow. *Agriculture, Ecosystems and Environment,,* 22/23**,** 41-69.

HENDTLASS, C., MORGAN, S. & D/, N. 2020. Coastal Systems & Sea Level Rise: What to look for in the future. Wellington: New Zealand Coastal Society

HESP, P. A. 2002. Foredunes and blowouts: initiation, geomorphology and dynamics *Geomorphology,* 48**,** 245-268.

HESP, P. A. & HILTON, M. J. 2013. Restoration of Foredunes and Transgressive Dunefields: Case Studies from New Zealand. *Restoration of Coastal Dunes.*

HESP, P. A. & SMYTH, T. A. G. 2021. CFD flow dynamics over model scarps and slopes. *Physical Geography,* 42**,** 1-24.

HEWITT, P. G. 2004. Bernoulli's principle. *The Science Teacher,* 71**,** 51-55.

HICKS, M., SEMADEMI-DAVIES, A., HADDADCHI, A., SHANKAR, U. & PLEW, D. R. 2019. Updated sediment load estimator for New Zealand. Ministry for the Environment.

HILTON, M., KONLECHNER, T., MCLACHLAN, K., LIM, D. & LORD, J. 2019. Long-lived seed banks of Ammophila arenaria prolong dune restoration programs. *Journal of Coastal Conservation,* 23**,** 461-471.

HILTON, M. J. & KONLECHNER, T. M. A review of the marram grass eradication program (1999–2009), Stewart Island, New Zealand. Proceeding of the 17th Australasian Weeds Conference, 26-30 September 2010 Christchurch, New Zealand 386-389.

HILTON, M. J. & KONLECHNER, T. M. 2021. *The Rakiura Dune Restoration Programme (1999–2021): Lessons Learned from 21 Years of Operations, Monitoring & Research.,* Dunedin, Otago Uniprint.

HIMES-CORNELL, A., PENDLETON, L. & ATIYAH, P. 2018. Valuing ecosystem services from blue forests: A systematic review of the valuation of salt marshes, sea grass beds and mangrove forests. *Ecosystem Services,* 30**,** 36-48.

HIMMELSTOSS, E. A., HENDERSON, R. E., KRATZMAN, M. G. & FARRIS, A. S. 2018. Digital Shoreline Analysis System (DSAS) Version 5.0 User Guide. *Open-File Report.* United States Geological Survey.

HOLLING, C. S. 1973. Resilience and Stability of Ecological Systems. *Annual Review of Ecology and Systematics,* 4**,** 1-23.

HOUTTUIJN BLOEMENDAAL, L. J., FITZGERALD, D. M., HUGHES, Z. J., NOVAK, A. B. & PHIPPEN, P. 2021. What controls marsh edge erosion? *Geomorphology,* 386.

HOWIE, A. H. & BISHOP, M. J. 2021. Contemporary Oyster Reef Restoration: Responding to a Changing World. *Frontiers in Ecology and Evolution,* 9.

HUGENHOLTZ, C. H., WHITEHEAD, K., BROWN, O. W., BARCHYN, T. E., MOORMAN, B. J., LECLAIR, A., RIDDELL, K. & HAMILTON, T. 2013. Geomorphological mapping with a small unmanned aircraft system (sUAS): Feature detection and accuracy assessment of a photogrammetrically-derived digital terrain model. *Geomorphology,* 194**,** 16-24.

HUNT, S., BRYAN, K. R. & MULLARNEY, J. C. 2015. The influence of wind and waves on the existence of stable intertidal morphology in meso-tidal estuaries. *Geomorphology,* 228**,** 158-174.

IPCC 2021a. Cliamte Change 2021: The Physical Science Basis. Contribution of Working Group I to the sixth Assessment Report of the Intergovernmental Panel on Climate Change. *In:* MASSON-DELMOTTE, V., ZHAI, P., PIRANI, A., CONNERS, S. L., PÉAN, C., BERGER, S., CAUD, N., CHEN, Y., GOLDFARB, M. I., GOMIS, M., HUANG, M.,

LEITZELL, K., LONNOY, E., MATTHEW, J. B. R., MAYCOCK, T. K., WATERFIELD, O., YELEKCI, O., YU, R. & ZHOU, B. (eds.).

IPCC 2021b. IPCC, 2021: Summary for Policymakers. *In:* MASSON-DELMOTTE, V., ZHAI, P., PIRANI, A., CONNORS, S. L., PÉAN, C., BERGER, S., CAUD, N., CHEN, Y., GOLDFARB, L., GOMIS, M. I., HUANG, M., LEITZELL, K., LONNOY, E., MATTHEWS, J. B. R., MAYCOCK, T. K., WATERFIELD, T., YELEKÇI, O., YU, R. & ZHOU, B. (eds.) *Climate Change 2021: The Physical Science Basis. Contribution of Working Group I to the Sixth Assessment Report of the Intergovernmental Panel on Climate Change* Cambridge Universirty Press.

JAUD, M., GRASSO, F., LE DANTEC, N., VERNEY, R., DELACOURT, C., AMMANN, J., DELOFFRE, J. & GRANDJEAN, P. 2016. Potential of UAVs for Monitoring Mudflat Morphodynamics (Application to the Seine Estuary, France). *ISPRS International Journal of Geo-Information,* 5.

JEFFS, A. G. & CREESE, R. G. 1996. Overview and bibliography of research on the Chilean oyster Tiostrea Chilensis (Philippi, 1845) from New Zealand waters. *Journal of Shellfish Research* 15**,** 305-311.

JIAN, Z., BO, L. & MINGYUE, W. 2018. Study on windbreak performance of tree canopy by numerical simulation method. *The Journal of Computational Multiphase Flows,* 10**,** 259-265.

JIANG, Z., BULLIDO-GARCIA, M., HOUBART, J.-C. & CÉLINE, B. CFD modeling of forest canopy flows- Input parameters, calibration and validation.pdf>. EWEA: Europe's Premier Wind Energy Event, 2013 Vienna, Austria. EWEA.

JIMÉNEZ, J., VALDEMORO, H., BOSOM, E., SÁNCHEZ-ARCILLA, A. & NICHOLLS, R. 2017. Impacts of sea-level rise-induced erosion on the Catalan coast. *Regional Environmental Change* 17**,** 593-603.

JOHNSON, P. & GERBEAUX, P. 2004. *Wetland Types in New Zealand,* Wellington, Department of Conservation.

JURJONAS, M. & SEEKAMP, E. 2018. Rural coastal community resilience: Assessing a framework in eastern North Carolina. *Ocean & Coastal Management,* 162**,** 137-150.

KABISCH, N., FRANTZESKAKI, N., PAULEIT, S., NAUMANN, S., DAVIS, M., ARTMANN, M., HAASE, D., KNAPP, S., KORN, H., STADLER, J., ZAUNBERGER, K. & BONN, A. 2016. Nature-based solutions to climate change mitigation and adaptation in urban areas: perspectives on indicators, knowledge gaps, barriers, and opportunities for action. *Ecology and Society,* 21.

KALMAN, R. 1960. A new approach to linear filtering and prediction problems *Journal of Basic Engineering* 82**,** 35-45.

KARIMPOUR, A., CHEN, Q. & TWILLEY, R. R. 2017. Wind Wave Behavior in Fetch and Depth Limited Estuaries. *Sci Rep,* 7**,** 40654.

KATRITSIS, D., KAIKTSIS, L., CHANIOTIS, A., PANTOS, J., EFSTATHOPOULOS, E. P. & MARMARELIS, V. 2007. Wall shear stress: theoretical considerations and methods of measurement. *Prog Cardiovasc Dis,* 49**,** 307-29.

KING, D. J., NEWNHAM, R. M., GEHRELS, W. R. & CLARK, K. J. 2020. Late Holocene sea-level changes and vertical land movements in New Zealand. *New Zealand Journal of Geology and Geophysics,* 64**,** 21-36.

KIRWAN, M. L., TEMMERMAN, S., SKEEHAN, E. E., GUNTENSPERGEN, G. R. & FAGHERAZZI, S. 2016. Overestimation of marsh vulnerability to sea level rise. *Nature Climate Change,* 6**,** 253-260.

KITTINGER, J. N. & AYERS, A. L. 2010. Shoreline Armoring, Risk Management, and Coastal Resilience Under Rising Seas. *Coastal Management,* 38**,** 634-653.

KNUTSON, T. R., MCBRIDE, J. L., CHAN, J., EMANUEL, K., HOLLAND, G., LANDSEA, C., HELD, I., KOSSIN, J. P., SRIVASTAVA, A. K. & SUGI, M. 2010. Tropical cyclones and climate change. *Nature Geoscience,* 3**,** 157.

KOCH, E. W., BARBIER, E. B., SILLIMAN, B. R., REED, D. J., PERILLO, G. M. E., HACKER, S. D., GRANEK, E. F., PRIMAVERA, J. H., MUTHIGA, N., POLASKY, S., HALPERN, B. S., KENNEDY, C. J., KAPPEL, C. V. & WOLANSKI, E. 2009. Non-linearity in ecosystem services: temporal and spatial variability in coastal protection. *Frontiers in Ecology and the Environment,* 7**,** 29-37.

KONLECHNER, T. M., RYU, W., HILTON, M. J. & SHERMAN, D. J. 2015. Evolution of foredune texture following dynamic restoration, Doughboy Bay, Stewart Island, New Zealand. *Aeolian Research,* 19**,** 203-214.

KOZLOWSKI, T. T. 1997. Responses of woody plants to flooding and salinity. *Tree Physiology,* 17**,** 490-519.

KRONVANG, B., FALKUM, Ø., SVENDSEN, L. M. & LAUBEL, A. 2017. Deposition of sediment and phosphorus during overbank flooding. *SIL Proceedings, 1922-2010,* 28**,** 1289-1293.

KÜHN, D. B. 2021. *Designing an effective engineering approach to rebuild a sand spit that has disintegrated due to its ad-hoc artificial breaching : Kalutara Lagoon, Sri Lanka.* IHE Delft Institute for Water Education.

KULELI, T., GUNEROGLU, A., KARSLI, F. & DIHKAN, M. 2011. Automatic detection of shoreline change on coastal Ramsar wetlands of Turkey. *Ocean Engineering,* 38**,** 1141-1149.

KULP, S. A. & STRAUSS, B. H. 2019. New elevation data triple estimates of global vulnerability to sea-level rise and coastal flooding. *Nat Commun,* 10**,** 4844.

LANE, E., WALTERS, R., GILLIBRAND, P. & UDDSTROM, M. 2009. Operational forecasting of sea level height using an unstructured grid ocean model. *Ocean Modelling,* 28**,** 88-96.

LAWRENCE, J., BELL, R., BLACKETT, P., STEPHENS, S. & ALLAN, S. 2018. National guidance for adapting to coastal hazards and sea-level rise: Anticipating change, when and how to change pathway. *Environmental Science & Policy,* 82**,** 100-107.

LEE, J.-M., PARK, J.-Y. & CHOI, J.-Y. 2013. Evaluation of Sub-aerial Topographic Surveying Techniques Using Total Station and RTK-GPS for Applications in Macrotidal Sand Beach Environment. *Journal of Coastal Research,* 65**,** 535-540.

LEE, W. G. & PARTRIDGE, T. R. 1983. Rates of spread ofSpartina anglicaand sediment accretion in the New River Estuary, Invercargill, New Zealand. *New Zealand Journal of Botany,* 21**,** 231-236.

LEONARDI, N., CARNACINA, I., DONATELLI, C., GANJU, N. K., PLATER, A. J., SCHUERCH, M. & TEMMERMAN, S. 2018. Dynamic interactions between coastal storms and salt marshes: A review. *Geomorphology,* 301**,** 92-107.

LEONARDI, N., GANJU, N. K. & FAGHERAZZI, S. 2016. A linear relationship between wave power and erosion determines salt-marsh resilience to violent storms and hurricanes. *Proc Natl Acad Sci U S A,* 113**,** 64-68.

LI, X., LEONARDI, N. & PLATER, A. J. 2019. Wave-driven sediment resuspension and salt marsh frontal erosion alter the export of sediments from macro-tidal estuaries. *Geomorphology,* 325**,** 17-28.

LIU, B., QU, J., ZHANG, W., TAN, L. & GAO, Y. 2014. Numerical evaluation of the scale problem on the wind flow of a windbreak. *Sci Rep,* 4**,** 6619.

LOCKERBIE, L. 1959. From Moa-Hunter to Classic Maori in Southern New Zealand. *In:* FREEMAN, J. D. & GEDDES, W. R. (eds.) *Anthropology in the South Seas: Essays presented to H.D. Skinner*. New Plymouth Thomas Avery & Sons Ltd.

LONG, J. W. & PLANT, N. G. 2012. Extended Kalman Filter framework for forecasting shoreline evolution. *Geophysical Research Letters,* 39**,** n/a-n/a.

LUISA MARTÍNEZ, M., MENDOZA-GONZÁLEZ, G., SILVA-CASARÍN, R. & MENDOZA-BALDWIN, E. 2014. Land use changes and sea level rise may induce a "coastal squeeze" on the coasts of Veracruz, Mexico. *Global Environmental Change,* 29**,** 180-188.

MADSEN, A. T., MURRAY, A. S., ANDERSEN, T. J. & PEJRUP, M. 2007. Temporal changes of accretion rates on an estuarine salt marsh during the late Holocene — Reflection of local sea level changes? The Wadden Sea, Denmark. *Marine Geology* 242**,** 221-233.

MAHGOUB, A. O. & GHANI, S. 2021. Numerical and experimental investigation of utilizing the porous media model for windbreaks CFD simulation. *Sustainable Cities and Society,* 65.

MARANI, M., D'ALPAOS, A., LANZONI, S. & SANTALUCIA, M. 2011. Understanding and predicting wave erosion of marsh edges. *Geophysical Research Letters,* 38**,** n/a-n/a.

MARCOS, M., JORDÀ, G., GOMIS, D. & PÉREZ, B. 2011. Changes in storm surges in southern Europe from a regional model under climate change scenarios. *Global and Planetary Change,* 77**,** 116-128.

MARIOTTI, G. & FAGHERAZZI, S. 2013. Wind waves on a mudflat: The influence of fetch and depth on bed shear stresses. *Continental Shelf Research,* 60**,** S99-S110.

MARKFORT, C. D., PEREZ, A. L. S., THILL, J. W., JASTER, D. A., PORTÉ-AGEL, F. & STEFAN, H. G. 2010. Wind sheltering of a lake by a tree canopy or bluff topography. *Water Resources Research,* 46.

MARTINELLI, L., ZANUTTIGH, B., DE NIGRIS, N. & PRETI, M. 2011. Sand bag barriers for coastal protection along the Emilia Romagna littoral, Northern Adriatic Sea, Italy. *Geotextiles and Geomembranes,* 29**,** 370-380.

MARTÍNEZ-CARRICONDO, P., AGÜERA-VEGA, F., CARVAJAL-RAMÍREZ, F., MESAS-CARRASCOSA, F.-J., GARCÍA-FERRER, A. & PÉREZ-PORRAS, F.-J. 2018. Assessment of UAV-photogrammetric mapping accuracy based on variation of ground control points. *International Journal of Applied Earth Observation and Geoinformation,* 72**,** 1-10.

MASUCCI, G. D., ACIERNO, A. & REIMER, J. D. 2019. Eroding diversity away: Impacts of a tetrapod breakwater on a subtropical coral reef. *Aquatic Conservation: Marine and Freshwater Ecosystems,* 30**,** 290-302.

MAY, S. M., ENGEL, M., BRILL, D., SQUIRE, P., SCHEFFERS, A. & KELLETAT, D. 2013. Coastal hazards from tropical cyclones and extratropical winter storms based on Holocene storm chronologies. *Coastal Hazards* Dordrecht: Springer.

MCCLENACHAN, G. M., DONNELLY, M. J., SHAFFER, M. N., SACKS, P. E. & WALTERS, L. J. 2020. Does size matter? Quantifying the cumulative impact of small-scale living shoreline and oyster reef restoration projects on shoreline erosion. *Restoration Ecology,* 28**,** 1365-1371.

MCCOMB, A. J. & DAVIS, J. A. 1993. Eutrophic waters of southwestern Australia. *Fertilizer Researcb,* 36**,** 105-114.

MCGLONE, M. 2009. Postglacial history of New Zealand

wetlands and implications for their conservation. *New Zealand Journal of Ecology,* 33.

MENÉNDEZ, M. & WOODWORTH, P. L. 2010. Changes in extreme high water levels based on a quasi-global tide-gauge data set. *Journal of Geophysical Research: Oceans,* 115.

MEYER, D. L., TOWNSEND, E. C. & THAYER, G. W. 1997. Stabilization and Erosion Control Value of Oyster Cultch for Intertidal Marsh. *Restoration Ecology,* 5**,** 93-99.

MFE, M. F. T. E. 2017. Coastal Hazards and Climate Change: Guidance for Local Government. Wellington, New Zealand

MILLER, F., OSBAHR, H., BOYD, E., THOMALLA, F., BHARWANI, S., ZIERVOGEL, G., WALKER, B., BIRKMANN, J., VAN DER LEEUW, S., ROCKSTRÖM, J., HINKEL, J., DOWNING, T., FOLKE, C. & NELSON, D. 2010. Resilience & vulnerability - complementary or conflicting concepts. *Ecology and Society,* 15.

MITSCH, W. J. & GOSSELINK, J. G. 2015. *Wetlands*, John Wiley & Sons, Incorporated.

MOESLUND, J. E., ARGE, L., BØCHER, P. K., NYGAARD, B. & SVENNING, J.-C. 2011. Geographically Comprehensive Assessment of Salt-Meadow Vegetation-Elevation Relations Using LiDAR. *Wetlands,* 31**,** 471-482.

MÖLLER, I. 2019. Applying Uncertain Science to Nature-Based Coastal Protection: Lessons From Shallow Wetland-Dominated Shores. *Frontiers in Environmental Science,* 7.

MÖLLER, I., KUDELLA, M., RUPPRECHT, F., SPENCER, T., PAUL, M., VAN WESENBEECK, B. K., WOLTERS, G., JENSEN, K., BOUMA, T. J., MIRANDA-LANGE, M. & SCHIMMELS, S. 2014. Wave attenuation over coastal salt marshes under storm surge conditions. *Nature Geoscience,* 7**,** 727-731.

MOLONEY, J. G., HILTON, M. J., SIRGUEY, P. & SIMONS-SMITH, T. 2018. Coastal Dune Surveying Using a Low-Cost Remotely Piloted Aerial System (RPAS). *Journal of Coastal Research,* 345**,** 1244-1255.

MONMONIER, M. 2005. Defining the Wind: The Beaufort Scale, and How a 19th Century Admiral Turned Science into Poetry. *The Professional Geographer,* 57**,** 474-475.

MOREIRA, A., VIEIRA, C. S., DAS NEVES, L. & LOPES, M. L. 2016. Assessment of friction properties at geotextile encapsulated-sand systems' interfaces used for coastal protection. *Geotextiles and Geomembranes,* 44**,** 278-286.

MORRIS, J. T., BARBER, D. C., CALLAWAY, J. C., CHAMBERS, R., HAGEN, S. C., HOPKINSON, C. S., JOHNSON, B. J., MEGONIGAL, P., NEUBAUER, S. C., TROXLER, T. & WIGAND, C. 2016. Contributions of organic and inorganic matter to sediment volume and accretion in tidal wetlands at steady state. *Earths Future,* 4**,** 110-121.

MORRIS, R. L., BILKOVIC, D. M., BOSWELL, M. K., BUSHEK, D., CEBRIAN, J., GOFF, J., KIBLER, K. M., LA PEYRE, M. K., MCCLENACHAN, G., MOODY, J., SACKS, P., SHINN, J. P., SPARKS, E. L., TEMPLE, N. A., WALTERS, L. J., WEBB, B. M., SWEARER, S. E. & COLEMAN, M. 2019. The application of oyster reefs in shoreline protection: Are we over-engineering for an ecosystem engineer? *Journal of Applied Ecology,* 56**,** 1703-1711.

MORRIS, R. L., KONLECHNER, T. M., GHISALBERTI, M. & SWEARER, S. E. 2018. From grey to green: Efficacy of eco-engineering solutions for nature-based coastal defence. *Glob Chang Biol,* 24**,** 1827-1842.

MORRIS, R. L., LA PEYRE, M. K., WEBB, B. M., MARSHALL, D. A., BILKOVIC, D. M., CEBRIAN, J., MCCLENACHAN, G., KIBLER, K. M., WALTERS, L. J., BUSHEK, D., SPARKS, E. L., TEMPLE, N. A., MOODY, J., ANGSTADT, K., GOFF, J., BOSWELL, M., SACKS, P. & SWEARER, S. E. 2021. Large-scale variation in wave attenuation of oyster reef living shorelines and the influence of inundation duration. *Ecol Appl,* 31**,** e02382.

MURTY, T. S. & FLATHER, R. A. 1994. Impact of Storm Surges in the Bay of Bengal. *Journal of Coastal Research,* 12**,** 149-161.

MURY, A., COLLIN, A., HOUET, T., ALVAREZ-VANHARD, E. & JAMES, D. 2020. Using Multispectral Drone Imagery for Spatially Explicit Modeling of Wave Attenuation through a Salt Marsh Meadow. *Drones,* 4.

MUTO, T. & STEEL, R. J. 1997. Principles of regression and transgression; the nature of the interplay between accommodation and sediment supply *Journal of Sedimentary Research,* 67**,** 994-1000.

MYERS, S. C., CLARKSON, B. R., REEVES, P. N. & CLARKSON, B. D. 2013. Wetland management in New Zealand: Are current approaches and policies sustaining wetland ecosystems in agricultural landscapes? *Ecological Engineering,* 56**,** 107-120.

NAGDEE, M. R. M. S., NURSE, L., INNISS, L., CHADWICK, A. & JOHNSON, T. 2019. Historical Shoreline Mapping: Application of the Digital Shoreline Analysis System to the Evolution of Worthing Beach, Barbados, Following Hurricanes Allen (1980) and Ivan (2004). *Journal of Coastal Research,* 36.

NARAYAN, S., BECK, M. W., REGUERO, B. G., LOSADA, I. J., VAN WESENBEECK, B., PONTEE, N., SANCHIRICO, J. N., INGRAM, J. C., LANGE, G. M. & BURKS-COPES, K. A. 2016. The Effectiveness, Costs and Coastal Protection Benefits of Natural and Nature-Based Defences. *PLoS One,* 11**,** e0154735.

NEEDHAM, H. R. 2011. *The context-specific roles of a bioturbating crab (Austrohelice crassa) on ecosystem functioning (PhD).* Doctor of Philosophy, The University of Waikato.

NELSON, E. J., KAREIVA, P., RUCKELSHAUS, M., ARKEMA, K., GELLER, G., GIRVETZ, E., GOODRICH, D., MATZEK, V., PINSKY, M., REID, W., SAUNDERS, M., SEMMENS, D. & TALLIS, H. 2013. Climate change's impact on key ecosystem services and the human well-being they support in the US. *Frontiers in Ecology and the Environment,* 11**,** 483-893.

NEREM, R. S., BECKLEY, B. D., FASULLO, J. T., HAMLINGTON, B. D., MASTERS, D. & MITCHUM, G. T. 2018. Climate-change-driven accelerated sea-level rise detected in the altimeter era. *Proc Natl Acad Sci U S A,* 115**,** 2022-2025.

NESSHOVER, C., ASSMUTH, T., IRVINE, K. N., RUSCH, G. M., WAYLEN, K. A., DELBAERE, B., HAASE, D., JONES-WALTERS, L., KEUNE, H., KOVACS, E., KRAUZE, K., KULVIK, M., REY, F., VAN DIJK, J., VISTAD, O. I., WILKINSON, M. E. & WITTMER, H. 2017. The science, policy and practice of nature-based solutions: An interdisciplinary perspective. *Sci Total Environ,* 579**,** 1215-1227.

NEW ZEALAND GOVERNMENT 2010. New Zealand Coastal Policy Statement 2010. *In:* GOVERNMENT, N. Z. (ed.). Wellington, New Zealand: Department of Conservation.

NEWNHAM, R. M., LOWE, D. J., MCCLONE, S., WILMSHURST, J. M. & HIGHAM, T. F. C. 1998. The Kaharoa Tephra as a critical datum for earliest human impact in northern New Zealand,. *Journal of Archaeological Science,* 25**,** 533-544.

NGUYEN, D., HILTON, M. J., WAKES, S. J. & SIMONS-SMITH, T. 2021. Incident wind angle and topographic steering through foredune notches. *Geomorphology,* 395**,** 1-19.

NGUYEN, H. T., TANAKA, H. & NGUYEN, T. X. Post-Tsunami Recovery and Morphology Change at Naruse Rivermouth, Japan. Proceedings of the 10th International Conference on Asian and Pacific Coasts, 25-28 September 2019 Hanoi, Vietnam 797-801.

NICHOLLS, R., HOOZEMANS, F. & MARCHAND, M. 1999. Increasing flood risk and wetland losses due to global sea-level rise: regional and global analyses. *Global Environmental Change,* 9**,** S69-S87.

NIXON, S. W. 1995. Coastal marine eutrophication: A definition, social causes, and future concerns. *Ophelia,* 41**,** 199-219.

NOAA. 2021. *What is a perigean spring tide?* [Online]. National Oceanic and Atmospheric Administration. Available: https://oceanservice.noaa.gov/facts/perigean-spring-tide.html [Accessed 23/06/21 2021].

NOLTE, S., KOPPENAAL, E. C., ESSELINK, P., DIJKEMA, K. S., SCHUERCH, M., DE GROOT, A. V., BAKKER, J. P. & TEMMERMAN, S. 2013. Measuring sedimentation in tidal marshes: a review on methods and their applicability in biogeomorphological studies. *Journal of Coastal Conservation,* 17**,** 301-325.

OH, S. M. & MOON, I.-J. 2012. Typhoon and storm surge intensity changes in a warming climate around the Korean Peninsula. *Natural Hazards,* 66**,** 1405-1429.

OKAYA, D., STERN, T., DAVEY, F., HENRYS, S. & COX, S. 2007. Continent-Continent Collision at the Pacific/Indo-Australian Plate Boundary: Background, Motivation, and Principal Results. *In:* OKAYA, D., STERN, T. & DAVEY, F. (eds.) *A Continental Plate Boundary : Tectonics at South Island, New Zealand.* 1 ed. Washington, DC: American Geophysical Union

ORC. 2020a. *Hungerford Point Saltmarsh* [Online]. Otago Regional Council Available: https://www.orc.govt.nz/managing-our-environment/water/wetlands-and-estuaries/clutha-district/hungerford-point-saltmarsh [Accessed 5th December 2022].

ORC 2020b. Natural Features and Natural Landscapes - Clutha District Section. Clutha.

OSSWALD, F., DOLCH, T. & REISE, K. 2019. Remobilizing stabilized island dunes for keeping up with sea level rise? *Journal of Coastal Conservation,* 23**,** 675-687.

OTAGO CATCHMENT BOARD REPORT 1979. Newhaven, Manuka Point & Pounawea Erosion.

OTAGO REGIONAL COUNCIL, O. 2010. Otago Estauries, State of the Environment Report.

OUMERACI, H. 1994. Review and analysis of vertical breakwater failures lessons learned. *Coastal Engineering,* 22**,** 3-29.

PALINKAS, C. M., SANFORD, L. P. & KOCH, E. W. 2017. Influence of Shoreline Stabilization Structures on the Nearshore Sedimentary Environment in Mesohaline Chesapeake Bay. *Estuaries and Coasts,* 41**,** 952-965.

PARTRIDGE, T. R. 1984. Salt Marshes or Catlins Lake and Estuary, South East Otago. Lincoln University

PARTRIDGE, T. R. & WILSON, J. B. 1988. Vegetation patterns in salt marshes of Otago, New Zealand. *New Zealand Journal of Botany,* 26**,** 497-510.

PARTRIDGE, T. R. & WILSON, J. B. 1989. Methods for investigating vegetation/environment relations — a test using the salt marsh vegetation of Otago, New Zealand. *New Zealand Journal of Botany,* 27**,** 35-47.

PENNINGS, S. & CALLAWAY, R. M. 1992. Salt Marsh Plant Zonation- The Relative Importance of Competition and Physical Factors. *Ecology and Society,* 73**,** 681-690.

PENNINGS, S. C., GRANT, M.-B. & BERTNESS, M. D. 2005. Plant zonation in low-latitude salt marshes: disentangling the roles of flooding, salinity and competition. *Journal of Ecology,* 93**,** 159-167.

PHILLIPS, J. D. 2018. Coastal wetlands, sea level, and the dimensions of geomorphic resilience. *Geomorphology,* 305**,** 173-184.

PIAZZA, B. P., BANKS, P. D. & LA PEYRE, M. K. 2005. The Potential for Created Oyster Shell Reefs as a Sustainable Shoreline Protection Strategy in Louisiana. *Restoration Ecology,* 13**,** 499-506.

PINSKY, M. L., GUANNEL, G. & ARKEMA, K. K. 2013. Quantifying wave attenuation to inform coastal habitat conservation. *Ecosphere,* 4.

PLEW, D. R., ZELDIS, J. R., DUDLEY, B. D., WHITEHEAD, A. L., STEVENS, L. M., ROBERTSON, B. M. & ROBERTSON, B. P. 2020. Assessing the Eutrophic Susceptibility of New Zealand Estuaries. *Estuaries and Coasts,* 43**,** 2015-2033.

POMPEI, M. & GROVE, P. 2010. Historic and current extent of Canterbury freshwater wetlands, and recent trends in remaining wetland areas. Christchurch: Environment Canterbury.

PONTEE, N. 2013. Defining coastal squeeze: A discussion. *Ocean & Coastal Management,* 84**,** 204-207.

PONTEE, N., NARAYAN, S., BECK, M. W. & HOSKING, A. H. 2016. Nature-based solutions: lessons from around the world. *Proceedings of the Institution of Civil Engineers - Maritime Engineering,* 169**,** 29-36.

PRAHALAD, V., SHARPLES, C., KIRKPATRICK, J. & MOUNT, R. 2014. Is wind-wave fetch exposure related to soft shoreline change in swell-sheltered situations with low terrestrial sediment input? *Journal of Coastal Conservation,* 19**,** 23-33.

PRANZINI, E., WETZEL, L. & WILLIAMS, A. T. 2015. Aspects of coastal erosion and protection in Europe. *Journal of Coastal Conservation,* 19**,** 445-459.

PUGH, D. & WOODWORTH, P. 2014. *Sea-Level Science: Understanding Tides, Surges, Tsunamis and Mean Sea-Level Changes,* Cambridge, Cambridge University Press.

PUGH, D. T. 2004. *Changing sea levels: effects of tides, weather, and climate:,* Cambridge, U.K. New York Cambridge University Press.

PULLEN, T., ALLSOP, N. W. H., BRUCE, T., KORTENHAUS, A., SCHÜTTRUMPF, H. & VAN DER MEER, J. W. 2007. EurOtop wave overtopping of sea defences and related structures: assessment manual. *Die Küste,* 73.

PYE, K. & BLOTT, S. 2008. Decadal-scale variation in dune erosion and accretion rates: An investigation of the significance of changing storm tide frequency and magnitude on the Sefton coast, UK. *Geomorphology,* 102**,** 652-666.

RAMAKRISHNAN, R., AGRAWAL, R., REMYA, P. G., NAGAKUMAR, K. C. V., DEMUDU, G., RAJAWAT, A. S., NAIR, B. & NAGESWARA RAO, K. 2018. Modelling coastal erosion: A case study of Yarada beach near Visakhapatnam, east coast of India. *Ocean & Coastal Management,* 156**,** 239-248.

RANGEL-BUITRAGO, N., WILLIAMS, A. T. & ANFUSO, G. 2018. Hard protection structures as a principal coastal erosion management strategy along the Caribbean coast of Colombia. A chronicle of pitfalls. *Ocean & Coastal Management,* 156**,** 58-75.

REES, J. G., RIDGWAY, J., ELLIS, S., O'B, R. W., NEWSHAM, R. & PARKES, A. 2000. Holocene sediment storage in the Humber Estuary *Geological Society* 166**,** 119-143.

REGISTER, J. 2004. Engineers against the Ocean: the St Clair Sea-wall. *E.nz Maginzine of Technical Enterprise,* 4**,** 36-38.

REGUERO, B. G., BECK, M. W., BRESCH, D. N., CALIL, J. & MELIANE, I. 2018. Comparing the cost effectiveness of nature-based and coastal adaptation: A case study from the Gulf Coast of the United States. *PLoS One,* 13**,** e0192132.

RIDDIN, T. & ADAMS, J. B. 2021. Salt marsh erosion in a microtidal estuary. *African Journal of Marine Science,* 43**,** 265-273.

ROBERTSON , B., M., ROBERTSON , B., P. & STEVENS, L. M. 2017. Catlins Estuary- Fine Scale Monitoring 2016:17.

ROBERTSON, H. 2016. Wetland reserves in New Zealand : the status of protected areas between 1990 and 2013. *New Zealand Journal of Ecology,* 40**,** 1-11.

ROBERTSON, H., AUSSEIL, A.-G., RANCE, B., BETTS, H. & POMEROY, E. 2018. Loss of wetlands since 1990 in Southland, New Zealand. *New Zealand Journal of Ecology*.

ROBIN, N., LEVOY, F., ANTHONY, E. J. & MONFORT, O. 2020. Sand spit dynamics in a large tidal-range environment- Insight from multiple LiDAR, UAV and hydrodynamic measurements on multiple spit hook development, breaching, reconstruction, and shoreline changes. *Earth Surface Processes and Landforms,* 45**,** 2706-2726.

RODRIGUEZ, A. B., FODRIE, F. J., RIDGE, J. T., LINDQUIST, N. L., THEUERKAUF, E. J., COLEMAN, S. E., GRABOWSKI, J. H., BRODEUR, M. C., GITTMAN, R. K., KELLER, D. A. & KENWORTHY, M. D. 2014. Oyster reefs can outpace sea-level rise. *Nature Climate Change,* 4**,** 493-497.

ROSS, A. N. & BAKER, T. P. 2012. Flow Over Partially Forested Ridges. *Boundary-Layer Meteorology,* 146**,** 375-392.

RUPPRECHT, F., MÖLLER, I., PAUL, M., KUDELLA, M., SPENCER, T., VAN WESENBEECK, B. K., WOLTERS, G., JENSEN, K., BOUMA, T. J., MIRANDA-LANGE, M. & SCHIMMELS, S. 2017. Vegetation-wave interactions in salt marshes under storm surge conditions. *Ecological Engineering,* 100**,** 301-315.

SALEH, F. & WEINSTEIN, M. P. 2016. The role of nature-based infrastructure (NBI) in coastal resiliency planning: A literature review. *J Environ Manage,* 183**,** 1088-1098.

SALVADOR DE PAIVA, J. N., WALLES, B., YSEBAERT, T. & BOUMA, T. J. 2018. Understanding the conditionality of ecosystem services: The effect of tidal flat morphology and oyster reef characteristics on sediment stabilization by oyster reefs. *Ecological Engineering,* 112**,** 89-95.

SCHOONEES, T., GIJÓN MANCHEÑO, A., SCHERES, B., BOUMA, T. J., SILVA, R., SCHLURMANN, T. & SCHÜTTRUMPF, H. 2019. Hard Structures for Coastal Protection, Towards Greener Designs. *Estuaries and Coasts,* 42**,** 1709-1729.

SCHUERCH, M., SPENCER, T., TEMMERMAN, S., KIRWAN, M. L., WOLFF, C., LINCKE, D., MCOWEN, C. J., PICKERING, M. D., REEF, R., VAFEIDIS, A. T., HINKEL, J., NICHOLLS, R. & BROWN, S. 2018. Future response of global coastal wetlands to SLR. *Nature,* 561.

SCOTT, D. B., FRAIL-GAUTHIER, J. & MUDIE, P. J. 2014a. Human intervention causing coastal problems. *Coastal Wetlands of the World.*

SCOTT, D. B., FRAIL-GAUTHIER, J. & MUDIE, P. J. 2014b. Physical aspects: geological, oceanic and climatic conditions. *Coastal Wetlands of the World.*

SCYPHERS, S. B., POWERS, S. P., HECK, K. L., JR. & BYRON, D. 2011. Oyster reefs as natural breakwaters mitigate shoreline loss and facilitate fisheries. *PLoS One,* 6**,** e22396.

SEDDON, N., CHAUSSON, A., BERRY, P., GIRARDIN, C. A. J., SMITH, A. & TURNER, B. 2020. Understanding the value and limits of nature-based solutions to climate change and other global challenges. *Philos Trans R Soc Lond B Biol Sci,* 375**,** 20190120.

SERVOLD, K. P., WEBB, B. M. & DOUGLASS, S. L. 2015. Effects of Low-Crested Living Shoreline Breakwaters on Wave Setup. *In:* WALLENDORF, L. & COX, D. (eds.) *Coastal Structure and Solutions to Coastal Disasters Joint Conference* Boston, Massachusetts: American Society of Civil Engineers

SHEPARD, C. C., CRAIN, C. M. & BECK, M. W. 2011. The protective role of coastal marshes: a systematic review and meta-analysis. *PLoS One,* 6**,** e27374.

SHI, B. W., YANG, S. L., WANG, Y. P., BOUMA, T. J. & ZHU, Q. 2012. Relating accretion and erosion at an exposed tidal wetland to the bottom shear stress of combined current–wave action. *Geomorphology,* 138**,** 380-389.

SILVA, R., MARTÍNEZ, M. L., VAN TUSSENBROEK, B. I., GUZMÁN-RODRÍGUEZ, L. O., MENDOZA, E. & LÓPEZ-PORTILLO, J. 2020. A Framework to Manage Coastal Squeeze. *Sustainability,* 12.

SIMONSON, T. & HALL, G. 2019. Vulnerable: the quantum of local government infrastructure exposed to sea level rise. Local Government New Zealand.

SLOBBE, E., VRIEND, H. J., AARNINKHOF, S., LULOFS, K., VRIES, M. & DIRCKE, P. 2012. Building with Nature: in search of resilient storm surge protection strategies. *Natural Hazards,* 65**,** 947-966.

SMITH, M. J., STEVENS, C. L., GORMAN, R. M., MCGREGOR, J. A. & NEILSON, C. G. 2001. Wind-wave development across a large shallow intertidal estuary: A case study of Manukau Harbour, New Zealand. *New Zealand Journal of Marine and Freshwater Research,* 35**,** 985-1000.

SMYTH, T. A. G. 2016. A review of Computational Fluid Dynamics (CFD) airflow modelling over aeolian landforms. *Aeolian Research,* 22**,** 153-164.

SOUTHALL, K. E., GEHRELS, W. R. & HAYWARD, B. W. 2006. Foraminifera in a New Zealand salt marsh and their suitability as sea-level indicators. *Marine Micropaleontology,* 60**,** 167-179.

SPALDING, M. D., RUFFO, S., LACAMBRA, C., MELIANE, I., HALE, L. Z., SHEPARD, C. C. & BECK, M. W. 2014. The role of ecosystems in coastal protection: Adapting to climate change and coastal hazards. *Ocean & Coastal Management,* 90**,** 50-57.

SPENCER, T., MÖLLER, I., RUPPRECHT, F., BOUMA, T. J., VAN WESENBEECK, B. K., KUDELLA, M., PAUL, M., JENSEN, K., WOLTERS, G., MIRANDA-LANGE, M. & SCHIMMELS, S. 2016a. Salt marsh surface survives true-to-scale simulated storm surges. *Earth Surface Processes and Landforms,* 41**,** 543-552.

SPENCER, T., SCHUERCH, M., NICHOLLS, R. J., HINKEL, J., LINCKE, D., VAFEIDIS, A. T., REEF, R., MCFADDEN, L. & BROWN, S. 2016b. Global coastal wetland change under sea-level rise and related stresses: The DIVA Wetland Change Model. *Global and Planetary Change,* 139**,** 15-30.

STANCHEVA, M., RANGEL-BUITRAGO, N., ANFUSO, G., PALAZOV, H., STANCHEV, H. & CORREA, I. 2011. Expanding Level of Coastal Armouring- Case Studies from Different Countries. *Journal of Coastal Research,* 64**,** 1815-1819.

STEPHENS, S., BELL, R. & LAWRENCE, J. 2017. Applying Principles of Uncertainty within Coastal Hazard Assessments to Better Support Coastal Adaptation. *Journal of Marine Science and Engineering,* 5.

STEPHENS, S., WADHWA, S., GORMAN, R. M., GOODHUE, N., PRITCHARD, M., OVENDEN, R. & REEVE, G. 2013. Coastal inundation by storm-tides and waves in the Auckland region. Prepared for Auckland Council. Auckland: NIWA.

STEVENS, L. M. & ROBERTSON , B., M 2017. Catlins Estuary- Board Scale Habitat Mapping 2016:17. Wriggle Coastal Management.

STŘEDOVÁ, H., PODHRÁZSKÁ, J., LITSCHMANN, T., STŘEDA, T. & ROŽNOVSKÝ, J. 2012. Aerodynamic Parameters of Windbreak Based on its Optical Porosity. *Contributions to Geophysics and Geodesy,* 42.

STRONG, S. 2017. Franz Josef business and community groups concerned about lack of consultation over wastewater upgrade. *Stuff*.

SUTTON-GRIER, A. E., WOWK, K. & BAMFORD, H. 2015. Future of our coasts: The potential for natural and hybrid infrastructure to enhance the resilience of our coastal communities, economies and ecosystems. *Environmental Science & Policy,* 51**,** 137-148.

SWALES, A. & HUME, T. 1995. Sedimentation history and potential future impacts of production forestry on the Wharekawa Estuary, Coromandel Peninsula.

TEICHBERG, M., FOX, S. E., OLSEN, Y. S., VALIELA, I., MARTINETTO, P., IRIBARNE, O., MUTO, E. Y., PETTI, M. A. V., CORBISIER, T. N., SOTO-JIMÉNEZ, M., PÁEZ-OSUNA, F., CASTRO, P., FREITAS, H., ZITELLI, A., CARDINALETTI, M. & TAGLIAPIETRA, D. 2010. Eutrophication and macroalgal blooms in temperate and tropical coastal waters: nutrient enrichment experiments with Ulv spp. *Global Change Biology,* 16**,** 2624-2637.

TEMMERMAN, S., DE VRIES, M. B. & BOUMA, T. J. 2012. Coastal marsh die-off and reduced attenuation of coastal floods: A model analysis. *Global and Planetary Change,* 92-93**,** 267-274.

TEMMERMAN, S., MEIRE, P., BOUMA, T. J., HERMAN, P. M., YSEBAERT, T. & DE VRIEND, H. J. 2013. Ecosystem-based coastal defence in the face of global change. *Nature,* 504**,** 79-83.

THANNHEISER, D. & HOLLAND, P. 1994. The Plant Communities of New Zealand Salt Meadows. *Global Ecology and Biogeography Letters,* 4**,** 107-115.

THOMSON, J. W. 1889. CATLINS IN 1863. *Clutha Leader*, 25 October 1889.

TRAILL, L. W., PERHANS, K., LOVELOCK, C. E., PROHASKA, A., MCFALLAN, S., RHODES, J. R. & WILSON, K. A. 2011. Managing for change: wetland transitions under sea-level rise and outcomes for threatened species. *Diversity and Distributions,* 17**,** 1225-1233.

TURNER, R. K., BURGESS, D., HADLEY, D., COOMBES, E. & JACKSON, N. 2007. A cost-benefit appraisal of coastal managed realignment policy. *Global Environmental Change,* 17**,** 397-407.

TYRRELL, A. R. 2006. *Pounawea: a Catlins township and its estuary* Dunedin, A.R. Tyrrell

USHIYAMA, T. 2009. Measurements of wind suppression effects of windbreak net using a wind tunnel for the purpose of applying numerical simulations. *Journal of Agricultural Meteorology (Japan),* 65**,** 273-281.

VAN EERDT , M. M. 1985. The influence of vegetation on erosion and accretion in salt marshes of the Oosterschelde, The Netherlands. *In:* BEEFTINK, W. G., ROZEMA, J. & HUISKES, A. H. L. (eds.) *Ecology of coastal vegetation.* Dordrecht: Springer.

VAN LOON-STEENSMA, J. M., SLIM, P. A., DECUYPER, M. & HU, Z. 2014. Salt-marsh erosion and restoration in relation to flood protection on the Wadden Sea barrier island Terschelling. *Journal of Coastal Conservation,* 18**,** 415-430.

VAN RIJN, L. C. 2011. Coastal erosion and control. *Ocean & Coastal Management,* 54**,** 867-887.

VONA, I., GRAY, M. & NARDIN, W. 2020. The Impact of Submerged Breakwaters on Sediment Distribution along Marsh Boundaries. *Water,* 12.

VUIK, V., BORSJE, B. W., WILLEMSEN, P. W. J. M. & JONKMAN, S. N. 2019. Salt marshes for flood risk reduction: Quantifying long-term effectiveness and life-cycle costs. *Ocean & Coastal Management,* 171**,** 96-110.

WALKER, I. J., HESP, P. A., DAVIDSON-ARNOTT, R. G. D. & OLLERHEAD, J. 2006. Topographic Steering of Alongshore Airflow over a Vegetated Foredune: Greenwich Dunes, Prince Edward Island, Canada. *Journal of Coastal Research,* 225**,** 1278-1291.

WALSH, K. J. E., MCBRIDE, J. L., KLOTZBACH, P. J., BALACHANDRAN, S., CAMARGO, S. J., HOLLAND, G., KNUTSON, T. R., KOSSIN, J. P., LEE, T.-C., SOBEL, A. & SUGI, M. 2016. Tropical cyclones and climate change. *Wiley Interdisciplinary Reviews: Climate Change,* 7**,** 65-89.

WAN, M., PAN, C., WANG, M. & JIN, Y. 2005. Application of the digitized measurement on windbreak porosity of farmland shelter–forests. *Arid Land Geography,* 29**,** 120-123.

WANG, H., VAN DER WAL, D., LI, X., VAN BELZEN, J., HERMAN, P. M. J., HU, Z., GE, Z., ZHANG, L. & BOUMA, T. J. 2017. Zooming in and out: Scale dependence of extrinsic and intrinsic factors affecting salt marsh erosion. *Journal of Geophysical Research: Earth Surface,* 122**,** 1455-1470.

WATSON, E. B., WIGAND, C., OCZKOWSKI, A. J., SUNDBERG, K., VENDETTUOLI, D., JAYARAMAN, S., SALIBA, K. & MORRIS, J. T. 2015. Ulva additions alter soil biogeochemistry and negatively impact Spartina alterniflora growth. *MARINE ECOLOGY PROGRESS SERIES,* 532**,** 59-72.

WEBB, B. M. & ALLEN, R. 2015. Wave Transmission through Artificial Reef Breakwaters. *In:* WALLENDORF, L. & COX, D. (eds.) *Coastal Structure and Solutions to Coastal Disasters Joint Conference.* Boston, Massachusetts: American Society of Civil Engineers

WESTON, N. B. 2013. Declining Sediments and Rising Seas: an Unfortunate Convergence for Tidal Wetlands. *Estuaries and Coasts,* 37**,** 1-23.

WIBERG, P. L., TAUBE, S. R., FERGUSON, A. E., KREMER, M. R. & REIDENBACH, M. A. 2018. Wave Attenuation by Oyster Reefs in Shallow Coastal Bays. *Estuaries and Coasts,* 42**,** 331-347.

WILLIAMS, S. 2019. *Building Living Shorelines with Oyster Shells* [Online]. Tensar Available: https://www.tensarcorp.com/resources/articles/building-living-shorelines-with-oysters [Accessed November 11 2022].

WILSON, G. A. 1993. The pace of indigenous forest clearance on farms in the Catlins District, South Island, New Zealand, 1861–1991. *New Zealand Geographer,* 49**,** 15-25.

WUNSCH, C., PONTE, R. M. & HEIMBACH, P. 2007. Decadal Trends in Sea Level Patterns: 1993–2004. *Journal of Climate,* 20**,** 5889-5911.

XU, W., FENG, G., MENG, L., ZHANG, A., AMPUERO, J. P., BÜRGMANN, R. & FANG, L. 2018. Transpressional Rupture Cascade of the 2016 Mw 7.8 Kaikoura Earthquake, New Zealand. *Journal of Geophysical Research: Solid Earth,* 123**,** 2396-2409.

YAN, D., YAO, X., LI, J., QI, L. & LUAN, Z. 2021. Shoreline Change Detection and Forecast along the Yancheng Coast Using a Digital Shoreline Analysis System. *Wetlands,* 41.

YE, C. & SUN, F. 2021. Development of a social value evaluation model for coastal wetlands. *Ecological Informatics,* 65.

YSEBAERT, T., WALLES, B., HANER, J. & HANCOCK, B. 2019. Habitat Modification and Coastal Protection by Ecosystem-Engineering Reef-Building Bivalves. *In:* C., S. A., FERREIRA, J. G., GRANT, J., PETERSON, J. K. & STRAND, Ø. (eds.) *Goods and Services of Marine Bivalves* Switzerland: SpringerOpen.

ZHANG, K., DOUGLAS, B. C. & LEATHERMAN, S. P. 2004. Global Warming and Coastal Erosion. *Climate Change,* 64**,** 41-58.

ZHU, Z., SLANGEN, A., ZHU, Q., GERKEMA, T., BOUMA, T. J. & YANG, Z. 2022. The role of tides and winds in shaping seed dispersal in coastal wetlands. *Limnology and Oceanography*.

ZUNIGA-TERAN, A. A., GERLAK, A. K., MAYER, B., EVANS, T. P. & LANSEY, K. E. 2020. Urban resilience and green infrastructure systems: towards a multidimensional evaluation. *Current Opinion in Environmental Sustainability,* 44**,** 42-47.

Appendix A

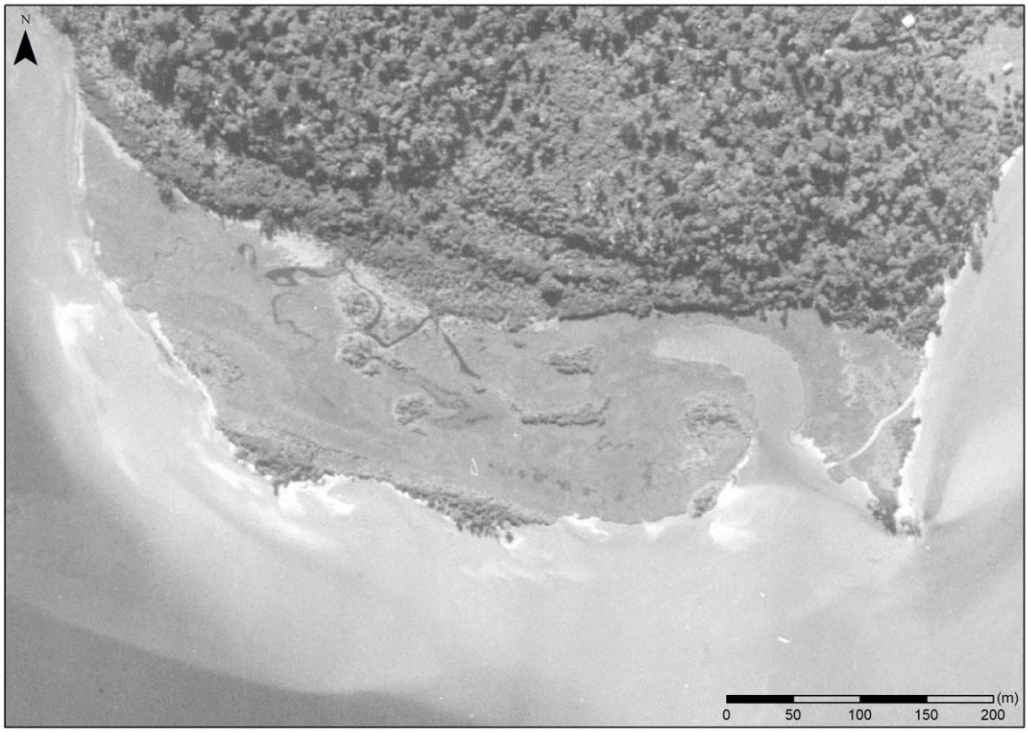

Figure A 1: 1948 aerial photograph of Pounawea Wetland.

Figure A 2: 1967 aerial photograph of Pounawea Wetland.

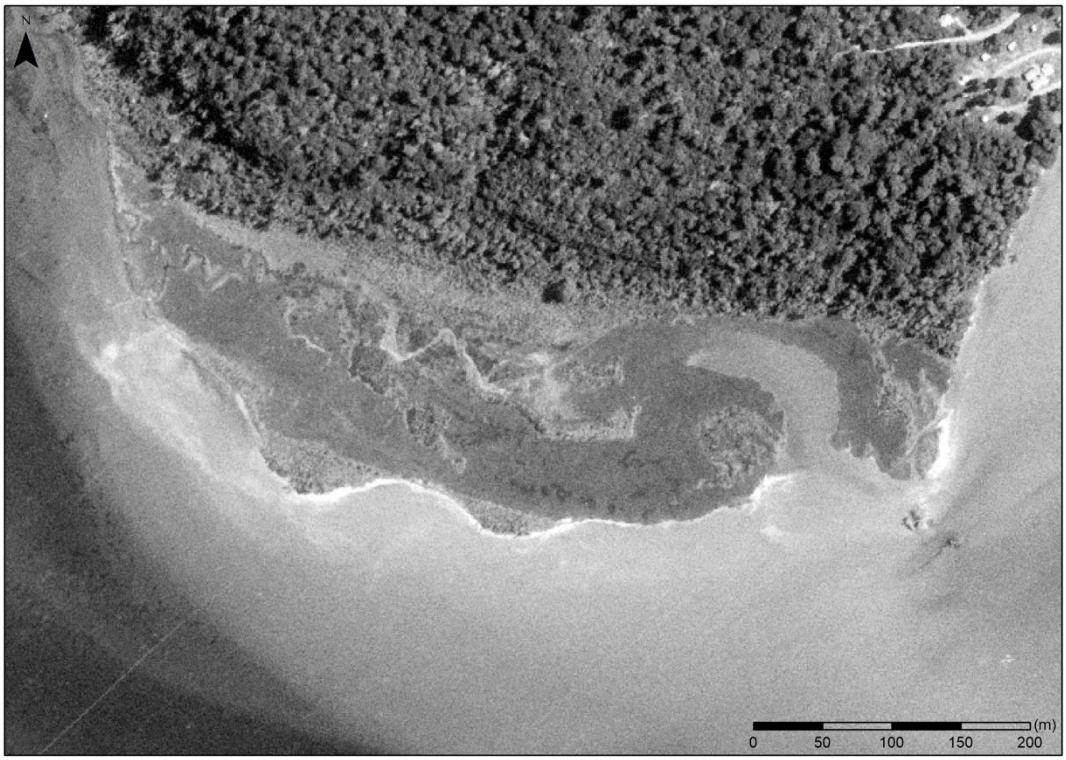

Figure A 3: 1978 aerial photograph of Pounawea Wetland.

Figure A 4: 1982 aerial photograph of Pounawea Wetland.

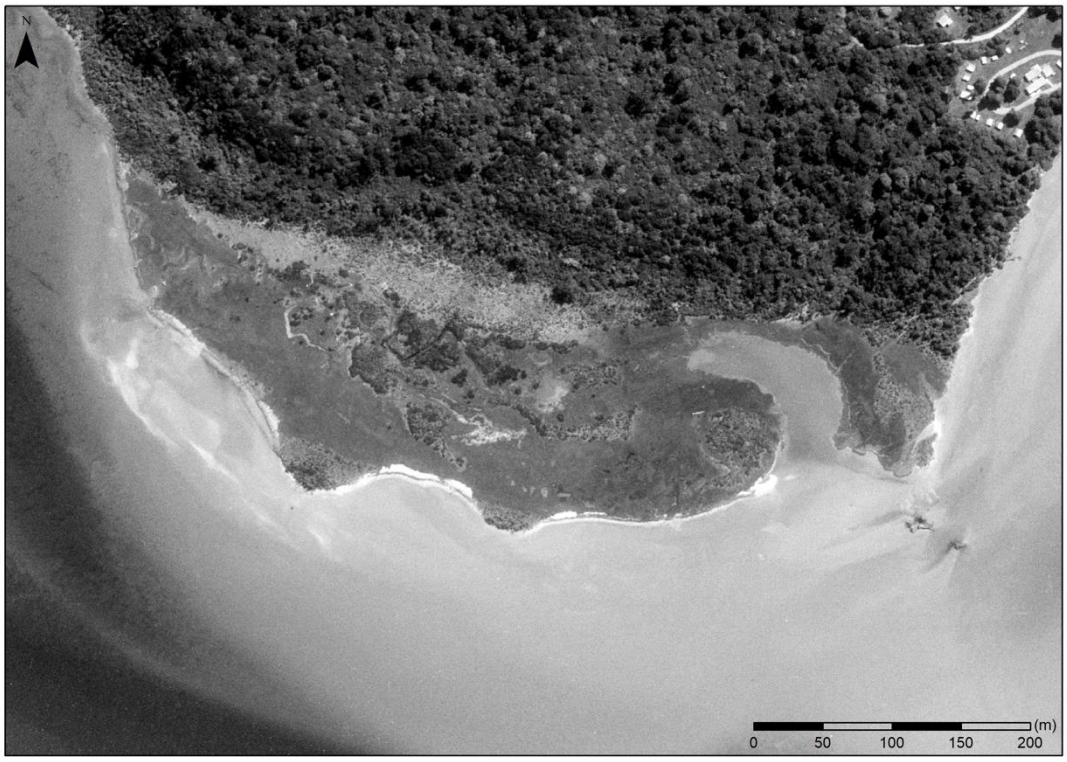

Figure A 5: 1985 aerial photograph of Pounawea Wetland.

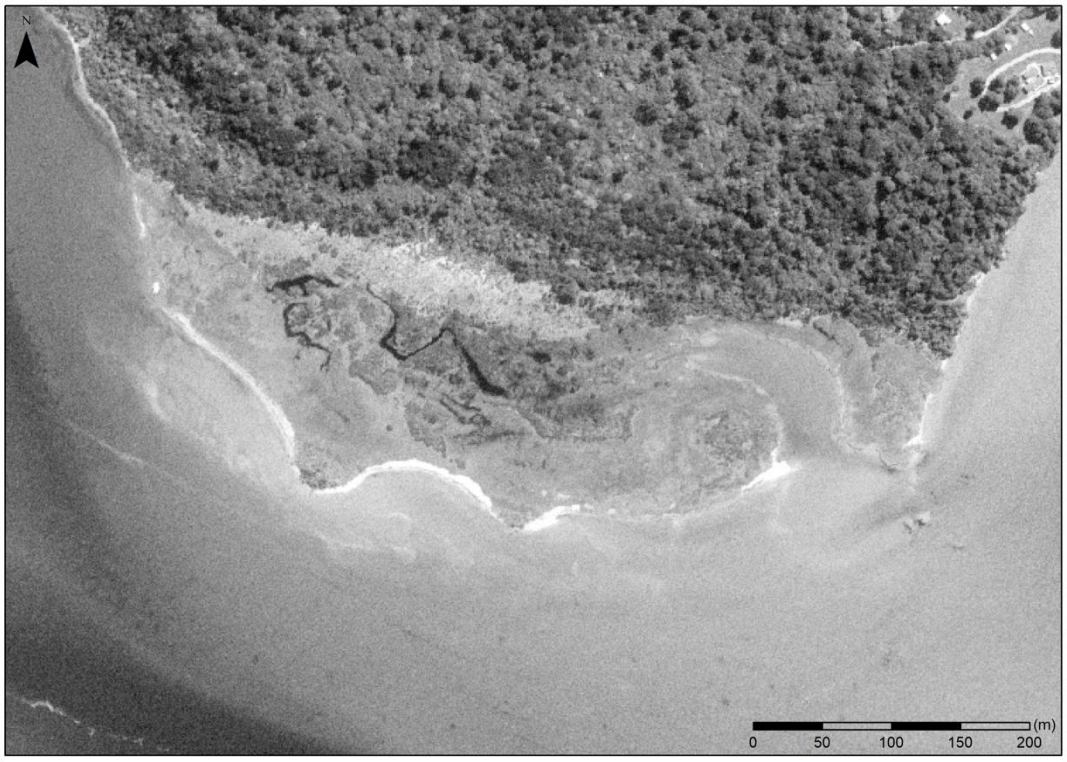

Figure A 6: 1995 aerial photograph of Pounawea Wetland.

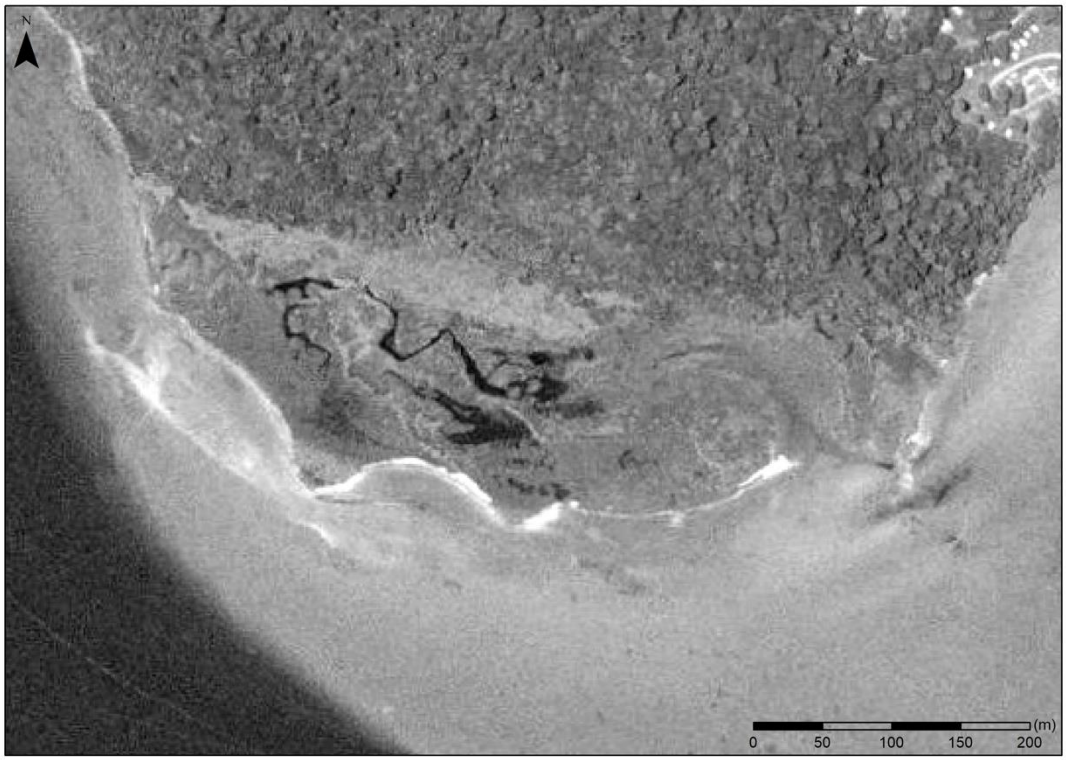

Figure A 7: 1997 aerial photograph of Pounawea Wetland.

Figure A 8: 2006 satellite image of Pounawea Wetland (Google Earth^{TM}).

2015

Figure A 9: 2015 satellite image of Pounawea Wetland (Google Earth™).

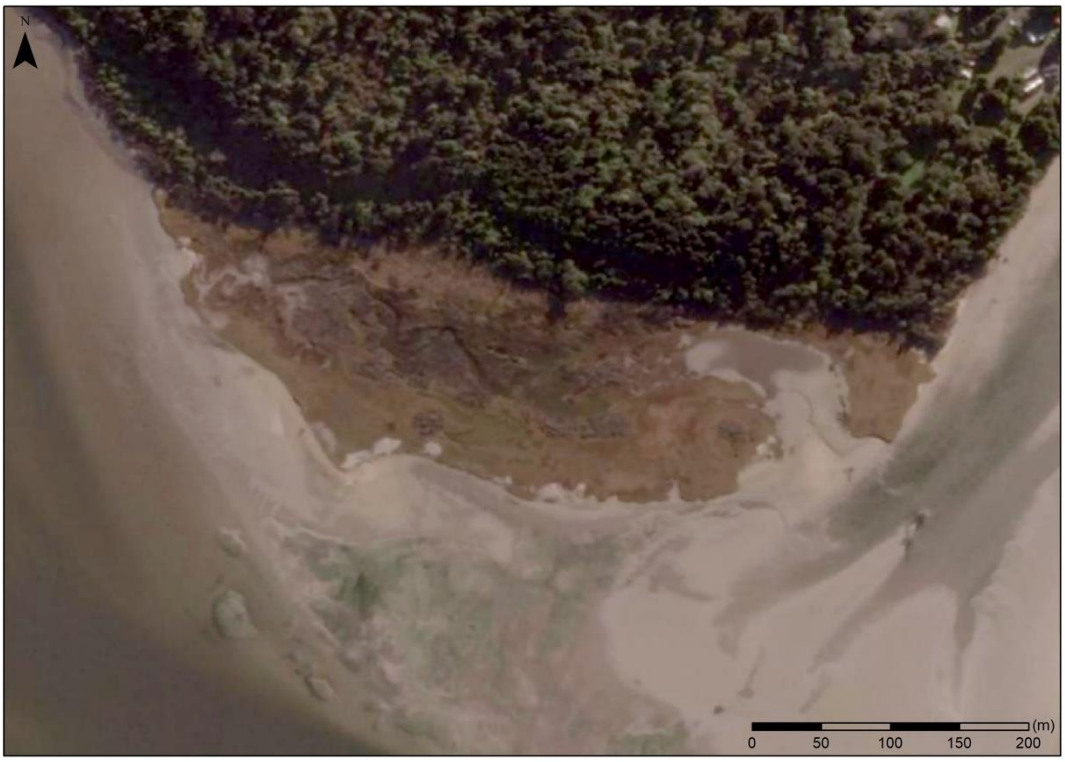

Figure A 10: 2019 satellite image of Pounawea Wetland (Google Earth™).

Figure A 11: Cartographic map of Owaka township from 1860, red squares outline Pounawea Wetland, Manuka Point and Cabbage Point

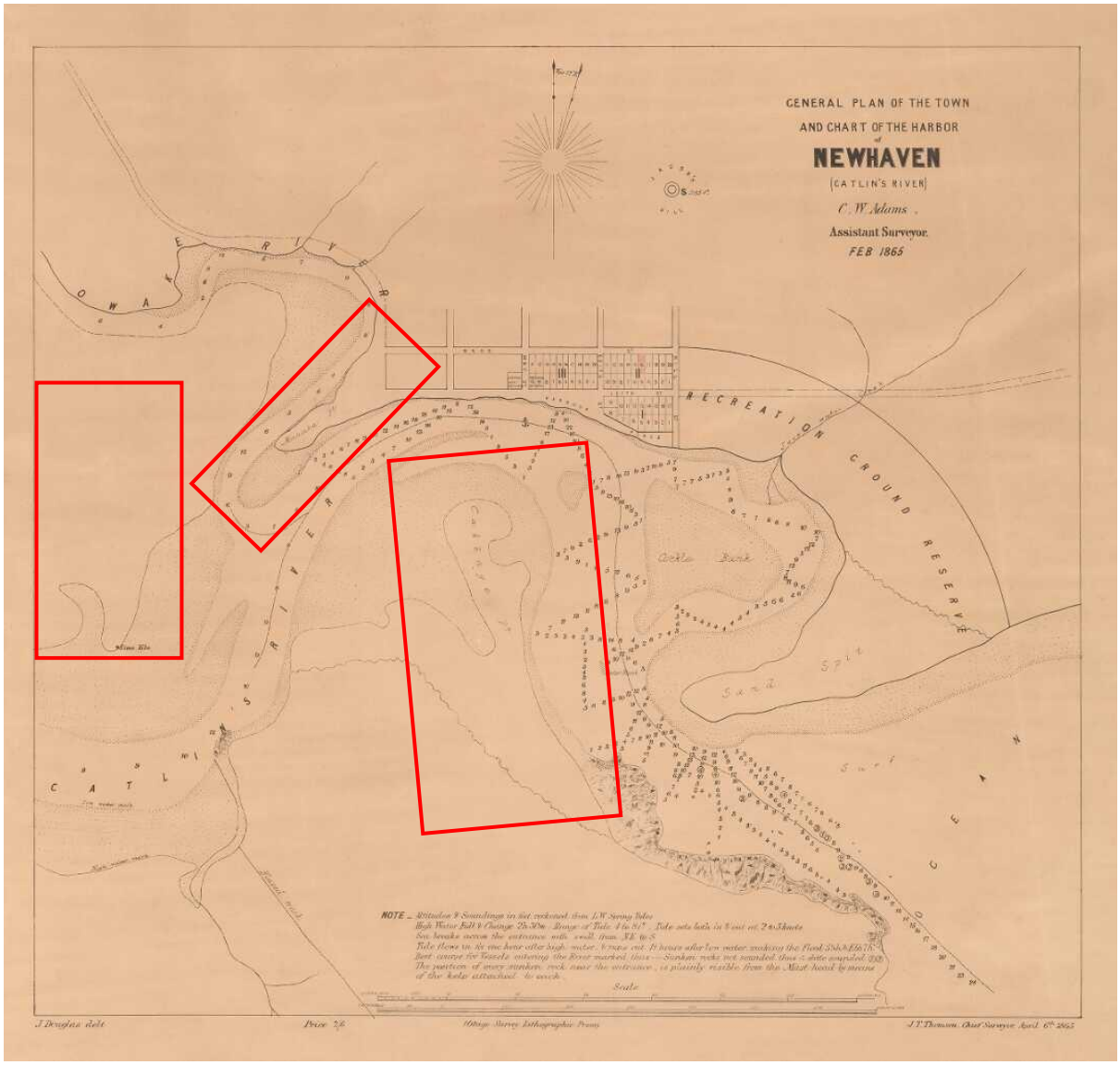

Figure A 12: Cartographic map of new haven 1890, red squares outline Pounawea Wetland, Manuka Point and Cabbage Point.

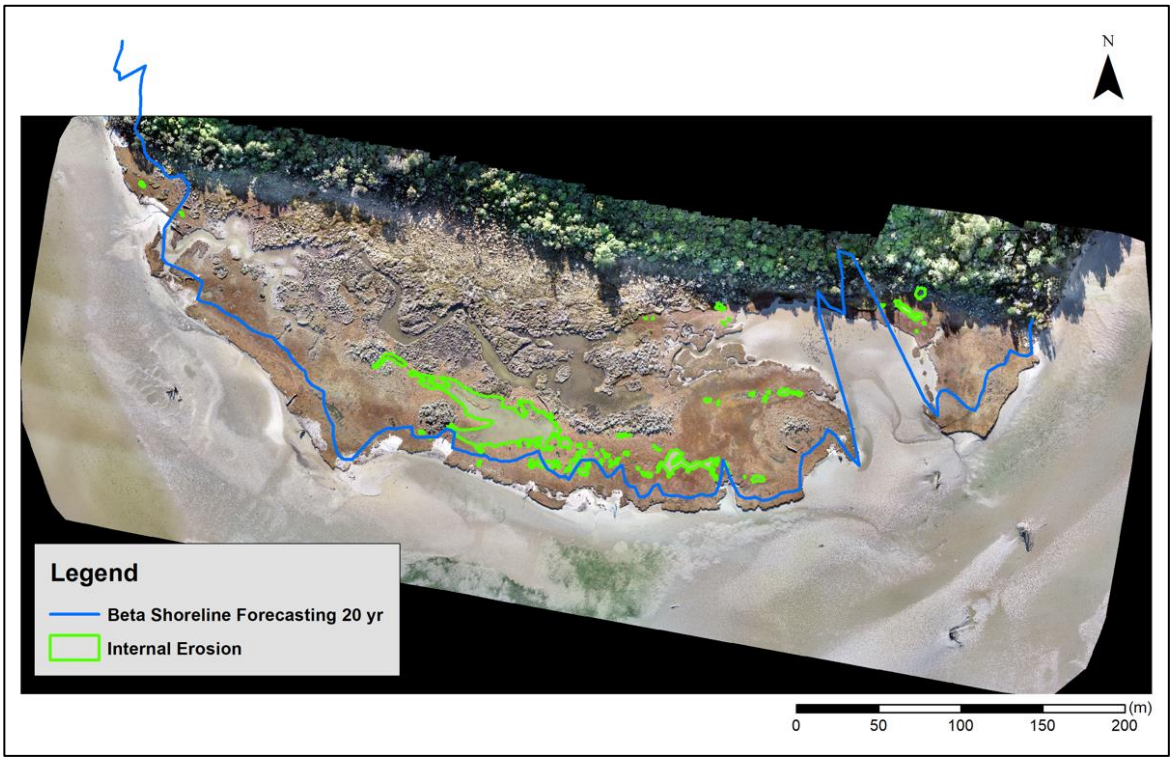

Figure A 13: DSAS beta shoreline forecast (20 yr) and 2022 internal erosion pools.

Appendix B

Wind velocity code: wind velocity is increased or decreased by changing the value highlighted in yellow.

```
#include "udf.h"
DEFINE_PROFILE(log_velocity,thread,index)
{
real y[ND_ND];
real x,z;
face_t f;
begin_f_loop(f,thread)
{
F_CENTROID(y,f,thread);
x = y[1];
z = y[2];
if (x<2)
{
F_PROFILE(f,thread,index) = 0.;
} else {
F_PROFILE(f,thread,index) = 7.5*log(x+0.0002/0.0002);
}
end_f_loop(f,thread)
}
}
```

Wind flow using “5.5*log” and C_D = 0.005

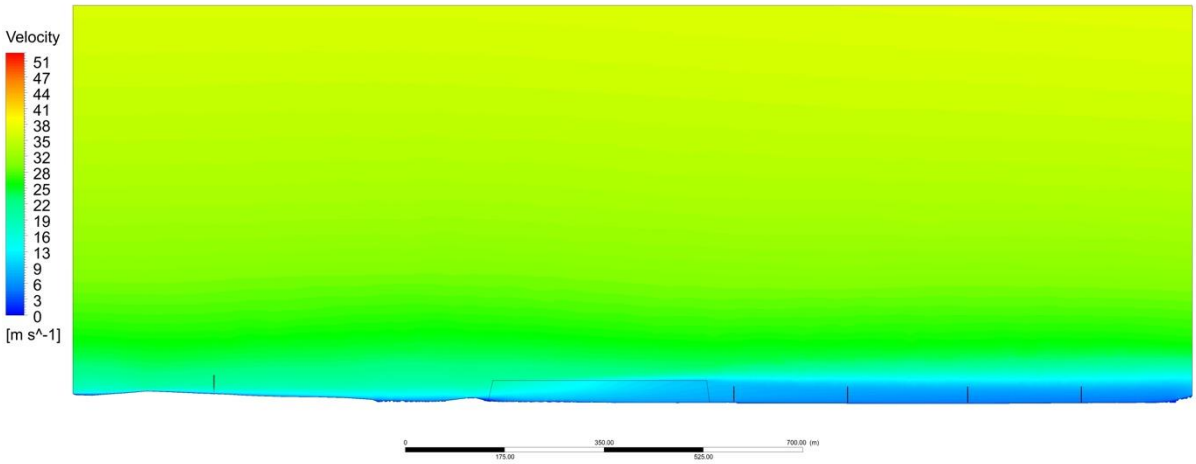

Figure B 1: Wind flow using 5.5*log and Cd = 0.005

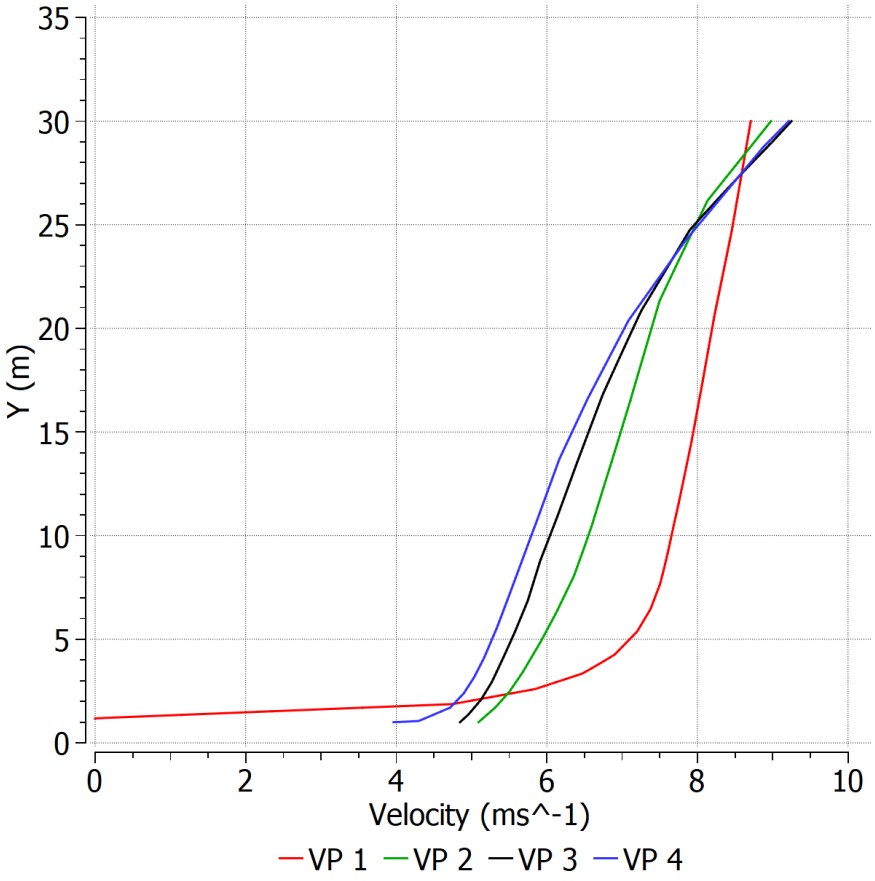

Figure B 2: Velocity profile of wind across the estuary using 5.5*log and Cd=0.005

Table B 1: Wind speeds across the Catlins Estuary recorded at each velocity profile under all Cd models.

Cd=0					
Y (m)	Inlet Velocity ($m\ s^{-1}$)	V1 ($m\ s^{-1}$)	V2 ($m\ s^{-1}$)	V3 ($m\ s^{-1}$)	V4 ($m\ s^{-1}$)
1	12.41	12.2	13.9	14.11	11.26
1.5	13.9	13.7	14.34	14.6	13.15
Cd=0.005					
Y (m)	Inlet Velocity ($m\ s^{-1}$)	V1 ($m\ s^{-1}$)	V2 ($m\ s^{-1}$)	V3 ($m\ s^{-1}$)	V4 ($m\ s^{-1}$)
1	12.35	7	6.78	6.53	5.22
1.5	13.83	7.95	7.02	6.73	6.06
Cd=0.009					
Y (m)	Inlet Velocity ($m\ s^{-1}$)	V1 ($m\ s^{-1}$)	V2 ($m\ s^{-1}$)	V3 ($m\ s^{-1}$)	V4 ($m\ s^{-1}$)
1	12.31	5.07	4.31	3.76	2.91
1.5	13.8	5.8	4.46	3.87	3.36
Cd = 0.05					
Y (m)	Inlet Velocity ($m\ s^{-1}$)	V1 ($m\ s^{-1}$)	V2 ($m\ s^{-1}$)	V3 ($m\ s^{-1}$)	V4 ($m\ s^{-1}$)
1	12.19	0.73	0.03	1.48	1.6
1.5	13.64	0.88	0.03	1.49	1.89
Cd=0.1					
Y (m)	Inlet Velocity ($m\ s^{-1}$)	V1 ($m\ s^{-1}$)	V2 ($m\ s^{-1}$)	V3 ($m\ s^{-1}$)	V4 ($m\ s^{-1}$)
1	12.15	0.03	0.85	1.97	1.99
1.5	13.61	0.03	0.87	2.02	2.51
Cd=0.15					
Y (m)	Inlet Velocity ($m\ s^{-1}$)	V1 ($m\ s^{-1}$)	V2 ($m\ s^{-1}$)	V3 ($m\ s^{-1}$)	V4 ($m\ s^{-1}$)
1	12.12	0.02	1.04	1.88	0.67
1.5	13.59	0.04	1.07	1.92	1.09

Appendix C

RMSE error Omega vs K-w vs RBR 203020

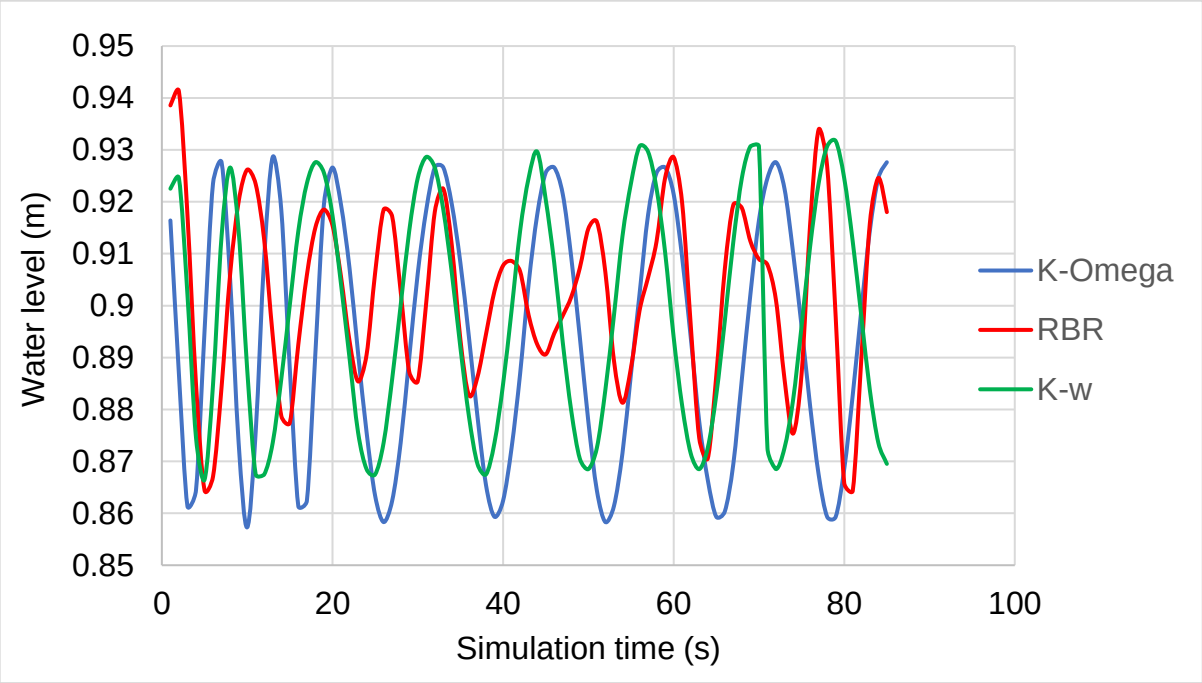

Figure C 1: Water level from observed and modelled inundation, RBR 203020 from location 'a' in Figure 5.1, k-omega and k-epsilon were the two models used for comparison.

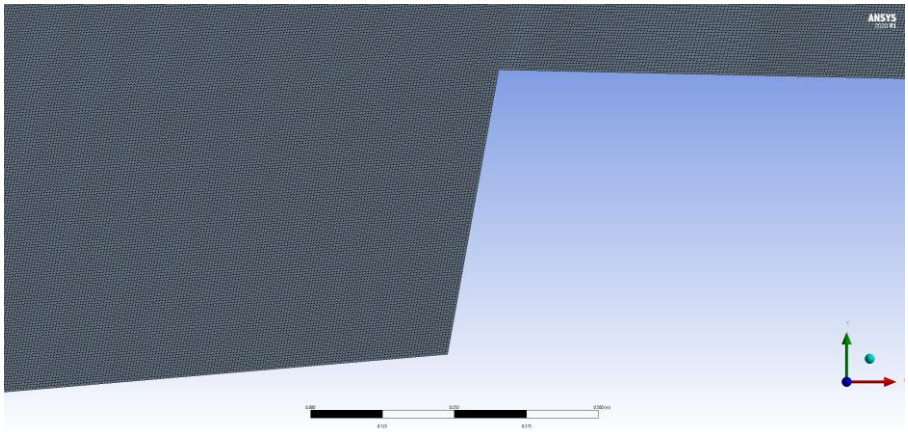

Figure C 2: CFD mesh of scarp edge.

Wetland inundation code

```
close all;
clear all;

%note files very large causing memeory crashs if have any bigger
consider
%using mapresize in loadfile.m function to decimiate.
dem_file='/media/Data-Drive/frado66p/finn/pounawea.tif';
photo_file='/media/Data-
Drive/frado66p/finn/Images/55m_Pounawea_gimp.tif';
photo_orginal_file='/media/Data-
Drive/frado66p/finn/Images/55m_Pounawea_gimp.tif';

aveage_local_pressure=1010;% this needs
year=2140;
SLR=(-1.36/1000)*(year-2022); %-1.36mm/y www.searise.co.nz
tide=(0:0.01:6)';
pressure=(900:1:1200);
[i,y]=size(pressure);
extra_tide=repmat((pressure-
aveage_local_pressure)*0.01,[length(tide),1]);
total_tide=(repmat(tide,[1,y])+extra_tide+SLR);

contourf(pressure,tide,total_tide,20);
title("For "+year+" total tide -1.36mm/y www.searise.co.nz");
ylabel('tide (m)');
xlabel('pressure hpa');
zlabel('total tide (m)');
colorbar
figure
[z,x]=readgeoraster(dem_file,'OutputType','double');
mapshow(z,x);
title('dem');
figure
[pz,px]=readgeoraster(photo_orginal_file,'OutputType','uint8');
%changed from single
pz=uint8(pz(:,:,1:3));
mapshow(pz,x);
title('orginal');
figure
final=pz;
%clear pz
hightide=1;%under 2m height can change value
final(z<hightide)=nan;
mapshow(final,x);
title(['Tide of ',num2str(hightide), 'm']);
axes_plot=gca;
axes_plot.TickDir='out';
axes_plot.XTickLabelRotation = 90;
cell_area=x.CellExtentInWorldX*x.CellExtentInWorldY;

%plot areas of beach bar graph
figure
z(z==-10000)=nan;
area_flood=z(~isnan(z));
histogram(area_flood,100,'normalization','cdf')
title(['normalized area with height of beach, 100 bins
',string(numel(area_flood)),' points']);
```

Table C 1: Sediment depth (cm) at each mat for all deployments

	18-19 May	19-20 May	20-21 May	31 May - 1 June	1-2 June	June 13-14
a	0.000598	0.001425	0.008815	0.000332	0.000302	0.022913
b	0.000314	0.003731	0.001781	0.000423	0.000755	0.002681
c	0.000489	0.001177	0.001111	0.000235	0.000658	0.000815
d	0.000326	0.000960	0.000513	0.000169	0.000254	0.001709
e	0.000664	0.003435	0.007191	0.000592	0.000513	0.020124
f	0.000374	0.001165	0.001232	0.000356	0.000471	0.001365
g	0.000374	0.000924	0.000574	0.000574	0.000592	0.001878
h	0.000284	0.000936	0.000525	0.000495	0.000368	0.002125

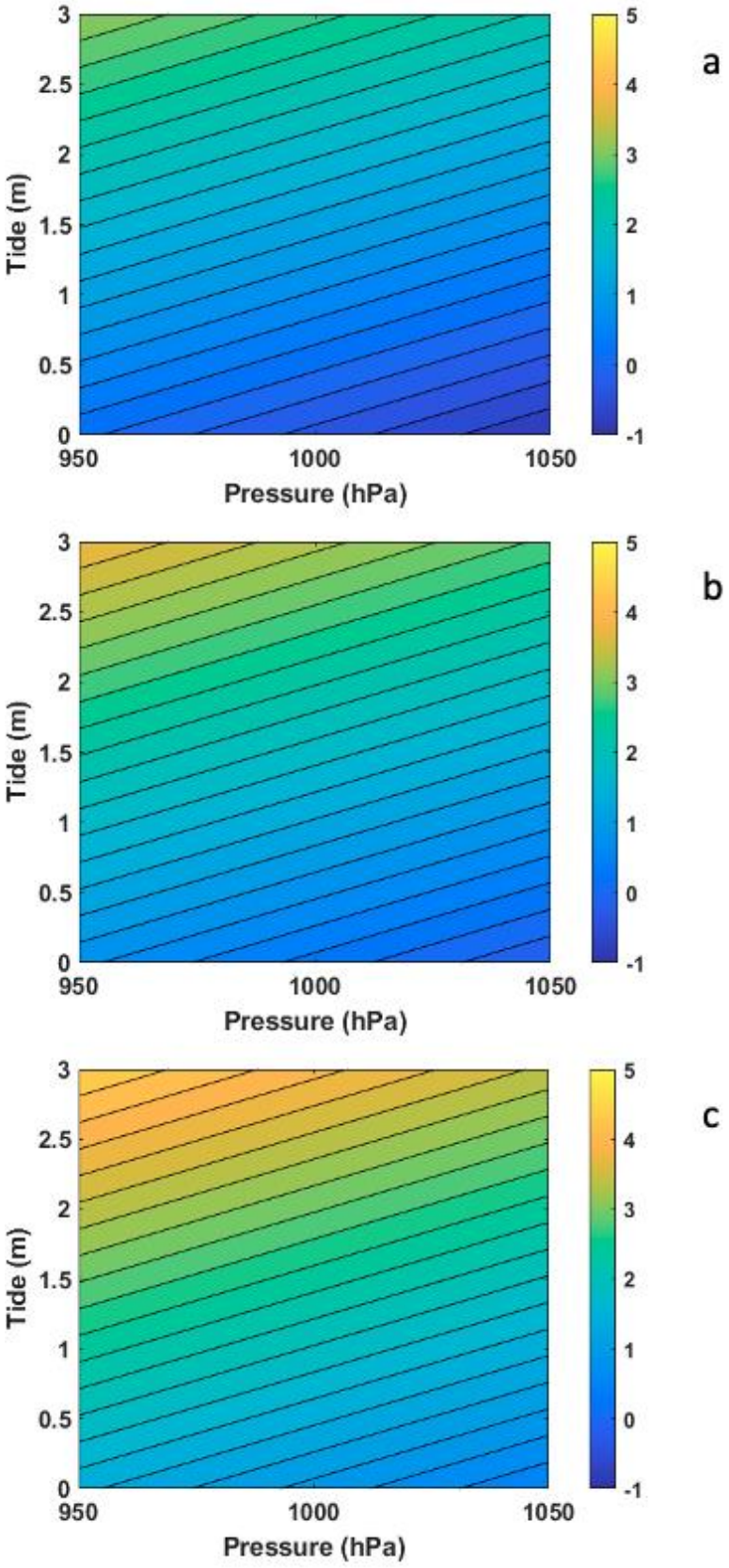

Figure C 3: The modelled effect of tide and pressure on water level (m); (a) 1900; (b) 2100; (c) 2300.

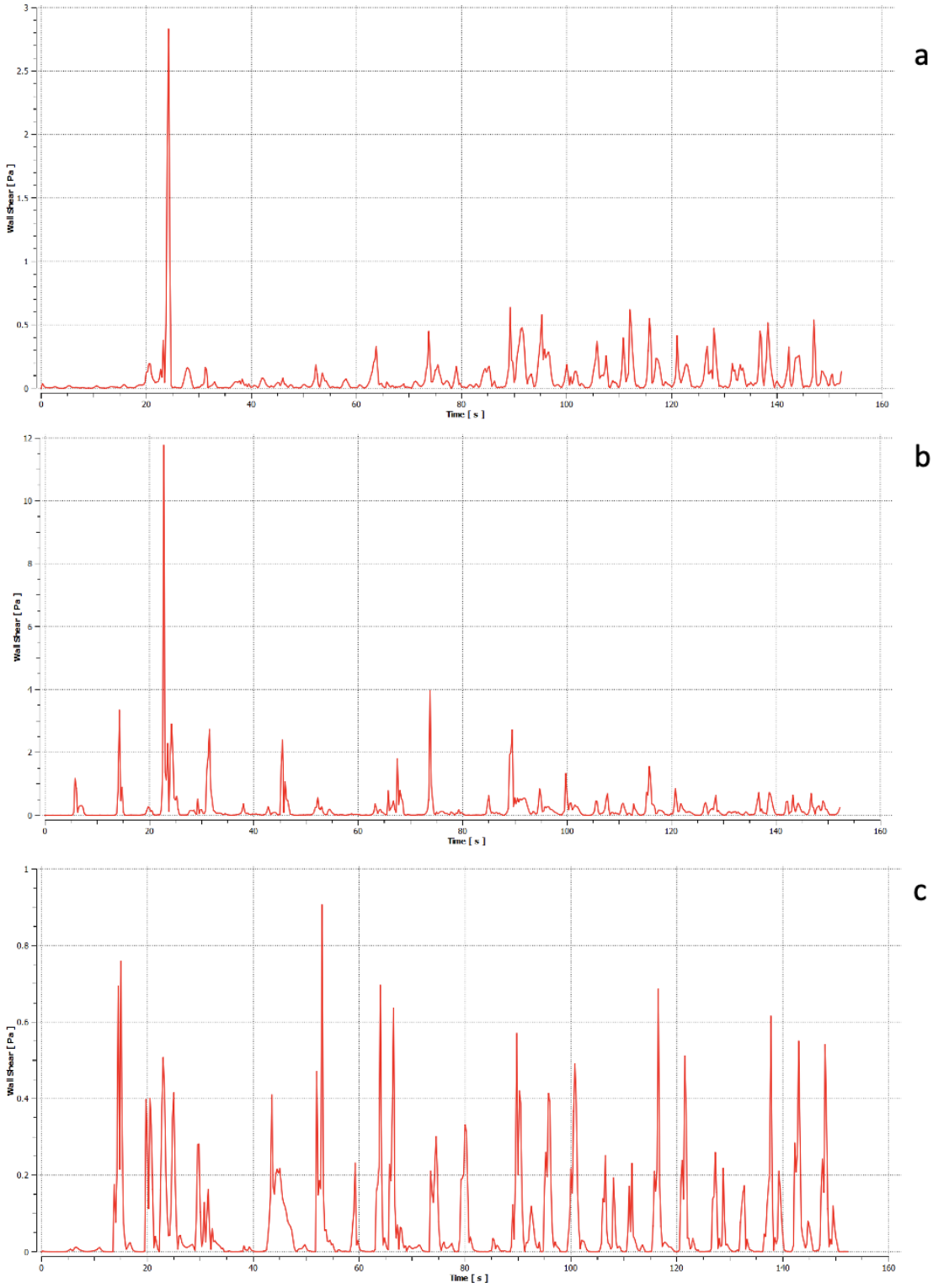

Figure C 4: Wall shear stress under 0.2 m water level; (a) top of the scarp; (b) middle of the scarp; (c) bottom of the scarp; note the scale differences at the y axis.

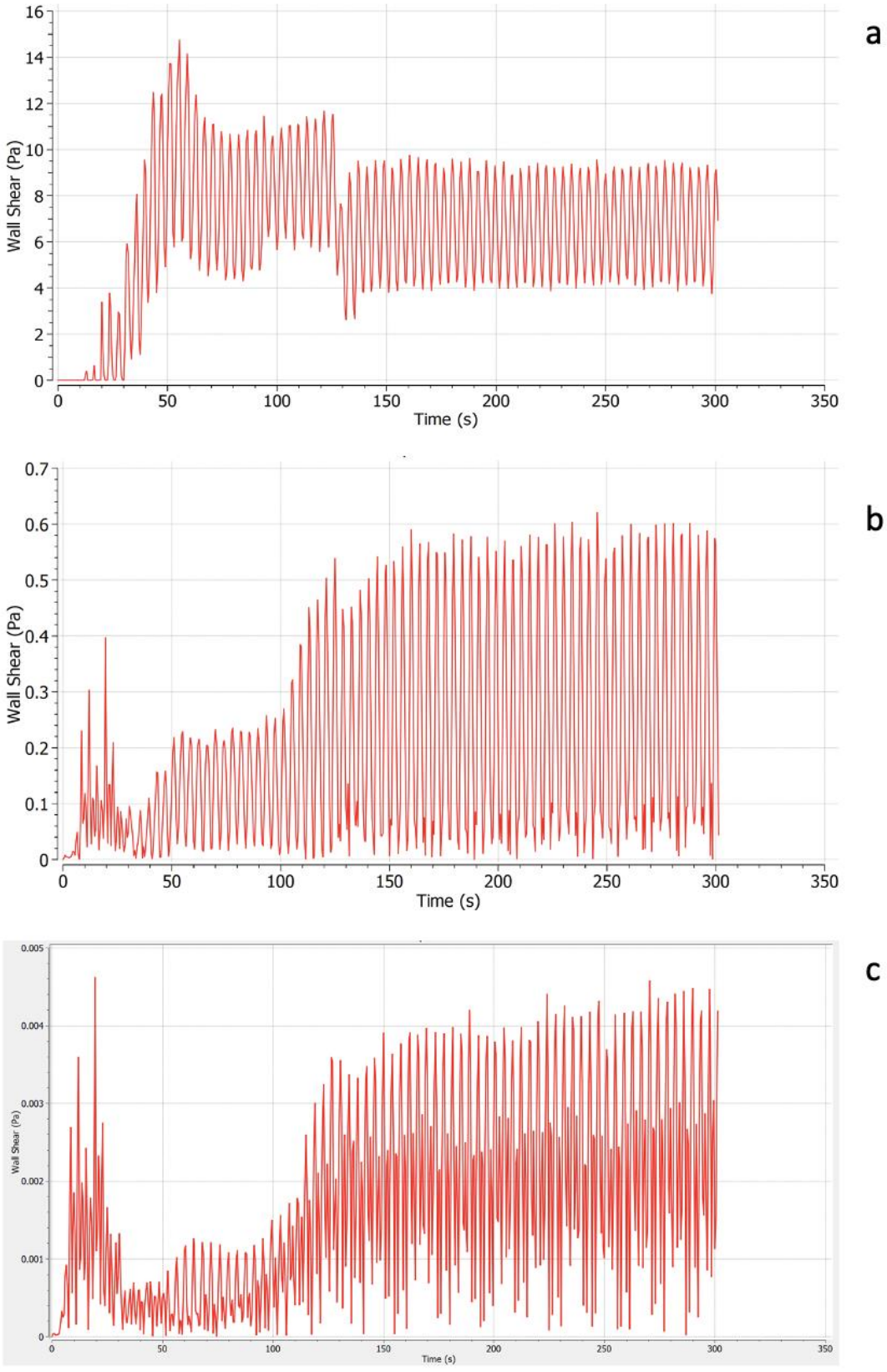

Figure C 5: Wall shear stress under 0.4 m water level; (a) top of the scarp; (b) middle of the scarp; (c) bottom of the scarp; note the scale differences at the y axis.

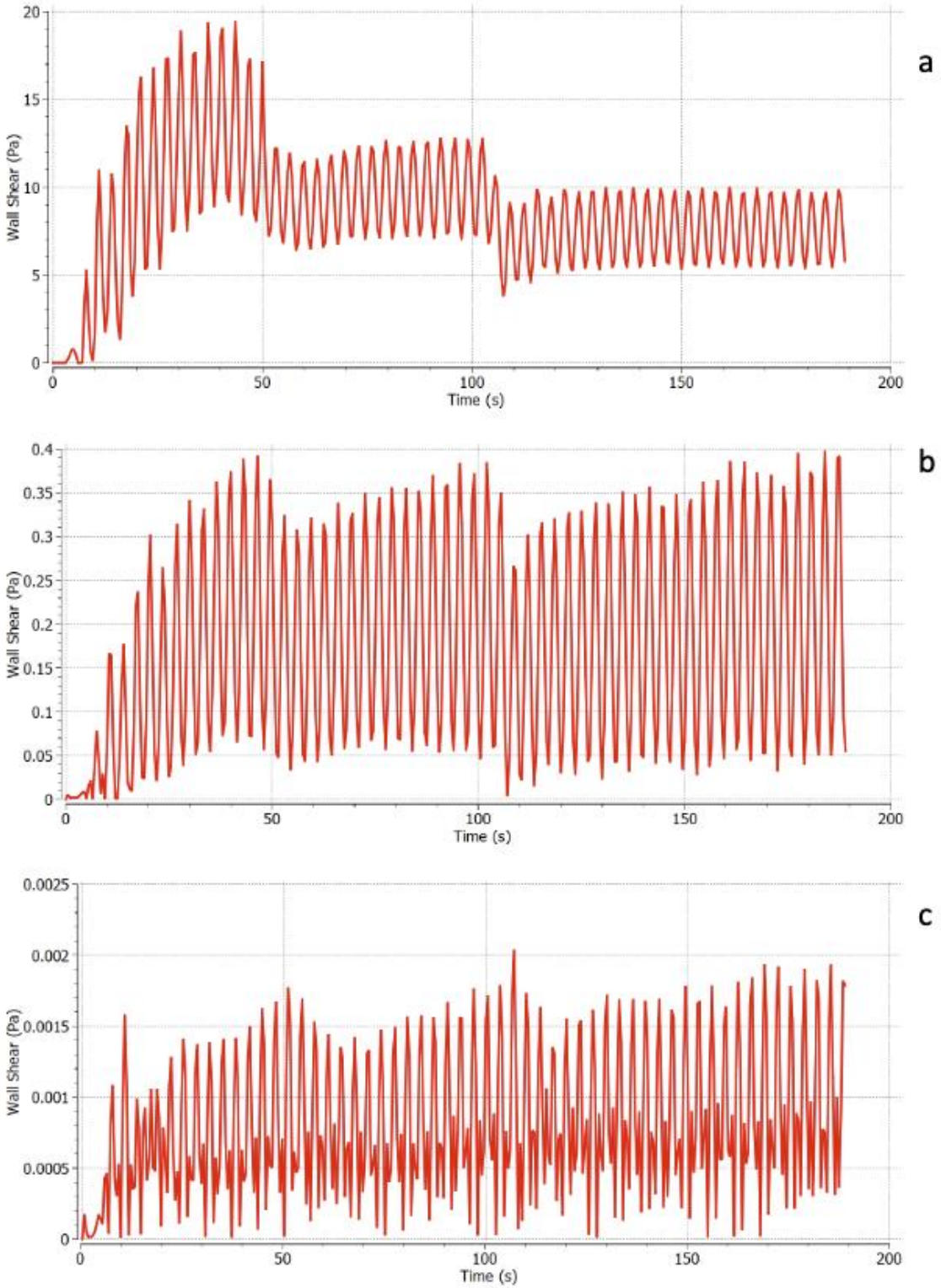

Figure C 6: Wall shear stress under 0.6 m water level; (a) top of the scarp; (b) middle of the scarp; (c) bottom of the scarp; note the scale differences at the y axis.

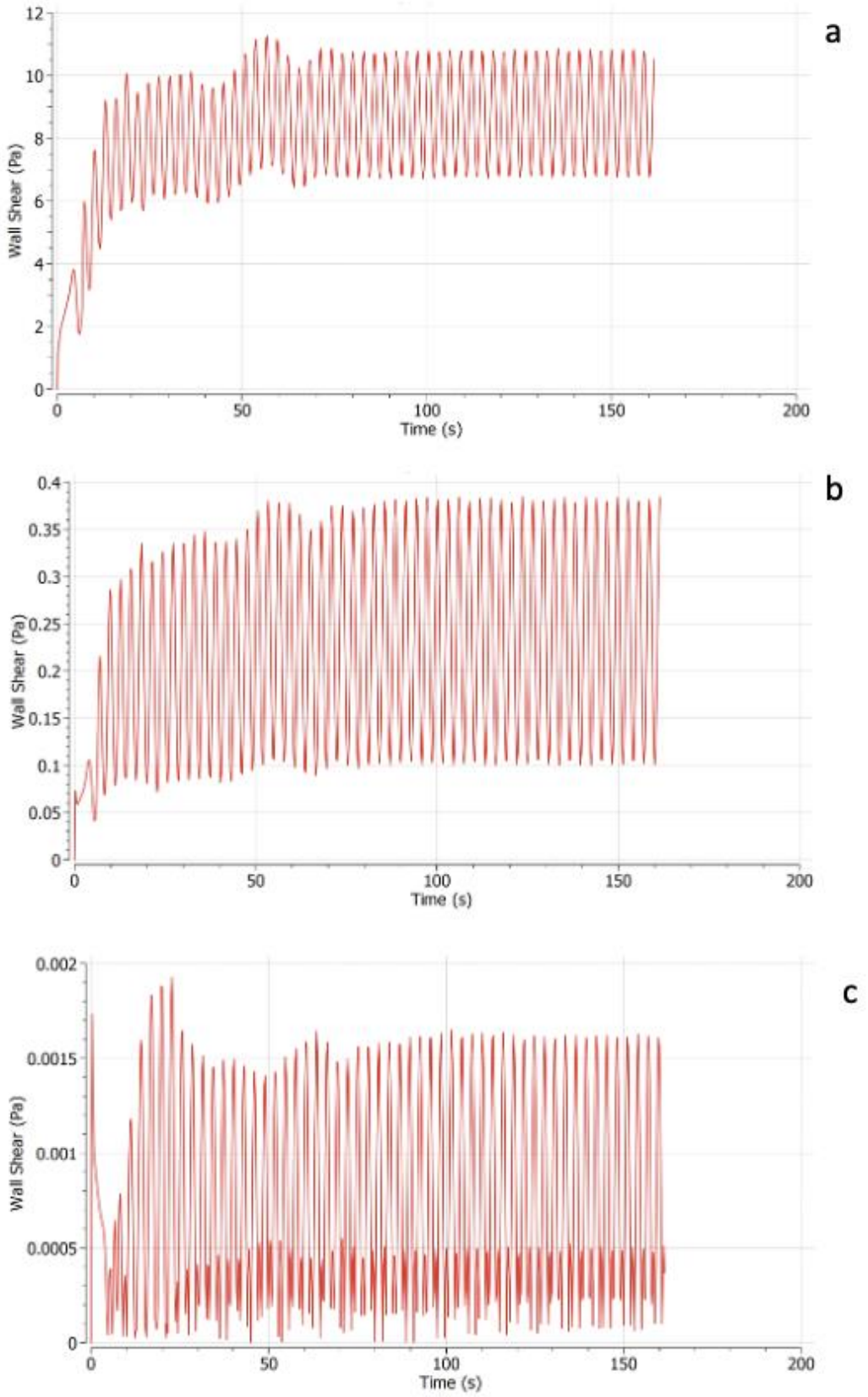

Figure C 7: Wall shear stress under 0.8 m water level; (a) top of the scarp; (b) middle of the scarp; (c) bottom of the scarp; note the scale differences at the y axis.

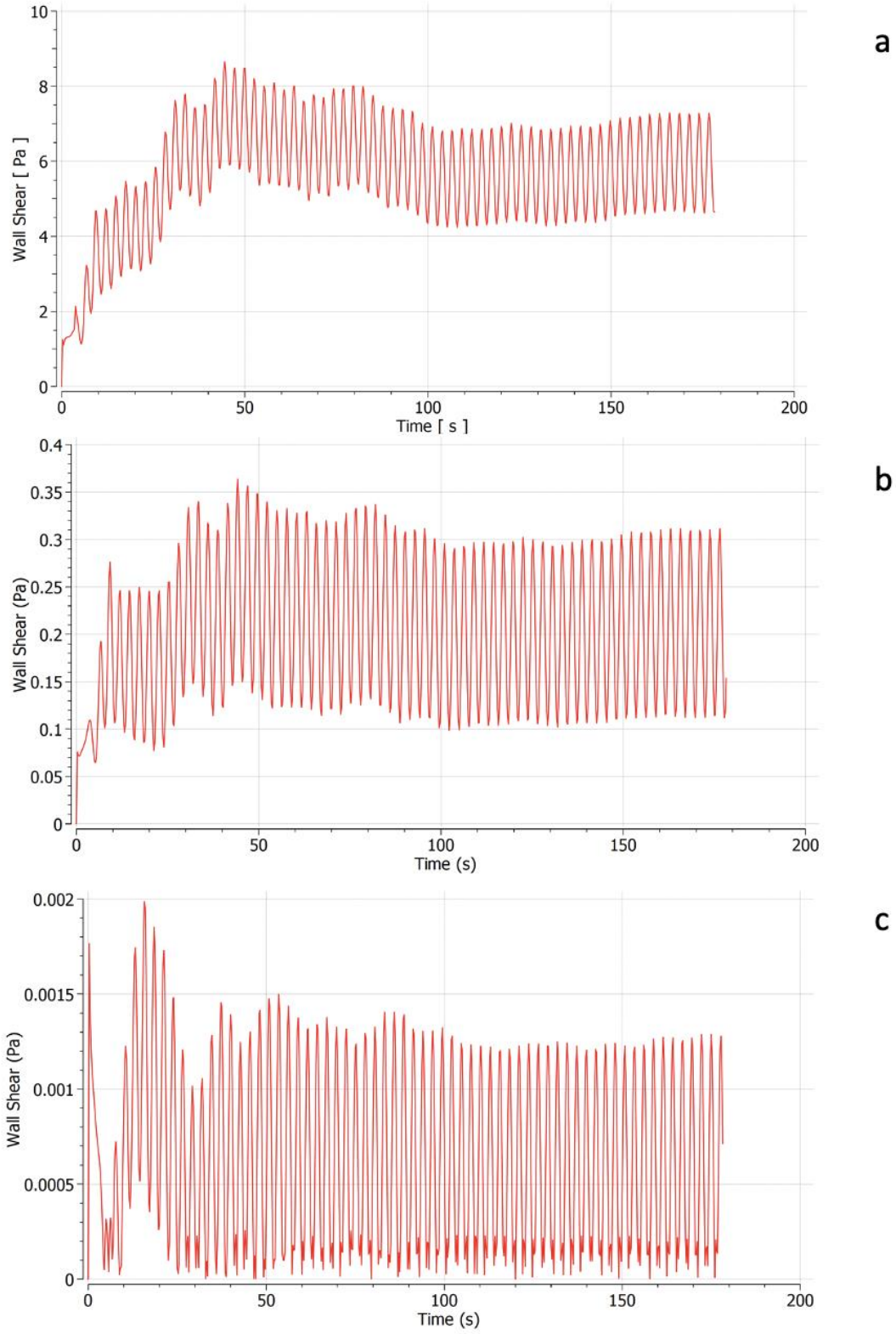

Figure C 8: Wall shear stress under 1 m water level; (a) top of the scarp; (b) middle of the scarp; (c) bottom of the scarp; note the scale differences at the y axis.

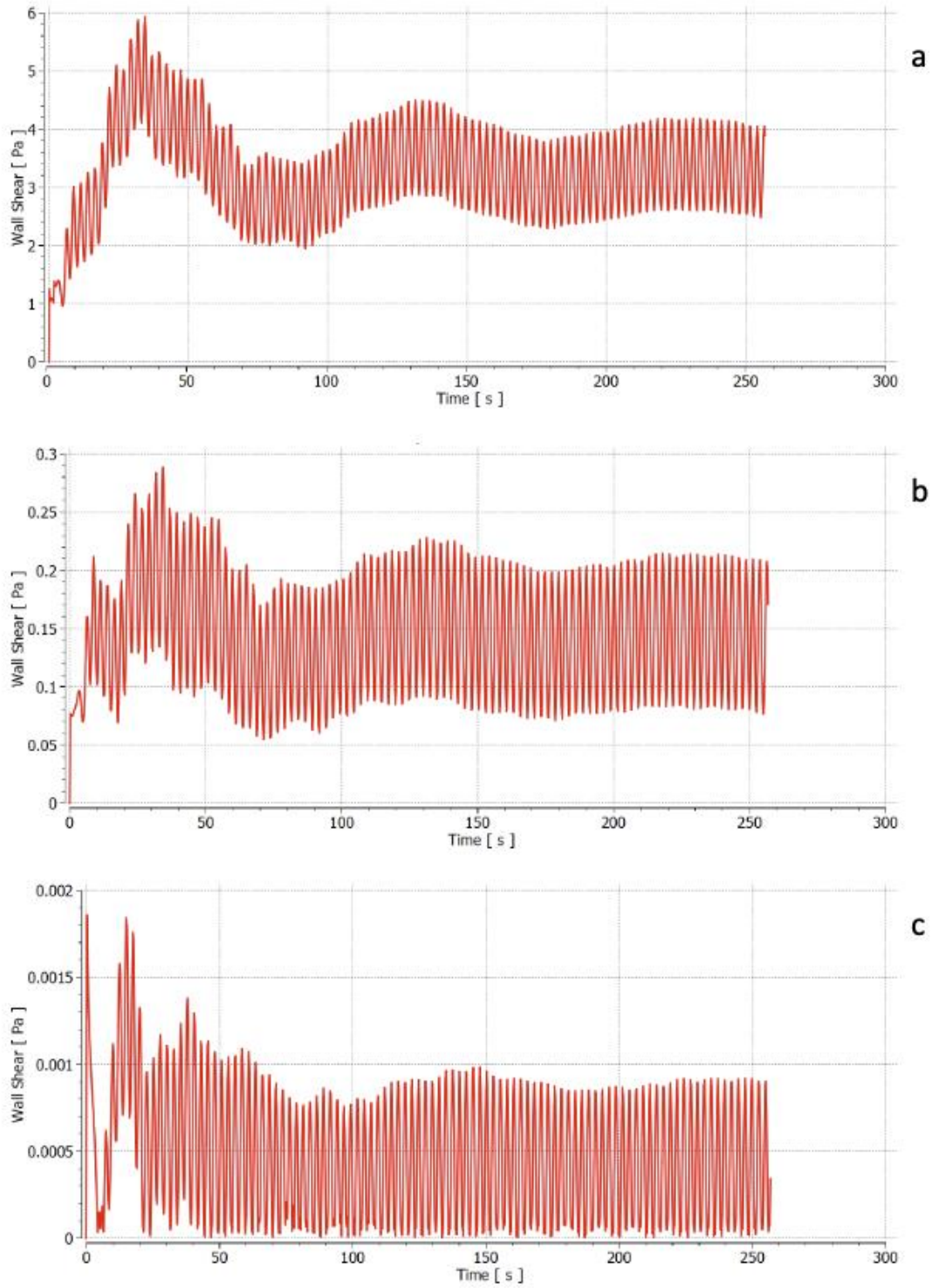

Figure C 9: Wall shear stress under 1.2 m water level; (a) top of the scarp; (b) middle of the scarp; (c) bottom of the scarp; note the scale differences at the y axis.

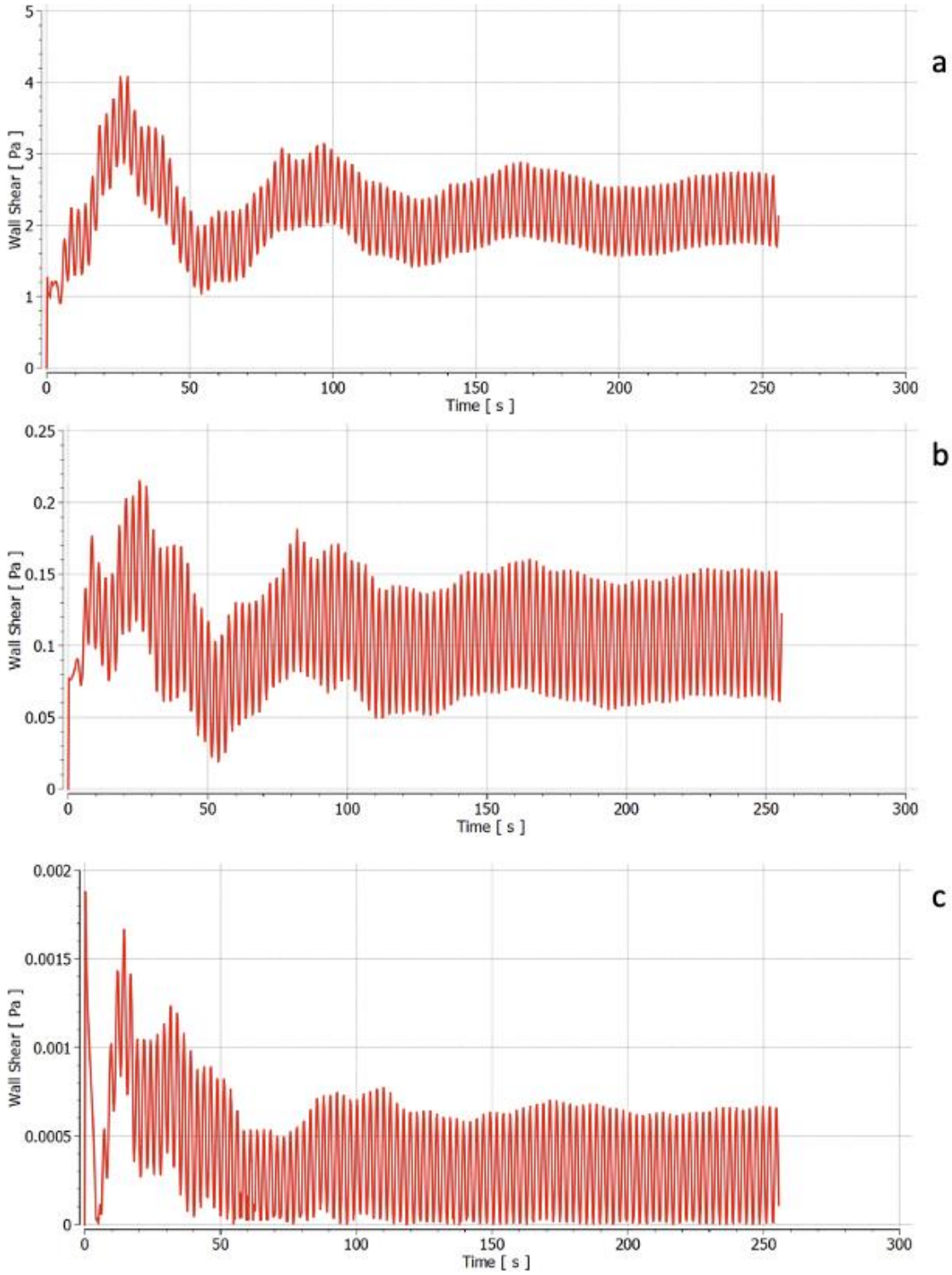

Figure C 10: Wall shear stress under 1.4 m water level; (a) top of the scarp; (b) middle of the scarp; (c) bottom of the scarp; note the scale differences at the y axis.